Evaluation of Practical Methods for the Evaluation of Concrete Walls

Blake D. Doepker

A thesis
submitted in partial fulfillment of the
requirements for the degree of

Master of Science in Civil Engineering

University of Washington
2008

Program Authorized to Offer Degree:
Department of Civil and Environmental Engineering

University of Washington
Graduate School

This is to certify that I have examined this copy of a master's thesis by

Blake D. Doepker

and have found that it is complete and satisfactory in all respects,
and that any and all revisions required by the final
examining committee have been made.

Committee Members:

____

Laura N. Lowes

____

Dawn E. Lehman

____

Gregory R. Miller

Date: ______________________________

In presenting this thesis in partial fulfillment of the requirements for a master’s degree at the University of Washington, I agree that the Library shall make its copies freely available for inspection. I further agree that extensive copying of this thesis is allowable only for scholarly purposes, consistent with “fair use” as prescribed in the U.S. Copyright Law. Any other reproduction for any purposes or by any means shall not be allowed without my written permission.

Signature ________________________

Date ___________________________

University of Washington

Abstract

Evaluation of Practical Methods for the Evaluation of Concrete Walls

Blake D. Doepker

Chair of the Supervisory Committee:
Associate Professor Laura N. Lowes
Department of Civil and Environmental Engineering

The determination of loads and displacement demands for seismic design of reinforced concrete walls is typically accomplished in practice using elastic shell-element models and response-spectrum analysis methods. Here, the results of a series of shake-table tests of reinforced concrete wall specimens are used to evaluate commonly used and newly proposed methods for determining the effective stiffness used in these analyses.

Newly proposed stiffness prediction methods use an iterative method of stiffness reduction with increased roof drift demands to capture stiffness loss due to cracking of concrete and yielding of reinforcing steel. Existing recommendations for modal damping are also evaluated. Stiffness and damping methods are evaluated on the basis of how accurately the period, building displacements, story accelerations and

load distribution are simulated. The results of this study include recommended methods for application of elastic, response-spectrum analysis for seismic design of concrete walls.

TABLE OF CONTENTS

Page

LIST OF FIGURES

Figure Number Page

LIST OF TABLES

Table Number Page

ACKNOWLEDGEMENTS

This thesis could not have been completed without the enormous support of my advisers: Professor Dawn Lehman and Professor Laura Lowes as well as committee member Professor Greg Miller. Additionally, I must acknowledge the help of my predecessors as well as my current colleagues. These include Aaron Sterns, Paul Oyen, Peter Brown, Claudio Esteban Osses-Henriquez and Danya Mohr. Additionally I would like to thank Richard Ranf for his enormous contributions, as well as my colleagues at the University of Illinois, Urbana Champaign, Chris Hart and Ken Marley, for their assistance on our project.

This work could not have been completed without the support of the National Science Foundation through the Network for Earthquake Engineering Simulation (NEESR) Program (award number CMS-0421577) that has funded me through a large portion of my project.

And lastly, I would like to thank my brother Byron for his enormous help in the final days, as well as all my friends and family who have endured boring talk about shear walls for the past two plus years.

Chapter 1: Introduction

Concrete shear walls are a frequently used lateral load resisting system for low-, mid- and high-rise construction in seismic areas. They provide an economical system for resisting seismic loads, and they can be incorporated in most architectural schemes. Given their prevalence in seismic areas, many studies have addressed analysis of walls to predict seismic demands for design. However, these many studies have not resulted in consensus. Currently, building codes, standards of practice for structural design, and research reports and papers provide a number of widely different recommendations for predicting shear wall response. These different recommendations address appropriate effective stiffness modifiers for linear elastic analysis, modal damping values, and methods of estimating effective fundamental periods. Despite the wide variation in recommendations and the extent of previous research, there has been little work done to systematically evaluate and compare recommendations for linear elastic, time history analyses. The objectives of this study are to evaluate some of the previously proposed methods for linear elastic, dynamic analysis of wall system as well as to develop and evaluate new methods for predicting stiffness loss associated with seismic loading that enable better prediction of response quantities used in design.

These objectives are achieved by using new and existing methods to simulate the dynamic response of four different structural walls subjected to shake table testing.

The simulation results are compared with measured response quantities to assess the methods' effectiveness.

The results of this study are presented in this thesis as follows. Previously proposed methods for analyzing walls and predicting wall response as well as a newly proposed method for predicting wall stiffness as a function of maximum story drift are presented in Chapter 2. Chapter 3 introduces the shake table test programs and data that were used to evaluate the analysis methods. Chapter 4 discusses numerical modeling of the shake table tests. Chapter 5 provides results of error analyses comparing simulated and measured response quantities for the shake table tests and evaluated the different analysis methods on the basis of this. A summary of the research effort, recommendations for practice, conclusions and recommendations for future research are presented in Chapter 6.

Chapter 2: Current Methods of Stiffness, Period and Damping Prediction

Linear elastic, response-spectrum analysis is the most commonly used method for determining seismic demands for design of lateral load resisting systems. Accomplishing this type of analysis to support design of a concrete wall requires the engineer to choose appropriate stiffness modification factors for the wall elements to account for concrete cracking and damage that occurs under service and design level loading as well as to choose appropriate modal damping values to represent energy dissipation associated with damage to nonstructural and structural elements. Accomplishing this type of analysis may require the engineer also to estimate the fundamental period of the structure to provide initial estimates of seismic demands.

Numerous recommendations for defining the effective stiffness, modal damping and fundamental period of concrete walls and walled buildings are provided in the literature in research papers and reports, code documents, and documents of standard practice. The current study seeks to evaluate previous recommendations as well as a newly proposed method for defining the effective stiffness of wall elements. The study then seeks to recommend preferred methods. The following sections present the previously and newly proposed methods for defining the effective stiffness of wall elements, appropriate modal damping values and the fundamental and effective period of walled buildings.

2.1 Review of Wall Stiffness Recommendations

The most commonly used methods for determining the effective stiffness of wall elements for elastic analysis under seismic loading are summarized in Table 2-1 and Table 2-2. In some cases, original notation has been changed slightly to provide greater continuity between different methods. These methods are discussed in greater detail in the following subsections.

Table 2-1: Summary of Wall Stiffness Recommendations

Source	**Description**	**Equation Number**
FEMA 356 – Uncracked Walls	Flexural Rigidity: $\left(E_c I_{eff}\right)_{flexure} = 0.8 E_c I_g$ Shear: $\left(E_c I_{eff}\right)_{shear} = 0.4 E_c I_g$ Axial: $\left(E_c I_{eff}\right)_{axial} = 1.0 E_c I_g$	(2-1) (2-2) (2-3)
FEMA 356 – Cracked Walls	Flexural Rigidity: $\left(E_c I_{eff}\right)_{flexure} = 0.5 E_c I_g$ Shear: $\left(E_c I_{eff}\right)_{shear} = 0.4 E_c I_g$ Axial: $\left(E_c I_{eff}\right)_{axial} = 1.0 E_c I_g$	(2-4) (2-5) (2-6)
ACI 318, 2002	$E_c I_{eff} = \left(\frac{M_{cr}}{M_a}\right)^3 * E_c I_g + \left[1 - \left(\frac{M_{cr}}{M_a}\right)^3\right] * E_c I_{cr}$	(2-7)
ACI 318, 2002	Uncracked: $E_c I_{eff} = 0.7 E_c I_g$ Cracked: $E_c I_{eff} = 0.35 E_c I_g$	(2-8) (2-9)
FIB 25, 2003	$E_c I_{eff} = \frac{E_c I_{cr}}{\mu_\Delta}$	(2-10)
FIB 27, 2003	$E_c I_{eff} = 0.3 E_c I_g$	(2-11)

Table 2-2: Continued from Table 2-1 – Summary of Wall Stiffness Recommendations

Paulay & Priestley, 1990	English Standard Units: $E_c I_{eff} = \left(\frac{14.5}{f_y} + \frac{P_u}{f_c^{'} * A_g} \right) * E_c I_g$ Metric Units: $E_c I_{eff} = \left(\frac{100}{f_y} + \frac{P_u}{f_c^{'} * A_g} \right) * E_c I_g$	(2-12) (2-13)
Adebar, et al., 2007	Upper-bound Effective Stiffness: $E_c I_{eff} = \left(0.6 + \frac{P_u}{f_c^{'} * A_g} \right) * E_c I_g \le E_c I_g$ Lower-bound Effective Stiffness: $E_c I_{eff} = \left(0.2 + 2.5 * \frac{P_u}{f_c^{'} * A_g} \right) * E_c I_g \le 0.7 * E_c I_g$	(2-15) (2-16)
Lestuzzi, 2002	Ranges from $E_c I_{eff} = 0.3 E_c I_g$ to $E_c I_{eff} = 0.1 E_c I_g$	
Brown, 2008	$E_c I_{eff} = 0.3 * \exp\left(-1.2 \left(\frac{\Delta_{roof}}{H} - 0.3 \right) \right) * E_c I_g \le 0.3 E_c I_g$	(2-18)

In Table 2-1 and Table 2-2, variables are defined as follows:

E_c = the elastic modulus of concrete,

I_{eff} = the effective moment of inertia of the wall section,

I_g = the gross moment of inertia of the wall section,

M_{cr} = the wall cracking moment,

I_{cr} = the cracked moment of inertia of the wall section,

M_a = the maximum moment in the stage where deflection is measured,

μ_Δ = the displacement ductility,

P_u = the axial load (compression is positive) acting on the wall during an earthquake (kips for ESU, MN for metric),

f_y = the yield strength of the steel (ksi for ESU, MPa for metric)

2.1.1 FEMA 356

FEMA 356, *Prestandard and Commentary for the Seismic Rehabilitation of Buildings* (ASCE, 2000) provides recommendations for the effective flexural, shear and axial stiffness of uncracked and cracked walls. These stiffness modification factors represent recommendations for structures designed by linear procedures. These values correspond to "the secant value to the yield point" of the shear wall in question (ASCE, 2000, 6.4.1.2). These recommendations are:

Uncracked walls (on inspection):

Flexural Rigidity: $\left(E_c I_{eff}\right)_{flexure} = 0.8 E_c I_g$ (2-1)

Shear: $\left(E_c I_{eff}\right)_{shear} = 0.4 E_c I_g$ (2-2)

Axial: $\left(E_c I_{eff}\right)_{axial} = 1.0 E_c I_g$ (2-3)

Cracked walls:

Flexural Rigidity: $\left(E_c I_{eff}\right)_{flexure} = 0.5 E_c I_g$ (2-4)

Shear: $\left(E_c I_{eff}\right)_{shear} = 0.4 E_c I_g$ (2-5)

Axial: $\left(E_c I_{eff}\right)_{axial} = 1.0 E_c I_g$ (2-6)

where all variables are as defined in Table 2-1 and Table 2-2.

2.1.2 ACI 318 Effective Stiffness Equation

ACI states that "any set of reasonable assumptions shall be permitted for computing relative flexural and torsional stiffness of columns, walls, floors and roof systems" (ACI 318, 2002, 8.6.1), and requires that these assumptions be used consistently through the analysis. Within the document it then provides two such possible assumptions, the first for the control of deflections (this section) and the second using magnified moments procedure (discussed in 2.1.3 below).

For use in determining deflections "unless stiffness values are obtained by a more comprehensive analysis" (ACI 318, 2002, 9.5.2.3) the 2002 version of the ACI Code recommends that the effective flexural stiffness of reinforced concrete members be defined as follows:

$$\mathrm{E_c} I_{eff} = \left(\frac{M_{cr}}{M_a}\right)^3 \mathrm{E_c} I_g + \left[1 - \left(\frac{M_{cr}}{M_a}\right)^3\right] \mathrm{E_c} I_{cr} \tag{2-7}$$

where all variables are as defined in Table 2-1 and Table 2-2.

2.1.3 ACI 318: Stiffness Modification Factors for Walls Designed by Magnified Moments Design Procedure

As mentioned in 2.1.2, ACI allows for any reasonable assumptions regarding concrete structural component stiffness. Section 10.11 "describes an approximate design procedure that uses the moment magnifier concept to account for slenderness effects" (ACI 318, 2002, R10.11). The factored axial forces and moments as well as relative story displacements shall be computed using a first-order frame analysis. The ACI 318 code allows for more complicated calculations of section properties however it also allows for the following to be assumed for walls:

Uncracked: $E_c I_{eff} = 0.7 E_c I_g$ (2-8)

Cracked: $E_c I_{eff} = 0.35 E_c I_g$ (2-9)

where all variables are as defined in Table 2-1 and Table 2-2.

The commentary goes on to say: “If the factored moments and shears from an analysis on the moment of inertia of a wall taken equal to $0.70I_g$ indicate that the wall will crack in flexure, based on the modulus of rupture, the analysis should be repeated with $E_cI_{eff} = 0.35E_cI_g$ in those stories where cracking is predicted at factored loads” (ACI 318, 2002, R10.11.1).

The values prescribed by ACI in this section were derived from “the results of frame tests and analyses and include an allowance for the variability of the computed deflections” (ACI 318, 2002, R10.11.1)

The recommended approach for predicting wall demands and deformations using this approach is to start with the uncracked stiffness to compute the loads. If the cracking load of the wall has been exceeded the system should be reanalyzed using the cracked stiffness in stories where cracking is predicted.

2.1.4 FIB 25 Ductility Based Effective Stiffness

The Federation Internationale du Beton (FIB) bulletin number 25, *Displacement-Based Seismic Design of Reinforced Concrete Buildings* (2003) outlines a secant stiffness approach first developed by Gulkan and Sozen (1974) on the basis of shake table tests of reinforced concrete single degree of freedom (SDOF) systems. Gulkan and Sozen found that an elastic SDOF behaving inelastically would exhibit a reduced stiffness and an increased level of damping. Gulkan and Sozen proposed that the effective stiffness was inversely proportional to the displacement ductility demand μ_Δ:

$$E_c I_{eff} = \frac{E_c I_{cr}}{\mu_\Delta} \tag{2-10}$$

where all variables are as defined in Table 2-1 and Table 2-2.

2.1.5 FIB 27 Effective Stiffness Recommendation

The FIB 27, *Seismic Design of Precast Concrete Building Structures* (2003) provides recommendations for equivalent monolithic precast systems. The key characteristic of equivalent monolithic precast systems is that the location and behavior of plastic hinges is “comparable to monolithic cast-in-place” concrete systems (FIB 27, 2003 4.4.4). Thus, these systems “by definition behave like cast-in-place reinforced concrete systems” (FIB 27, 2003 4.6.6). For equivalent monolithic precast walls, FIB 27 recommends the following effective stiffness seen in Eq. 2-11:

$$\mathrm{E_c} I_{eff} = 0.3\mathrm{E_c} I_g \tag{2-11}$$

variables are as defined previously in Table 2-1 and Table 2-2.

The commentary points out that effective stiffness in reality depends upon numerous factors, including but not limited to, axial force, member strength and reinforcement ratio. As these factors are likely not all known at the time of design, some iteration may be required. The recommended value is representative of "current trends in design philosophy" (FIB 27, 2003 4.6.6).

2.1.6 Paulay and Priestley Effective Stiffness Equation

The title of the document referenced by Paulay and Priestley suggests that the study was specifically looking at masonry cantilever wall buildings; however it is assumed based on the way the information was presented in *Seismic Design of Reinforced Concrete and Masonry Buildings* that this relationship was found to be appropriate for concrete walls as well. (Paulay and Priestley, 1990)

Paulay and Priestley outline analysis procedures for structures with shear walls as their primary lateral force resisting system. They provide a means to estimate the effective member stiffness in order to estimate the fundamental period of the structure, story displacements, and the distribution of lateral forces. They found the stiffness of cantilever walls subjected to flexural deformation is related to the equivalent moment of inertia (I_{eff}) at the first yield of the extreme fiber.

The function is described in United States Customary Units in Eq. 2-12 as well as metric units in Eq. 2-13.

$$E_c I_{eff} = \left(\frac{14.5}{f_y} + \frac{P_u}{f_c^{'} * A_g} \right) * E_c I_g \tag{2-12}$$

$$E_c I_{eff} = \left(\frac{100}{f_y} + \frac{P_u}{f_c^{'} * A_g} \right) * E_c I_g \tag{2-13}$$

all variables are as defined in Table 2-1 and Table 2-2.

2.1.7 Adebar Effective Stiffness Equation

Adebar et al. (2007) provide recommendations for defining the effective stiffness of slender walls. These recommendations were developed using a number of simplifying assumptions regarding the rigidity, geometric properties, moment distribution and lateral force distribution up the height of the wall. Adebar et al. concluded that the most important parameter is the axial compression applied at the wall base.

The relationships were validated by a single large-scale test of a bar-bell cantilever wall with an aspect ratio (height divided by length) of 7 subjected to pseudo-static cyclic shear loading as well as constant axial load at the top of the wall specimen. On the basis of these experimental data, Adebar et al recommend the following relationship for prediction of effective stiffness up to first yield:

$$E_c I_{eff} = E_c I_{cr} + \left[3 * \left(\frac{M_l}{M_n} \right)^{a} - 2 * \left(\frac{M_l}{M_n} \right)^{1.6a} \right] \left(E_c I_g - E_c I_{cr} \right) \le E_c I_g \tag{2-14}$$

where:

$a = 1.1(I_{ce}/I_g)-0.4$

Adebar et al. propose that the effective stiffness defined by Eq. 2-14 may be estimated as falling between the following upper and lower bound functions.

Upper bound: $$E_c I_{eff} = \left(0.6 + \frac{P_u}{f_c' * A_g}\right) * E_c I_g \le E_c I_g \tag{2-15}$$

Lower bound: $$E_c I_{eff} = \left(0.2 + 2.5 * \frac{P_u}{f_c' * A_g}\right) * E_c I_g \le 0.7 * E_c I_g \tag{2-16}$$

where all variables are as defined in Table 2-1 and Table 2-2.

2.1.8 Lestuzzi Effective Stiffness Recommendation

Lestuzzi (2002) provides observations of the effective stiffness seen in shake table testing of six 1/3-scale planar wall specimens. Testing was done using the shake table at the Institute of Structural Engineering of the Swiss Federal Institute of Technology (ETH) in Zurich Switzerland. From these tests, Lestuzzi found that the measured fundamental frequency of the wall specimens correspond, initially, to an effective stiffness equal to approximately 30% of that calculated using gross section dimensions. The effective stiffness dropped to less than 10% after a few tests using relatively weak earthquake ground motions and remained constant until failure.

Although Lestuzzi specifies effective stiffness values ranging from 30% to 10% of the gross-section stiffness, no guidance is provided linking the reduction in effective stiffness to wall demands.

2.1.9 Brown Drift Based Stiffness

Brown (2008) investigated the effects of numerous design aspects on the effective stiffness for walls using data from pseudo-static, cyclic and monotonic tests of planar and barbell walls. From this study, Brown developed a relationship between drift and effective flexural stiffness. Eq. 2-18 shows the proposed relationship and Figure 2-1 shows the relationship with the experimental data, where K_{eff} is the effective stiffness modifier defined as in Eq. 2-17:

$$E_c I_{eff} = (K_{eff}) E_c I_g \qquad (2\text{-}17)$$

The study also investigated the effect of the aspect ratio (ranging from 1.0 to 6.6), axial load ratio (ranging from 0% to 35%) and reinforcement ratios (ranging from 0.45% to 4.1%) and found no significant correlation.

$$E_c I_{eff} = 0.3 * \exp\left(-1.2\left(\frac{\Delta_{roof}}{H} - 0.3\right)\right) * E_c I_g \leq 0.3 E_c I_g \qquad (2\text{-}18)$$

where all parameters are as defined in Table 2-1 and Table 2-2.

Due to the significant scatter of the data at low drifts, the relationship is capped at the effective stiffness of $0.3E_cI_g$ which was the average effective stiffness for under 0.3% roof drift.

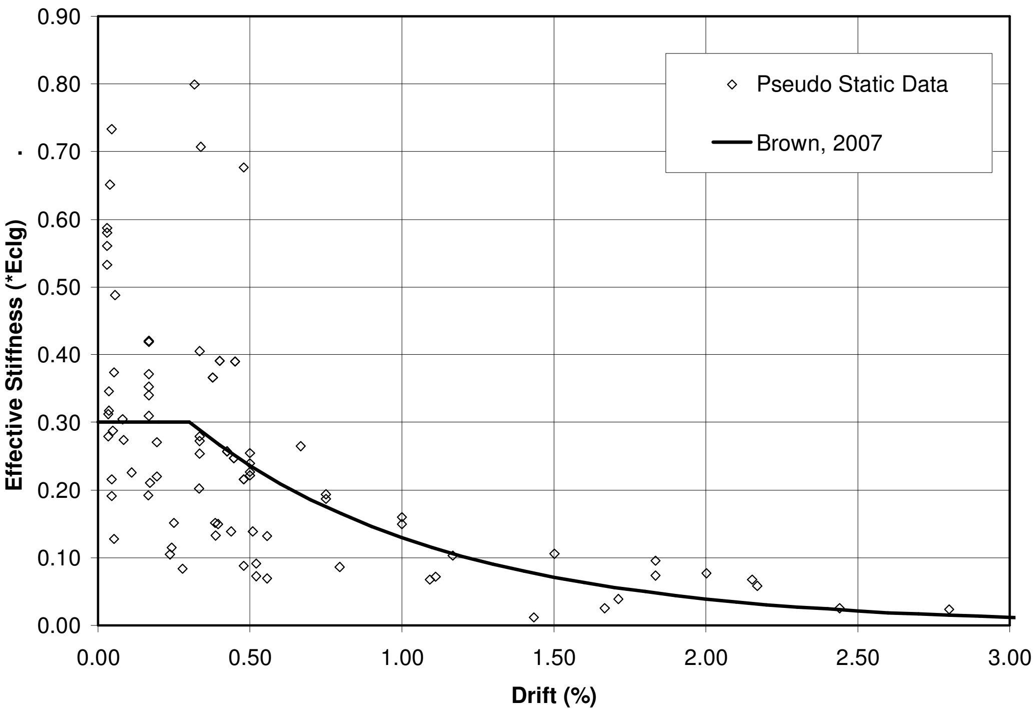

Figure 2-1: Effective Stiffness versus Drift for Planar and Barbell Rectangular Walls (Brown, 2008)

2.1.10 Comparison of effective stiffness models

The effective stiffness models introduced here attempt to model the behavior of wall structures by providing a uniform effective stiffness value regardless of structural demands as well as methods based on axial load ratio. Figure 2-2 shows the stiffness derived from Adebar et al. (2007) and Paulay and Priestley (1990) with respect to axial load ratio along with the uniform stiffness methods that provide recommendations independent of axial load ratio. These values of stiffness are compared to the uniform stiffness to match the period of the first test of four shake table test programs (to be introduced in Chapter 3). The results appear to indicate that for the first test, the effective stiffness is over predicted by the FEMA and ACI uncracked ($0.8E_cI_g$ and $0.75E_cI_g$ respectively) stiffness, the FEMA cracked ($0.5E_cI_g$) stiffness and the Adebar upper bound axial load ratio related method. The single value stiffness methods of ACI cracked ($0.35E_cI_g$), FIB 27 ($0.3E_cI_g$) as well as the Adebar lower bound and Paulay and Priestley methods all find themselves with stiffness predictions within the range of the low excitation experimental data.

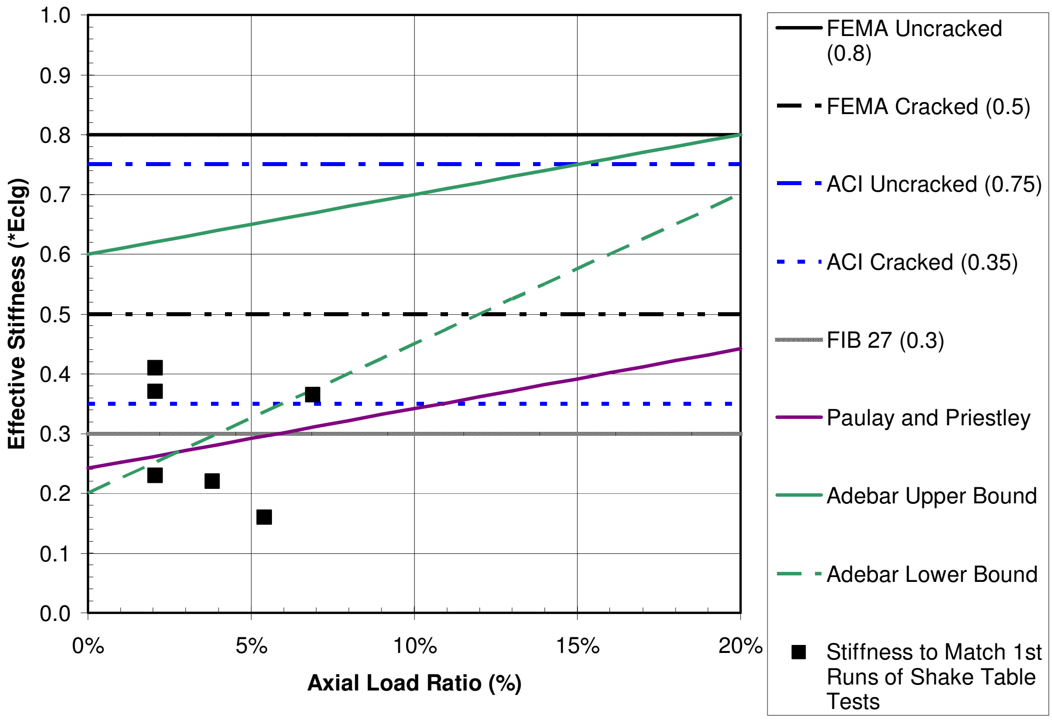

Figure 2-2: Comparison of Axial Load Ratio Based Methods with Uniform Stiffness Methods and the 1st Run of the Shake Table Test Programs

Figure 2-3 shows the stiffness derived from the Brown drift based stiffness function (2008) as well as the uniform stiffness methods that provide recommendations regardless of roof drift demand. These values of stiffness are compared to the stiffness of pseudostatic tests as well as shake table tests (to be introduced in Chapter 3).

In very low drift ranges, methods such as FIB 27 ($0.3E_cI_g$) and ACI cracked ($0.35E_cI_g$) appear near the mean of the pseudostatic data, however beyond 0.5% drift these methods appear to over predict the stiffness. FEMA uncracked and cracked as well as ACI uncracked stiffness values tend to over predict the pseudostatic data with the exception of a small number of data points in the very low drift range. The Brown method was derived using the pseudostatic data and as such matches this data, along with the shake table data, very well for all drift ranges.

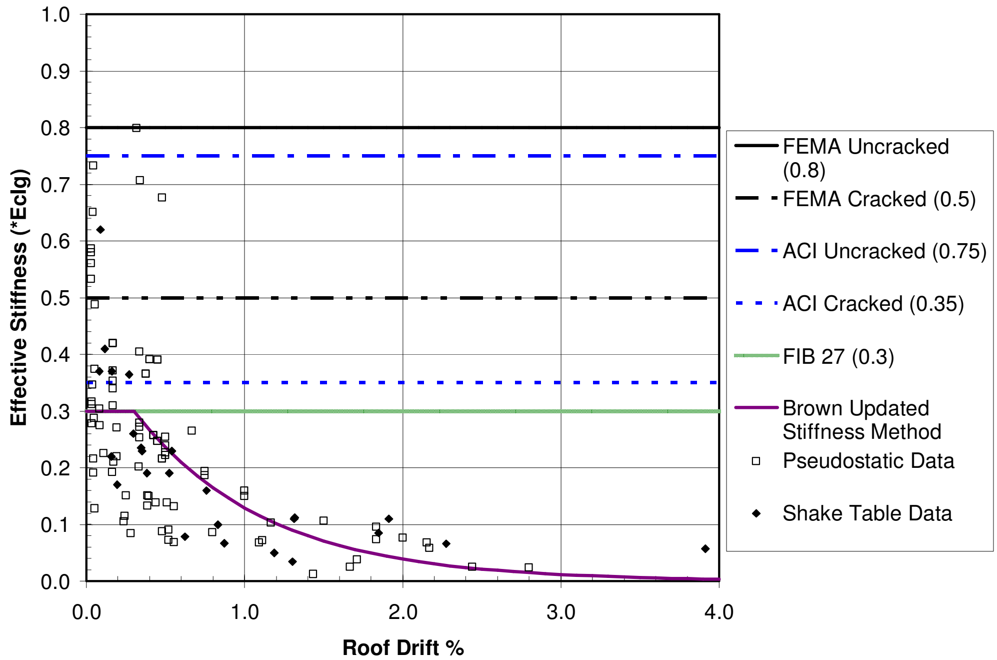

Figure 2-3: Comparison of Drift Based Stiffness Methods with Uniform Stiffness Methods and Experimental Data

2.2 Review of Period Approximation Recommendations

A review of the literature produced several methods for estimating the fundamental period of vibration of wall buildings. Some methods provide estimates of the initial fundamental period, while others provide estimates of the effective fundamental period as a function of the displacement ductility demand of the wall. These methods are summarized in Table 2-3 and discussed in detail in the following subsections. In some cases, the original notation used by the authors has been changed to facilitate comparison of different methods.

Table 2-3: Summary of Period Approximation Recommendations

Source	**Description**	**Equation Number**
FEMA 440	Relationship to determine effective period with respect to displacement ductility demand For $1.0 < \mu_\Delta < 4.0$: $\frac{T_{eff}}{T_0} = \left[G(\mu_\Delta - 1)^2 + H(\mu_\Delta - 1)^3 + 1\right]$	(2-19)
	For $4.0 < \mu_\Delta < 6.5$: $\frac{T_{eff}}{T_0} = \left[I + J(\mu_\Delta - 1) + 1\right]$	(2-20)
	For $\mu_\Delta > 6.5$: $\frac{T_{eff}}{T_0} = \left\{K\left[\sqrt{\frac{(\mu_\Delta - 1)}{1 + L(\mu_\Delta - 2)}} - 1\right] + 1\right\}$	(2-21)
FEMA 450	Approximate Fundamental Period $T_0 = C_r h_n^x$	(2-22)
Newmark and Hall, 1982	Estimate of Fundamental Period for Concrete Shear-Wall Buildings $T_0 = \frac{0.05H}{\sqrt{L}}$	(2-26)

In Table 2-3, variables are defined as follows:

T_{eff} = the effective period

T_0 = the fundamental period of vibration

G, H, I, J, K and L = coefficients defined by Table 2-4.

μ_Δ = the displacement ductility demand,

h_n = height in feet or meters above the base to the highest level of the structure,

C_r = period parameter based on structure type. C_r = 0.02 (metric 0.0488) for shear walls,

x = period parameter based on structure type. x = 0.75 for shear walls,

H = height of building in feet, and

L = the plan dimension in feet in the direction of analysis

2.2.1 FEMA 440: Ductility Based Effective Period

FEMA 440 (ATC, 2005) provides recommendations for approximating the effective fundamental period of a generic structure as a function of the ductility demand on the structure as well as characteristics of the expected response history for the structure. This method is described as equivalent linearization and it attempts to model the peak displacement of a nonlinear system by using a linear system with an effective period and effective damping. The basic relationship defining effective period is provided in Eq. 2-19, 2-20 and 2-21. Table 2-4 defines coefficients for use with these equations that provide a best fit for idealized, single-degree-of-freedom oscillators with different response histories.

For $1.0 < \mu_\Delta < 4.0$:

$$\frac{T_{eff}}{T_0} = \left[G(\mu_\Delta - 1)^2 + H(\mu_\Delta - 1)^3 + 1\right] \tag{2-19}$$

For $4.0 < \mu_\Delta < 6.5$:

$$\frac{T_{eff}}{T_0} = \left[I + J(\mu_\Delta - 1) + 1\right] \tag{2-20}$$

For $\mu_\Delta > 6.5$:

$$\frac{T_{eff}}{T_0} = \left\{K\left[\sqrt{\frac{(\mu_\Delta - 1)}{1 + L(\mu_\Delta - 2)}} - 1\right] + 1\right\} \tag{2-21}$$

where coefficients G, H, I, J, K and L are defined in Table 2-4 and all other variables as are defined previously in Table 2-3. FEMA 440 (ATC, 2005) also provides a series of functions for estimating the effective fundamental period that are independent of the expected hysteretic response and post-elastic stiffness of the system. The coefficients are found at the bottom of Table 2-4.

Table 2-4: Coefficients for use in Equations for Effective Period (ATC, 2005)

Model	α(%)	G	H	I	J	K	L
Bilinear hysteretic	0	0.11	–0.017	0.27	0.090	0.57	0.00
Bilinear hysteretic	2	0.10	–0.014	0.17	0.12	0.67	0.02
Bilinear hysteretic	5	0.11	–0.018	0.09	0.14	0.77	0.05
Bilinear hysteretic	10	0.13	–0.022	0.27	0.10	0.87	0.10
Bilinear hysteretic	20	0.10	–0.015	0.17	0.094	0.98	0.20
Stiffness degrading	0	0.17	–0.032	0.10	0.19	0.85	0.00
Stiffness degrading	2	0.18	–0.034	0.22	0.16	0.88	0.02
Stiffness degrading	5	0.18	–0.037	0.15	0.16	0.92	0.05
Stiffness degrading	10	0.17	–0.034	0.26	0.12	0.97	0.10
Stiffness degrading	20	0.13	–0.027	0.11	0.11	1.0	0.20
Strength degrading	–3a	0.18	–0.033	0.17	0.18	0.76	–0.03
Strength degrading	–5a	0.20	–0.038	0.25	0.17	0.71	–0.05
Model Independent		0.20	-0.038	0.28	0.13	0.89	0.05

where:

α = the post elastic stiffness ratio

The model independent function, as well as an example of a stiffness degrading model (with post elastic stiffness ratio of 2%) and a bilinear hysteretic model can be seen in Figure 2-4.

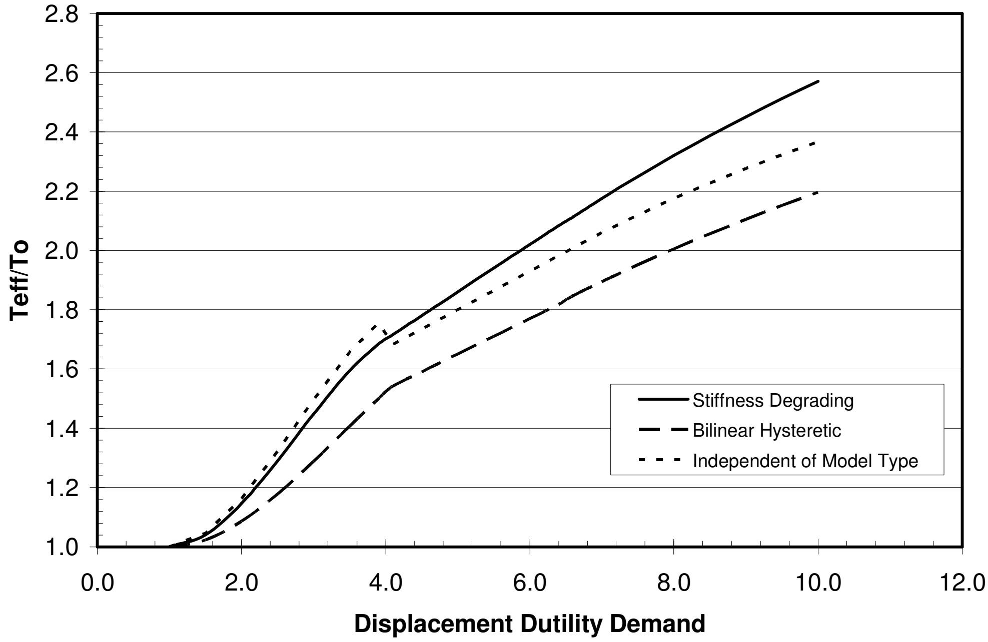

Figure 2-4: Effective Period with Respect to Ductility for Stiffness Degrading Post-elastic Stiffness Ratio Model and Bilinear Hysteretic Models, (α=2%) and Model Independent of α

2.2.2 FEMA 450 – NEHRP Approximate Fundamental Period

The FEMA 450 - *NEHRP Recommended Provisions for Seismic Regulations for New Buildings and Other Structures* (BSSC, 2003) provides a simple equation to approximate the fundamental period of structures of different types to be used in an equivalent lateral force analysis:

$$T_0 = C_r h_n^x \tag{2-22}$$

where x = 0.75 for shear walls and all other variables are as previously defined in Table 2-3. This relationship can be seen in Figure 2-5.

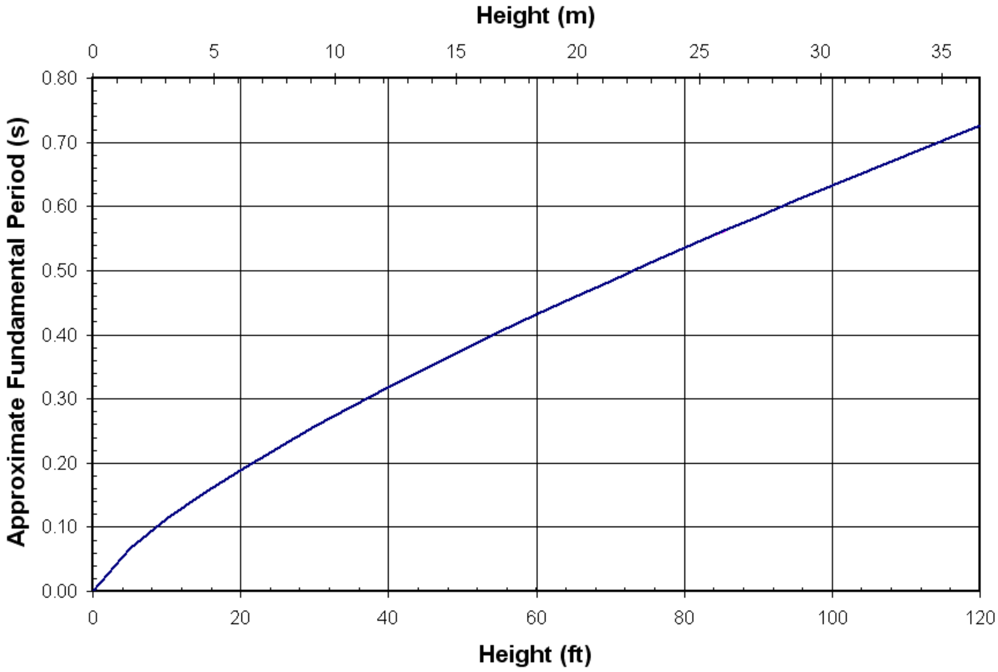

Figure 2-5: Approximate Fundamental Period with Respect to Building Height for Shear Wall Structures

Alternatively, "the approximate fundamental period for masonry or concrete shear wall structures is permitted to be determined from the following equation" (BSSC, 2003, 5.2.2.1)

$$T_a = \frac{0.0019}{\sqrt{C_w}} h_n \tag{2-23}$$

The metric equivalent is:

$$T_a = \frac{0.0062}{\sqrt{C_w}} h_n \tag{2-24}$$

where:

$$C_w = \frac{100}{A_B}\sum_{i=1}^{n}\left(\frac{h_n}{h_i}\right)^2 \frac{A_i}{\left[1+0.83\left(\frac{h_i}{L_i}\right)^2\right]} \qquad (2\text{-}25)$$

where:

A_B = base area of the structure,

A_i = cross sectional area of shear wall i,

L_i = length of shear wall i,

h_n = height above the base to the highest level of the structure,

h_i = height of shear wall i, and

n = number of shear walls in the building effective in resisting lateral forces in the direction under consideration

These relationships are the result of analyses of data from the U.S. Geological Survey and the California Division of Mines and Geology collected from instrumented buildings in zones of high seismic activity.

2.2.3 Newmark and Hall Approximate Period of Shear Wall Structures

Newmark and Hall (1982) provide a simple equation for estimating the initial period of a shear wall building for use in preliminary design:

$$T_0 = \frac{0.05H}{\sqrt{L}} \qquad (2\text{-}26)$$

where all variables are as defined previously in Table 2-3.

2.2.4 Comparison of Period Prediction Methods

The aforementioned methods provide recommendations for prediction of the effective and fundamental periods. FEMA 440 (ATC, 2005) uses a ductility demand based method to determine the effective period requiring an estimate of the hysteretic behavior as well as the post-elastic response (Eq. 2-19, 2-20, and 2-21). FEMA 450 (Eq. 2-22) (BSSC, 2003) as well as Newmark and Hall (Eq. 2-26) (1982) provide means of estimating the fundamental period based on initial geometric assumptions. This fundamental difference between the method outlined in FEMA 440 and those outlined in FEMA 450 as well as Newmark and Hall makes comparison difficult.

The two geometric methods are compared below in Figure 2-6. As the function from FEMA 450 is independent of wall length, only one is displayed. Several examples of different wall lengths are used with the function described by Newmark and Hall. For reference these are compared with the fundamental period of a 63’ tall 10’ long planar wall specimen tested at the University of California, San Diego. This specimen is discussed in greater detail in Chapter 3.

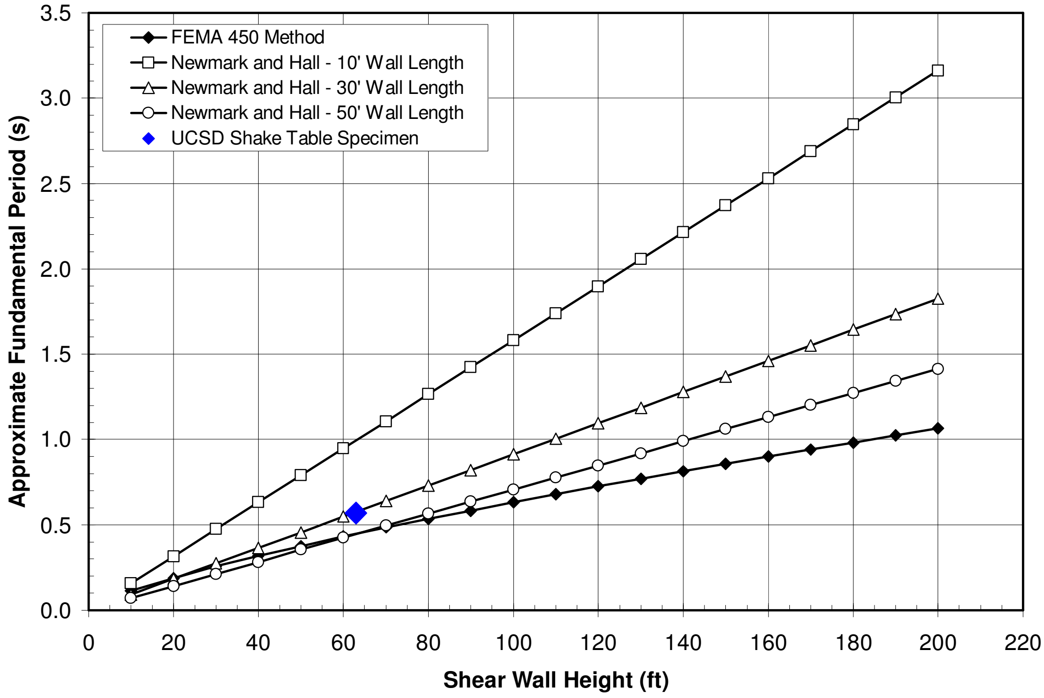

Figure 2-6: Comparison of Fundamental Period Prediction Methods for Different Wall Heights and Lengths (UCSD 63' tall 10' Long Wall Specimen Used for Comparison)

For this particular specimen, the Newmark and Hall function provides a very poor prediction of the period for the proper 10' wall length. By comparison, FEMA 450 provides a much better prediction.

2.3 Review of Modal Damping Recommendations

Typically, in a linear, elastic dynamic analysis, energy dissipation due to hysteretic response of structural elements as well as damage to non-structural elements is simulated through the introduction of viscous damping. Previous research has resulted in recommendations for appropriate equivalent viscous damping, defined typically as a fraction of the critical damping coefficient, for use. Some commonly used recommendations are listed in Table 2-5. In some cases the original notation used by the authors has been changed to facilitate comparison of the recommendations. These relationships are discussed in greater detail in the following subsections.

Table 2-5: Summary of Damping Recommendations

Source	**Description**	**Equation or Reference Number**
FEMA 440, 2005	Damping as it relates to ductility demand For $1.0<\mu_\Delta<4.0$: $\beta_{eff} = A(\mu_\Delta - 1)^2 + B(\mu_\Delta - 1)^3 + \beta_0$ For $4.0<\mu_\Delta<6.5$: $\beta_{eff} = C + D(\mu_\Delta - 1) + \beta_0$ For $\mu_\Delta>6.5$: $\beta_{eff} = E\left[\frac{F(\mu_\Delta - 1) - 1}{[F(\mu_\Delta - 1)]^2}\right]\left(\frac{T_{eff}}{T_0}\right) + \beta_0$	(2-27) (2-28) (2-29)
FIB 25, 2003	Damping as it relates to ductility demand $\beta_{eff} = 0.2\left(1 - \frac{1}{\sqrt{\mu_\Delta}}\right) + 0.02$	(2-30)
Newmark and Hall, 1982	Working stress, no more than about ½ yield point: Well-reinforced concrete (only slight cracking) $\beta_{eff} = 2 - 3\%$ Working stress, no more than about ½ yield point: Reinforced concrete with considerable cracking $\beta_{eff} = 5 - 7\%$ At or just below yield point $\beta_{eff} = 7 - 10\%$	Table 2-7

In Table 2-5 variables are defined as follows:

β_{eff} = the effective damping.

β_0 = initial elastic demand with damping,

μ_Δ = the displacement ductility demand,

A, B, C, D, E, and F are coefficients as defined by Table 2-6,

T_{eff} = the effective period

T_0 = the fundamental period

2.3.1 FEMA 440: Ductility-Based Modal Damping

FEMA 440 (ATC, 2005) provides recommendations also for effective viscous damping ratio as a function of the ductility demand on the structure. This method is described as equivalent linearization and it attempts to model the peak displacement of a nonlinear system by using a linear system with an effective period and effective damping:

For $1.0<\mu_\Delta<4.0$:

$$\beta_{eff} = A(\mu_\Delta - 1)^2 + B(\mu_\Delta - 1)^3 + \beta_0 \tag{2-27}$$

For $4.0<\mu_\Delta <6.5$:

$$\beta_{eff} = C + D(\mu_\Delta - 1) + \beta_0 \tag{2-28}$$

For $\mu_\Delta >6.5$:

$$\beta_{eff} = E\left[\frac{F(\mu_\Delta - 1) - 1}{[F(\mu_\Delta - 1)]^2}\right]\left(\frac{T_{eff}}{T_0}\right) + \beta_0 \tag{2-29}$$

where variables are as defined previously following Table 2-5. In the above function, b_0 is intended to account for damping due to nonstructural components while the remainder of the equation is intended to define equivalent viscous damping. The coefficients A, B, C, D, E and F are as defined in Table 2-6. FEMA also provides a series of functions that have been designed to be independent of hysteretic model type or alpha value. The coefficients corresponding to this are found in the last row of Table 2-6.

Table 2-6: Coefficients for use in Equations for Effective Damping (ATC, 2005)

Model	α (%)	A	B	C	D	*E*	*F*
Bilinear hysteretic	0	3.2	–0.66	11	0.12	19	0.73
Bilinear hysteretic	2	3.3	–0.64	9.4	1.1	19	0.42
Bilinear hysteretic	5	4.2	–0.83	10	1.6	22	0.40
Bilinear hysteretic	10	5.1	–1.1	12	1.6	24	0.36
Bilinear hysteretic	20	4.6	–0.99	12	1.1	25	0.37
Stiffness degrading	0	5.1	–1.1	12	1.4	20	0.62
Stiffness degrading	2	5.3	–1.2	11	1.6	20	0.51
Stiffness degrading	5	5.6	–1.3	10	1.8	20	0.38
Stiffness degrading	10	5.3	–1.2	9.2	1.9	21	0.37
Stiffness degrading	20	4.6	–1.0	9.6	1.3	23	0.34
Strength degrading	-3	5.3	–1.2	14	0.69	24	0.90
Strength degrading	-5	5.6	–1.3	14	0.61	22	0.90
Model Independent		4.9	-1.1	14	0.32	19	0.64

where:

α = the post elastic stiffness ratio

2.3.2 FIB 25: Ductility-Based Modal Damping

FIB 25 (2005) outlines a secant stiffness approach for damping as a function of ductility. This method is implemented by determining an appropriate effective damping for a target displacement ductility demand.

$$\beta_{eff} = 0.2\left(1 - \frac{1}{\sqrt{\mu_\Delta}}\right) + 0.02 \quad (2\text{-}30)$$

where variables are as defined previously following Table 2-5. This relationship was developed using data from shake-table tests of reinforced concrete systems and is intended to approximate the energy dissipation that occurs during the hysteretic response of reinforced concrete elements.

2.3.3 Newmark and Hall Damping Values

Newmark and Hall (1982) provide recommendations for damping ratios for structures responding in the pre-yield to incipient yield range. The values are included in Table 2-7 below. The higher values in the provided ranges are intended for ordinary structures while the lower values are intended for structures designed more conservatively. (Chopra, 2004).

Table 2-7: Recommended Damping Values (Newmark and Hall, 1982)

Stress Level	Type and Condition of Structure	Damping Ratio β_{eff} (%)
Working Stress, no more than about 1/2 yield point	Welded steel, prestressed concrete, well-reinforced concrete (only slight cracking)	2-3
	Reinforced concrete with considerable cracking	3-5
At or just below yield point	Reinforced concrete	7-10

2.3.4 Comparison of Damping Prediction Methods

These methods are included together below in Figure 2-7. For the Newmark and Hall (written as N&H in Figure 2-7) recommendations, the lower value in the provided range was used. The ductilities used for the Newmark and Hall terms are approximate. It was assumed that the damage state of slight cracking and significant cracking would be representative of a ductility between 0 and 0.5 while the ductilities for a system at incipient yield would be somewhere between 0.5 and 1.0.

For the FEMA plots, three different models were plotted. The first is a model using stiffness degrading parameters. The second is based on a bilinear hysteretic response. Both of these use an initial elastic damping demand (β_0) of 3% and a post elastic stiffness ratio (α) of 2%. The third FEMA plot is based off of a method that is independent of response model.

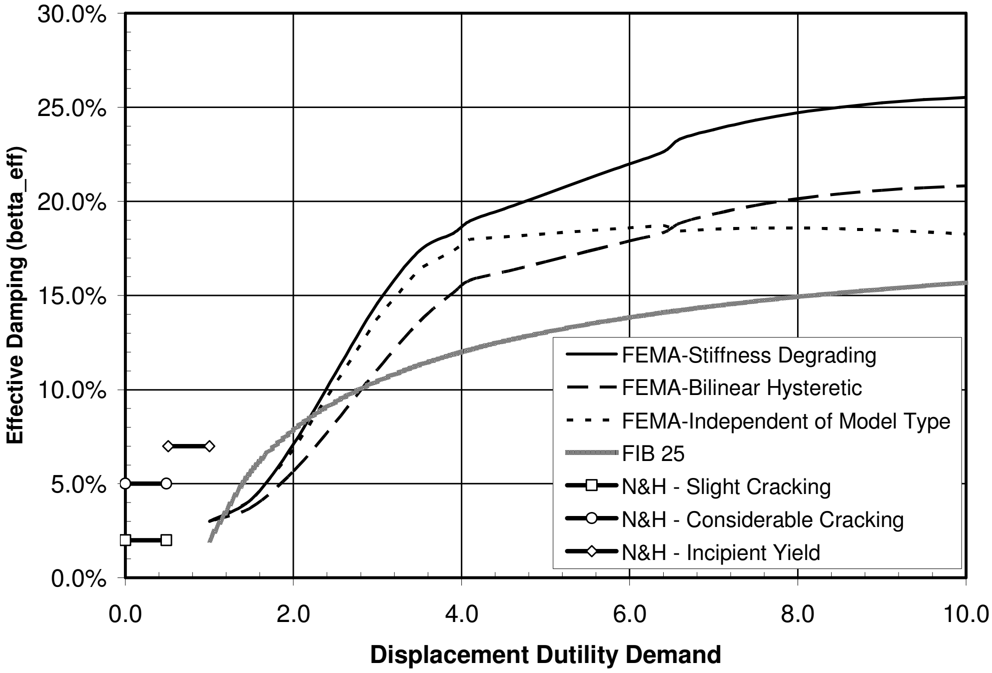

Figure 2-7: Different Recommendations for Effective Damping with Respect to Ductility

2.4 Proposed Iterative Methods for Wall Stiffness Prediction

As discussed, most methods do not take into account stiffness loss due to performance. Methods of this form can thus be described as in Figure 2-8. FEMA 440 provided a function to estimate the effective period as it relates to ductility. This method however can be cumbersome as there are numerous methods for approximating ductility that all yield significantly different results.

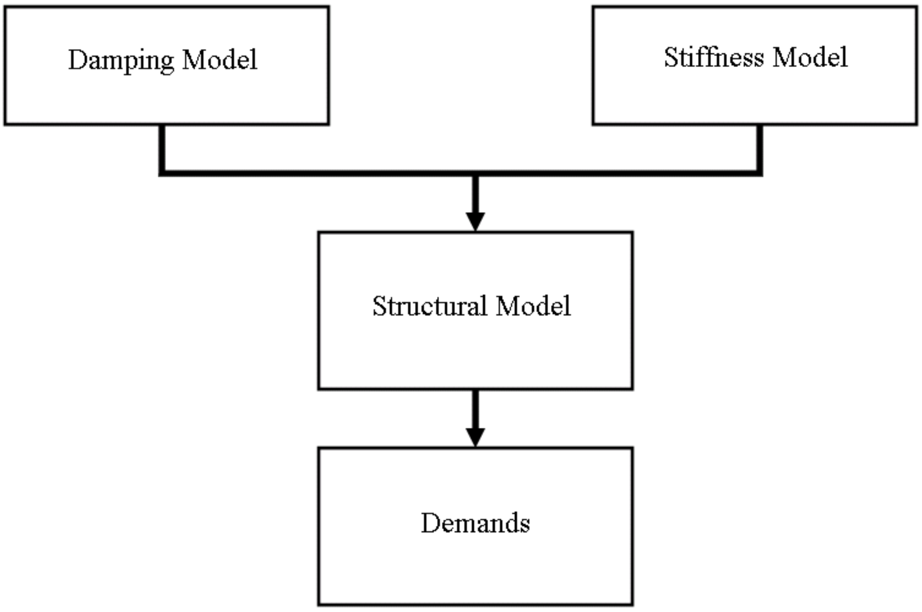

Figure 2-8: Common Existing Methodology

With this concept in mind, the goal of this study was to establish methods that would be able predict the reduction in stiffness with increased drift as was observed by Brown (2008) and use terms such as roof drift and effective stiffness that can be used and compared directly with most linear elastic analysis software on the market today. The methodology proposed follows the same basic framework outlined by the ductility based effective period and effective damping equations as seen in FEMA 440 (ATC, 2005). This methodology can be seen in Figure 2-9.

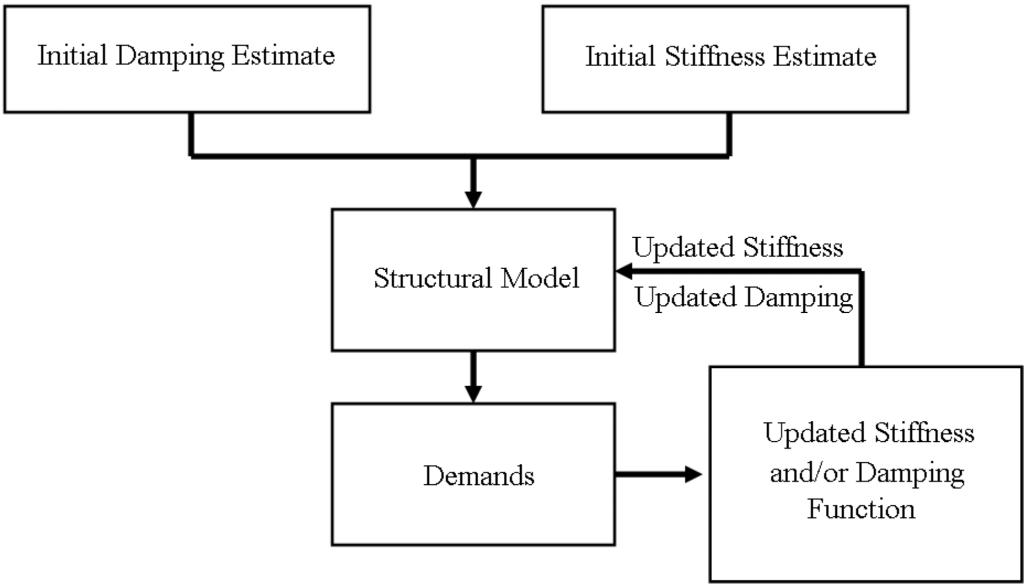

Figure 2-9: Updated Stiffness and/or Damping Methodology

Three updated stiffness methods are presented here. The first is an implementation of Brown's (2008) function to obtain a reduced uniform effective stiffness. The second is an implementation of Brown's (2008) function at each story to provide a variable stiffness. The third, referred to as the Doepker method, uses a new relationship between uniform effective stiffness and roof drift that was developed using Brown's data set plus data from shake table tests discussed in Chapter 3. In this new relationship, the initial effective stiffness is $0.80E_cI_g$, which may be compared with the initial effective stiffness of $0.30E_cI_g$ recommended by Brown.

2.4.1 Implementation of Brown 2008 Equation to Yield an Updated Uniform Stiffness

Brown's function (Eq. 2-18) is proposed to be implemented through a two step analysis method using linear elastic time history tools such as SAP and ETABS. The method uses an initial stiffness of $0.3E_cI_g$, to provide an initial estimate of the expected roof drift. Using this drift in Eq. 2-18 the updated stiffness is determined. In the event that the structure is expected to be subjected to multiple motions, subsequent analyses would use the resulting stiffness from the analysis that preceded it. In the context of lab experiments used in this study, the specimens underwent repeated ground motions. As the ground motions resulted in increased damage, and thus reduced stiffness, each simulation after the first measured ground motion started by using the end stiffness of the test preceding it. This methodology can be seen in Figure 2-10.

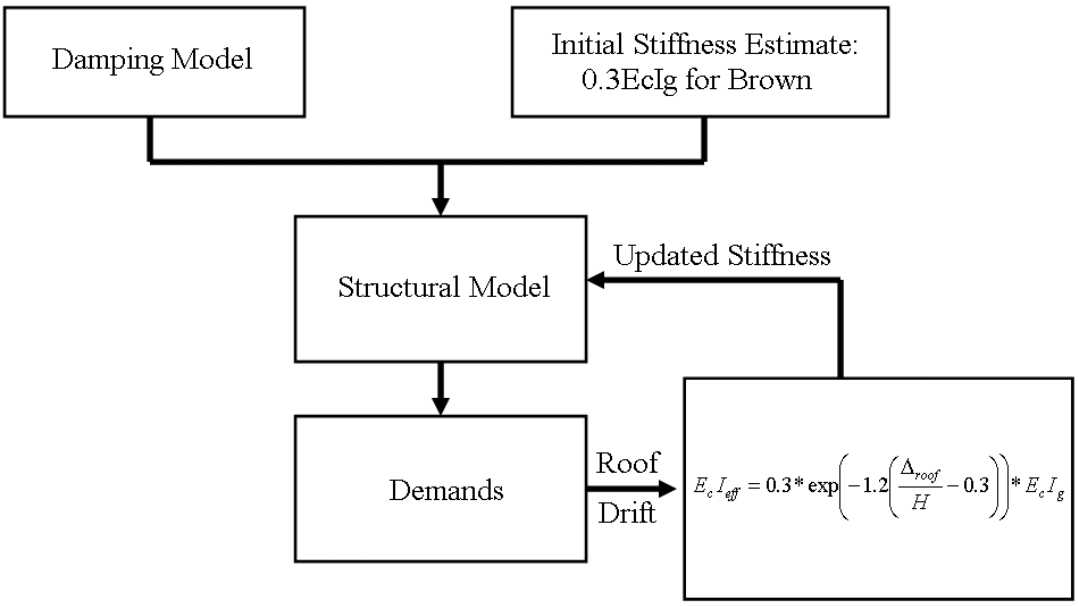

Figure 2-10: Methodology for Brown Updated Stiffness Method

The following methods take the initial framework described above and elaborate through a variety of means.

2.4.2 Implementation of Brown 2008 Equation to Yield an Updated Stiffness Varying with Height

To capture the variation in stiffness over the height of the wall that could be expected under earthquake loading, Brown's function was implemented also at the story level. This methodology is represented by the flow chart in Figure 2-11. Here, an initial analysis is done using a uniform flexural stiffness of $0.3E_cI_g$. Then, the computed story drifts, with rigid body rotation subtracted, are used as inputs for Brown's equation to determine new effective stiffness modifiers for each story. Finally, a second analysis is done using the revised effective stiffnesses.

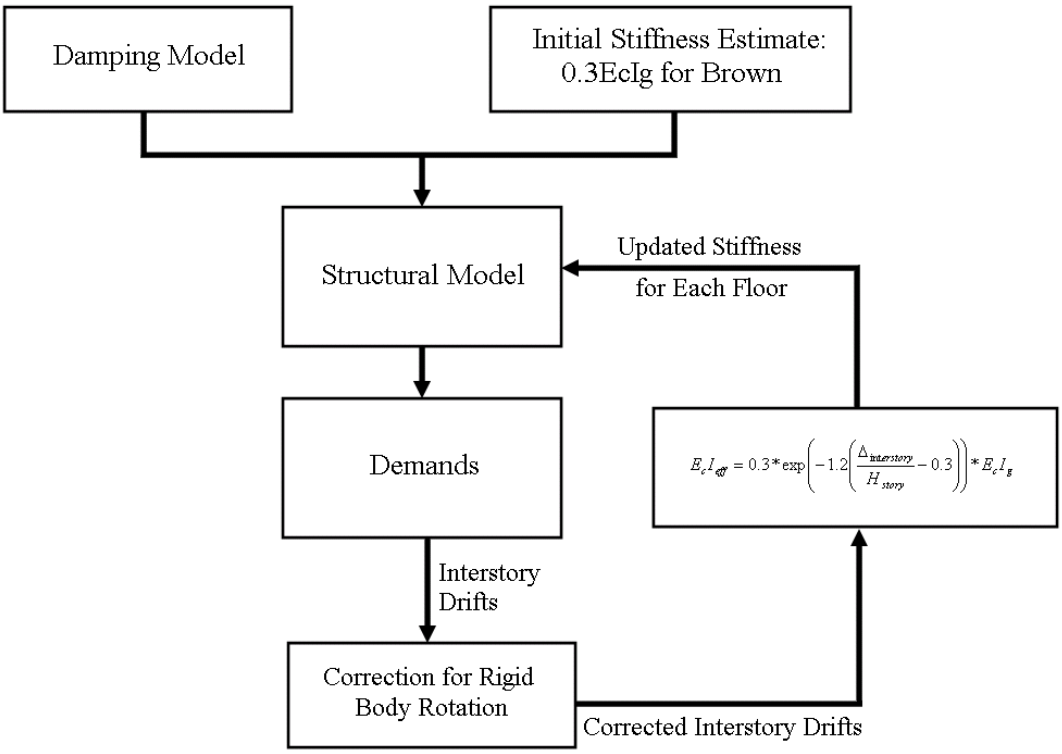

Figure 2-11: Methodology for Brown Updated Varying Stiffness Method

This method was initially evaluated using data from the UCSD test program and found to consistently provide results that were significantly worse than those resulting from application of the uniform stiffness methods. Thus, this method was not investigated further. A discussion of the application of this method, the approach used to subtract rigid body displacements to compute story drifts and the reasons for the poor performance of this method can be found in Appendix C.

2.4.3 Doepker Method for an Updated Uniform Stiffness

The data set used for development of Brown's equation saw a huge variation in stiffness, from approximately $0.8E_cI_g$ to less than $0.1E_cI_g$ for low drift ranges (between 0% and 0.5% roof drift, see Figure 2-12). With that in mind, a concern for Brown's function is that it has the potential to initially under predict the stiffness. This can result in significant error when iteration further reduces the stiffness. Further, Brown's stiffness drops to near $0.0E_cI_g$ for drift ranges of 3.0% drift. As such, a method was desired that would have the potential to capture the high stiffness, while seeing a rapid drop in stiffness for increased drift while never dropping below $0.05E_cI_g$. With this in mind the following function was determined to fit the above mentioned criteria:

$$E_cI_{eff} = \left[0.8 * \exp\left(0.05 * \frac{\Delta_{roof}}{H}\right) - 0.7 * \left(\frac{\Delta_{roof}}{H}\right)^{0.2}\right] * E_cI_g \tag{2-31}$$

Figure 2-12 shows effective flexural stiffness as estimated using Eq. 2-31 and Brown's equation (Eq. 2-18). The functions overlay data obtained from various pseudostatic tests as well as shake table tests to be further discussed in Chapter 3.

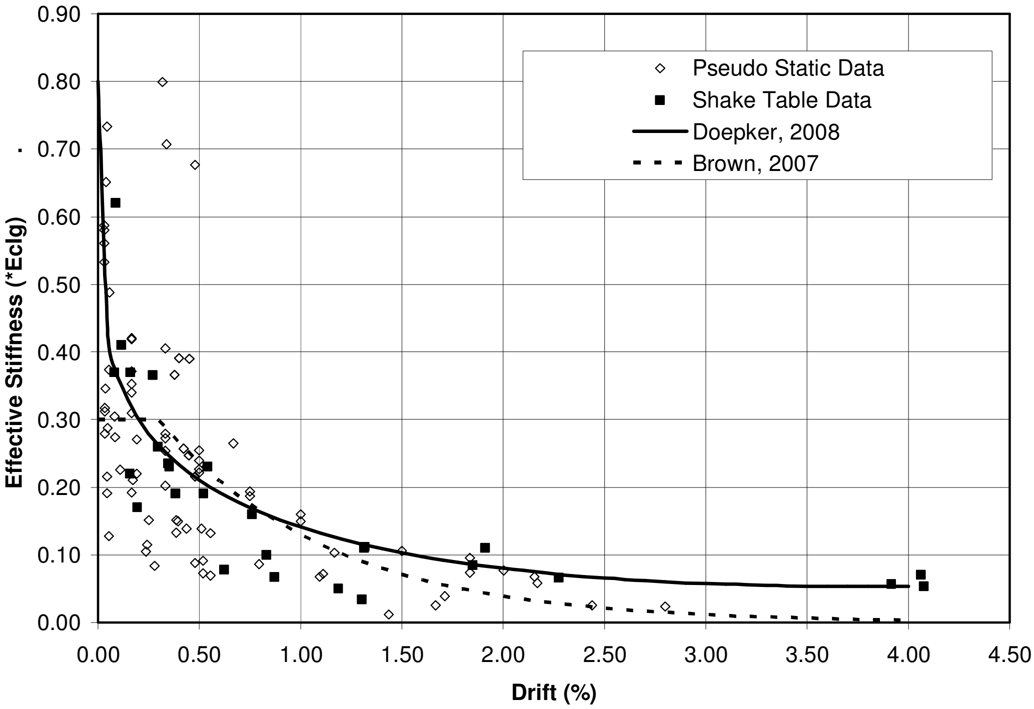

Figure 2-12: Comparison of Doepker Method with Brown Method

This function would be implemented in the same manner as Brown's uniform iterated stiffness. This methodology can be seen in Figure 2-13.

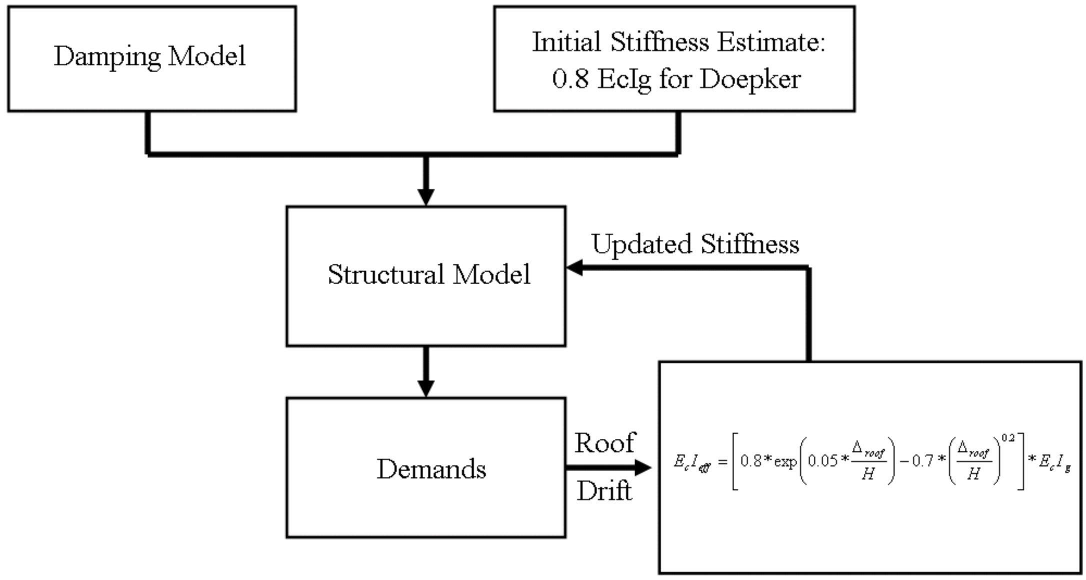

Figure 2-13: Methodology for Doepker Updated Stiffness Method

2.5 Summary of Methods

Several methods were reviewed for estimation of a shear wall structure's effective stiffness, fundamental and effective period and effective viscous damping ratio. The methods intend to capture the response through the variation of different parameters. Values prescribed in ACI (2002) and FEMA 356 (ASCE 2000) documents provide a single uniform effective stiffness, while methods developed by Paulay and Priestley (1990) as well as Adebar et al. (2007) provide stiffness recommendations related to the axial load ratio experienced in the wall. The Brown and Doepker methods by contrast provide recommendations for effective stiffness with respect to roof drift demands.

Period prediction models varied from those who attempted to predict the fundamental period such as FEMA 450 (BSSC, 2003) and Newmark and Hall (1982) while FEMA 440 (ATC, 2005) provides a model for the effective period as it relates to drift ductility demand.

Viscous damping ratios were recommended based on basic assumptions of expected damage, as in the case of Newmark and Hall (1982), as well as more complicated ductility demand based methods such as those prescribed by FEMA 440 (ATC, 2005) and FIB 25 (2003).

These methods are evaluated to varying degrees by modeling the tests described in Chapter 3. The results can be found in Chapter 5.

Chapter 3: Review of Experimental Shake Table Test

Data from four shake table test programs were used to evaluate existing and new methods for estimating the effective stiffness, effective viscous damping and fundamental period of walls. These four test programs included planar, C-shaped and H shaped walls as well as walls that ranged from one to seven stories in height. This information is summarized in Table 3-1. Chapter 3 presents information about these tests including specimen geometry, material properties, ground motions, and observed damage.

Table 3-1: Summary of Test Programs

Experiment	# of Specimens	Wall Configuration and Description	# of Stories	Scale	Aspect Ratio	Fundamental Period
UCSD 7 Story Planar Wall	1	A Planar wall was the main system resisting lateral loads. The system also included pin connected steel tube columns to support a portion of the gravity load, a flange wall perpendicular to the web wall as well as a post-tensioned pier. Slabs were at each story level. The specimen was excited only in direction of planar wall.	7	1:1	5.3	0.57
CAMUS 2000	1	The specimen was excited in two directions. Two Planar Walls resisted lateral loads in one direction while steel braces supported the out of plane direction. Slabs were at each story level.	5	1:3	2.65	0.16
CAMUS C	4	The specimen was C-shaped and excited in the direction of the flanges of the C. The only slabs were found at the base and the roof. Additional weight was added by masses at the top.	1	0.6	4.2	0.28
CAMUS Ecoleader X direction	1	The specimen was excited in two directions. Two Planar Walls resisted lateral loads in one direction while a coupled wall supported the out of plane direction. Slabs were at each story level.	5	1:3	2.81	0.27
CAMUS Ecoleader Y direction					2.88	0.22

3.1 UCSD 7-Story Planar Wall Specimen

Shake table tests of a full-scale, seven-story, wall building were conducted by Panagiotou, Restrepo, Conte and Englekirk (2006) using the University of California, San Diego (UCSD) Network for Earthquake Engineering Simulation (NEES) shake table. The test specimen can be seen Figure 3-1. The building was subjected to four ground motions of increasing severity in the direction of the wall web. The objective of these tests was to investigate the effects of using less than code recommended reinforcement.

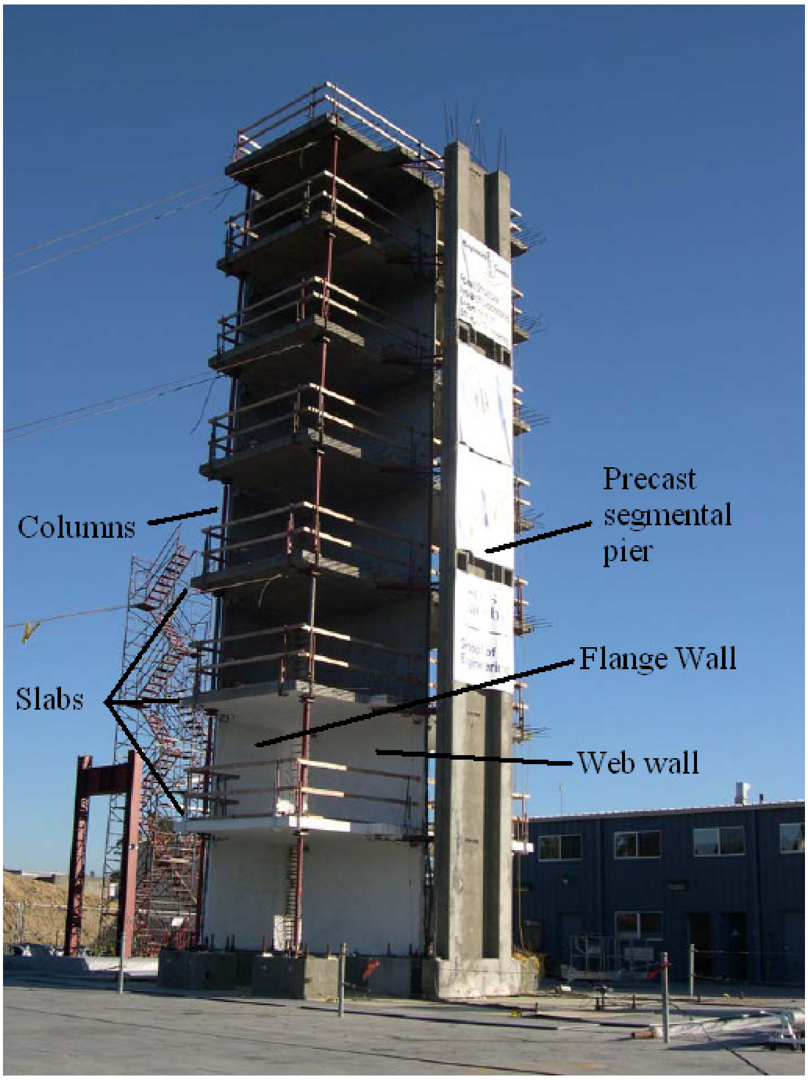

Figure 3-1: UCSD NEES 7-Story Specimen (NEES@UCSD, 2007)

3.1.1 Geometry and Reinforcement

Figure 3-2 and Figure 3-3 show, respectively, a plan and elevation view of the seven-story wall building shown in Figure 3-1. As indicated in these figures, the structural components of the test specimen included a web wall oriented in the direction of excitation, a flange wall oriented perpendicular to the ground motion, as well as floor slabs, pinned gravity columns, a post-tensioned pier and angles connecting the pier to the slab. The specimen cross section is T-shaped, however the load in the flange wall was limited by a notched slab resulting in a hinge-like slab behavior. The relative dimensions and other information are summarized in Table 3-2.

Table 3-2: Summary of UCSD Specimen Geometry

Member	**Property**	**Dimensions (in)**	**Aspect Ratio**
Web Walls	Story Height	108	5.25
	Height	756	
	Length	144	
	Thickness, floor 1+7	8	
	Thickness floor 2-6	6	
Flange Wall	Height	768	4.00
	Length	192	
	Thickness, floor 1+7	8	
	Thickness floor 2-6	6	
Slabs (*7)	Thickness	8	-
Specimen	Scale	Approx. 1:1	-

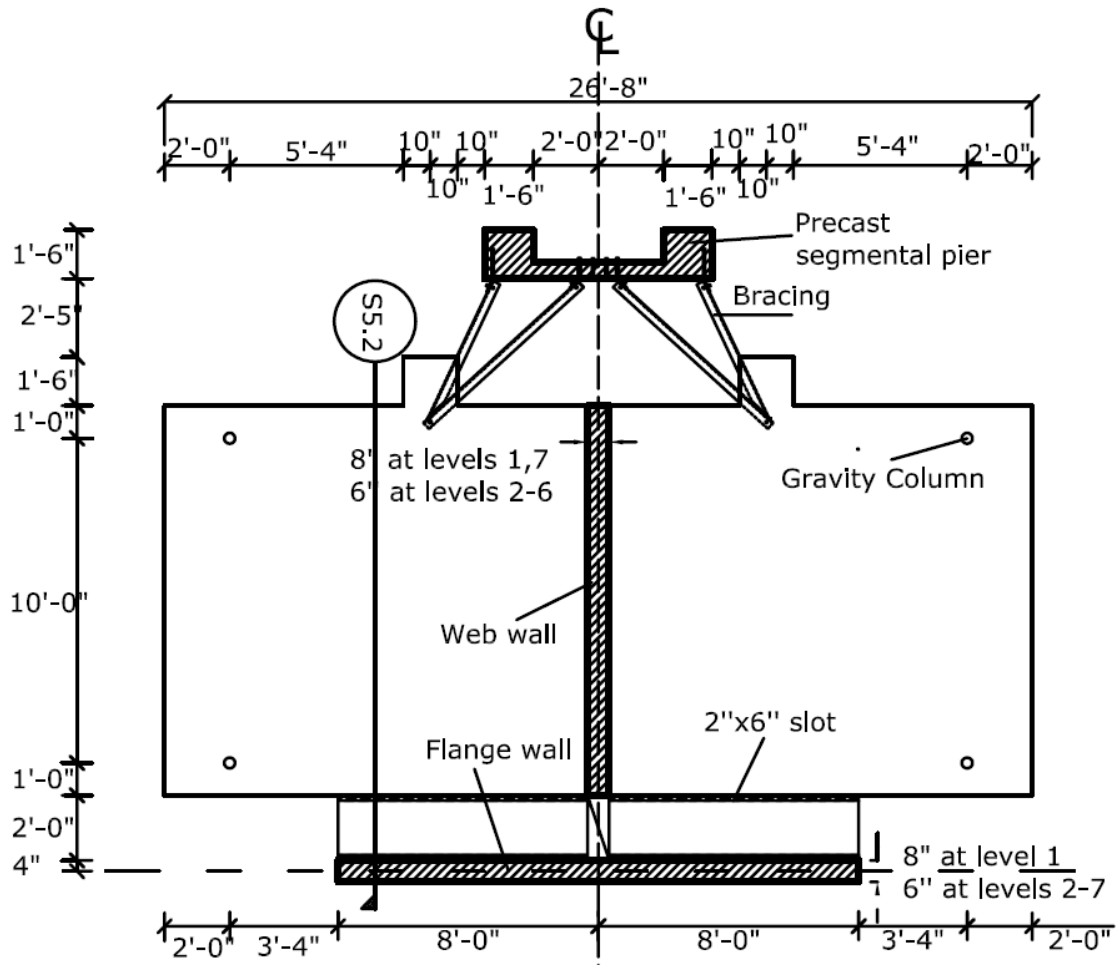

Figure 3-2: UCSD Specimen Plan (NEES@UCSD, 2007)

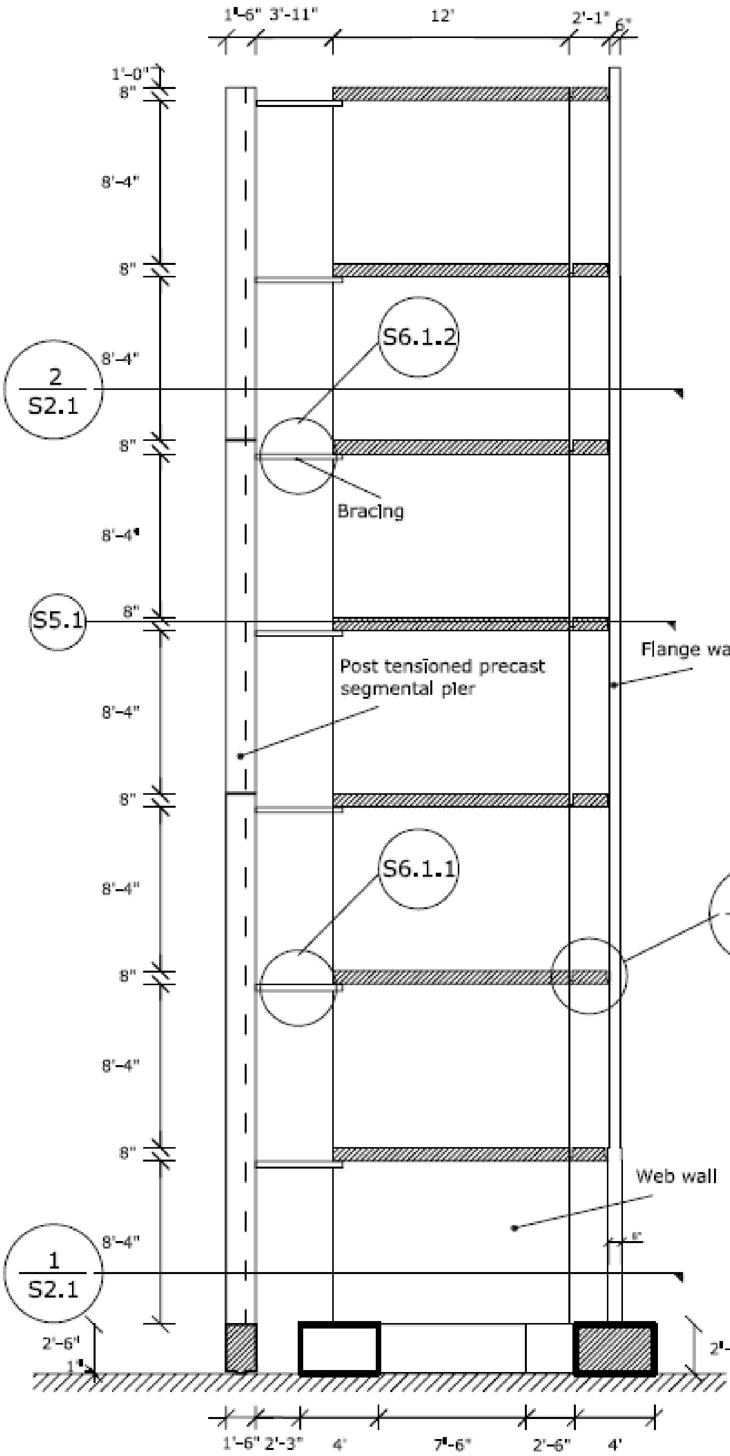

Figure 3-3: UCSD Specimen Elevation (NEES@UCSD, 2007)

The wall reinforcement for the specimen varied up the height of the structure. Table 3-3 summarizes the reinforcement in the web and flange wall. Figure 3-4 shows a cross section of the specimen and depicts the reinforcement layout at the base.

Table 3-3: UCSD Wall Reinforcement Summary

	Floor	**Vertical Reinforcement Ratio**			**Transverse Reinforcement Ratio**	
		Average ρv	**Wall ρv**	**Boundary Element ρv**	**Wall ρh**	**Boundary Element ρh**
Web Wall	flr 1	0.66%	0.28%	2.21%	0.31%	0.69%
	flr 2-6	0.81%	0.32%	2.86%	0.42%	0.42%
	flr 7	0.66%	0.66%	N/A	0.31%	N/A
Flange Wall	flr 1	0.36%	0.18%	1.43%	0.21%	0.69%
	flr 2-6	0.36%	0.24%	1.05%	0.28%	0.28%
	flr 7	0.36%	0.36%	N/A	0.28%	N/A

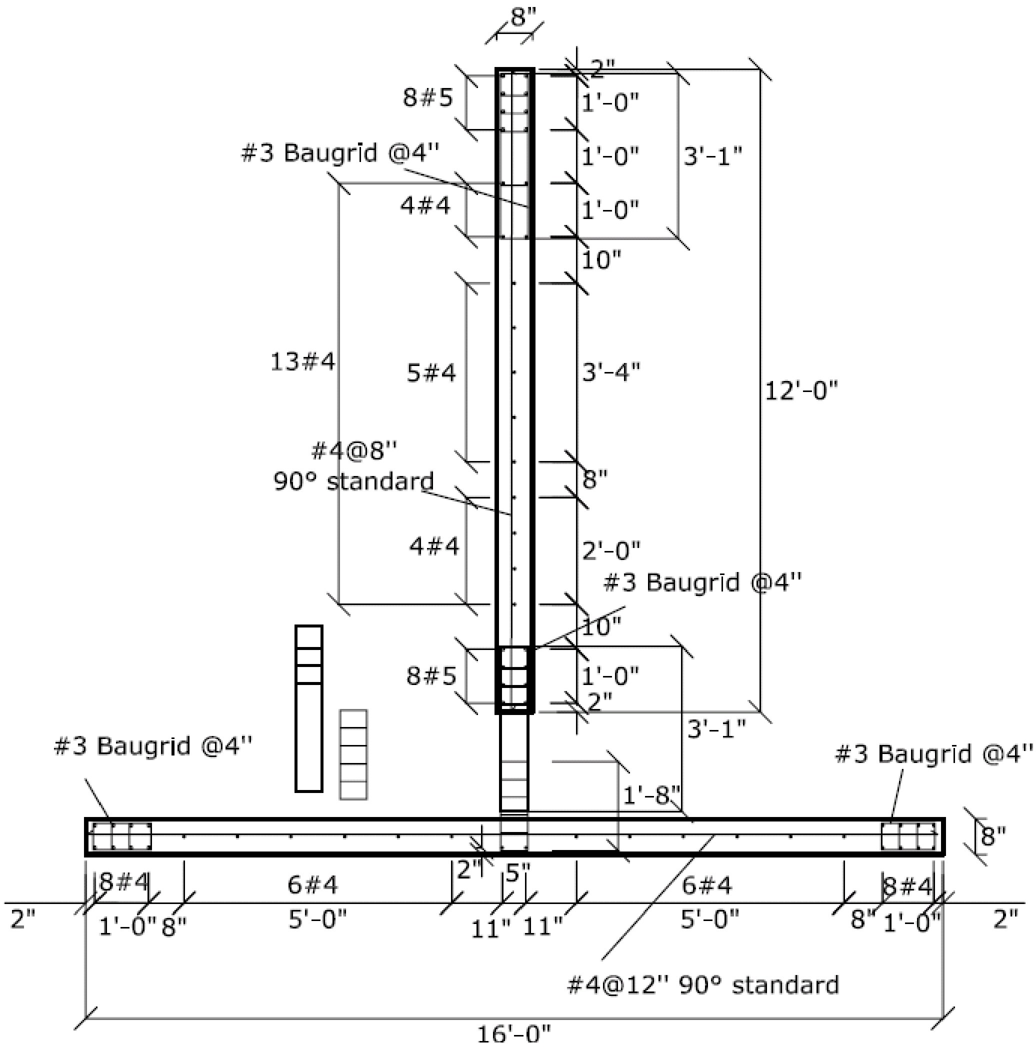

Figure 3-4: UCSD Level 1 Wall Reinforcement Cross Section at Level 1 (NEES@UCSD, 2007)

3.1.2 Material Properties

Table 3-4 and Table 3-5 below show the material properties of the concrete and steel respectively. The concrete was normal weight, and the strength was determined from concrete cylinder compressive tests.

Table 3-4: Average Concrete Properties (NEES@UCSD, 2007)

f'_c (ksi)	E_c (ksi)	ε_{cu} (in/in)
6.00	4241	-0.00235

Table 3-5: Average Reinforcing Steel Properties (NEES@UCSD, 2007)

f_y (ksi)	f_{su} (ksi)	ε_{sh} (in/in)	ε_{su} (in/in)
66.5	106.8	0.0068	0.10

3.1.3 Specimen Mass

The specimen had no additional weight added. The total weight of the specimen is summarized in Table 3-6.

Table 3-6: Calculated Weights in kips (NEES@UCSD, 2007)

Structural Component	**Weight (kips)**
Foundation	47.3
Slabs	224
Web Wall	55
Flange Wall	73.3
PT column + foundation	66.5
Gravity Columns + foundation	10.4
Braces	0.4
Total	476.9
W/(f'c*Ag)	6.90%

3.1.4 Table Specifications

The specimen was tested on the NEES Large High Performance Outdoor Shake Table (LHPOST) at the University of California, San Diego. The shake table facility can be seen in Figure 3-5, although note that the specimen displayed in the figure is not meant to represent the specimen considered for this study. The table is capable of unidirectional loading.

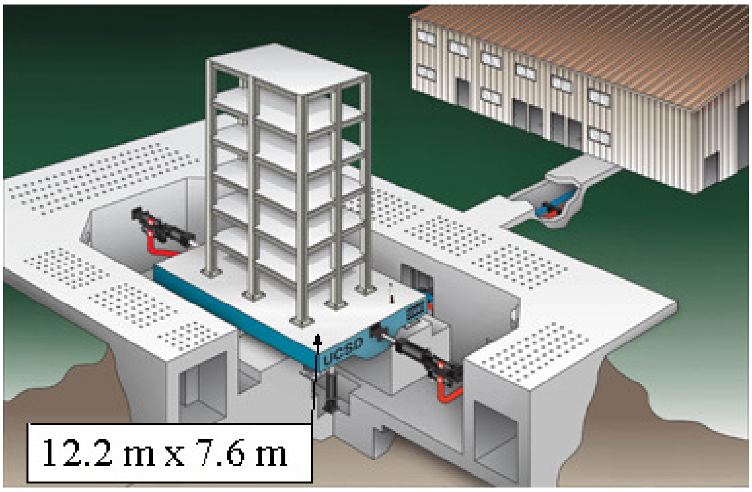

Figure 3-5: NEES LHPOST Facility at UCSD (NEES@UCSD, 2007)

3.1.5 Table Rocking Observations

The shake table was found to have some flexibility which had a modest contribution to the response. The researchers provided a model for the rotational spring stiffness of the base due to the table's flexibility. These stiffness values can be seen in Table 3-7 and Table 3-8.

Table 3-7: Rotational Spring Stiffness Due to Table Flexibility Only (kips-ft/rad)*10^7 (NEES@UCSD, 2007)

Relative Displacement	Spring stiffness (kips-ft/rad)*10^7			
	EQ1	EQ2	EQ3	EQ4
East	3.857	3.509	3.882	1.436
West	3.916	3.791	2.254	1.591

Table 3-8: Rotational Spring Stiffness Due to Combined Flexibility of Table and Foundation (kips-ft/rad)*10^7 (NEES@UCSD, 2007)

Relative Displacement	Spring stiffness (kips-ft/rad)*10^7			
	EQ1	**EQ2**	**EQ3**	**EQ4**
East	1.326	0.883	0.711	0.831
West	1.378	0.888	0.684	0.746

3.1.6 Instrumentation

Specimen response was monitored using a wide array of internal and external instrumentation. Traditional instrumentation comprised 58 displacement transducers, 28 string potentiometers, 314 strain gages and 23 pressure transducers. Additionally, to measure displacements, a photogrammetric system was employed using GPS devices with 1 mm resolution and a data collection rate of 50 Hz (Panagiotou et al., “Seismic Response”, 2006). Instrumentation was most densely deployed in the lower two levels of the building, where most of the inelastic action was expected.

A total of 139 accelerometers were also used. Figure 3-6 shows the typical location of horizontal accelerometers for each floor. In addition to this, “nine vertical accelerometers [were] placed at every floor. Two horizontals, one transverse and two vertical accelerometers were placed on top of the post tensioned pier and the flange wall. An additional horizontal accelerometer was placed at the mid-height of every level of the web wall” (Panagiotou et al., “Seismic Response” 5, 2006).

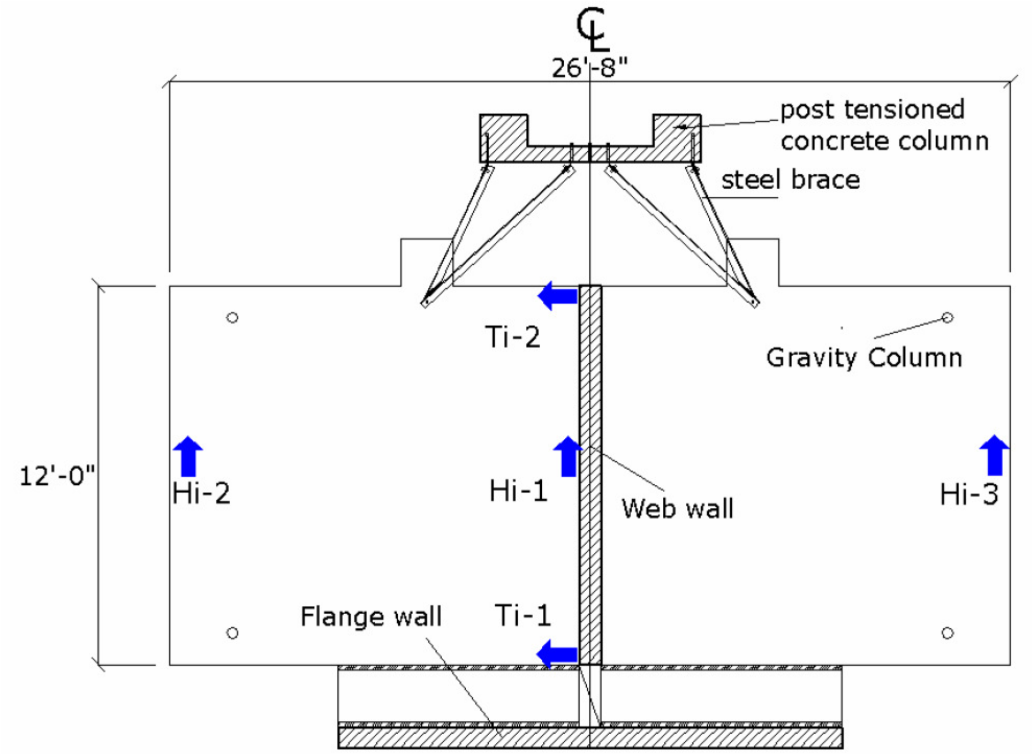

Figure 3-6: Horizontal and Transverse Accelerometers for a Typical Floor (Panagiotou et al., "Seismic Response", 2006)

3.1.7 Applied Earthquake Excitation

A total of four tests were run using the UCSD specimen. The first motion (VNUY longitudinal component from the 1971 San Fernando earthquake) was a low intensity ground motion. The second (VNUY transverse component from 1971 San Fernando earthquake) and third (WHOX longitudinal component of the 1994 Northridge earthquake) were "somewhat above the site response spectra for the period of the building for 50% probability of exceedance event" (Panagiotou et al., "Shake Table Test" 12, 2007). The fourth motion (Sylmar Olive View Med 360^{o} component record from the 1994 Northridge earthquake) was slightly above "the site response spectra for 10% probability of exceedance in 50 years" (Panagiotou et al., "Shake Table Test" 13, 2007). Table 3-9 shows the peak ground accelerations of each test and Figure 3-7 shows the response spectra. The strong motion portion of the acceleration time histories for each motion can be found in Appendix E.

Table 3-9: Peak Ground Acceleration for Four Ground Motions

Ground Motion	Peak Ground Acceleration (g)
EQ1	0.15
EQ2	0.26
EQ3	0.34
EQ4	0.94

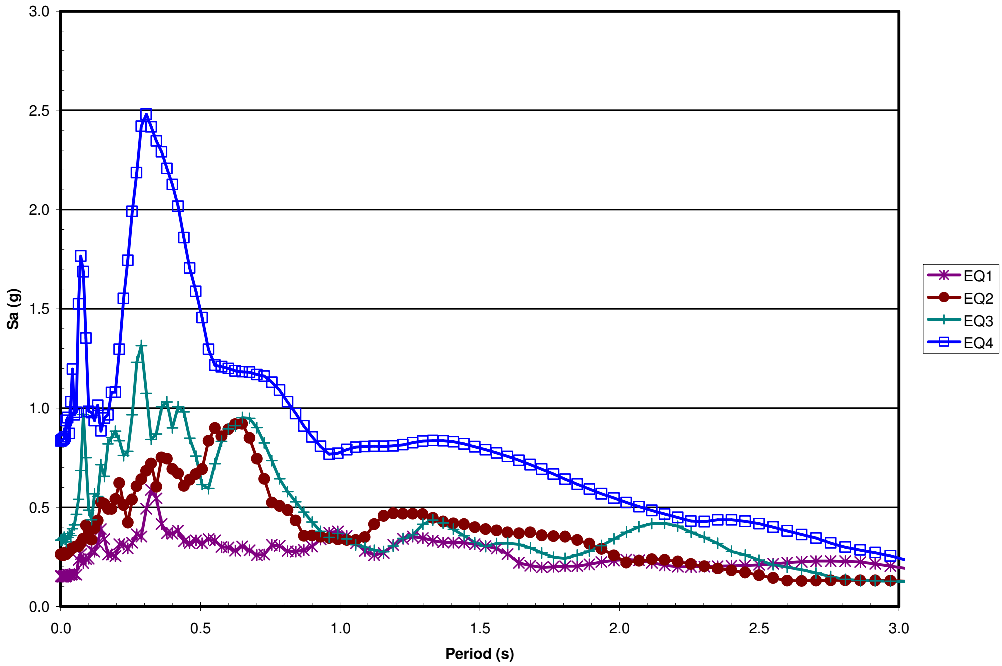

Figure 3-7: UCSD Acceleration Response Spectra – 5% damping

3.1.8 Wall Performance

Information provided by Panagiotou et al ("Shake Table Test", 2007) suggests that initially wall response was determined primarily by flexure as crack patterns are consistent with flexure in the web wall. However, during EQ4 a crack in the lap splice in the web wall was observed. The splice degraded throughout the run resulting in considerable bond slip although it never fully lost its integrity.

The following provides observations of test specimen response and damage made by Panagiotou et al ("Shake Table Test", 2007).

"During test EQ1 tensile strains [in web wall longitudinal reinforcement] were very small and only exceeded the cracking strain for concrete" (Panagiotou et al., "Shake Table Test" 26, 2007). The crack orientation following EQ 1 can be seen in Figure 3-8. This figure shows minimal cracking, isolated mostly in the first story.

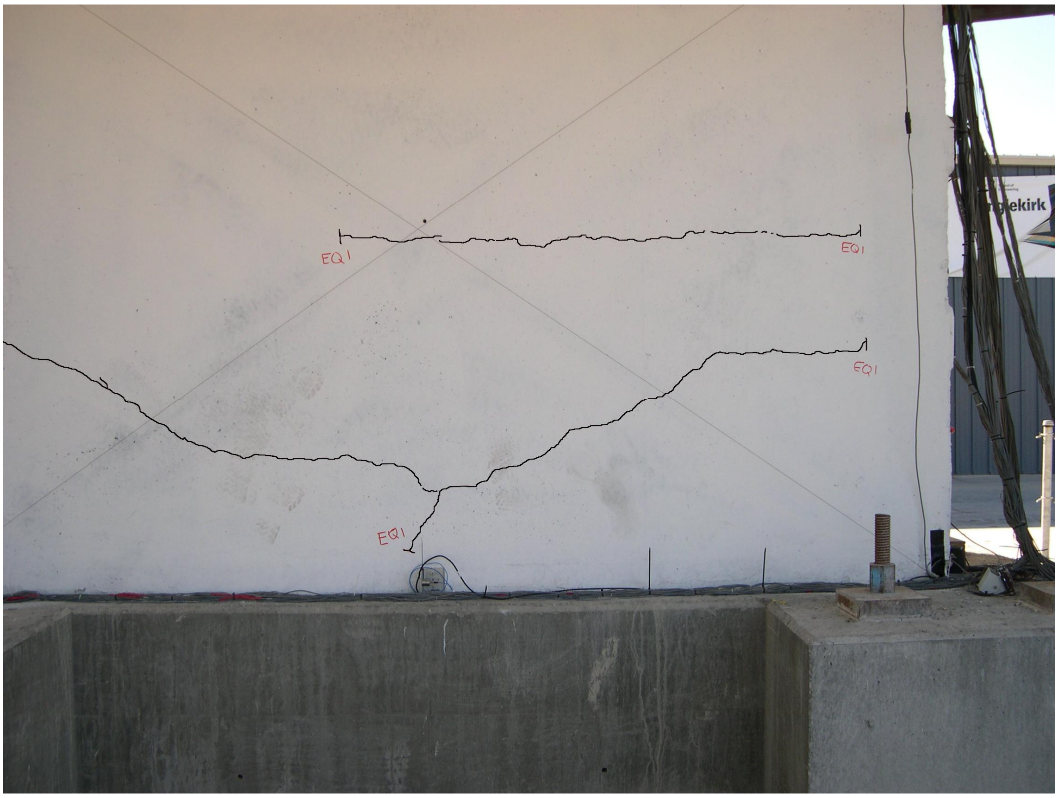

Figure 3-8: Crack Patterns in Level 1 of Web Wall Following EQ 1 (NEES Central, 2007, with crack lines darkened by author)

As a result of EQ2 and EQ3, the wall exhibited minor cracking “due to limited inelastic response and the maximum bar strains of 1.7% were recorded at the base of Level 1” (Panagiotou et al., “Shake Table Test” 26, 2007). Figure 3-9 shows crack patterns at the first story, and Figure 3-10 shows flexural cracks developing at the edge of the wall following EQ 2. Wall response to “EQ4 was characterized also by limited spalling of the concrete cover at the base of the wall, and by an unexpected large split crack at the west lap-splice at the base of the second level” (Panagiotou et al., “Shake Table Test” 26, 2007).

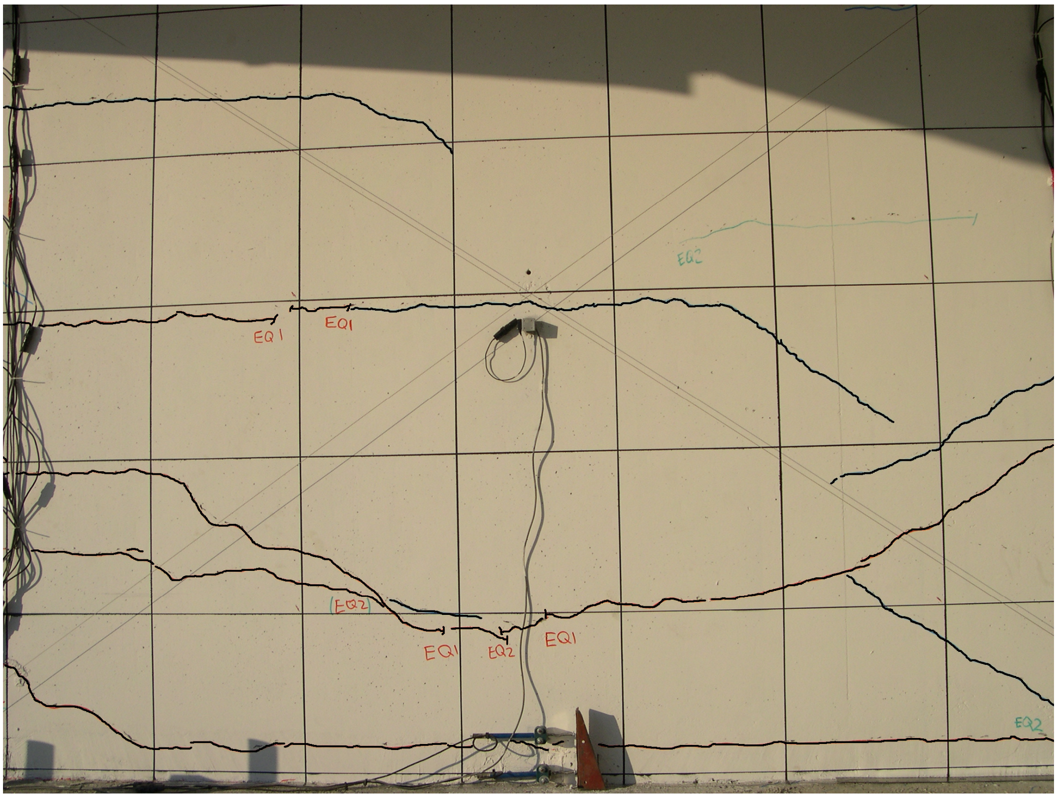

Figure 3-9: Crack Patterns in Level 1 of Web Wall Following EQ 2 (NEES Central, 2007, with crack lines darkened by author)

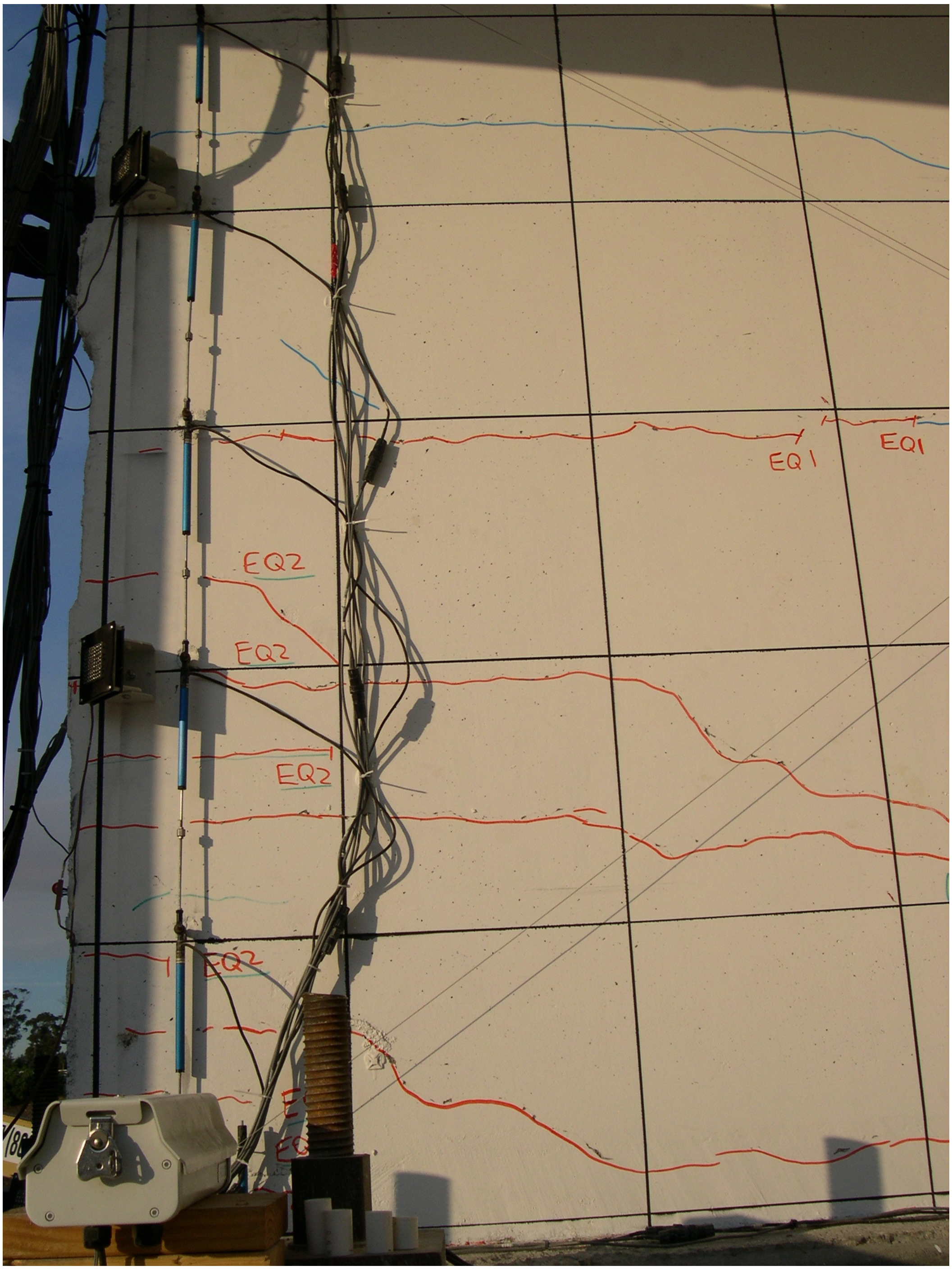

Figure 3-10: Crack Patterns in Web Wall Level 1 Following EQ 2 (NEES Central, 2007)

As a result of EQ4 significant cracking and spalling was observed as can be seen in Figure 3-11 through Figure 3-13. The lap splice can be seen in Figure 3-14. “The lap-splice maintained its integrity all throughout the test program and even during peak loading in test EQ4 but deteriorated in a subsequent large-amplitude cycle” (Panagiotou et al., “Shake Table Test” 26, 2007).

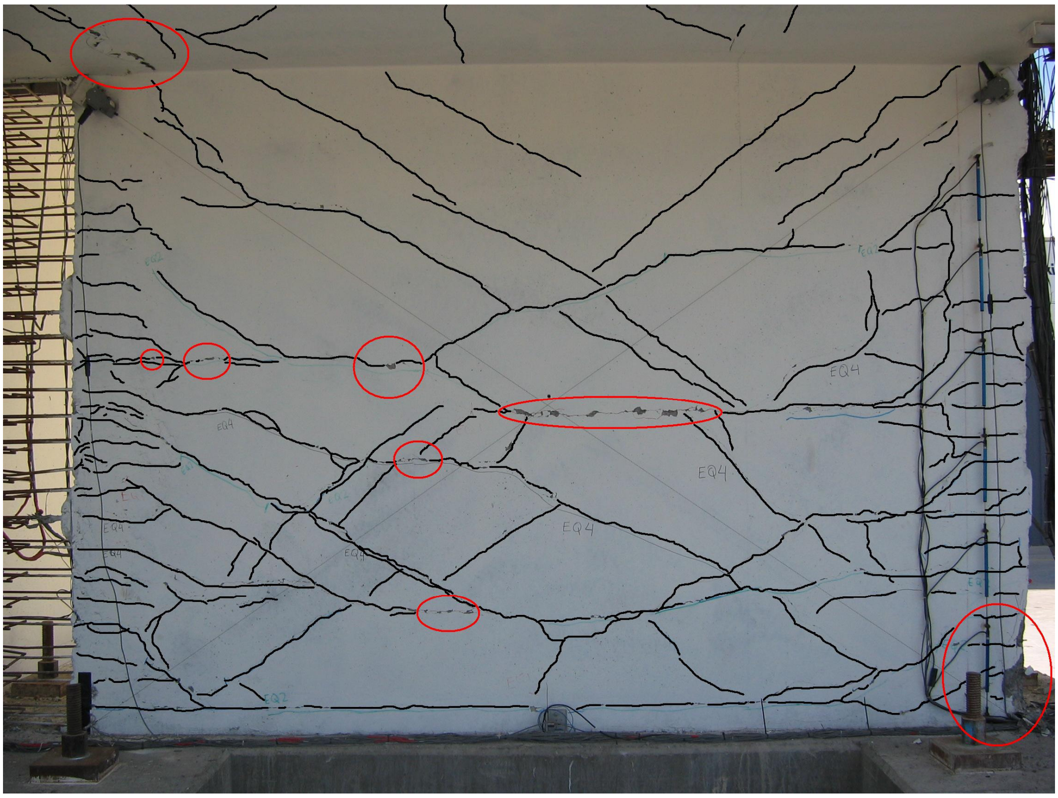

Figure 3-11: Crack Patterns in North Face of Web Wall Level 1 Following EQ 4. Areas Circled in Red Denote Regions of Spalling (NEES Central, 2007)

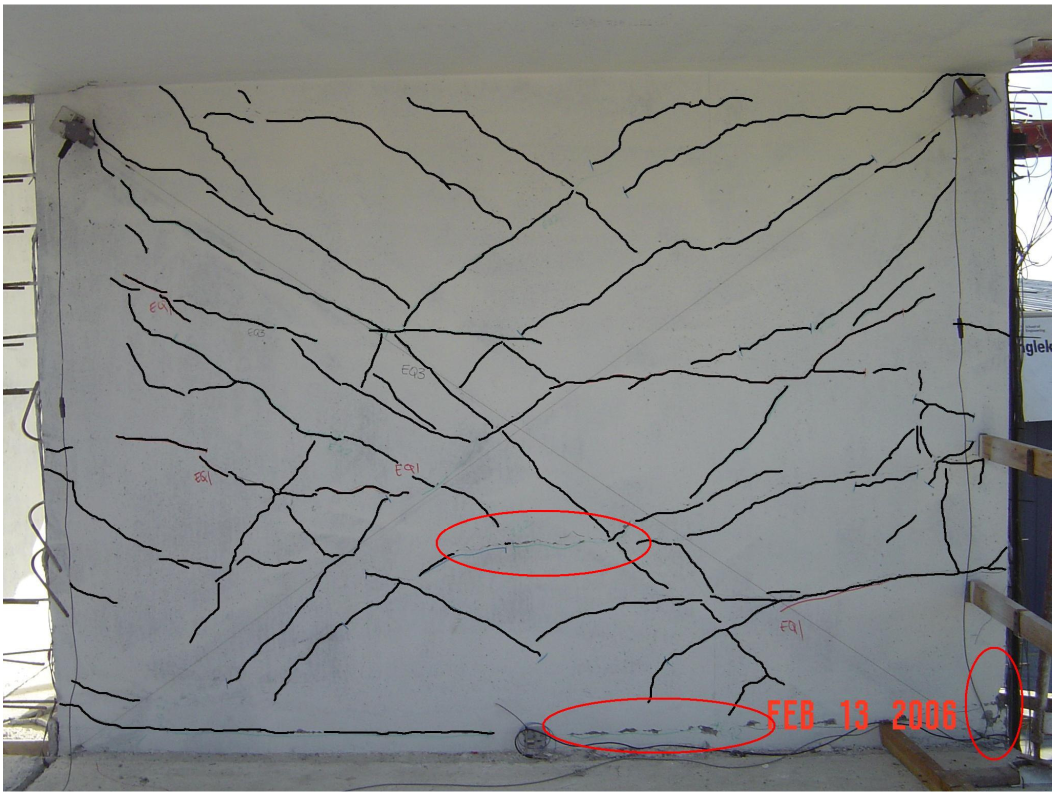

Figure 3-12: Crack Patterns in North Face of Web Wall Level 2 Following EQ 4. Areas Circled in Red Denote Regions of Spalling (NEES Central, 2007)

Figure 3-13: Spalling at Ends of Web Wall Following EQ 4 (NEES Central, 2007)

Figure 3-14: Split Crack at Web-Splice at Base of 2nd Floor Following EQ 4 (NEES Central, 2007)

During EQ4, "peak longitudinal bar strains of 2.7% were recorded at the wall base when the roof drift ratio was 2.1%" (Panagiotou et al., "Shake Table Test" 27, 2007). Following EQ4 there was a residual roof displacement of 0.5 in and residual crack widths of the order of 0.05 in. According to the researchers, "for such level of damage the 'building' could perhaps not be immediately occupied but would only have required minimum repairs" (Panagiotou et al., "Shake Table Test" 28, 2007).

The concrete strains on the west and east end of the web wall, measured from external transducers, can be seen in Figure 3-15. The steel strains measured from foil strain gauges on the longitudinal bars can be seen in Figure 3-16. The external transducers as well as the internal strain gauges showed that the steel and concrete had similar strains for EQ 1, EQ 2 and EQ 3; however the EQ 4 saw a significant difference in concrete and steel strains due to "bond slip caused by deterioration of the lap splice of the west most web wall longitudinal bars" (Panagiotou et al., "Shake Table Test" 26, 2007).

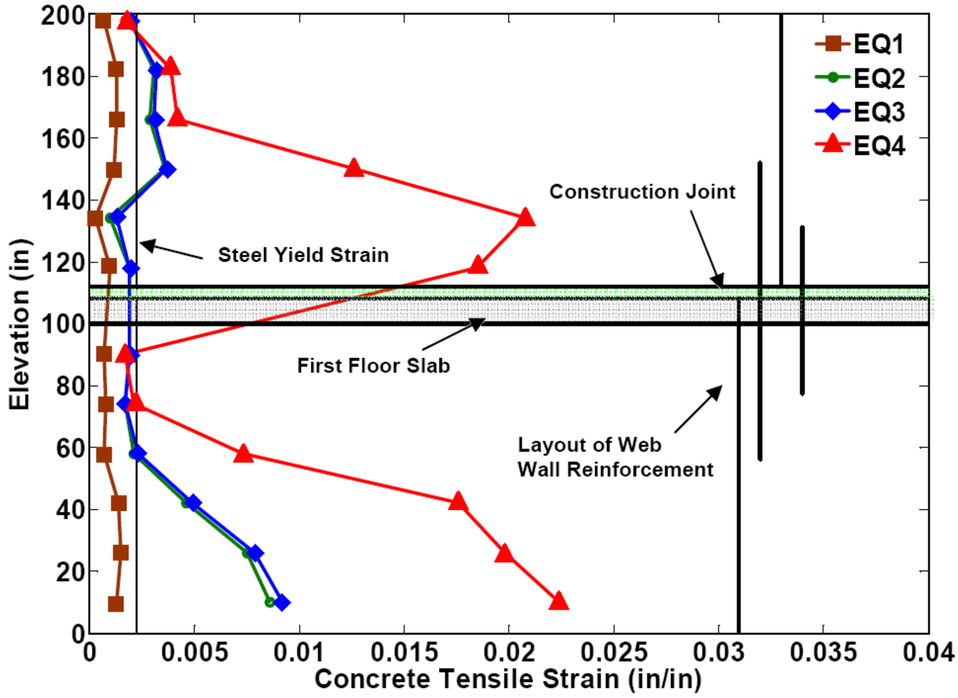

a) West End

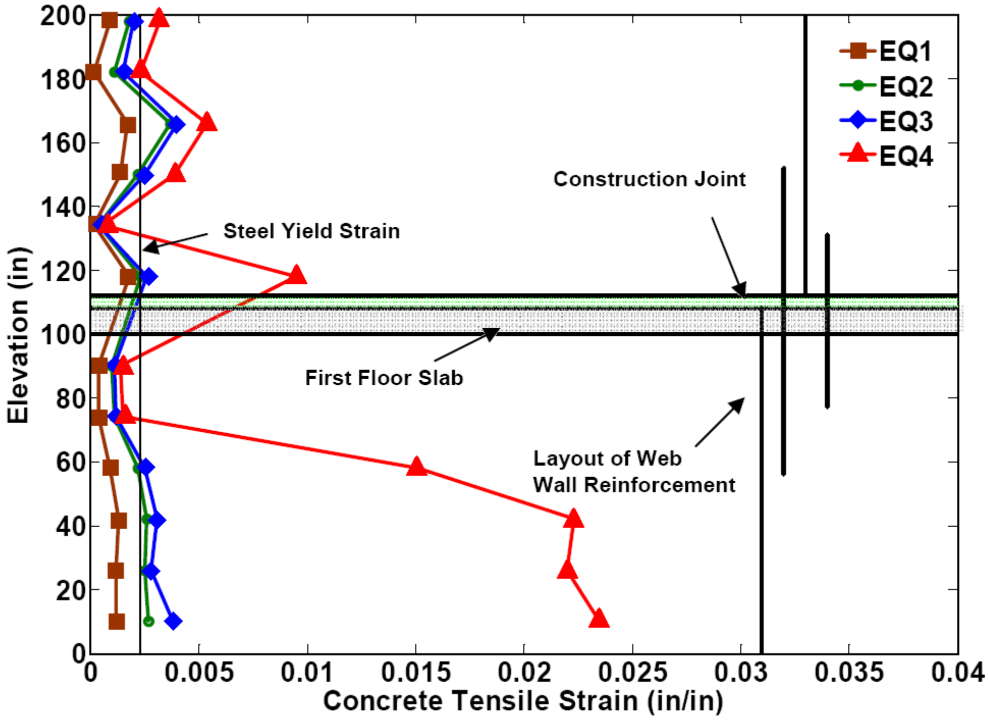

b) East End

Figure 3-15: Concrete Tensile Strain Envelopes (Panagiotou et al., "Shake Table Test", 2007)

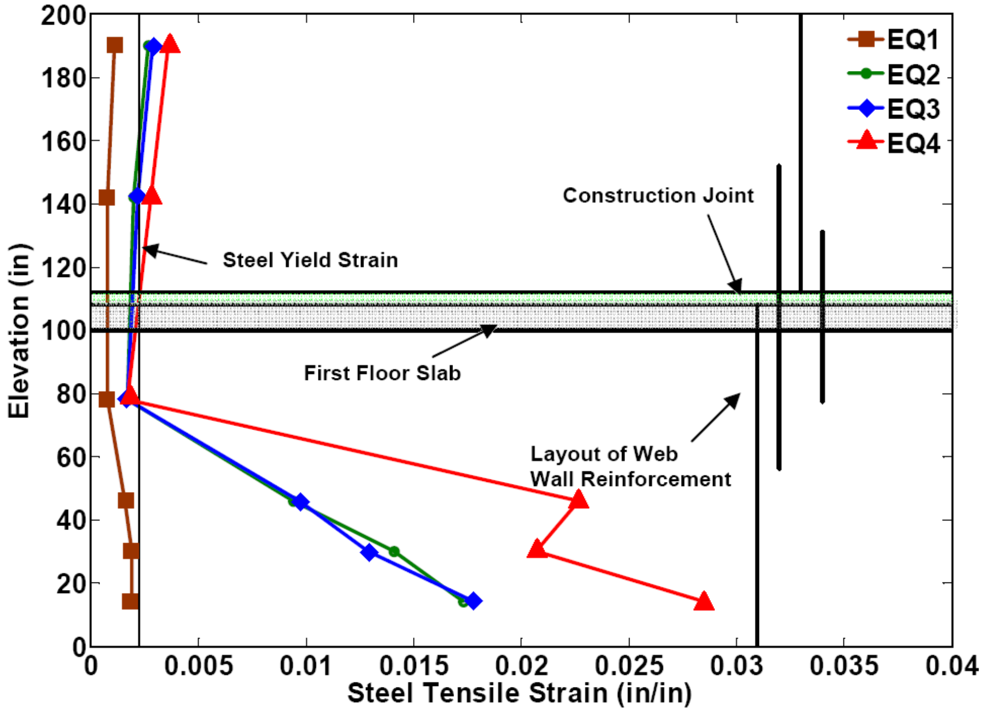

a) West End

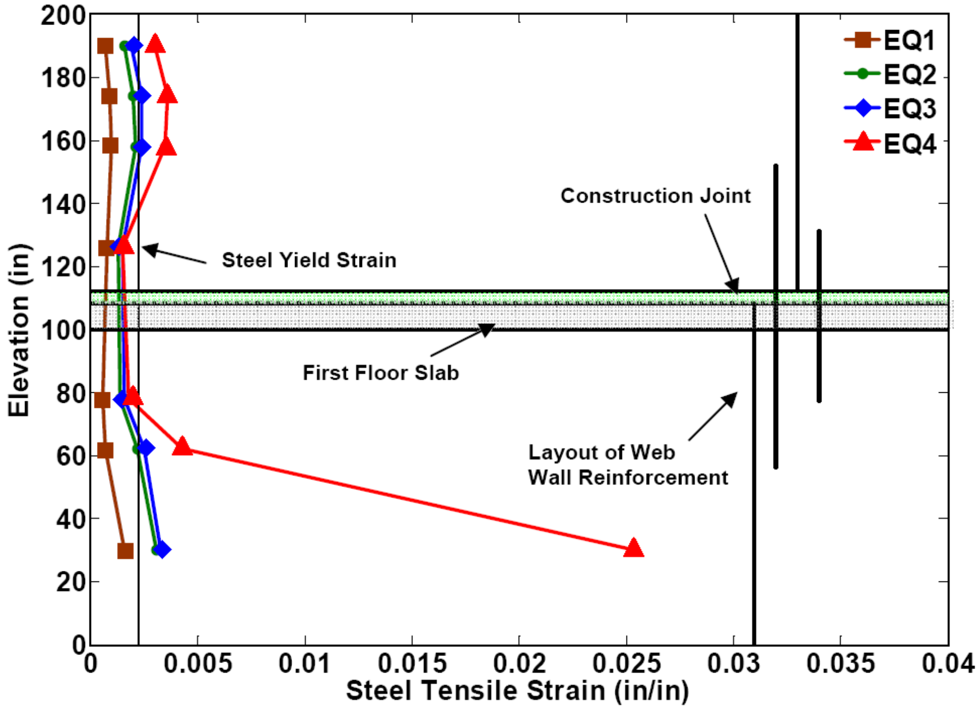

b) East End

Figure 3-16: Steel Strain Tensile Envelopes (Panagiotou et al., 2007)

3.2 CAMUS 2000: Parallel Wall Specimen with Chevron Braces

The CAMUS 2000 wall specimen was tested as part of a collaborative effort by a number of researchers from different European universities. The working group leader was J. M. Reynouard from the Institute National des Sciences Appliques de Lyon (INSA-Lyon).

The specimen was a five-story 1/3-scale structure comprising two parallel concrete walls connected via concrete slabs at each floor and a steel chevron brace system that provided lateral resistance in the out-of-plane direction of the walls. The structure was built and tested on the Azalee shaking table operated by the Commissariat à l'Energie Atomique (CEA) at the Saclay Nuclear Center in Lisbon (Combescure et al., 2002). Figure 3-17 shows the specimen on the table as well as a drawing of the specimen. The specimen was subjected to earthquake excitation in the directions parallel and perpendicular to the concrete walls.

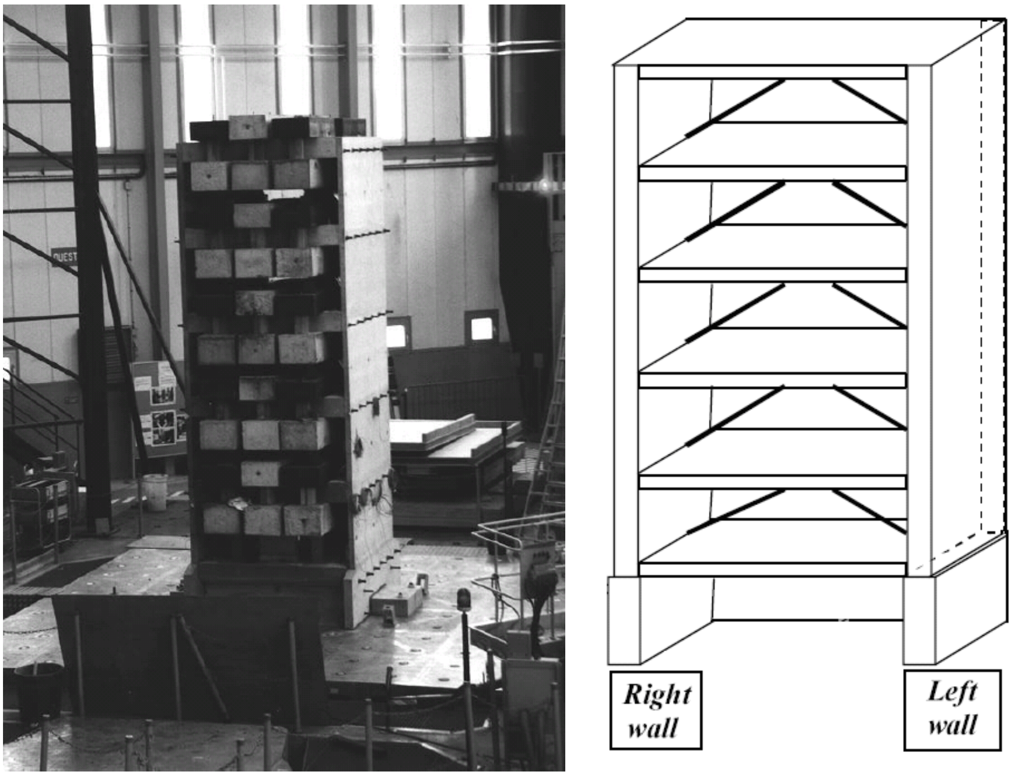

Figure 3-17: CAMUS 2000 Specimen (Combescure et al., 2002)

3.2.1 Geometry and Reinforcement

The specimen consisted of two parallel walls in one direction and steel braces in the other direction. The specimen had slabs connecting the braces and walls at each story level. Table 3-10 summarizes the dimensions of the specimen. Figure 3-18 through Figure 3-20 show the basic geometry.

Table 3-10: Summary of CAMUS 2000 Specimen Geometry

Member	Property	Dimensions (cm)	Dimensions (in)	Aspect Ratio
Walls (*2)	Story Height	90	35.43	2.65
	Height	450	177.17	
	Length	170	66.93	
	Thickness	6	2.36	
Slabs (*5)	Length	170	66.93	-
	Width	170	66.93	
	Thickness	21	8.27	
Out of Plane Braces - HEB 240	Depth	24	9.45	-
	Width	24	9.45	
	Flange Thickness	1.7	0.67	
	Web Thickness	1.0	0.39	
Specimen	Scale	1/3		-

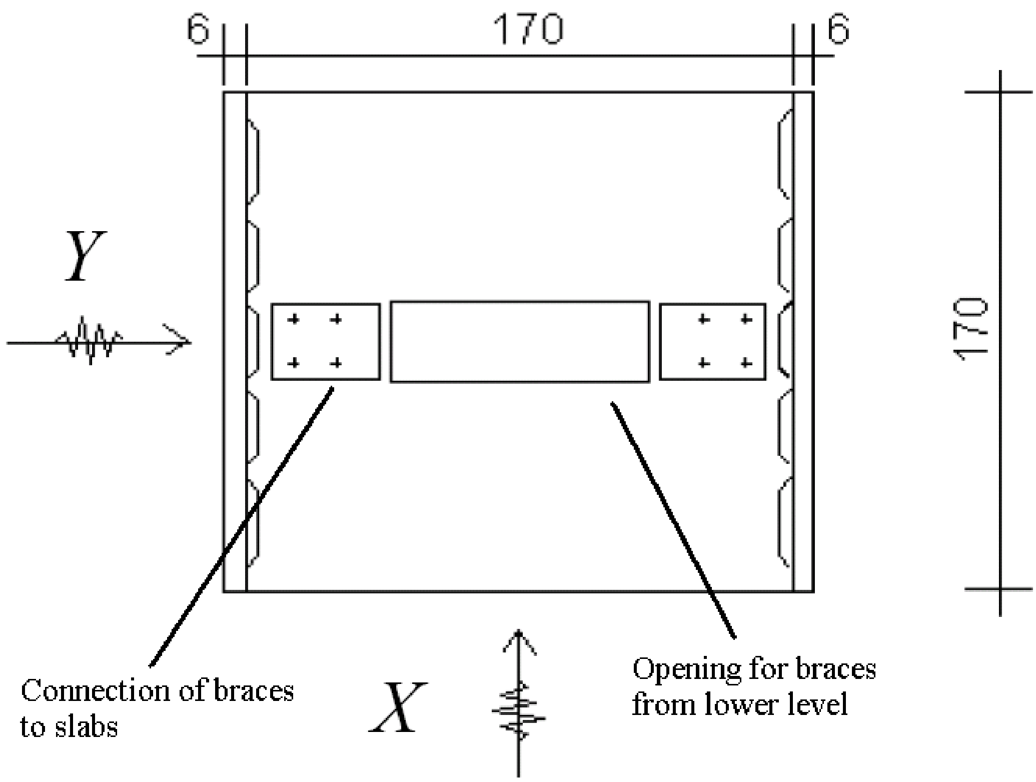

Figure 3-18: CAMUS 2000 Specimen Plan View, units in centimeters (Ile and Reynouard, 2003)

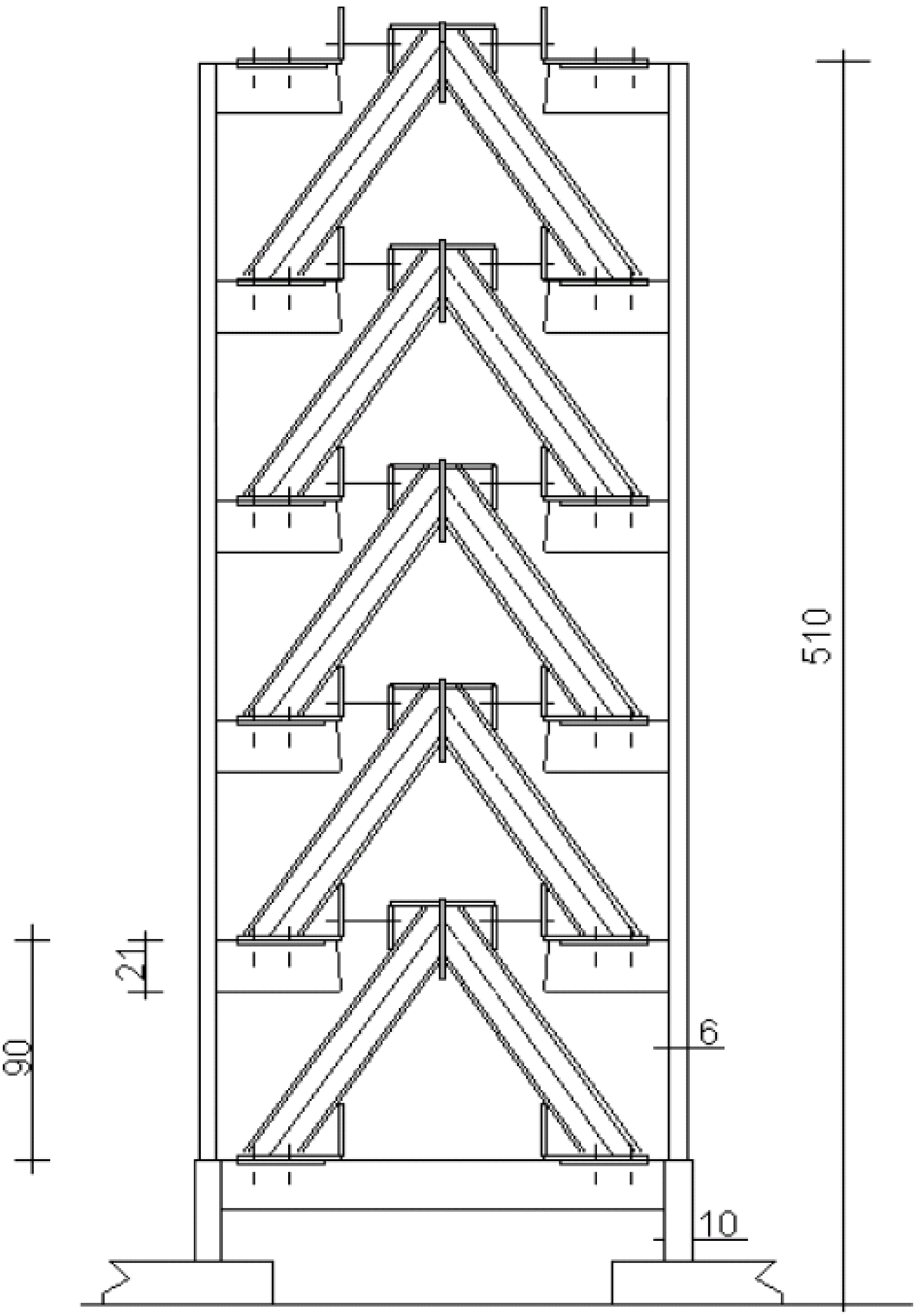

Figure 3-19: CAMUS 2000 Specimen Elevation, units in centimeters (Ile and Reynouard, 2003)

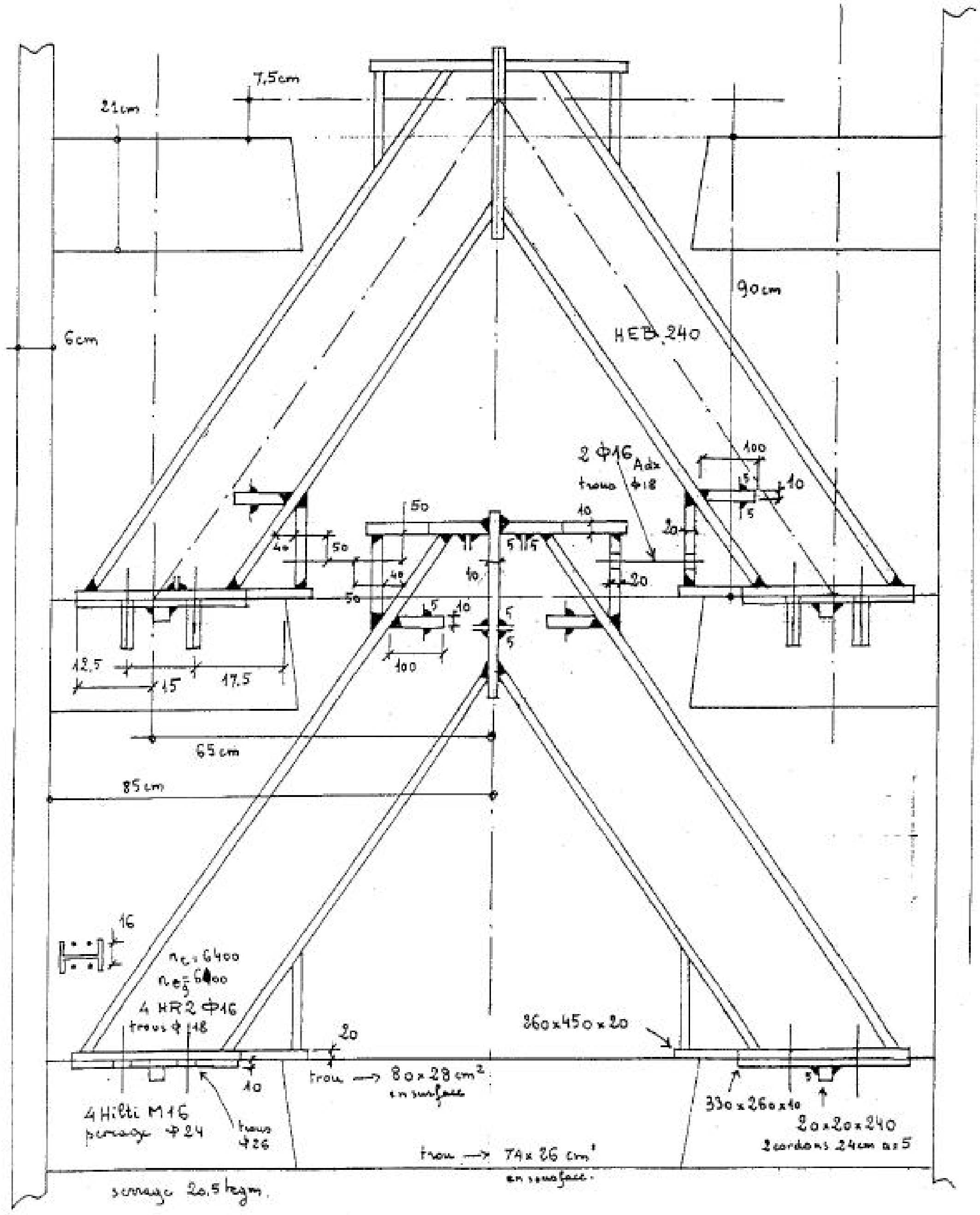

Figure 3-20: Steel Brace Detail, units in centimeters (Combescure et al., 2002)

Table 3-11 lists the reinforcement ratios for vertical and horizontal steel for the laboratory specimen. Figure 3-21 shows an elevation view of the reinforcement layout. Reinforcement was lumped at the ends rather than distributed through the entire wall. Reference documents do not precisely locate the steel reinforcement, so the average reinforcement ratios provided in Table 3-11 were used in all calculations.

Table 3-11: CAMUS 2000 Wall Reinforcement Summary

Floor	**Average ρv**	**Boundary Element Wall ρh**
Floor 1, Lift 1	0.19%	0.39%
Floor 1, Lift 2	0.16%	0.39%
Floor 1, Lift 3	0.12%	0.39%
Floor 2, Lift 1	0.09%	0.39%
Floor 2, Lift 2	0.06%	0.39%
Floor 2, Lift 3	0.03%	0.47%
Floors 3-5	0.03%	0.47%

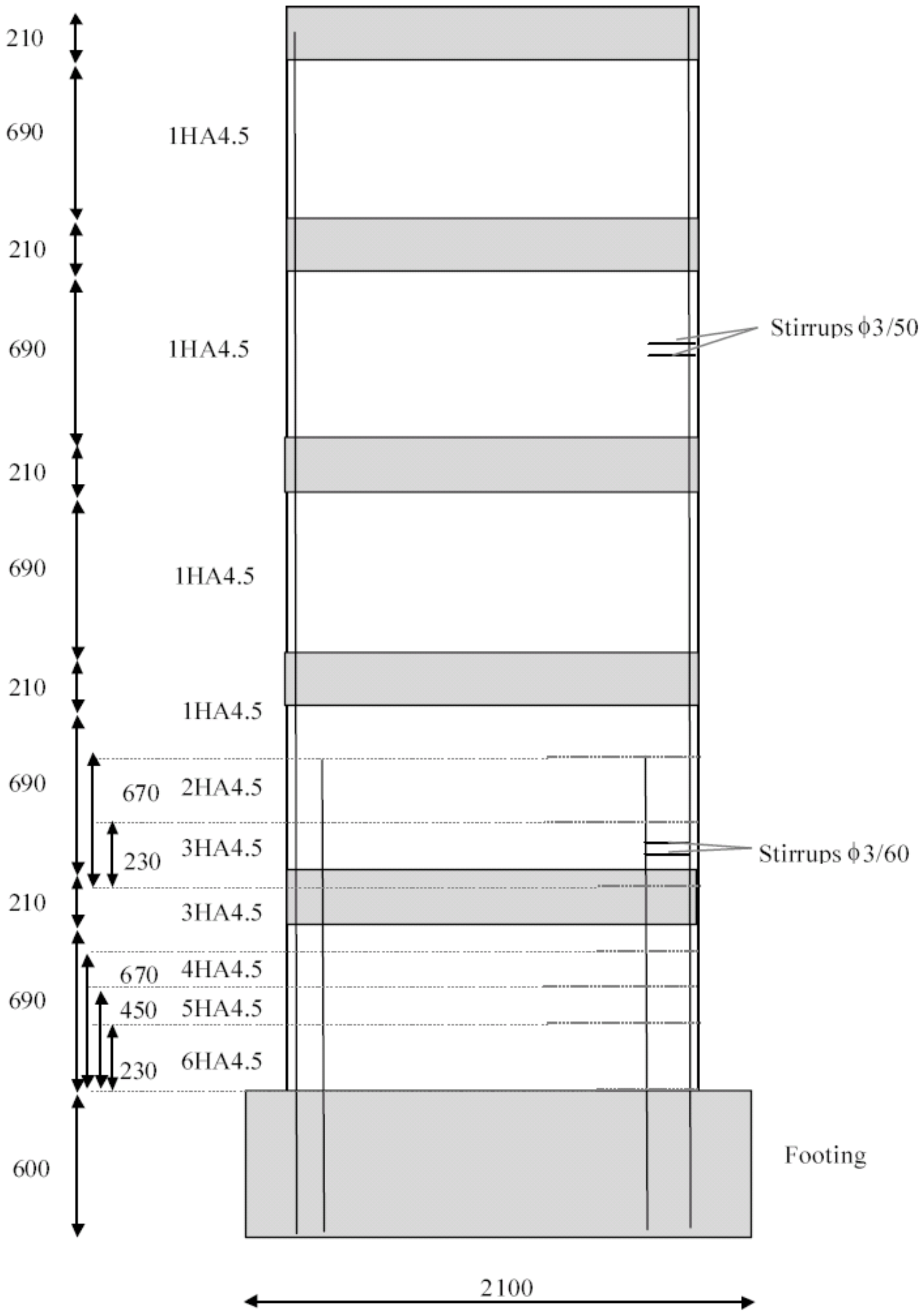

Figure 3-21: CAMUS 2000 Reinforcement Layout (Combescure et al., 2002)

3.2.2 Material Properties

Material properties for the concrete and steel used to construct the CAMUS 2000 specimen are listed in Table 3-12 through Table 3-15. The specimen was constructed using normal weight concrete, and the concrete material properties listed in Table 3-12 were determined from compressive and splitting tests of 160 mm diameter concrete cylinders. The reinforcing steel used in construction had significantly larger yield strength (90+ ksi) than is used typically in the United States. This is likely due to the fact that very small diameter bars (diameter equal to 4.5 mm, which is equivalent to a No 2 or 3 at full scale) were used, necessitating fabrication of deformations on the bars via mechanical action and resulting in work hardening of the steel.

Table 3-12: Average Concrete Properties, metric (Combescure et al., 2002)

Specified		Measured		
f'_c (MPa)	E_c (MPa)	f'_c (MPa)	E_c (MPa)	Density (kg/m^3)
25	28000	32.35	27475	2245

Table 3-13: Average Concrete Properties, English standard units

Specified		Measured		
f'_c (ksi)	E_c (ksi)	f'_c (ksi)	E_c (ksi)	Density (lb/ft^3)
3.6	4061.1	4.7	3985	140.2

Table 3-14: Average Reinforcing Steel Properties, metric (Combescure et al., 2002)

Specified	Measured		
f_y (MPa)	f_y (MPa)	f_{su} (MPa)	ε_{su} (%)
500	664	733	2.20%

Table 3-15: Average Reinforcing Steel Properties, English standard units

Specified	Measured		
f_y (ksi)	f_y (ksi)	f_{su} (ksi)	e_{su} (%)
72.5	96.3	106.3	2.20%

3.2.3 Specimen Mass

When scaling a specimen, the volume and thus the mass decrease by the scale factor cubed. The area by contrast decreases by the scale factor squared. Thus the stresses due to self weight decrease by the scale factor when they should stay the same. For this reason, the researchers provided additional weight at each story level to simulate typical axial loading for a structural wall. These masses as well as those of the structural elements are summarized below in Table 3-16 and can be seen pictorially in Figure 3-22.

Table 3-16: Masses of Structural Elements (Combescure et al., 2002)

Structural element	**Mass of each element *1000 kg**	**Total mass * 1000 kg**	**Total Weight (kips)**
Wall (5 stories)	1.100*2	2.200	4.8
Footing	1.422 + 1.390	2.812	6.2
Weight of slab per floor	1.316		
Concrete blocks per floor (lower side)	0.288*6		
Concrete blocks per floor (upper side)	0.240*2		
Steel blocks per floor	0.628*4		
Total mass of floors	6.036*5	30.180	66.5
Lateral bracing system	0.214 *5 + 0.048	1.1180	2.5
Total weight		36.310	80.0
W/(f'c*Ag) (%)		5.40%	

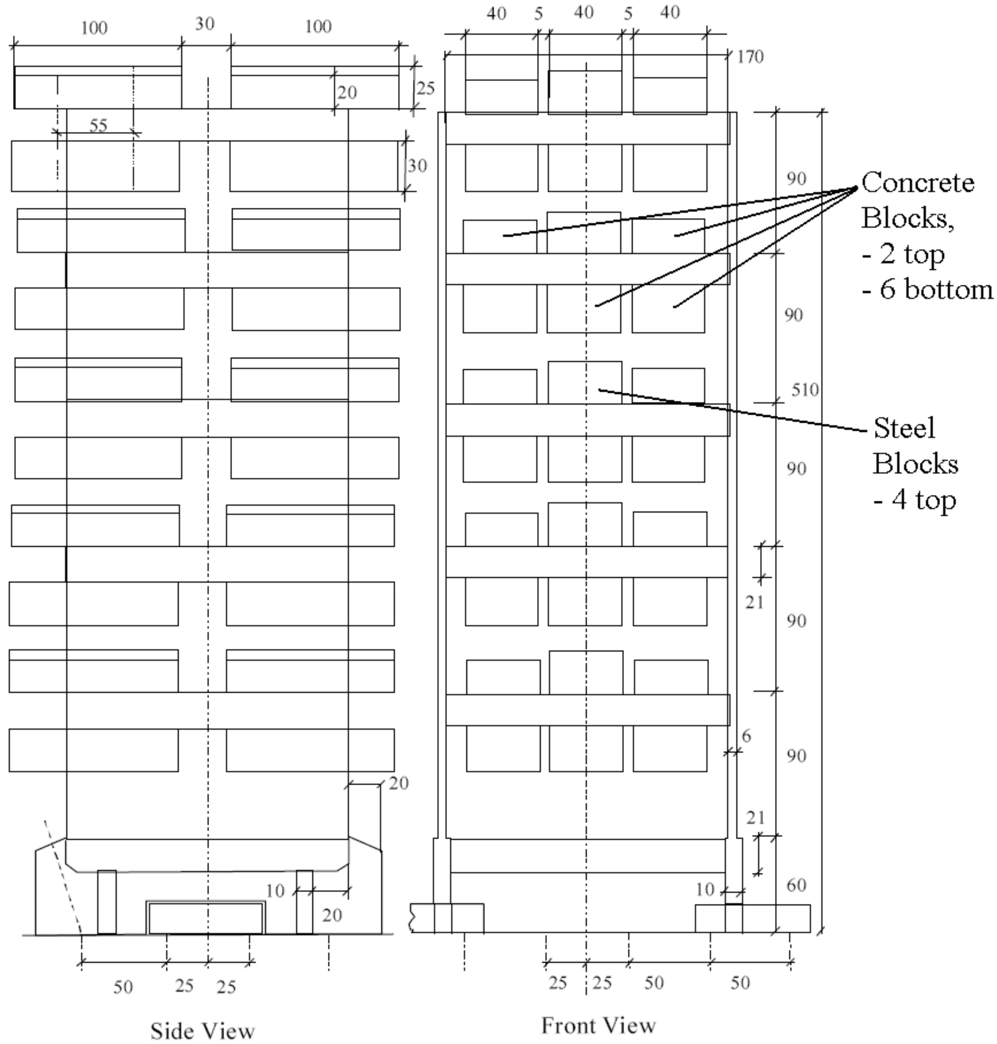

Figure 3-22: Distribution of Additional Masses (Combescure et al., 2002)

3.2.4 Table Specifications and Anchorage

The specimen was tested on the Azalee shaking table of the EMSI Laboratory of the CEA; the table can be seen in Figure 3-23. Figure 3-24 shows the layout of anchors used to tie the specimen to the table.

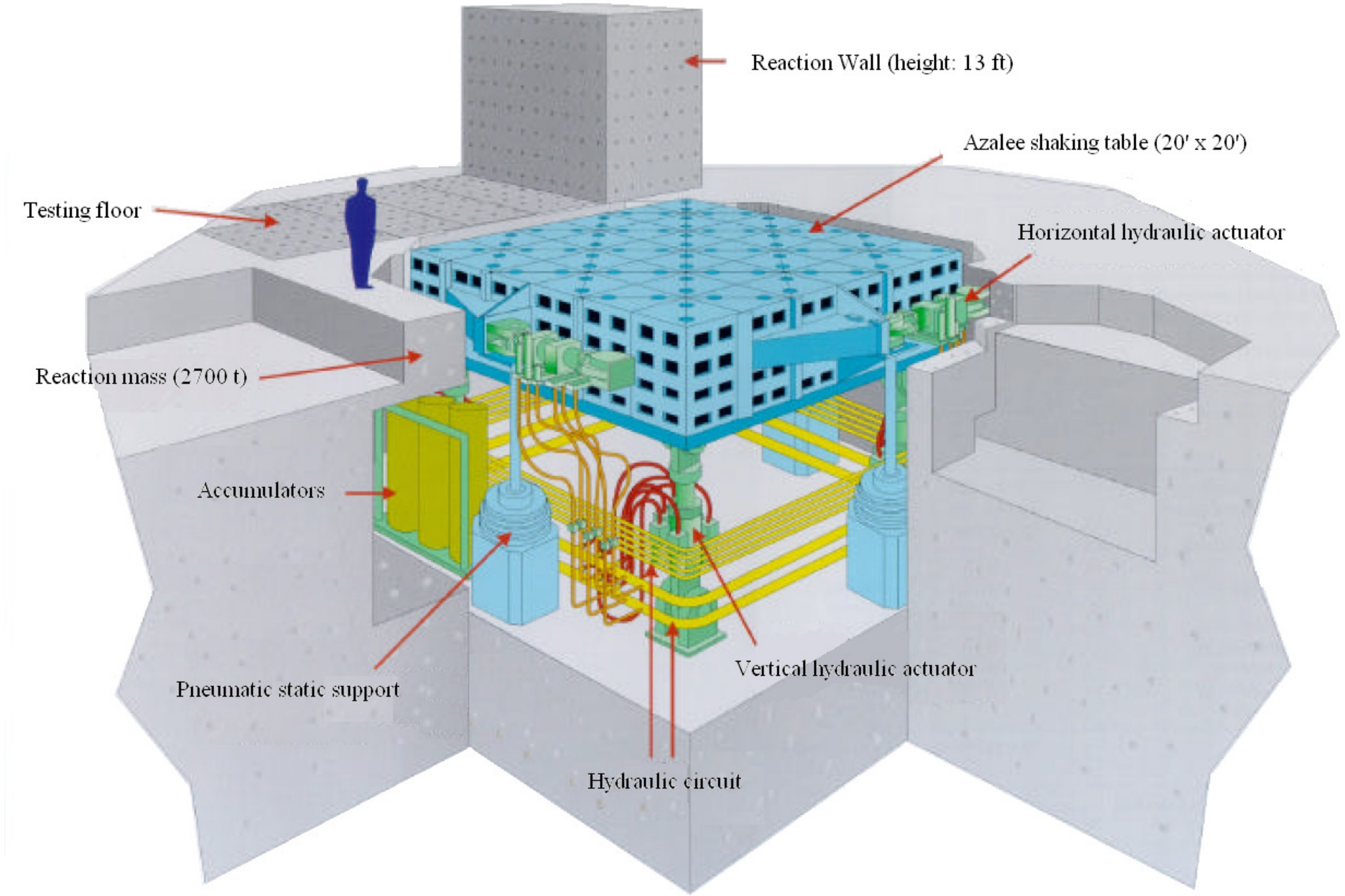

Figure 3-23: Azalee Shaking Table (Combescure et al., 2002)

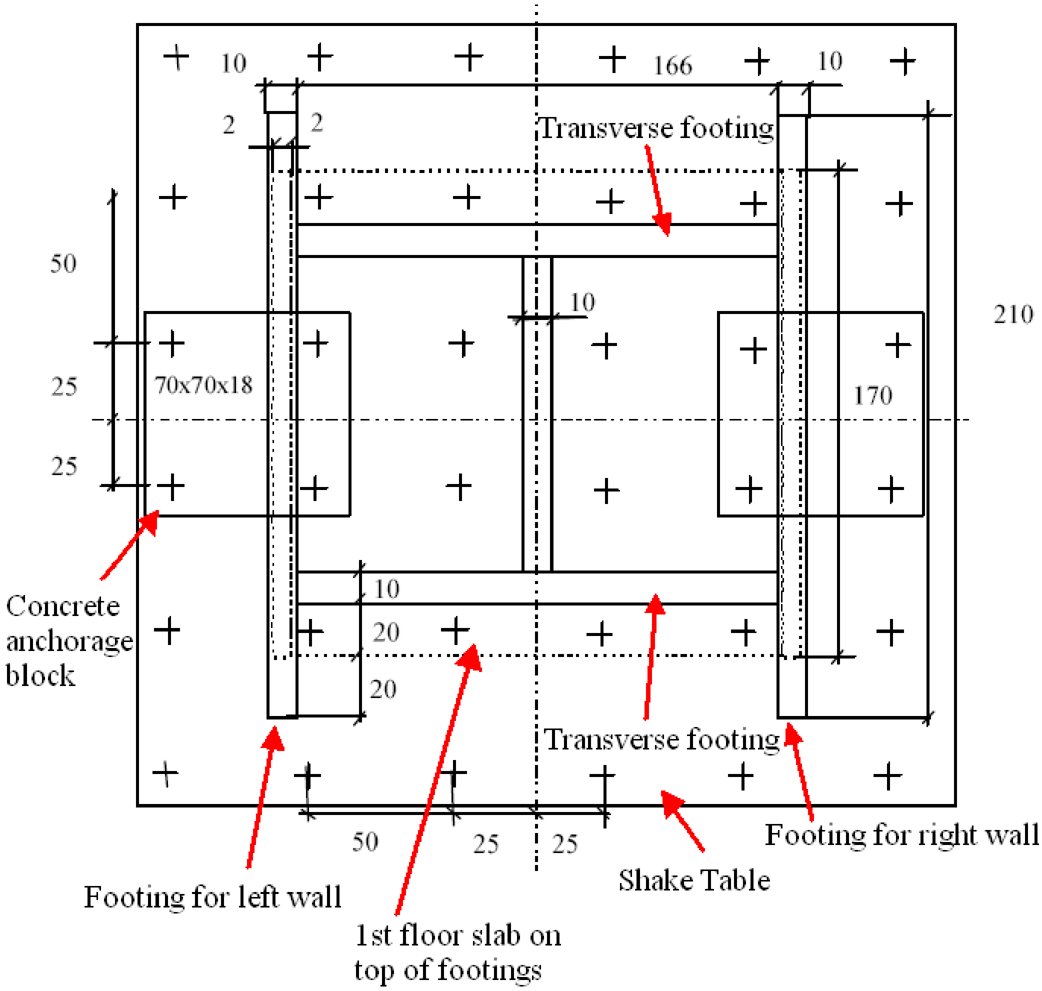

Figure 3-24: Anchorage Locations (+) on the Shake Table (Combescure et al., 2002)

3.2.5 Table Rocking Observations

The referenced report made mention that significant rocking occurred during the test and provided a recommended model to capture this response. (Combescure et al., 2002) This can be seen in Figure 3-25.

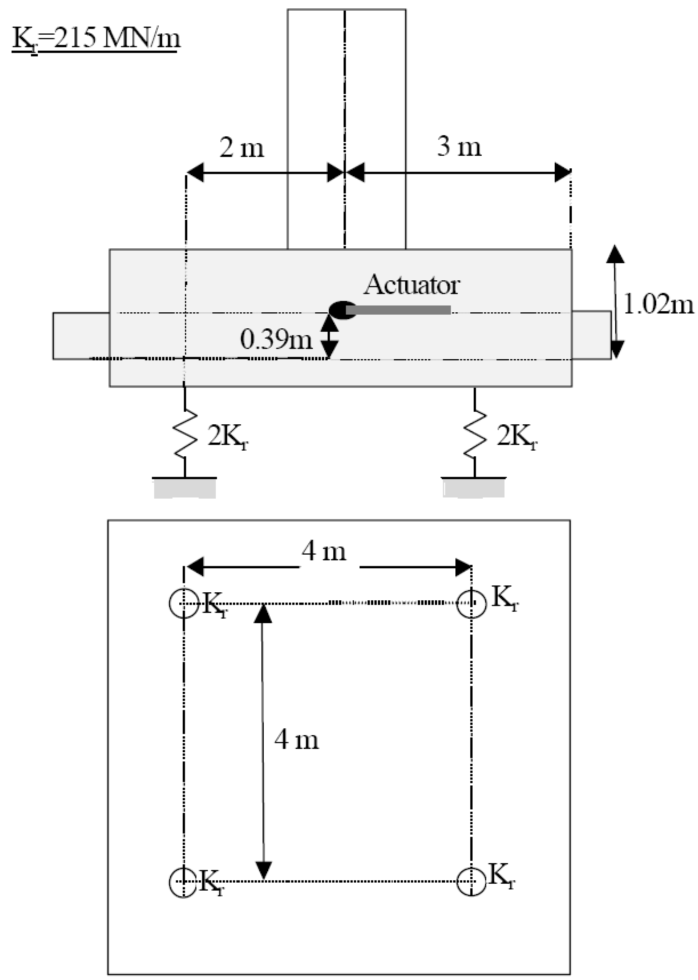

Figure 3-25: Suggested Model for Azalee Shaking Table (Combescure et al., 2002)

3.2.6 Instrumentation

The CAMUS 2000 specimen was instrumented to provide information on the global and local behavior of the specimen as well as to measure the response of the shake table. Figure 3-26 and Figure 3-27 show the location of floor accelerometers that measured the accelerations of the left and right walls in the X, Y and Z directions at the story levels as well as the location of displacement transducers used to measure the absolute displacement of the wall. Figure 3-28 shows the location of displacement transducers used to measured wall deformation. Figure 3-29 shows the location of strain gauges. Figure 3-30 shows the location of table instrumentation used to measure acceleration and displacements of the shake table.

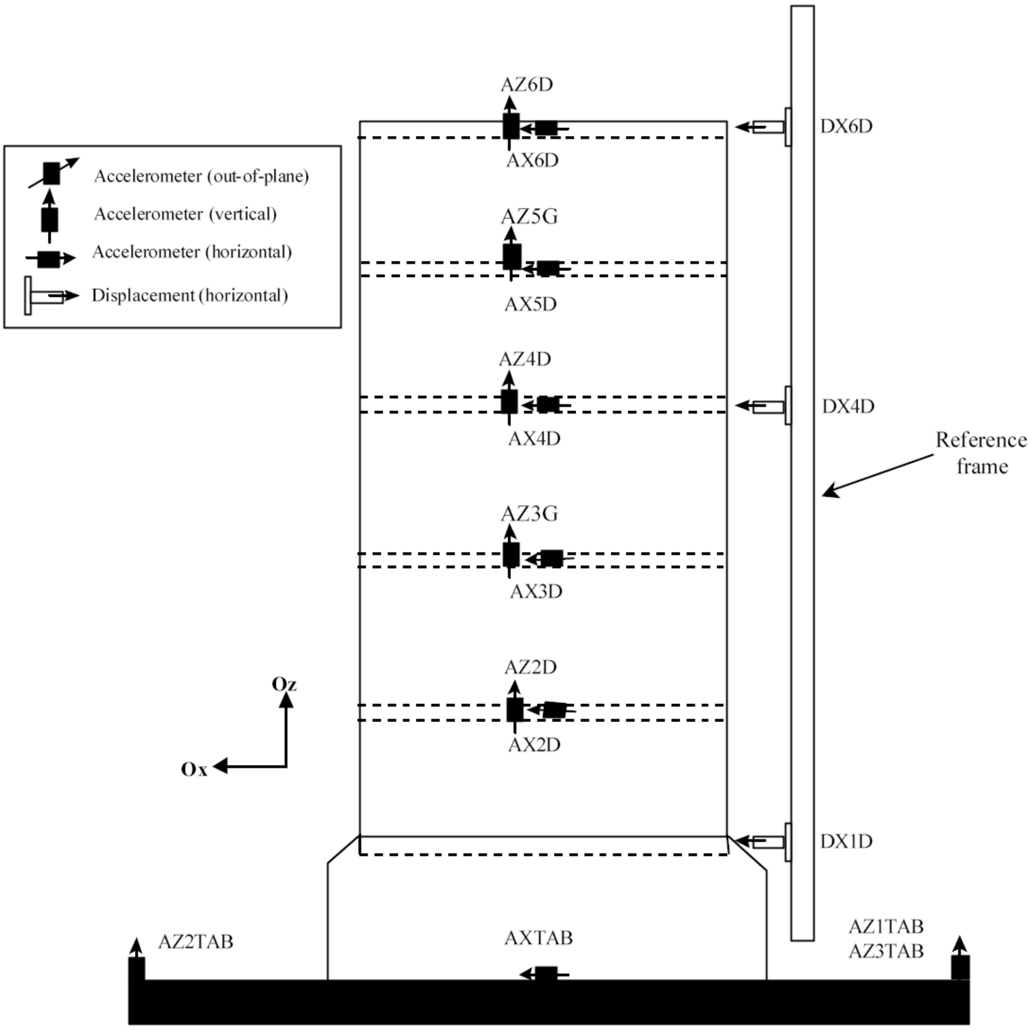

Figure 3-26: Location of Displacement Transducers and Accelerometers on Right Wall. (Combescure et al., 2002)

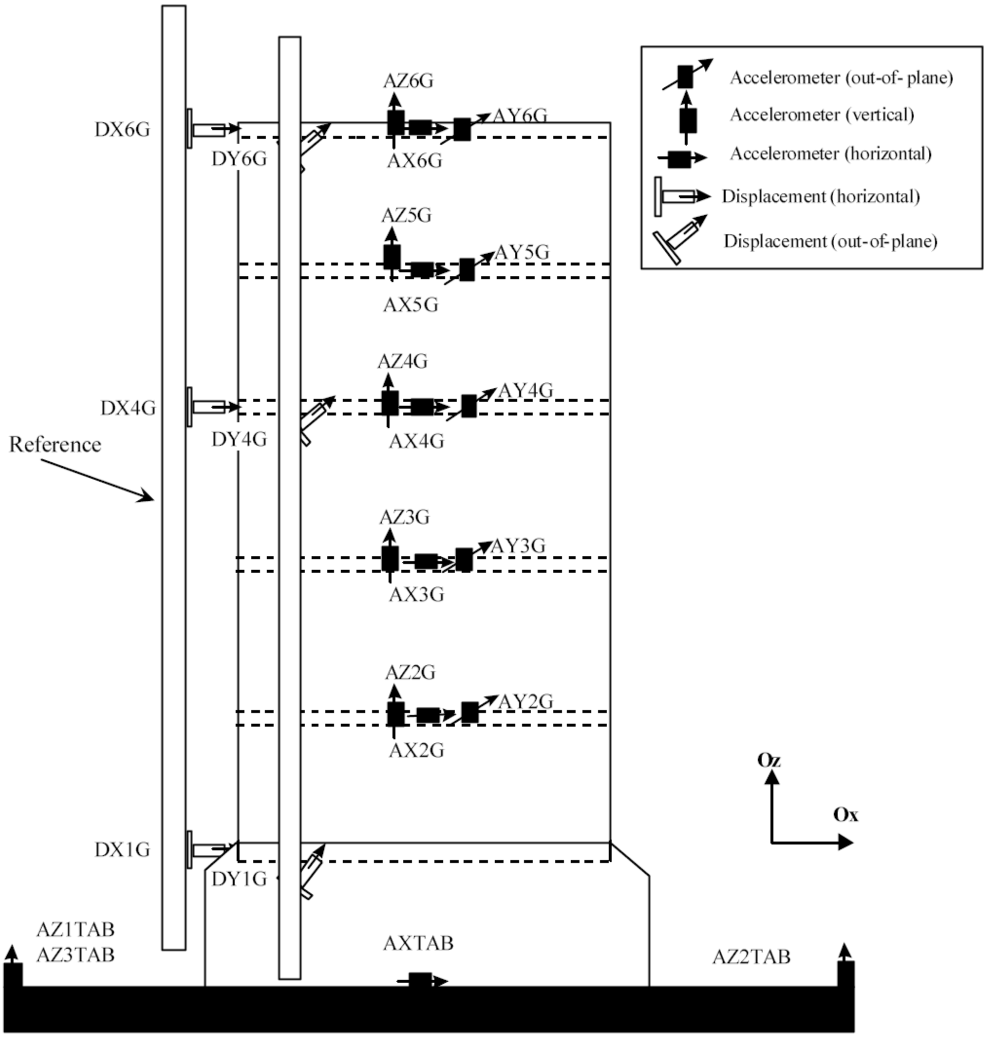

Figure 3-27: Location of Displacement Transducers and Accelerometers on Left Wall. (Combescure et al., 2002)

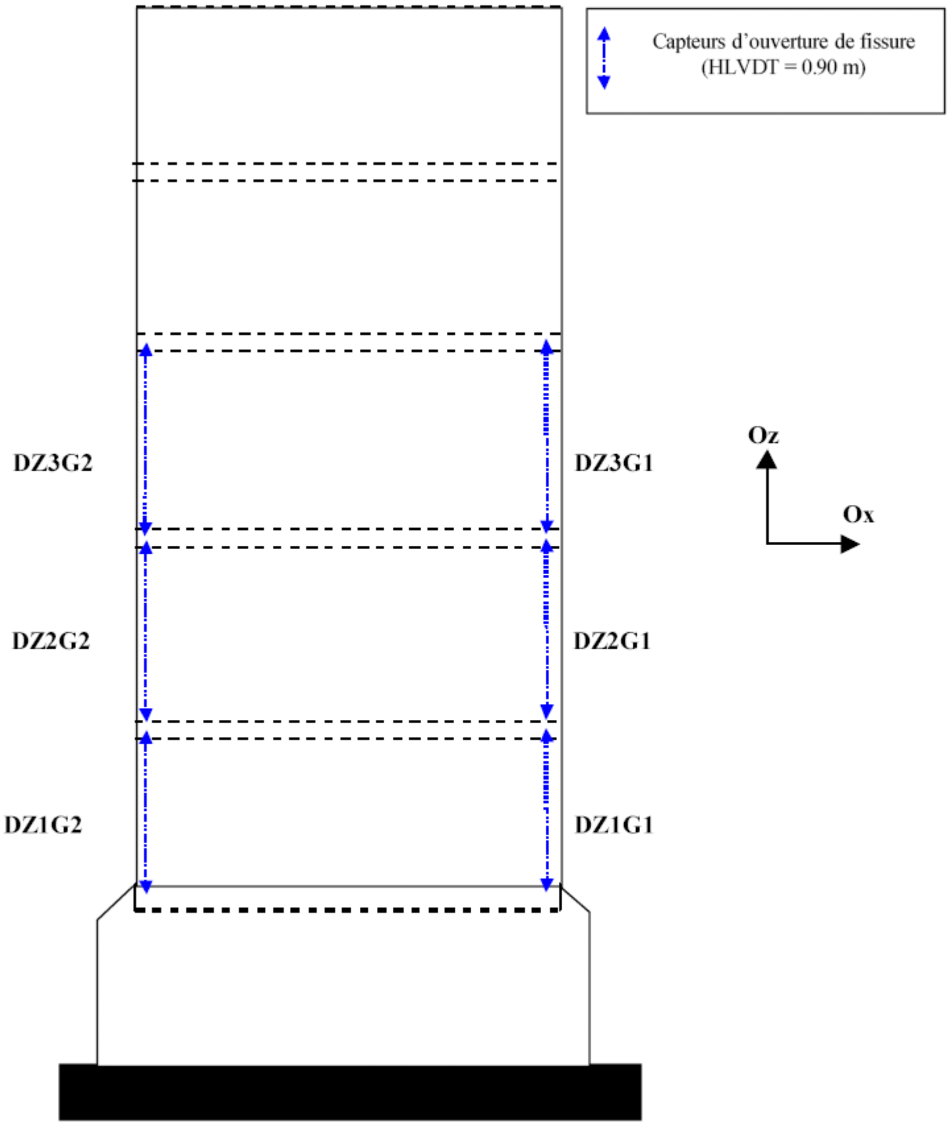

Figure 3-28: Position of Transducers Measuring Crack Openings, Left Wall (Combescure et al., 2002)

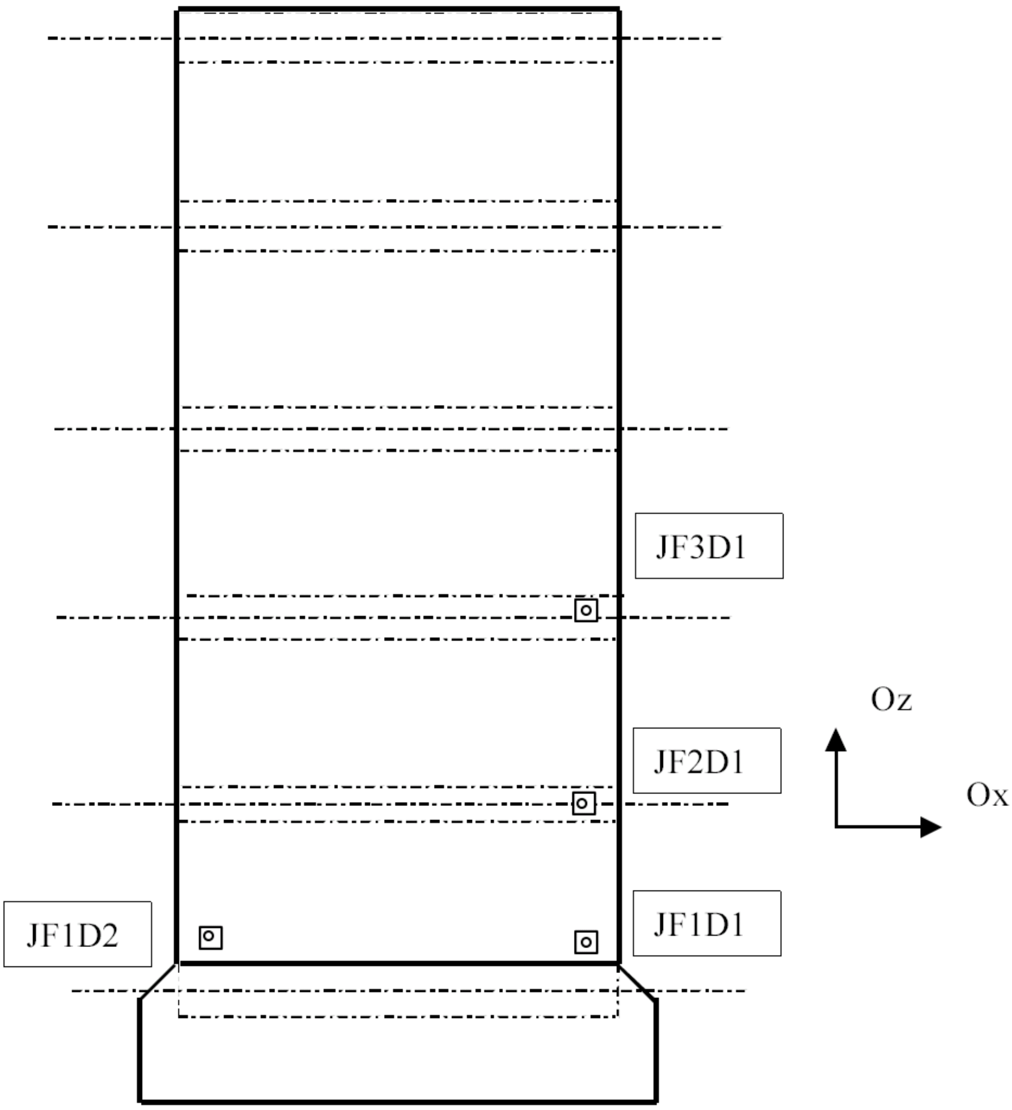

Figure 3-29: Position of Strain Gauges, Left Wall (Combescure et al., 2002)

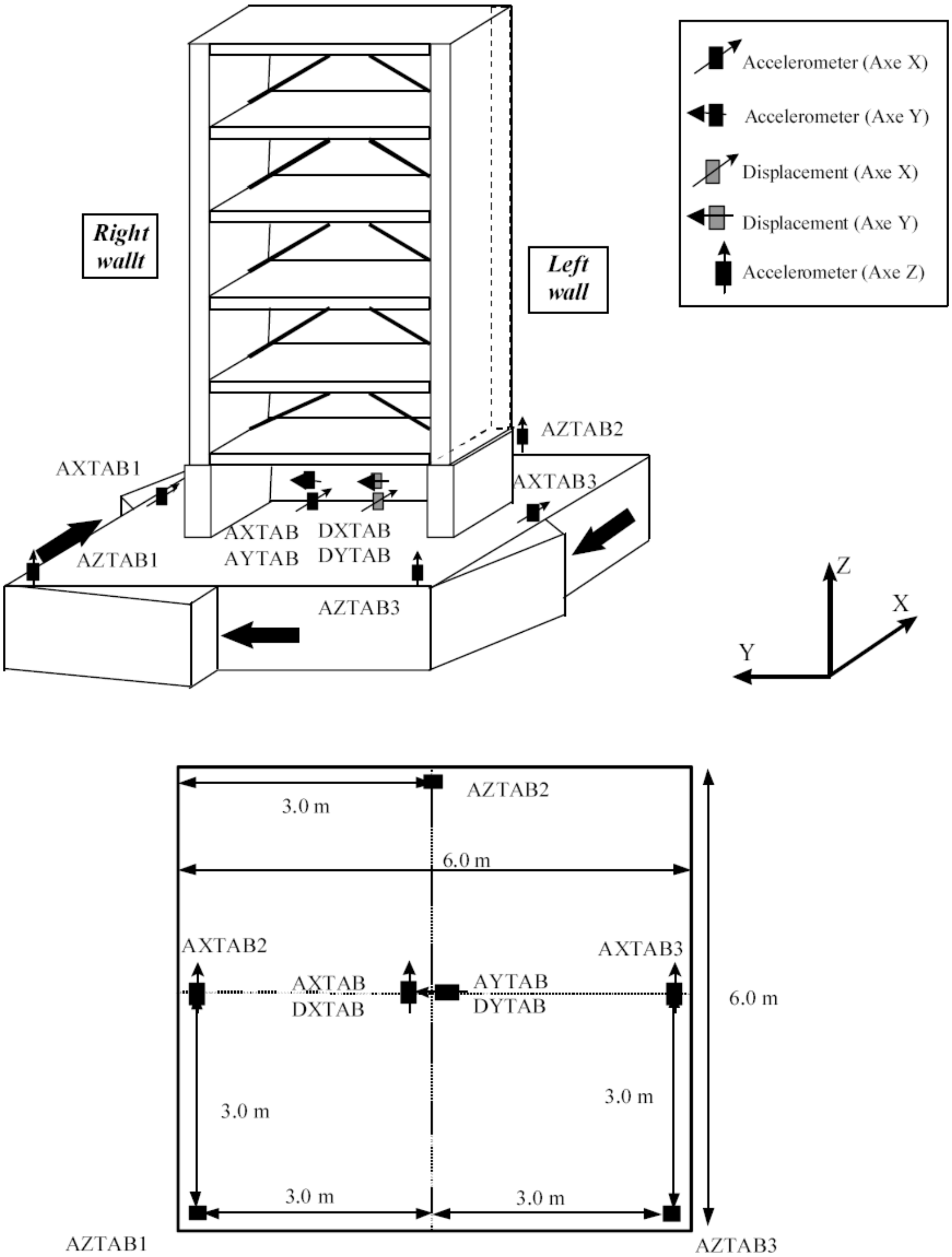

Figure 3-30: Location of Table Instrumentation (Combescure et al., 2002)

3.2.7 Applied Earthquake Excitation

The specimen was subjected to three ground motions. Each motion consisted of two uncorrelated synthetic acceleration records in the X- and Y-direction (where the X-direction is parallel to the concrete walls and the Y-direction is perpendicular). To account for the 1/3 geometric scale of the specimens, the time scale of the ground motion records were scaled by $(1/3)^{1/2}$. Table 3-17 shows the peak ground accelerations (Combescure et al., 2002). Figure 3-31 and Figure 3-32 show the acceleration response spectra in the X- and Y-directions, respectively. Acceleration records for the period of strong motion for the X- and Y-directions for each of the three ground motions can be found in Appendix E.

Table 3-17: Peak Ground Accelerations for Each Run in the X and Y Direction (Combescure et al., 2002)

Tests	**Run 1**	**Run 2**	**Run 3**
Peak ground acceleration, x direction	0.22g	0.62g	0.67g
Peak ground acceleration, y direction	0.22g	0.70g	0.97g

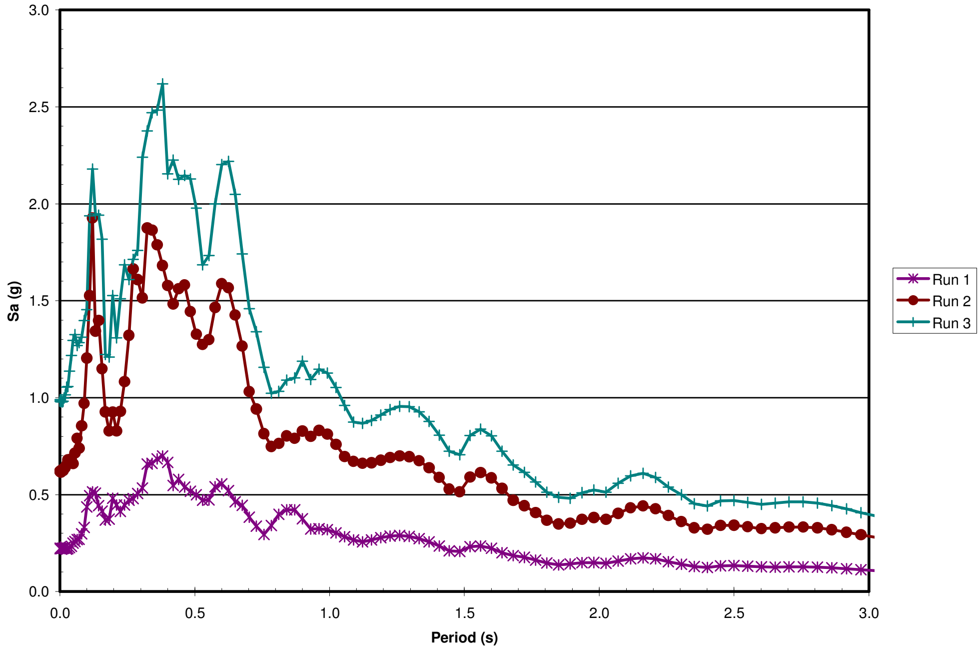

Figure 3-31: CAMUS 2000 Acceleration Response Spectra, Wall (X) direction – 5% damping

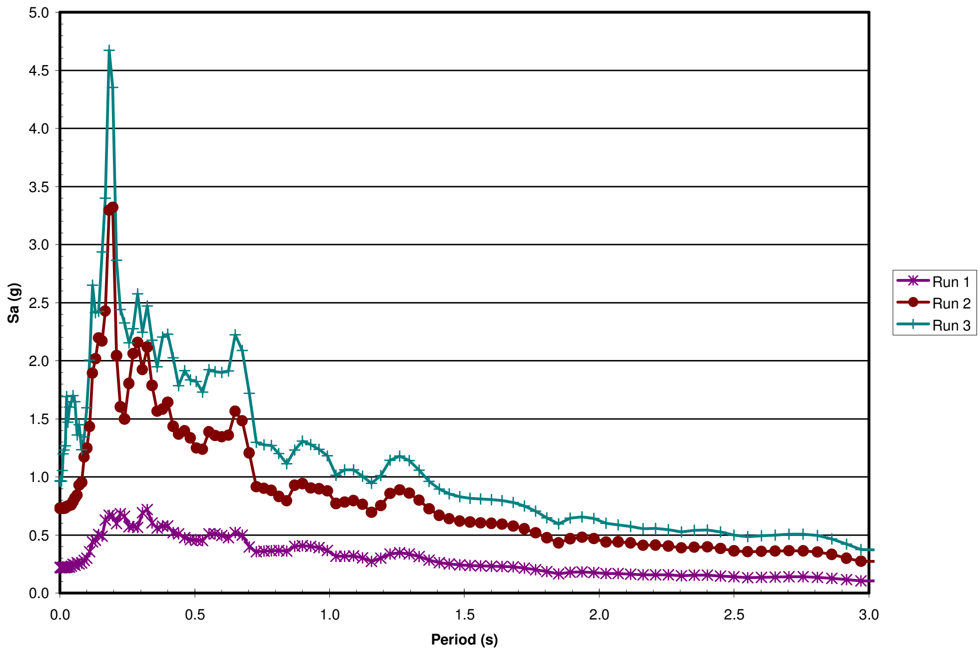

Figure 3-32: CAMUS 2000 Acceleration Response Spectra, Brace (Y) direction – 5% damping

3.2.8 Wall Performance

Information provided by Combescure et al. (2002) suggests that in addition to flexure, the shaking of the table had a large impact on the response. Little information is provided regarding the performance in the first two runs; however the third run saw a sudden and unexpected sliding shear failure.

Combescure et al. characterize wall response primarily on the basis of maximum concrete crack width and steel strain. Data on the crack openings at the extremities of the lower 3 stories of both walls and maximum strain values from strain gauges are listed in Table 3-18 and Table 3-19. No information is provided regarding the spacing or orientation of cracking. Figure 3-33 and Figure 3-34 show damage after Run 3; the figures appear to show a sliding shear failure in the walls at the second floor slab. This failure is surprising as it did not occur at the interface between the wall and the foundation. This could be a result of the fact that the amount of reinforcement was reduced significantly between the foundation element (6-4.5 mm bars per side per wall) and the second floor slab (3-4.5 mm bars per side per wall)

Table 3-18: CAMUS 2000 Damage Data, metric (Combescure et al., 2002)

Location	Wall	Units	Run 1	Run 2	Run 3
Roof Displacement	Left wall	mm	3.59	13.20	18.70
	Right wall	mm	4.25	16.10	18.30
Roof Drift	Left wall	mm	0.080%	0.293%	0.416%
	Right wall	mm	0.094%	0.358%	0.407%
Crack opening at 3rd story	Left wall	mm	-0.084	0.97	3.50
		mm	0.202	-0.26	-0.29
	Right wall	mm	-0.074	0.84	1.41
		mm	0.172	-0.20	-0.41
Crack opening at 2rd story	Left wall	mm	-0.122	0.99	7.59
		mm	0.286	-0.39	-0.40
	Right wall	mm	-0.152	1.47	3.52
		mm	0.338	-0.37	-0.59
Crack opening at 1st story	Left wall	mm	-0.214	2.35	2.97
		mm	0.43	-0.53	-1.68
	Right wall	mm	-0.199	3.86	3.73
		mm	0.423	-0.51	-0.84
Strain at 1st storey	Left wall	με	-860	3540	4150
		με	3330	-1260	-1540
	Right wall	με	-580	3680	4280
		με	1440	-1270	-1350

Table 3-19: CAMUS 2000 Damage Data, English standard units

Location	Wall	Units	Run 1	Run 2	Run 3
Roof Displacement	Left wall	in	0.14	0.52	0.74
	Right wall		0.17	0.63	0.72
Roof Drift	Left wall	in	0.080%	0.293%	0.416%
	Right wall		0.094%	0.358%	0.407%
Crack opening at 3rd story	Left wall	in	-0.0033	0.0382	0.1378
		in	0.0080	-0.0102	-0.0114
	Right wall	in	-0.0029	0.0331	0.0555
		in	0.0068	-0.0079	-0.0161
Crack opening at 2rd story	Left wall	in	-0.0048	0.0390	0.2988
		in	0.0113	-0.0154	-0.0157
	Right wall	in	-0.0060	0.0579	0.1386
		in	0.0133	-0.0146	-0.0232
Crack opening at 1st story	Left wall	in	-0.0084	0.0925	0.1169
		in	0.0169	-0.0209	-0.0661
	Right wall	in	-0.0078	0.1520	0.1469
		in	0.0167	-0.0201	-0.0331
Strain at 1st storey	Left wall	με	-860	3540	4150
		με	3330	-1260	-1540
	Right wall	με	-580	3680	4280
		με	1440	-1270	-1350

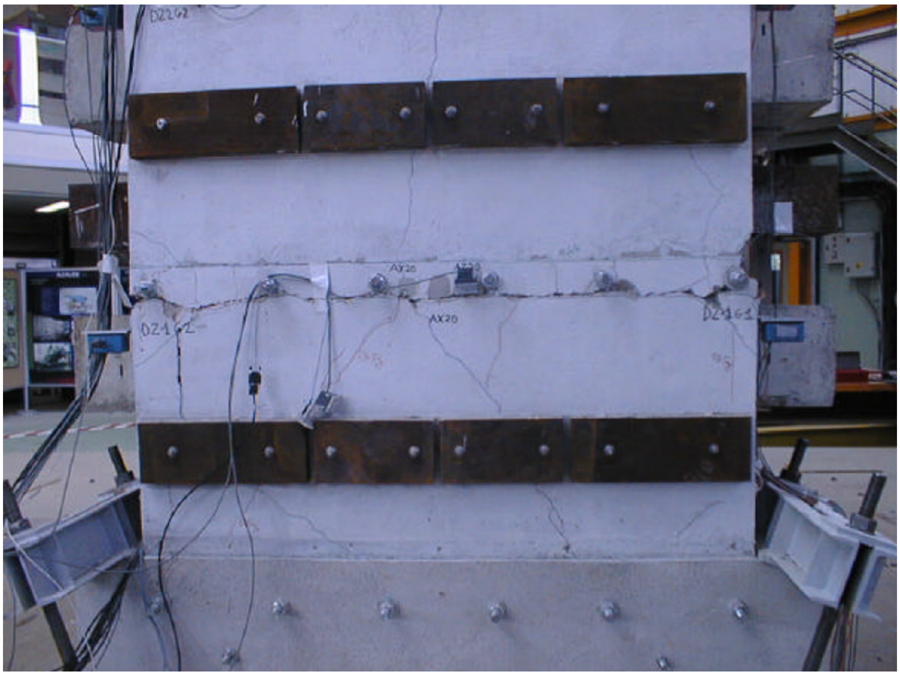

Figure 3-33: Main Damage at Base after Run 3 (Combescure et al., 2002)

Figure 3-34: Failure at Bottom Slab Level (Combescure et al., 2002)

3.3 CAMUS C-Shaped Wall Specimens

In addition to the CAMUS 2000 rectangular wall specimen described above, four c-shaped specimens were tested on the Azalee shaking table of the CEA at the Saclay Nuclear Center in Lisbon. The c-shaped specimens were all one-story structures, constructed at 3/5-scale and excited in the direction of the flange walls (Reynouard and Fardis, 2001). Figure 3-35 shows an isometric view of the specimen, including the roof slab.

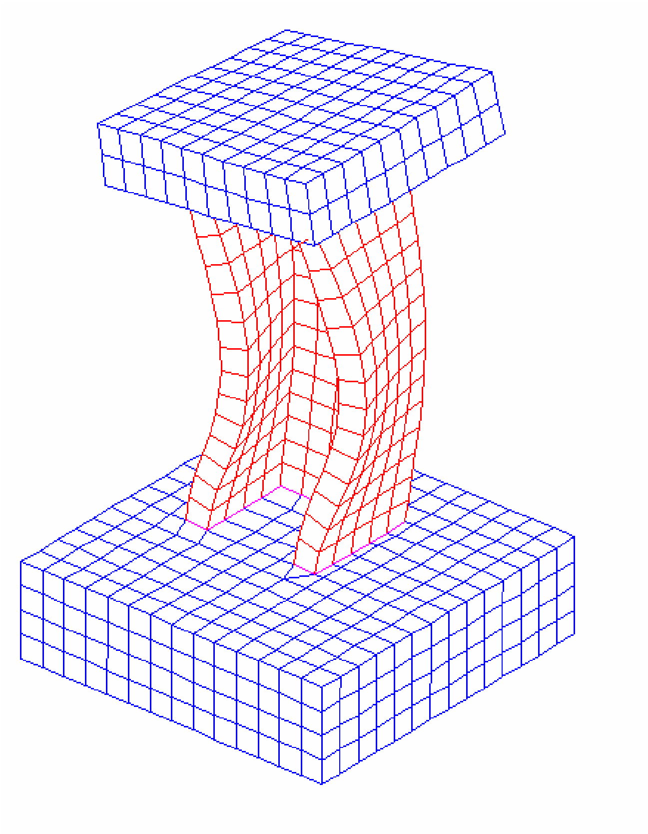

Figure 3-35: CAMUS C-Shaped Specimen Isometric (Reynouard and Fardis, 2001)

3.3.1 Geometry and Reinforcement

Four different c-shaped specimens were tested as part of this test program. The specimens were geometrically equivalent and differed only in the spacing of the stirrups used to confine the boundary element concrete. Table 3-20 summarizes the dimensions of the specimen, and the basic specimen geometry is shown in Figure 3-36 through Figure 3-38. Figure 3-39 shows the reinforcement layout for the specimens; Table 3-12 lists reinforcement ratios for the specimens. In Figure 3-40, boundary-element stirrups spacing is defined as a function of parameters "A" and "B". The value of parameters "A" and "B" for each specimen and the resulting transverse reinforcement ratios are provided in Table 3-21.

Table 3-20: Summary of CAMUS U Specimen Geometry

Member	Property	Dimensions (cm)	Dimensions (in)	Aspect Ratio
Flange Walls (*2)	Story Height	315	124.0	4.20
	Height	315	124.0	
	Length	75	29.5	
	Thickness	15	5.9	
Web Wall	Story Height	315	124.0	3.50
	Height	315	124.0	
	Length	90	35.4	
	Thickness	15	5.9	
Slab (*1)	Length	120	47.2	-
	Width	120	47.2	
	Thickness	15	5.9	
Additional Weights (*1)	Length	197	77.6	-
	Width	197	77.6	
	Thickness	198	78.0	
Specimen	Scale	0.60		

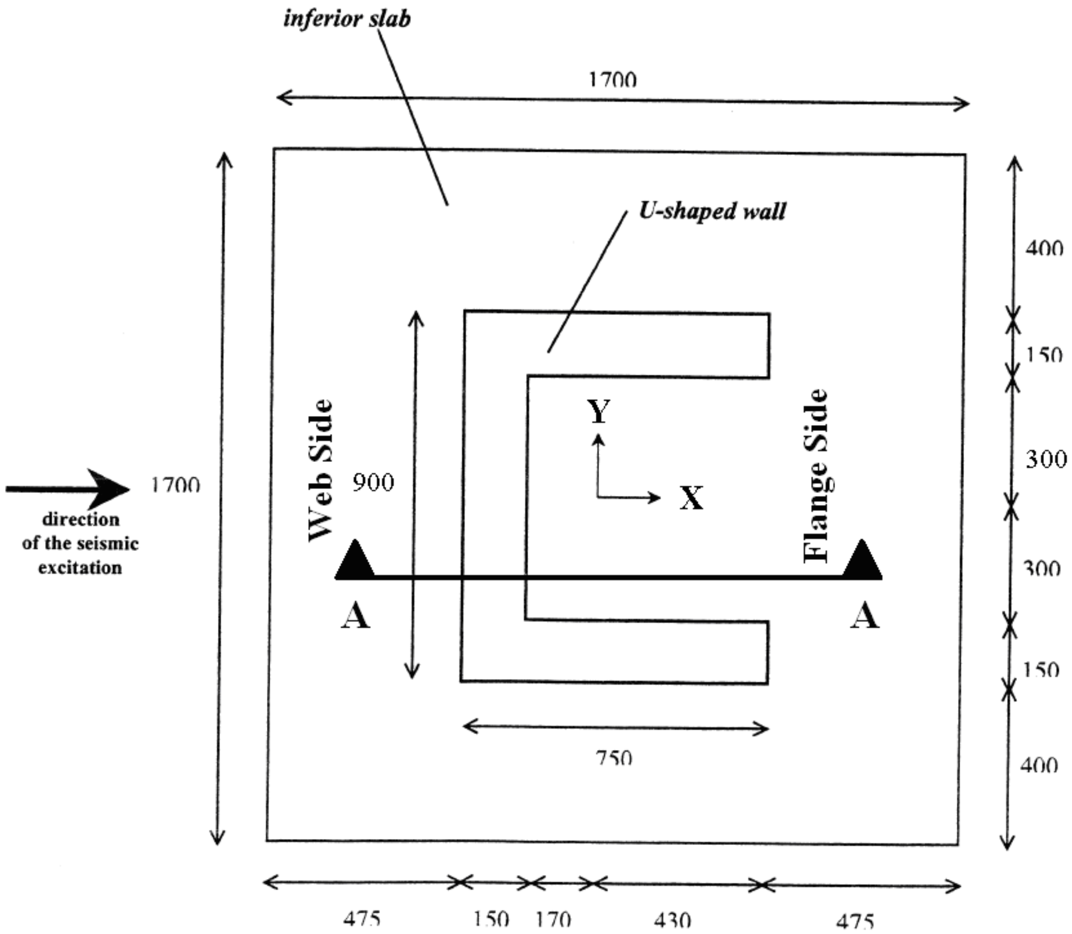

Figure 3-36: C-shaped Specimen Plan, units in millimeters (Reynouard and Fardis, 2001)

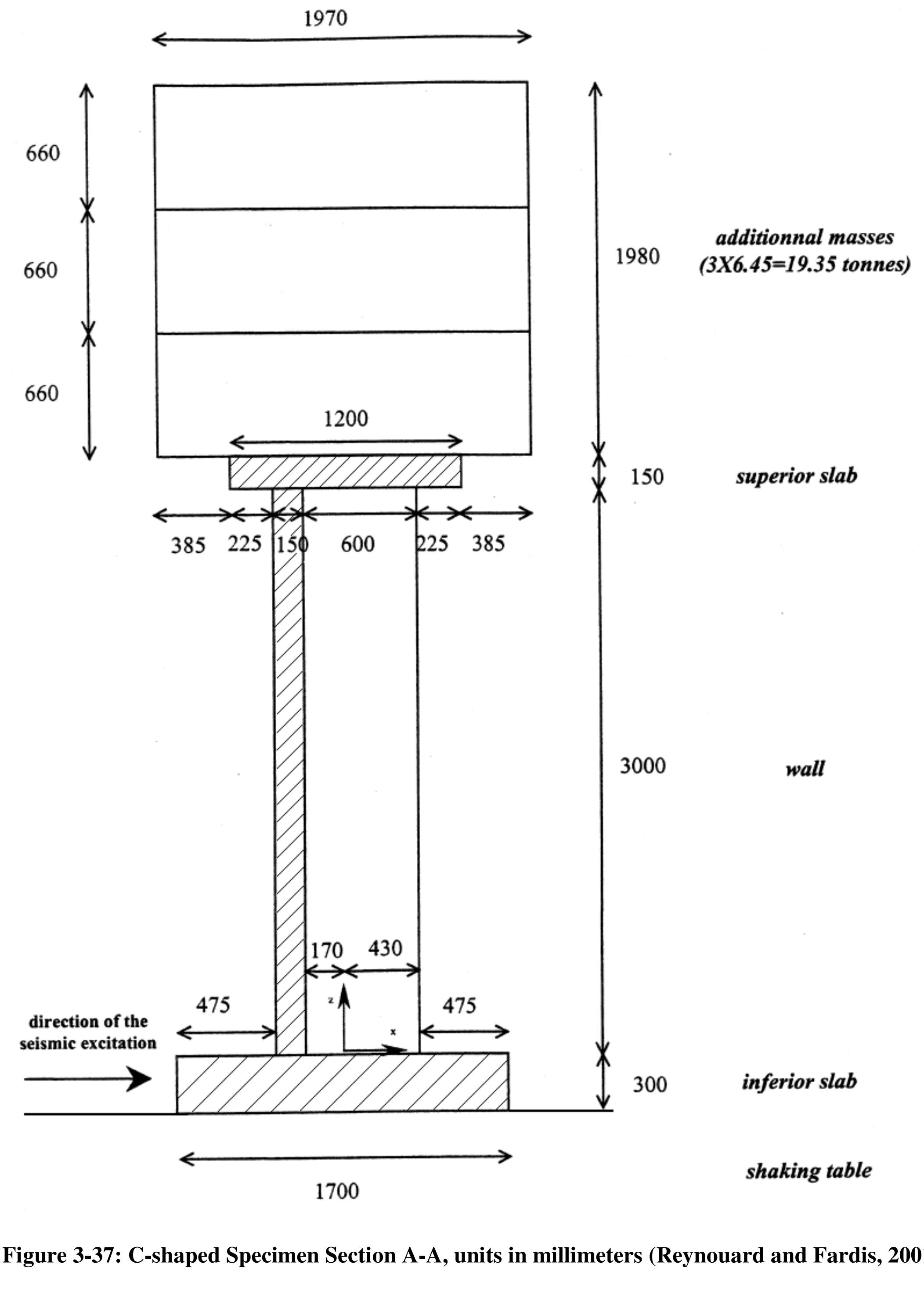

Figure 3-37: C-shaped Specimen Section A-A, units in millimeters (Reynouard and Fardis, 2001)

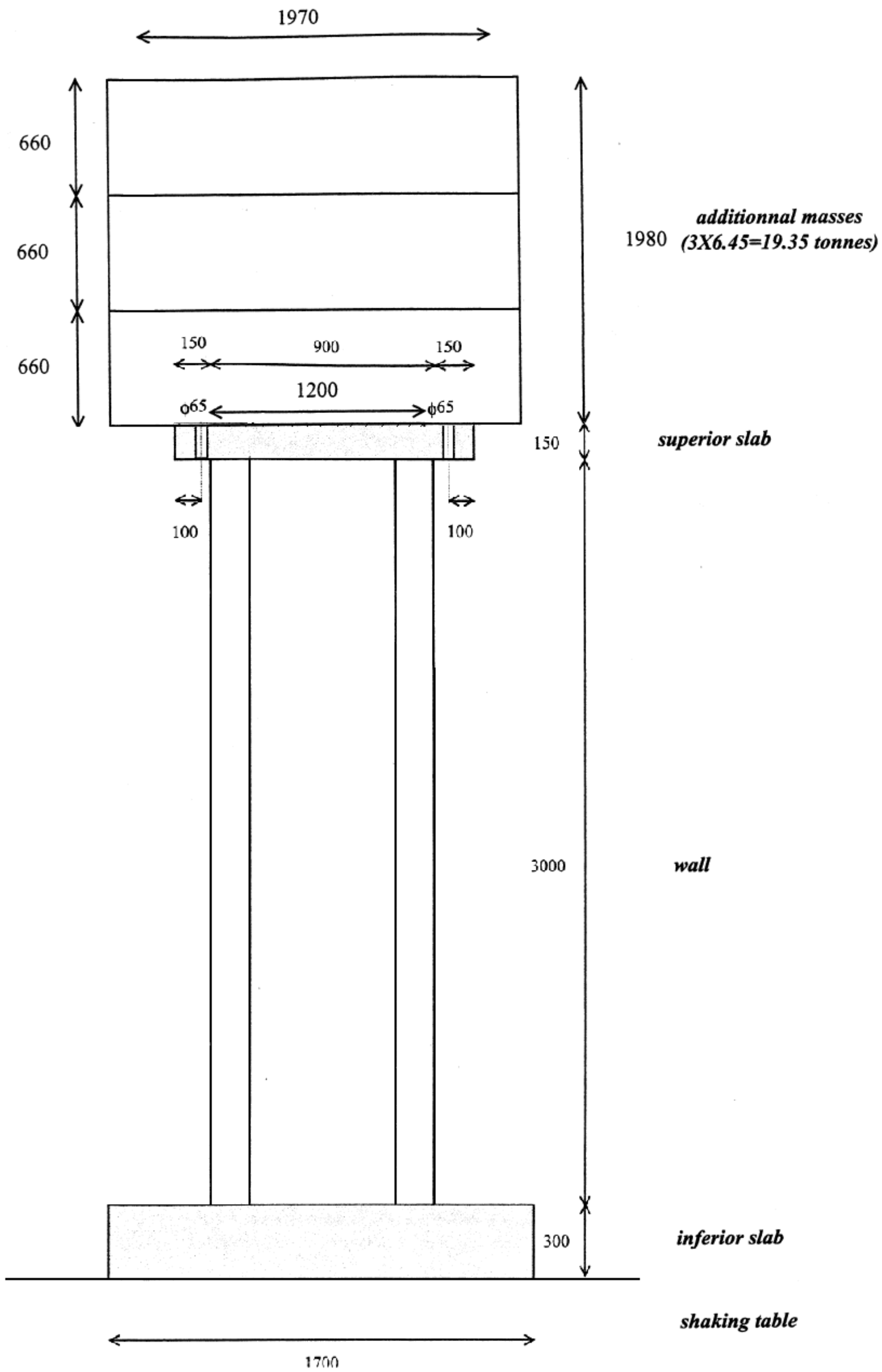

Figure 3-38: C-shaped Front Elevation, units in millimeters (Reynouard and Fardis, 2001)

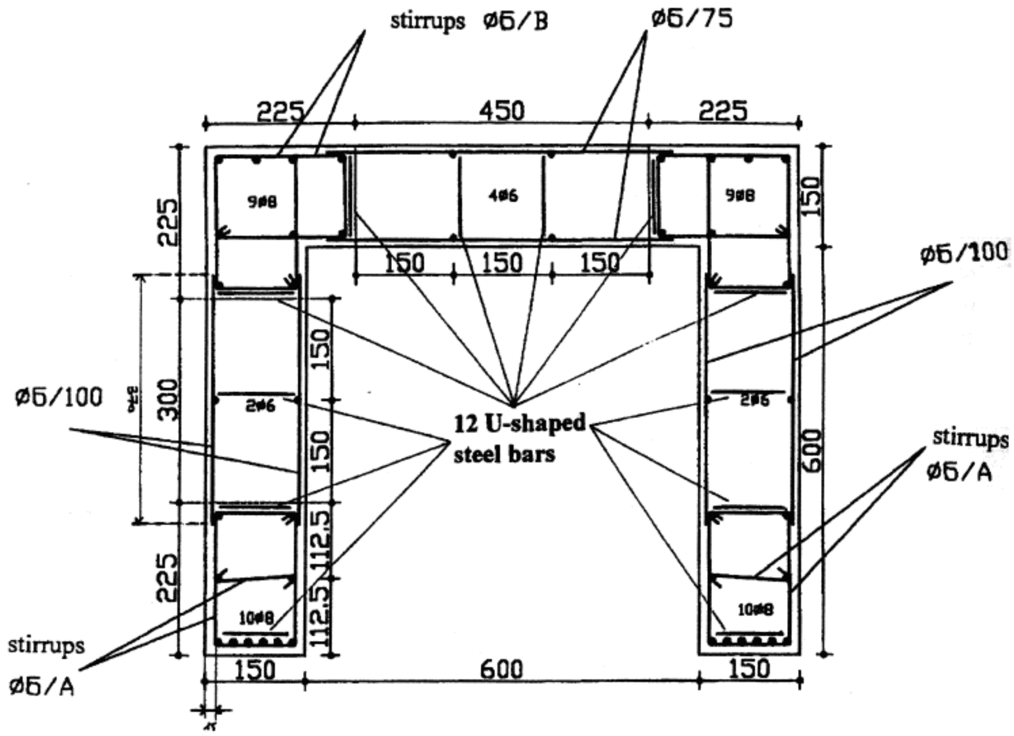

Figure 3-39: Horizontal Section Displaying Location of Longitudinal and Transverse Reinforcement, units in millimeters (Reynouard and Fardis, 2001)

Table 3-21: CAMUS U Wall Reinforcement Summary

	Specimen	Vertical Reinforcement Ratio			Transverse Reinforcement Ratio		
		Average ρv	Interior Wall ρv	Boundary Element ρv	Spacing of stirrups cm *	Interior Wall ρh	Boundary Element ρh
Flange Walls	0	0.81%	0.13%	1.49%	A = 4	0.38%	0.94%
	1				A = 10		0.38%
	2				A = 10		0.94%
	3				A = 4		0.94%
Web Wall	0	0.61%	0.11%	1.04%	B = 4	0.50%	0.94%
	1				B = 10		0.38%
	2				B = 4		0.38%
	3				B = 4		0.94%

* Where "spacing of stirrups" in the flange walls implies the stirrup spacing in the boundary elements on the flange side and the spacing in the web implies the boundary element region shared by the flange and web on the web side of the specimen

3.3.2 Material Properties

The specimens were constructed using normal weight concrete. The reinforcing steel used in construction had significantly larger yield strength (approximately 90 ksi) than is used typically in the United States. This is likely due to the fact that very small diameter bars (diameter equal to 6 mm, which is equivalent to a No 2 or 3 at full scale) were used, necessitating fabrication of deformations on the bars via mechanical action and resulting in work hardening of the steel. The concrete properties are listed in Table 3-22 and Table 3-23 and the steel properties are listed in Table 3-24 and Table 3-25. The concrete properties were determined by compressive and splitting tests on 100 mm diameter by 320 mm cylinders. For each specimen, six compressive cylinders and three tensile cylinders were tested.

Table 3-22: Average Concrete Properties, metric (Reynouard and Fardis, 2001)

Wall	Specified		Measured		
	f'_c (MPa)	E_c (MPa)	f'_c (MPa)	f_r (MPa)	E_c (MPa)
0	25	30500	Information not provided		
1	25	30500	32.3	3.64	25937
2	25	30500	32.8	3.23	26957
3	25	30500	43.9	3.83	29530

Table 3-23: Average Concrete Properties, English standard units (Reynouard and Fardis, 2001)

Wall	Specified		Measured		
	f'_c (ksi)	E_c (ksi)	f'_c (ksi)	f_r (ksi)	E_c (ksi)
0	3.6	4423.7	Information not provided		
1	3.6	4423.7	4.7	0.5	3761.8
2	3.6	4423.7	4.8	0.5	3909.8
3	3.6	4423.7	6.4	0.6	4283.0

Table 3-24: Average Reinforcing Steel Properties, metric (Reynouard and Fardis, 2001)

Steel diameter (mm)	Specified	Measured			
	f_y (MPa)	E (MPa)	f_y (MPa)	f_{su} (MPa)	ε_{su} (%)
6	500	190744	604	625	1.034
8	500	206830	643	660	1.026

Table 3-25: Average Reinforcing Steel Properties, English standard units (Reynouard and Fardis, 2001)

Steel diameter (in)	Specified	Measured			
	f_y (ksi)	E (ksi)	f_y (ksi)	f_{su} (ksi)	ε_{su} (%)
6	72.5	27665.1	87.6	90.6	1.034
8	72.5	29998.2	93.3	95.7	1.026

In Table 3-25, f_{su} is the failure stress and ε_{su} is the ultimate strain.

3.3.3 Specimen Mass

When scaling a specimen, the volume and thus the mass decrease by the scale factor cubed. The area by contrast decreases by the scale factor squared. Thus the stresses due to self weight decrease by the scale factor when they should stay the same. For this reason, the researchers provided additional weight at the top story to simulate typical axial loading for a wall building. The added masses as well as the masses of the structural elements are summarized below in Table 3-26.

Table 3-26: Masses and Weights of Specimen (Reynouard and Fardis, 2001)

Structural element	Mass of each element (*1000 kg)	Weight of each element (kips)
Wall specimen	2.36	5.20
Footing	2.18	4.81
Top slab	0.54	1.19
Total mass of specimen	5.08	11.03
3 Additional masses	3 x 6.45 = 19.35	42.67
Total mass	24.35	53.70
W/(f'c*Ag) (%)	2.07%	

3.3.4 Table and Anchorage Specifications

The specimens were tested on the Azalee shaking table of the EMSI Laboratory of the CEA; the same table as was used to test the previously discussed CAMUS 2000 parallel wall specimen. Figure 3-40 provides a plan view of the interior (footing) slab and the location of holes used to connect the slab to the table. Figure 3-41 shows the location of the anchors used for each test. Some available anchor locations were not used due to poor casting of the slab. Specimen 0 and 2 were the first to be tested. During the tests, significant damage was observed in the footing slab. In order to mitigate the damage in subsequent tests several steel plates were added to the footing slab.

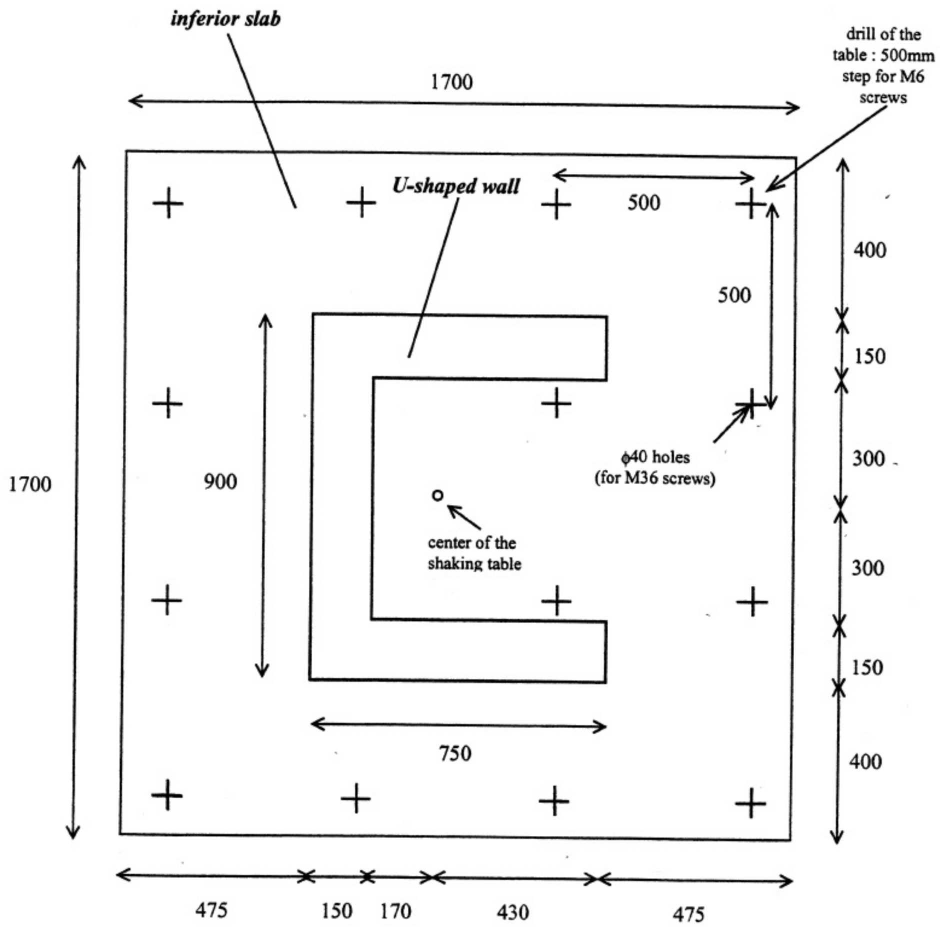

Figure 3-40: Footing Slab of Specimen and Location of Potential Connections (Reynouard and Fardis, 2001)

Note: Bottom slab covers entire shake table

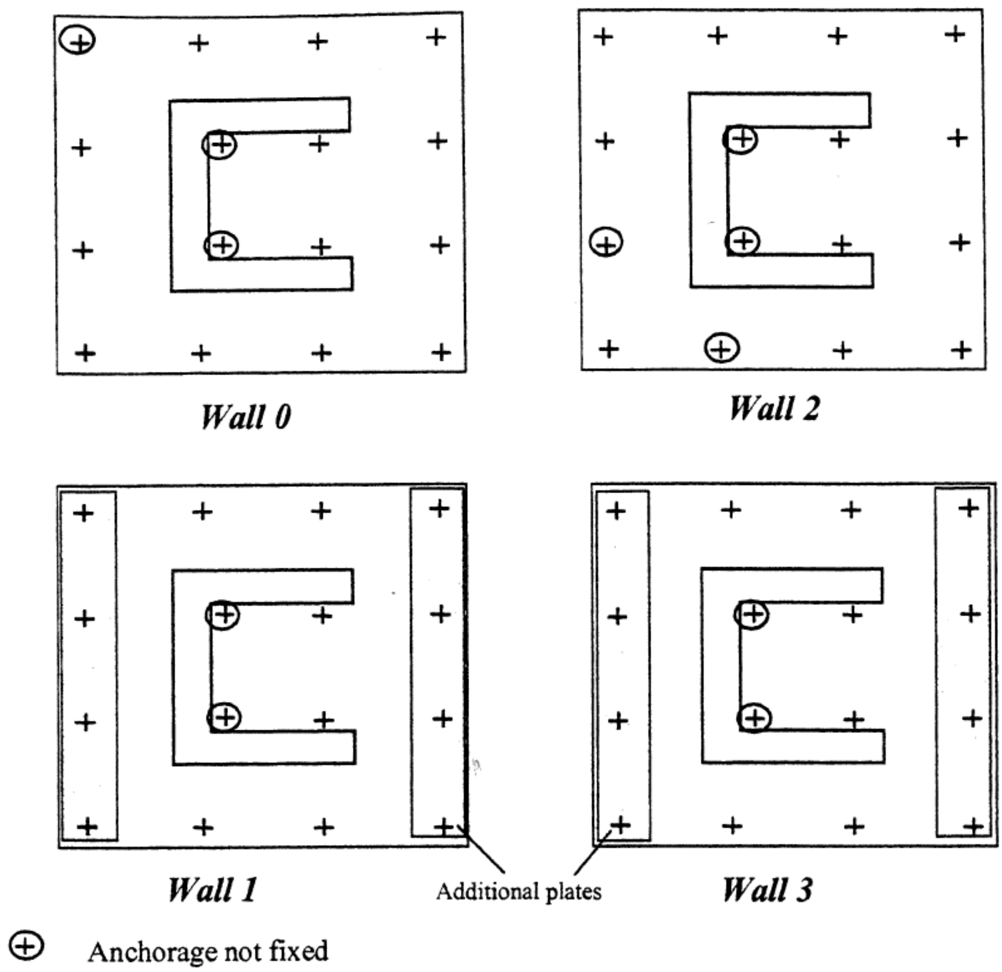

Figure 3-41: Anchorage Conditions and Location of Additional Plates for Wall Specimens (Reynouard and Fardis, 2001)

3.3.5 Table Rocking Observations

Although the specimens were tested on the same table as the CAMUS 2000 specimen, no mention was made about table rocking. It is unclear whether the model suggested for the CAMUS 2000 specimen is appropriate for this specimen as well.

3.3.6 Instrumentation

The specimen was instrumented to measure the absolute displacement and acceleration of the specimen at different locations on the wall plan and up the height. Relative measurements were also taken of wall, specifically targeting crack openings on the flanges, shear deformation on the flanges and strain of vertical reinforcement as well as stirrups. The table was also instrumented using accelerometers to record both in-plane motion as well as any undesired out-of-plane motion due to table rocking. Although the report by Reynouard and Fardis (2001) discusses numerous instruments and data sets, not all of these data were available for use in the current study. Figure 3-42 provides a visual representation of instrumentation locations made available for this study.

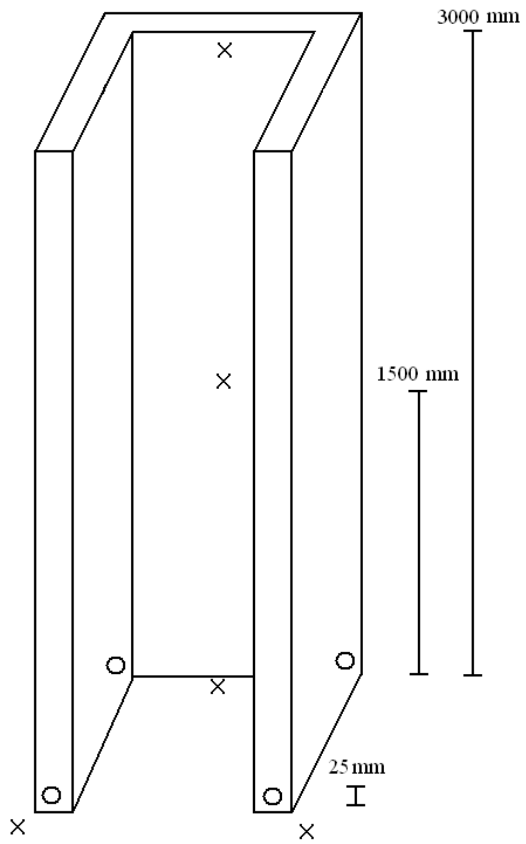

Figure 3-42: Location of Instrumentation. Symbol 'X' Refers to Location of Accelerometers in the X, Y and Z directions. Symbol 'O' refers to Location of Strain Gauges. (Not to Scale)

3.3.7 Applied Earthquake Excitation

The c-shaped walls were excited in only one direction, the X-direction, which is the direction of the flanges (Figure 3-36). Artificial ground motions were used; these were generated from recorded acceleration records by modifying the recorded record to produce a response spectrum that matched the design spectrum specified in Eurocode 8 (EC8) (European Committee for Standardization, 1998). Specifically, "the generation method consists in creating artificial accelerograms from the natural ones, by preserving the phases and changing iteratively the amplitudes to fit as much as possible the EC8 spectrum" (Reynouard and Fardis 166, 2001). Additionally, for one record, ACC3, the time scale was contracted by a scale factor of $(0.6)^{1/2}$ to reduce the maximum displacement. The recorded earthquake acceleration records from which the synthetic records were created are listed in Table 3-27.

Table 3-27: Input Acceleration Description (Reynouard and Fardis, 2001)

Acceleration	Description
ACC1	Kobe, January 17th, 1995 Port-Island
ACC2	Imperial Valley, May 18th, 1940 El Centro Site Imperial Valley Irrigation District
ACC3	San Fernando, February 9th, 1971 900 South Fremont Av., Basement Alhambra
ACC4	Hollister, April 8th, 1961 Hollister City Hall
ACC5	San Fernando, February 9th, 1971 Reservoir, Fairmont Reservoir

Each specimen was subjected to one or more of the synthetic records, scaled to a peak ground acceleration ranging from 0.1 to 1.0 g. The peak ground acceleration for each of the four c-shaped specimens and each stage (or ground motion history) is listed in Table 3-28. This approach to testing the specimens was intended to provide an ample range in the severity of ground excitation. A peak ground acceleration of approximately 0.25g was considered a low-level test, 0.6g an intermediate-level test, and 0.8g to 1.0g a high-level test (Reynouard and Fardis, 2001). Figure 3-43 through

Figure 3-46 show the response spectrum for the each wall specimen for each stage of testing.

Table 3-28: Peak Ground Accelerations for C-shaped Specimen Test (Reynouard and Fardis, 2001)

Specimen	Peak ground acceleration (g)				
	Stage 1	Stage 2	Stage 3	Stage 4	Stage 5
0 *	0.70	0.12	0.24	0.65	0.73
1 +	0.30	0.10	0.25	0.60	0.80
2 +	0.20	0.26	0.63	0.83	1.00
3 +	0.10	0.25	0.61	0.83	1.05

* Values were computed from the acceleration records

\+ Values were provided in the documents and verified through analysis of the acceleration records

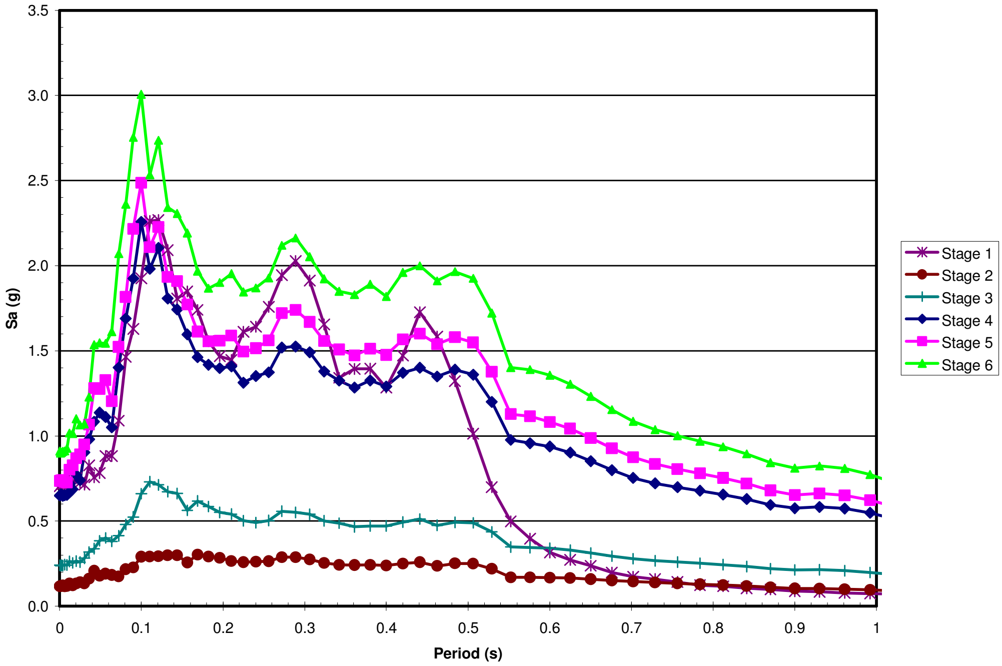

Figure 3-43: CAMUS C Shaped Wall Response Spectrum – 5% Damping, Wall 0

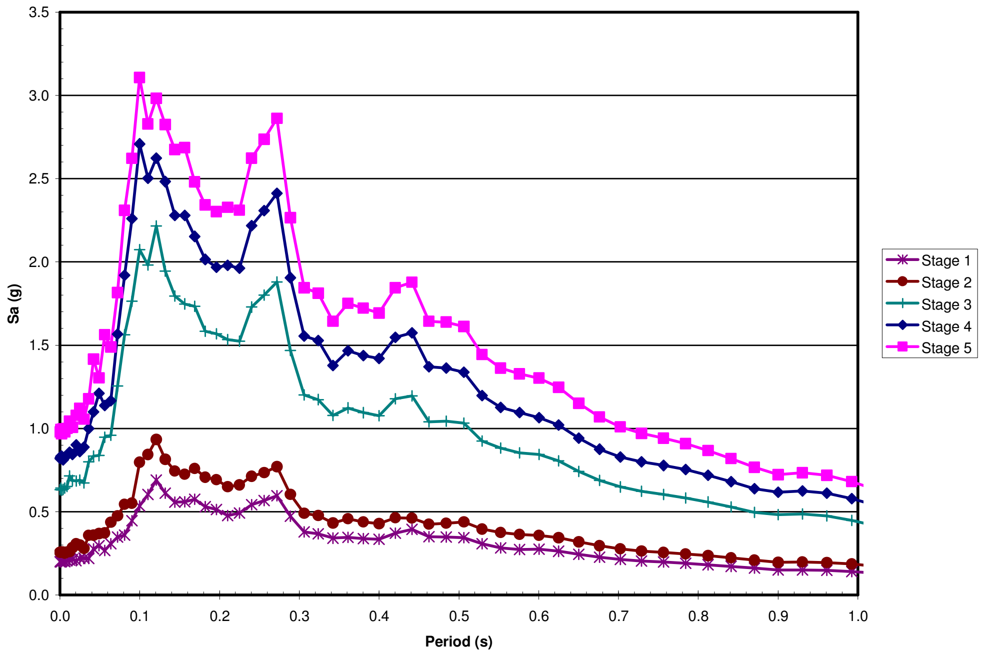

Figure 3-44: CAMUS C Shaped Wall Response Spectrum – 5% Damping, Wall 1

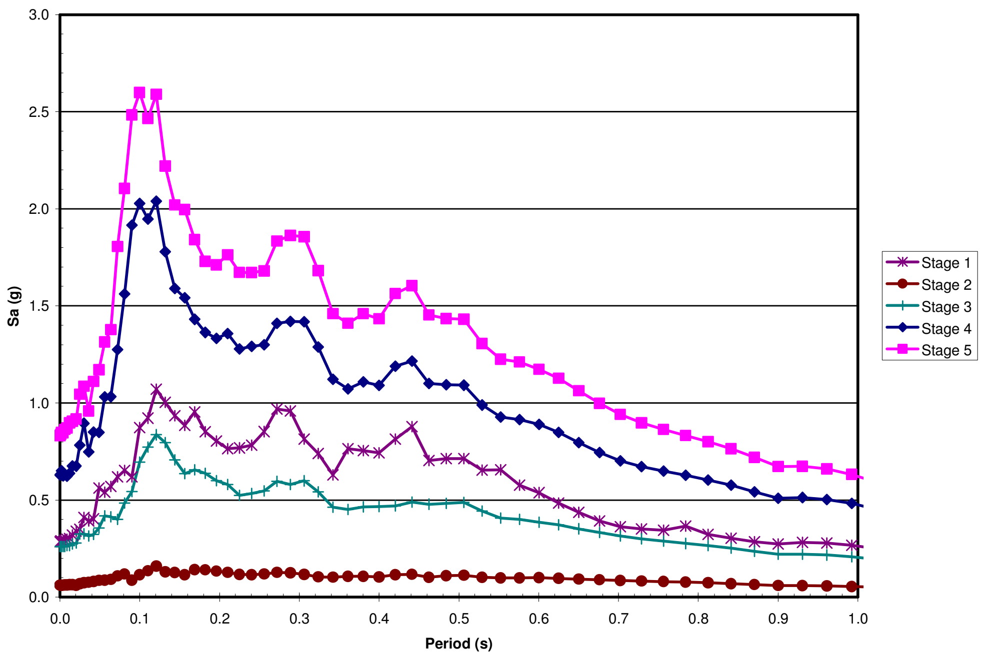

Figure 3-45: CAMUS C Shaped Wall Response Spectrum – 5% Damping, Wall 2

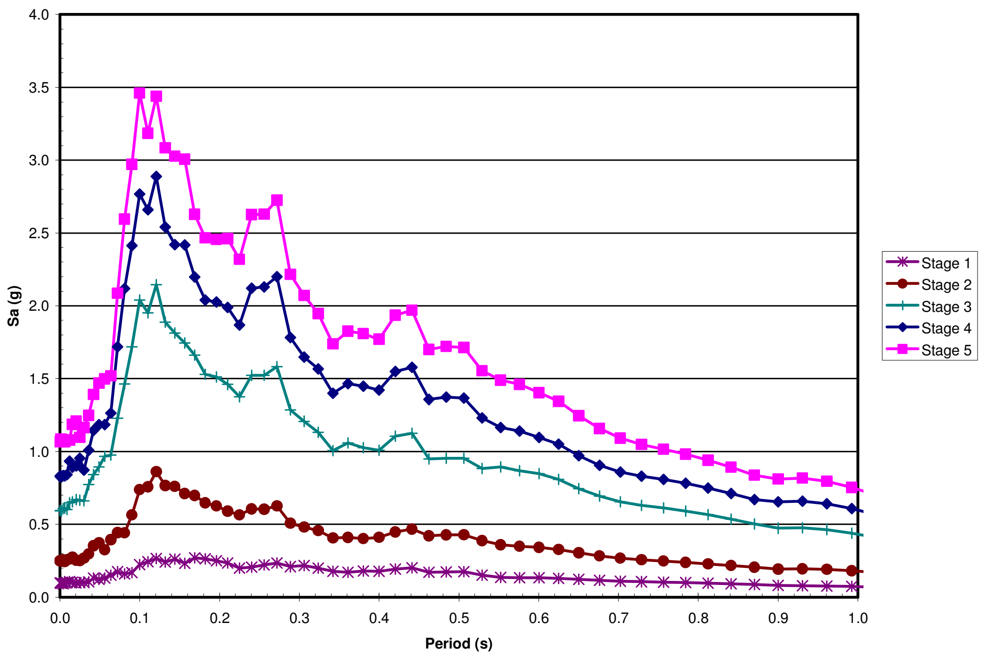

Figure 3-46: CAMUS C Shaped Wall Response Spectrum – 5% Damping, Wall 3

The five synthetic records, created from the five recorded acceleration records, were scaled in the time domain and used as input motions for the specimens. Reynouard and Fardis (2001) do not specifically identify the input motion used for each run and specimen. However, as acceleration records were provided for each run and specimen, the results of response spectrum analyses were used to identify the motions and associated specific motions with specimens and runs. Motion 1 was applied to specimen 1 in stage 1 through 5 as well as specimen 3 in stage 2 through 5. Motion 2 was applied to specimen 0 in stages 4, 5 and 6. Motion 3 was applied to specimen 2 in stages 3, 4, and 5. Motion 4 was applied to specimen 0 in stage 3 and specimen 2 in stage 2. Motion 5 was applied to specimen 0 in stage 1 and 2 as well as to specimen 2 stage 1 and specimen 3 stage 1. Examples of some of the acceleration records can be found in Appendix E.

3.3.8 Wall Performance

Very limited damage data are provided in the report by Reynouard and Fardis, (2001). However, from the report it is seen that all the specimens tested behaved in a similar manner. Low intensity runs exhibited flexural cracking that ultimately led to buckling and failure in the longitudinal reinforcement in more severe runs. The footing slab for the test program as a hole saw significant unexpected damage, particularly in high amplitude tests. The following summarizes the provided response data as well as the overall response mechanism surmised from these data.

Specimen 0: No response data were provided for specimen 0.

Specimen 1: The provided data suggest that wall response was controlled by flexural yielding with fracture of longitudinal steel in the web wall (back side shown in Figure 3-38) at the wall-foundation slab interface causing failure during loading stage 5. Response data reported by Reynouard and Fardis include the following:

- In investigating the limited damage data, the response appeared to be largely flexural.
- The specimen exhibited cracking near the base of the wall following stage 1 of the test. No information about crack orientation or spacing was provided.

- Yielding of the longitudinal reinforcement began in stage 3 and became more extensive during stage 4. Fracture of longitudinal reinforcement occurred on the web (back) side (Figure 3-38) during stage 5.
- Transverse reinforcement did not yield during the test. It reached a maximum strain of 1700 $\mu\varepsilon$ during stage 5.
- No spalling or crushing of the concrete was recorded.

Crack widths, strains, roof displacement and rotations are summarized below in Table 3-29 and Table 3-30.

Table 3-29: Response Data for C-Shaped Specimen 1, metric units (Reynouard and Fardis, 2001)

	Z Location (mm)	Units	Stage 1	Stage 2	Stage 3	Stage 4	Stage 5
Max Displacement at top of wall	3150	mm	10.91	16.25	40.81	57.74	121.20
	3150	Drift	0.35%	0.52%	1.30%	1.83%	3.85%
Absolute Rotation from base	820	mrad	2.95	4.16	10.00	16.00	44.00
	25	mrad	1.97	1.91	5.50	9.58	13.00
Crack Opening (back/flange side)	820	mm	1.60	2.18	5.14	8.41	21.50
	575	mm	1.33	1.78	4.44	7.66	21.50
	320	mm	0.98	1.28	3.52	6.82	21.00
	25	mm	1.12	1.28	3.75	4.98	17.80
Crack Opening (front/web side)	820	mm	1.45	2.01	4.67	7.73	5.19
	575	mm	1.18	1.67	4.13	7.21	4.82
	320	mm	0.75	1.06	2.95	6.03	25.20
	25	mm	0.37	0.55	1.52	5.56	2.50
Strain in Long. reinf (back/flange side)	25	$\mu\varepsilon$	560	240	4250	28000	10900
Strain in Long. reinf (front/web side)	25	$\mu\varepsilon$	250	590	5380	12400	6860
Strain in B.E. stirrups	25	$\mu\varepsilon$	279	174	310	890	1700

Table 3-30: Response Data for C-Shaped Specimen 1, English standard units (Reynouard and Fardis, 2001)

	Z Location (in)	Units	Stage 1	Stage 2	Stage 3	Stage 4	Stage 5
Max Displacement at top of wall	124.0	in	0.43	0.64	1.61	2.27	4.77
	124.0	Drift	0.01%	0.02%	0.05%	0.07%	0.15%
Absolute Rotation from base	32.3	mrad	2.95	4.16	10.00	16.00	44.00
	1.0	mrad	1.97	1.91	5.50	9.58	13.00
Crack Opening (back/flange side)	32.3	in	0.06	0.09	0.20	0.33	0.85
	22.6	in	0.05	0.07	0.17	0.30	0.85
	12.6	in	0.04	0.05	0.14	0.27	0.83
	1.0	in	0.04	0.05	0.15	0.20	0.70
Crack Opening (front/web side)	32.3	in	0.06	0.08	0.18	0.30	0.20
	22.6	in	0.05	0.07	0.16	0.28	0.19
	12.6	in	0.03	0.04	0.12	0.24	0.99
	1.0	in	0.01	0.02	0.06	0.22	0.10
Strain in Long. reinf (back/flange side)	1.0	$\mu\varepsilon$	560	240	4250	28000	10900
Strain in Long. reinf (front/web side)	1.0	$\mu\varepsilon$	250	590	5380	12400	6860
Strain in B.E. stirrups	1.0	$\mu\varepsilon$	279	174	310	890	1700

Specimen 2: The provided data suggest that wall response was controlled by flexural yielding with fracture of longitudinal steel in the front and back of the specimen (front and back sides shown in Figure 3-38) at the wall-foundation slab interface. The specimen saw failure of the footing slab, and for that reason experimenters could not run the 1.0 g test. Response data reported by Reynouard and Fardis include the following:

- In investigating the limited damage data, the response appeared to be largely flexural.
- Significant cracking did not initiate until stage 3. Cracks were largely localized near the base.
- Front and back reinforcement yielded in stage 4.

- Transverse reinforcement did not yield during the test. It reached a maximum strain of 1190 με during stage 5.
- No spalling or crushing of the reinforcement was recorded (Reynouard and Fardis, 2001).
- Footing slab saw significant damage throughout the test resulting in failure in stage 5.

Crack widths, strains, roof displacement and rotations are summarized below in Table 3-31 and Table 3-32.

Table 3-31: Performance and Damage Details for C Specimen 2, metric (Reynouard and Fardis, 2001)

	Z Location (mm)	Units	Stage 1	Stage 2	Stage 3	Stage 4	Stage 5
Max Displacement at top of wall	3150	mm	5.00	2.52	16.99	60.83	120.80
	3150	Drift	0.16%	0.08%	0.54%	1.93%	3.83%
Absolute Rotation from base	820	mrad	1.16	0.55	4.35	11.00	13.00
	25	mrad	0.78	0.40	2.09	7.78	21.00
Crack Opening (back/flange side)	820	mm	0.42	0.20	2.48	6.77	2.78
	575	mm	0.38	0.19	1.81	5.86	2.64
	320	mm	0.30	0.13	1.17	4.38	2.25
	25	mm	0.57	0.27	1.40	5.42	7.89
Crack Opening (front/web side)	820	mm	0.71	0.28	2.32	6.52	4.29
	575	mm	0.54	0.21	1.64	5.67	3.76
	320	mm	0.43	0.17	1.64	5.76	3.28
	25	mm	0.30	0.17	0.54	2.33	2.55
Strain in Long. reinf (back/flange side)	25	με	920	580	2050	10500	950
Strain in Long. reinf (front/web side)	25	με	1140	510	2200	10300	4110
Strain in B.E. stirrups	25	με	390	56	262	899	1190

Table 3-32: Performance and Damage Details for C Specimen 2, English standard units

	Z Location (in)	Units	Stage 1	Stage 2	Stage 3	Stage 4	Stage 5
Max Displacement at top of wall	124.0	in	0.20	0.10	0.67	2.39	4.76
	124.0	Drift	0.01%	0.00%	0.02%	0.08%	0.15%
Absolute Rotation from base	32.3	mrad	1.16	0.55	4.35	11.00	13.00
	1.0	mrad	0.78	0.40	2.09	7.78	21.00
Crack Opening (back/flange side)	32.3	in	0.02	0.01	0.10	0.27	0.11
	22.6	in	0.01	0.01	0.07	0.23	0.10
	12.6	in	0.01	0.01	0.05	0.17	0.09
	1.0	in	0.02	0.01	0.06	0.21	0.31
Crack Opening (front/web side)	32.3	in	0.03	0.01	0.09	0.26	0.17
	22.6	in	0.02	0.01	0.06	0.22	0.15
	12.6	in	0.02	0.01	0.06	0.23	0.13
	1.0	in	0.01	0.01	0.02	0.09	0.10
Strain in Long. reinf (back/flange side)	1.0	με	920	580	2050	10500	950
Strain in Long. reinf (front/web side)	1.0	με	1140	510	2200	10300	4110
Strain in B.E. stirrups	1.0	με	390	56	262	899	1190

Specimen 3: The provided data suggest that wall response was controlled by flexural yielding with fracture of longitudinal steel in the web wall (back side shown in Figure 3-38) at the wall-foundation slab interface causing failure during loading in stage 5. Response data reported by Reynouard and Fardis include the following:

- In investigating the limited damage data, the response appeared to be largely flexural.
- Cracking was largely localized near the base.
- Front and back reinforcement yielded in stage 3 and continued in stage 4 and 5 until fracture occurred in stage 5.
- According to strain gauge measurements, yielding of the confinement at the base occurred during stage 5.

- No spalling or crushing of the reinforcement was recorded.

Crack spacing, strains, roof displacement and rotations are summarized below in Table 3-33 and Table 3-34.

Table 3-33: Performance and Damage Details for C Specimen 3, metric (Reynouard and Fardis, 2001)

	Z Location (mm)	Units	Stage 1	Stage 2	Stage 3	Stage 4	Stage 5
Max Displacement at top of wall	3150	mm	3.57	10.87	41.30	70.59	125.70
	3150	Drift	0.11%	0.35%	1.31%	2.24%	3.99%
Absolute Rotation from base	820	mrad	0.79	2.80	9.31	14.00	22.00
	25	mrad	0.91	1.50	7.47	8.71	14.00
Crack Opening (back/flange side)	820	mm	0.33	1.78	4.87	6.22	9.87
	575	mm	0.28	1.34	4.07	5.59	9.49
	320	mm	0.24	0.85	2.86	4.49	*
	25	mm	1.15	1.80	7.82	10.40	13.20
Crack Opening (front/web side)	820	mm	0.45	1.62	4.85	7.25	11.60
	575	mm	0.44	1.32	4.04	6.42	11.60
	320	mm	0.27	0.88	2.99	5.44	*
	25	mm	0.19	0.36	1.19	3.80	8.75
Strain in Long. reinf (back/flange side)	25	με	1220	2510	12900	10900	37300
Strain in Long. reinf (front/web side)	25	με	1210	2190	24100	36200	47700
Strain in B.E. stirrups	25	με	52	242	283	635	4860

* Data not provided

Table 3-34: Performance and Damage Details for C Specimen 3, English standard units

	Z Location (in)	Units	Stage 1	Stage 2	Stage 3	Stage 4	Stage 5
Max Displacement at top of wall	124.0	in	0.14	0.43	1.63	2.78	4.95
	124.0	Drift	0.00%	0.01%	0.05%	0.09%	0.16%
Absolute Rotation from base	32.3	mrad	0.79	2.80	9.31	14.00	22.00
	1.0	mrad	0.91	1.50	7.47	8.71	14.00
Crack Opening (back/flange side)	32.3	in	0.01	0.07	0.19	0.24	0.39
	22.6	in	0.01	0.05	0.16	0.22	0.37
	12.6	in	0.01	0.03	0.11	0.18	*
	1.0	in	0.05	0.07	0.31	0.41	0.52
Crack Opening (front/web side)	32.3	in	0.02	0.06	0.19	0.29	0.46
	22.6	in	0.02	0.05	0.16	0.25	0.46
	12.6	in	0.01	0.03	0.12	0.21	*
	1.0	in	0.01	0.01	0.05	0.15	0.34
Strain in Long. reinf (back/flange side)	1.0	$\mu\varepsilon$	1220	2510	12900	10900	37300
Strain in Long. reinf (front/web side)	1.0	$\mu\varepsilon$	1210	2190	24100	36200	47700
Strain in B.E. stirrups	1.0	$\mu\varepsilon$	52	242	283	635	4860

* Data not provided

3.4 CAMUS Ecoleader: Parallel Flange Wall Specimen with Coupled Web Wall

The CAMUS Ecoleader wall specimen was tested by doctoral candidate Xuan Huy Nguyen under the guidance of C. La Borderie, N. Ile, P. Perrortin, J. Mazars and P. Kotronis on the shaking table of LNEC (National Laboratory for Civil Engineering) in Lisbon. The specimen was a 5-story H-shaped wall in which rectangular flange walls were joined by a coupled web wall. Simulated earthquake motions were applied in the X (parallel to the rectangular flange walls) and Y (parallel to the coupled web wall) direction. A plan view of the specimen, showing the flange walls and the coupled web wall, is provided in Figure 3-47.

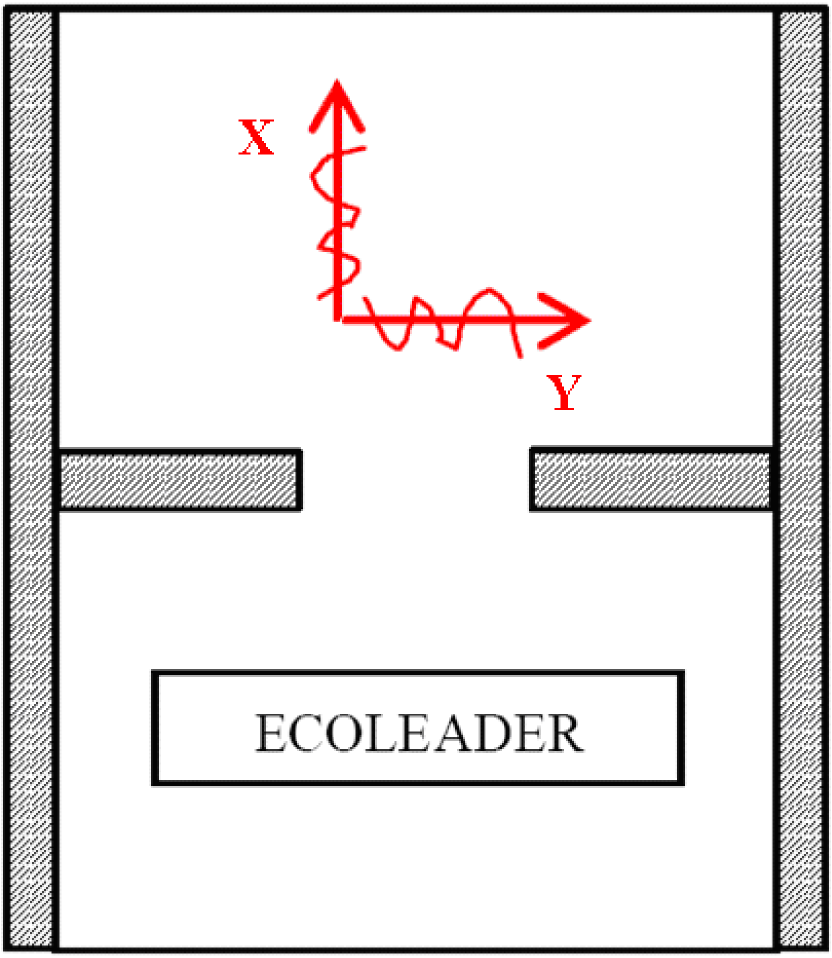

Figure 3-47: Basic CAMUS Ecoleader Plan View (Nguyen, 2006)

3.4.1 Geometry and Reinforcement

The five-story h-shaped specimen comprised two parallel rectangular flange walls joined by a coupled web wall and slabs at each story level. Table 3-35 summarizes the specimen geometry and Figure 3-48, Figure 3-49 and Figure 3-50 show elevation and plan views of the specimen.

Table 3-35: Summary of Ecoleader Specimen Geometry

Member	Property	Dimensions (cm)	Dimensions (in)	Aspect Ratio
Flange Walls (*2)	Story Height	90	35.4	2.81
	Height	450	177.2	
	Length	160	63.0	
	Thickness	6	2.36	
Coupled Web Wall	Story Height	90	35.4	2.88
	Height	450	177.2	
	Length	156	61.4	
	Thickness	6	2.36	
	Coupling Beam Length	27	10.6	
	Coupling Beam Depth	23	9.06	
	Bm Length/Depth	1.17	0.46	
Slabs (*5)	Length	160	63.0	-
	Width	156	61.4	
	Thickness	21	8.27	
Specimen	Scale	1/3		

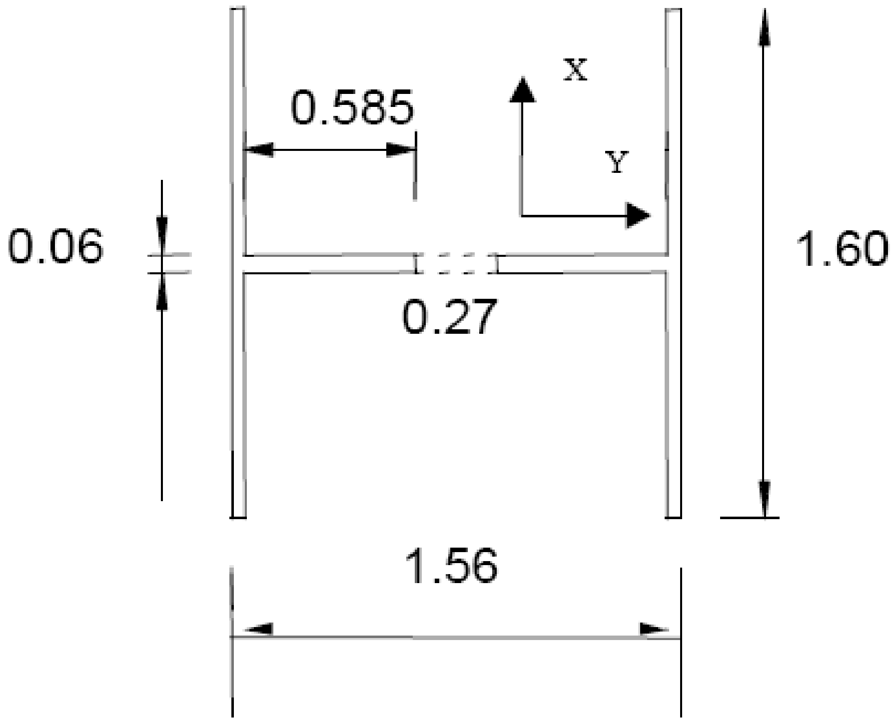

Figure 3-48: CAMUS Ecoleader Specimen Plan View, units in meters (Nguyen, 2006)

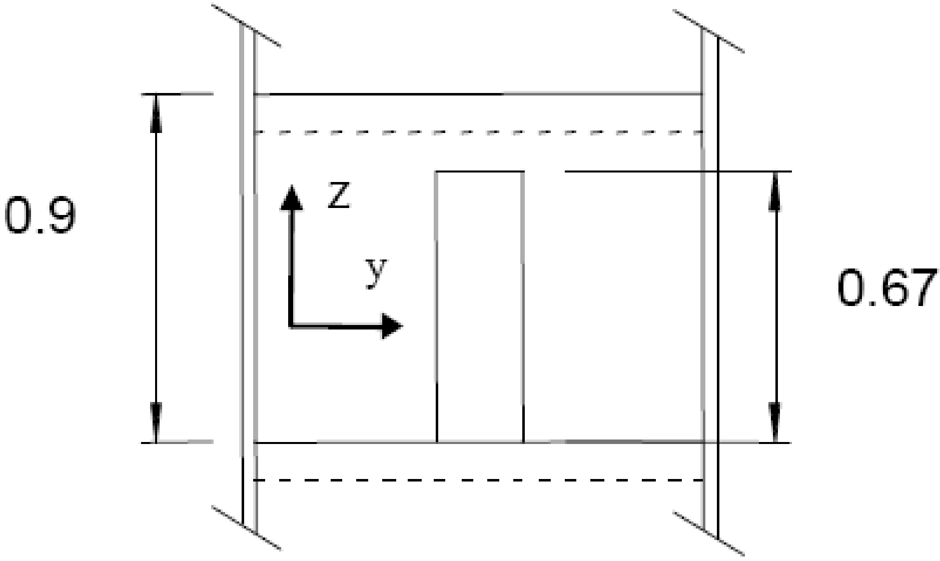

Figure 3-49: CAMUS Ecoleader Specimen Floor Elevation View, units in meters (Nguyen, 2006)

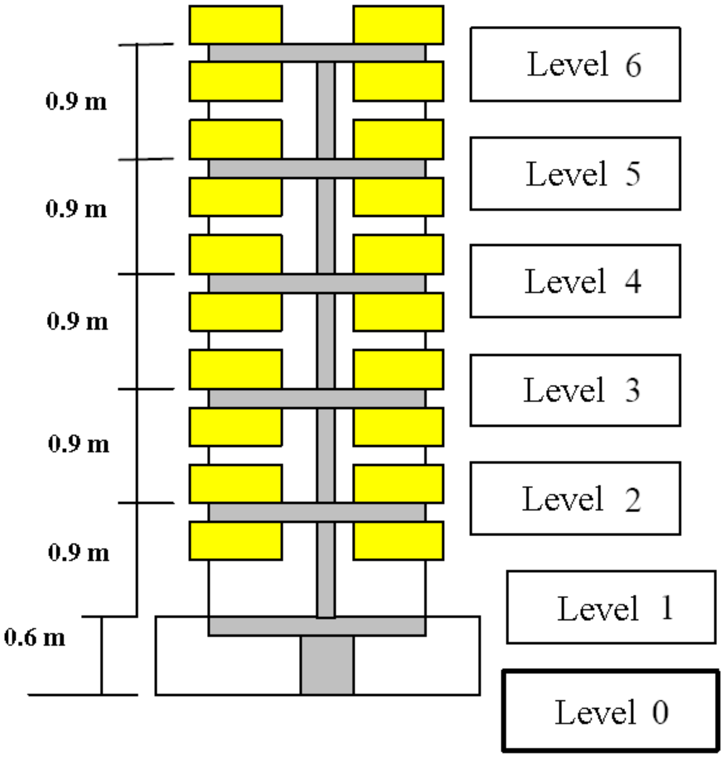

Figure 3-50: CAMUS Ecoleader Specimen Elevation View, units in meters (Nguyen, 2006)

The average reinforcement ratios for the laboratory specimen are included in Table 3-36. Figure 3-51 and Figure 3-52 show the distribution of the reinforcement. Longitudinal reinforcement was heavier in the boundary elements.

Table 3-36: CAMUS Ecoleader Wall Reinforcement Summary

		Vertical Reinforcement Ratio			Transverse Reinforcement Ratio		
	Floor	**Average ρv**	**ρv at Flange Web Connection**	**Boundary element ρv**	**Wall ρh**	**ρh at Flange Web Connection**	**Boundary element ρh**
Flange Walls	flr 1-2	0.12%	0.88%	1.61%	0.52%	0.52%	0.12%
	flr 2-3	0.09%	0.88%	1.02%	0.52%	0.52%	0.12%
	flr 3-4	0.07%	0.88%	0.59%	0.52%	0.52%	0.12%
	flr 4-5	0.05%	0.88%	0.29%	0.52%	0.52%	0.12%
	flr 5-6	0.05%	0.88%	0.29%	0.52%	0.52%	0.12%
Coupled Web Wall	flr 1-2	0.31%	0.88%	2.81%	0.52%	0.52%	0.12%
	flr 2-3	0.31%	0.88%	2.81%	0.52%	0.52%	0.12%
	flr 3-4	0.27%	0.88%	2.41%	0.52%	0.52%	0.12%
	flr 4-5	0.23%	0.88%	2.00%	0.52%	0.52%	0.12%
	flr 5-6	0.15%	0.88%	1.18%	0.52%	0.52%	0.12%

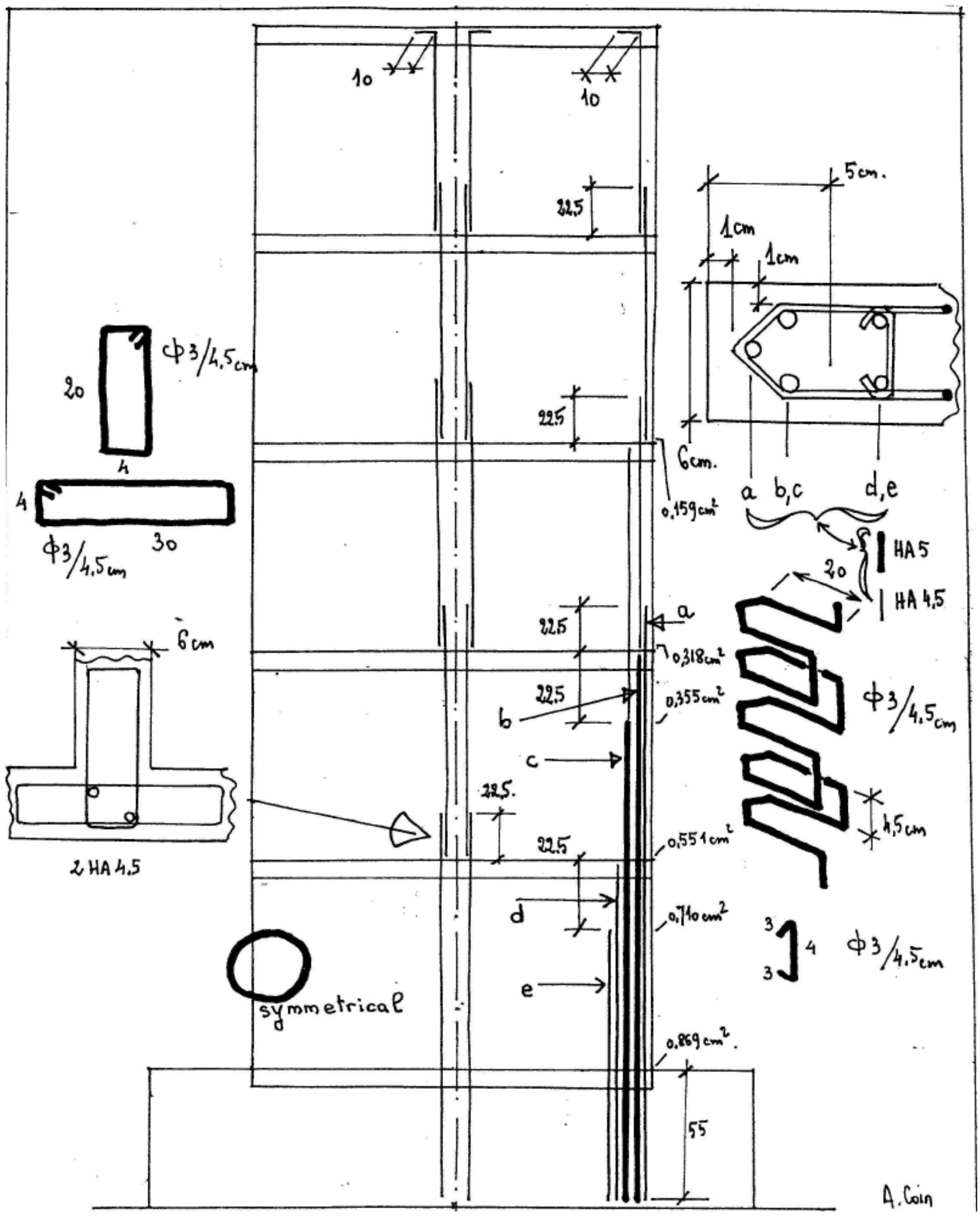

Figure 3-51: CAMUS Ecoleader Reinforcement Layout, Flange Walls (Nguyen, 2006)

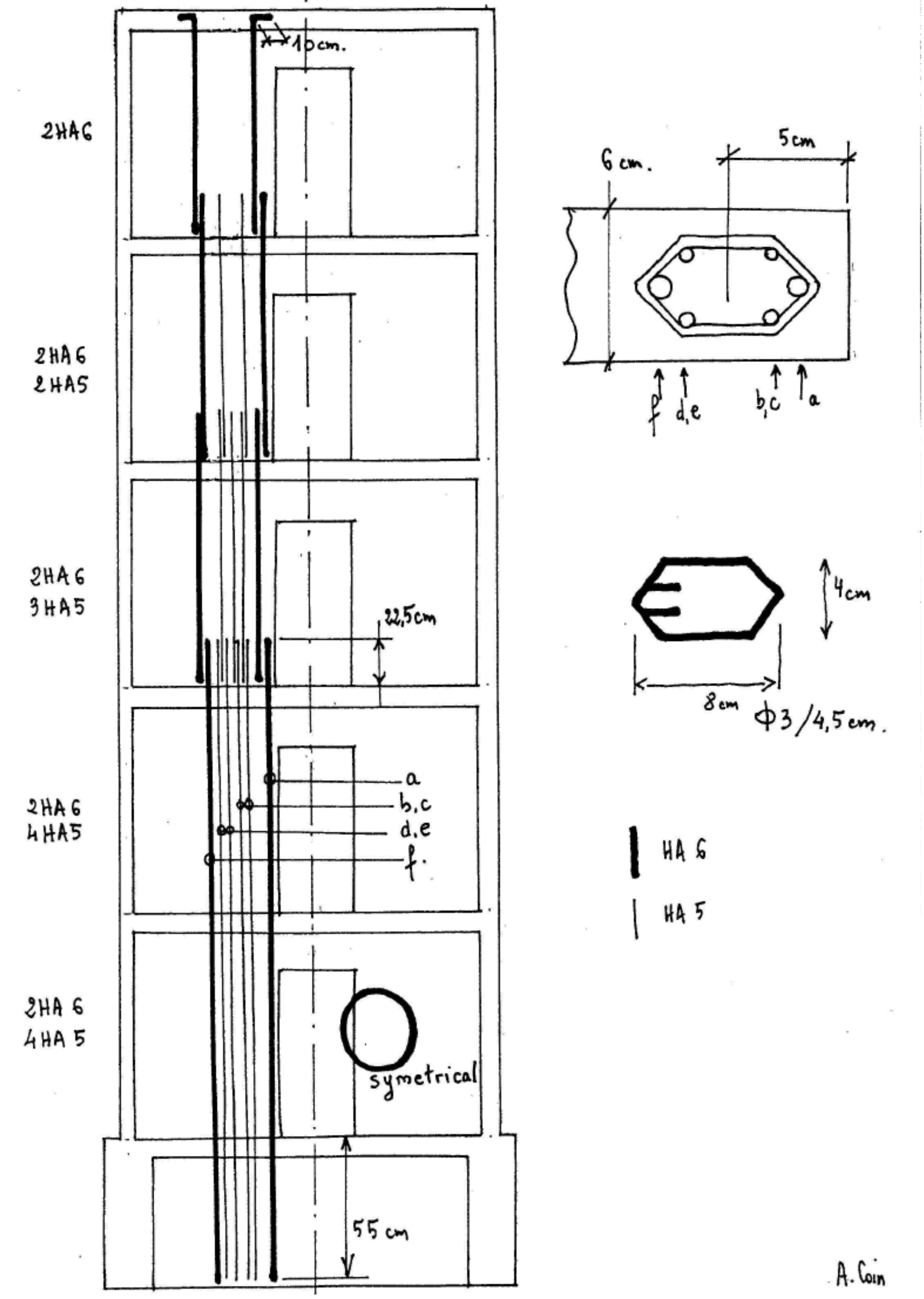

Figure 3-52: CAMUS Ecoleader Reinforcement Layout, Coupled Web Wall (Nguyen, 2006)

3.4.2 Material Properties

The CAMUS Ecoleader walls were constructed using normal weight concrete. Concrete properties were determined by testing cubes at 7 and 28 days. The reinforcing steel used in construction had a significantly larger yield strength (90+ ksi) than is used typically in the United States. This is likely due to the fact that very small diameter bars (diameter equal to 5 and 6 mm, which is equivalent to a No 2 or 3 at full scale) were used, necessitating fabrication of deformations on the bars via mechanical action and resulting in work hardening of the steel. The steel and 28 day concrete properties are provided in Table 3-37, Table 3-38, Table 3-39, and Table 3-40.

Table 3-37: Average 28-Day Concrete Properties, metric (Nguyen, 2006)

Specified			Measured		
f'_c (MPa)	f'_r (MPa)	E_c (MPa)	f'_c (MPa)	f'_r (MPa)	E_c (MPa)
29.8	3	20000	41.7	*	*

Table 3-38: Average 28-Day Concrete Properties, English standard units

Specified			Measured		
f'_c (ksi)	f'_r (ksi)	E_c (ksi)	f'_c (ksi)	f_r (ksi)	E_c (ksi)
4.3	0.435	2900.0	6.0	*	*

* Measured f_r and E_c not included in report.

Table 3-39: Average Reinforcing Steel Properties, metric (Nguyen, 2006)

Specified		Measured		
E (MPa)	f_y (MPa)	E (MPa)	f_y (MPa)	f_{su} (MPa)
200000	460	201267	621.29	688.33

Table 3-40: Average Reinforcing Steel Properties, English standard units

Specified		Measured		
E (ksi)	f_y (ksi)	E (ksi)	f_y (ksi)	f_{su} (ksi)
29000	66.7	29184	90.09	99.81

3.4.3 Specimen Mass

When scaling a specimen, the volume and thus the mass decrease by the scale factor cubed. The area by contrast decreases by the scale factor squared. Thus the stresses due to self weight decrease by the scale factor when they should stay the same. For this reason, the researchers provided additional weight at each story level to simulate typical axial loading for a structural wall. The added masses as well as the masses of the structural elements are summarized in Table 3-26 and can be seen in Figure 3-53.

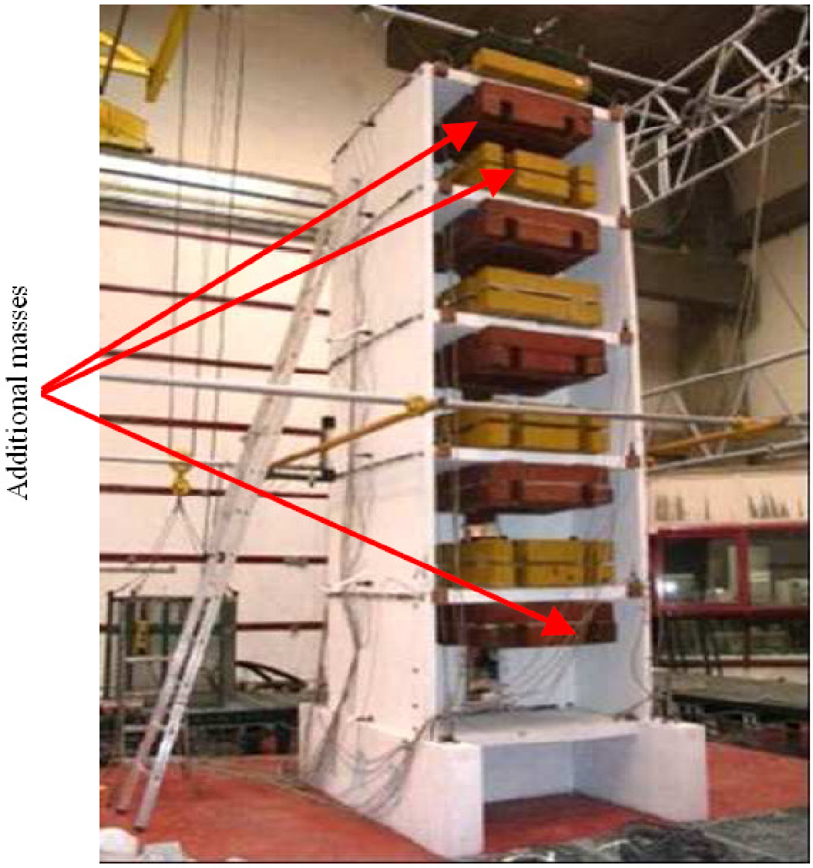

Figure 3-53: Additional Masses on Specimen (Nguyen, 2006)

Table 3-41: Axial Load on System by Story (Nguyen, 2006)

Floor	Height	Total mass (*1000 kg)	Total Weight (kips)
6	5.06m	0	0.0
5	4.16m	5.8	12.8
4	3.26m	11.6	25.6
3	2.36m	17.4	38.4
2	1.46m	23.2	51.1
1	0.56m	29	63.9
0	0	31.2	68.8
W/(f'c*Ag) (%)		3.81%	

3.4.4 Table and Anchorage Specifications

The specimen was tested on the shaking table of LNEC (National Laboratory for Civil Engineering) in Lisbon. The basic schematics of the table can be seen below in Figure 3-54.

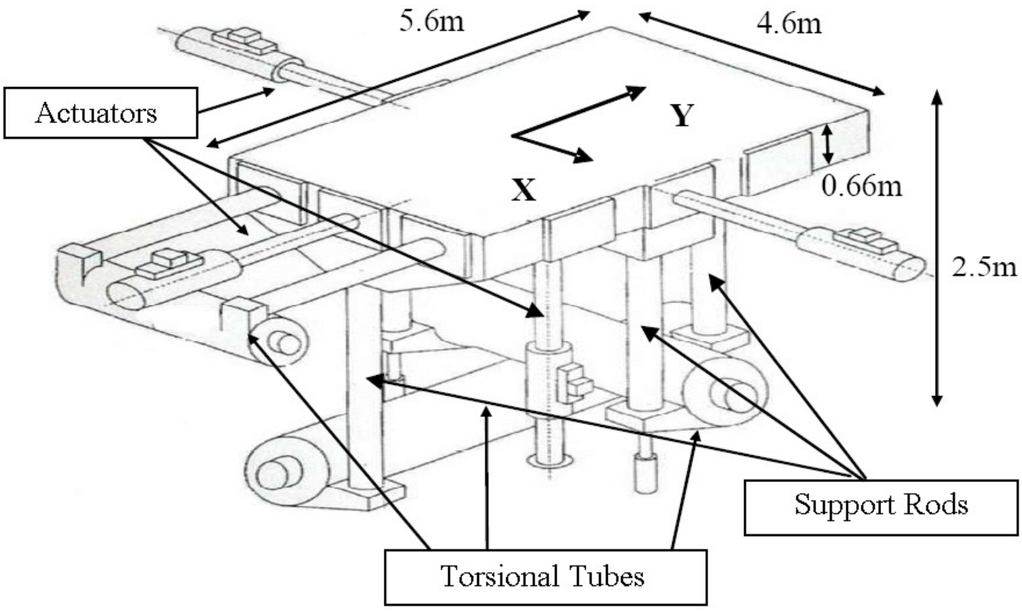

Figure 3-54: LNEC Shake Table Schematics (Nguyen, 2006)

3.4.5 Table Rocking Observations

There was no discussion regarding rocking at the base. Rather, the report made mention that the table was not instrumented due to the assumption that the foundation behaved rigidly. Figure 3-55 below shows the location of accelerometers. As can be seen, no measurements of accelerations were taken on the table surface, denoted here as “Floor 0”. As table rocking was a significant issue for the UCSD and CAMUS 2000 test programs, the choice to not measure the table is believed to have been unwise.

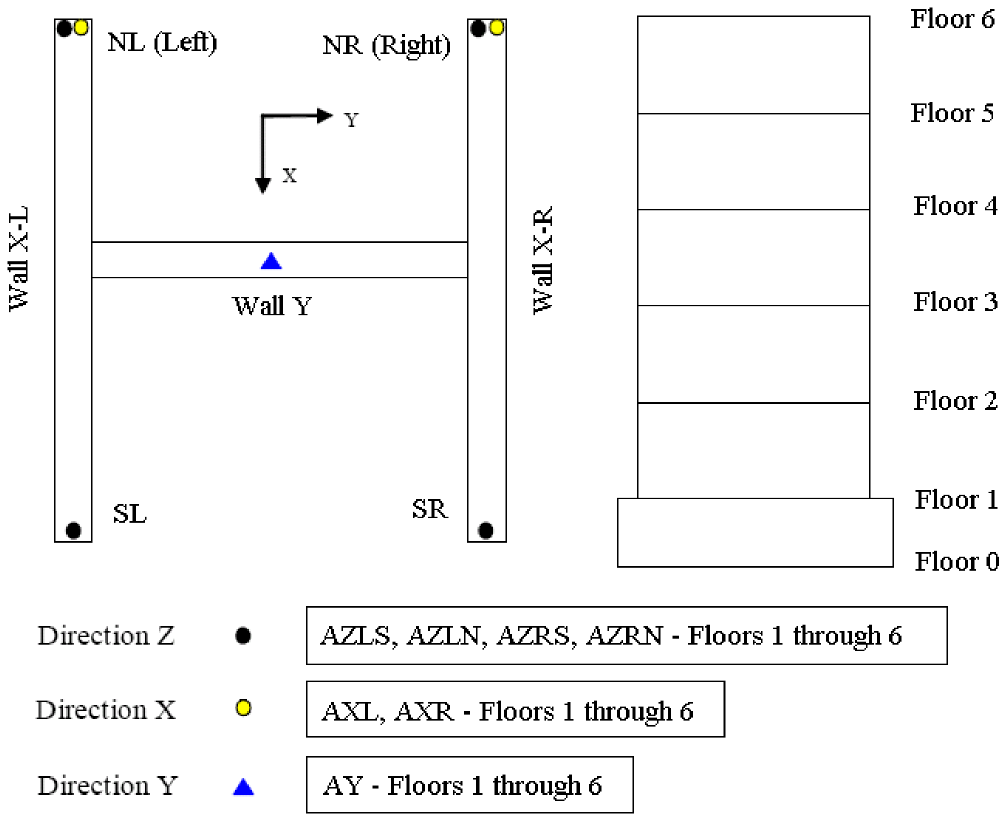

Figure 3-55: Location of Accelerometers (Nguyen, 2006)

Unfortunately, displacement outputs made available for this study were not at every floor, as such it was difficult to determine how much of the flexibility the specimen exhibited was due to table rocking and how much was due to normal expected flexural deformation. As such, no model was devised to correct for potential rocking.

3.4.6 Instrumentation

Instrumentation for the Ecoleader specimen included accelerometers, linear variable differential transformers (LVDT's), strain gauges and a photogrammetric system for measuring displacements. The location of accelerometers was previously shown in Figure 3-55 in Section 3.4.5. The location of LVDT's on the X and Y walls can be seen in Figure 3-56. Figure 3-57 shows the displacements measured from the optical systems. Figure 3-58 shows the location of strain gauges attached to longitudinal steel. Of the data recorded using this instrumentation, only roof acceleration and base shear and moment, computed from story acceleration histories, were provided by Nguyen (2006) for use in this study.

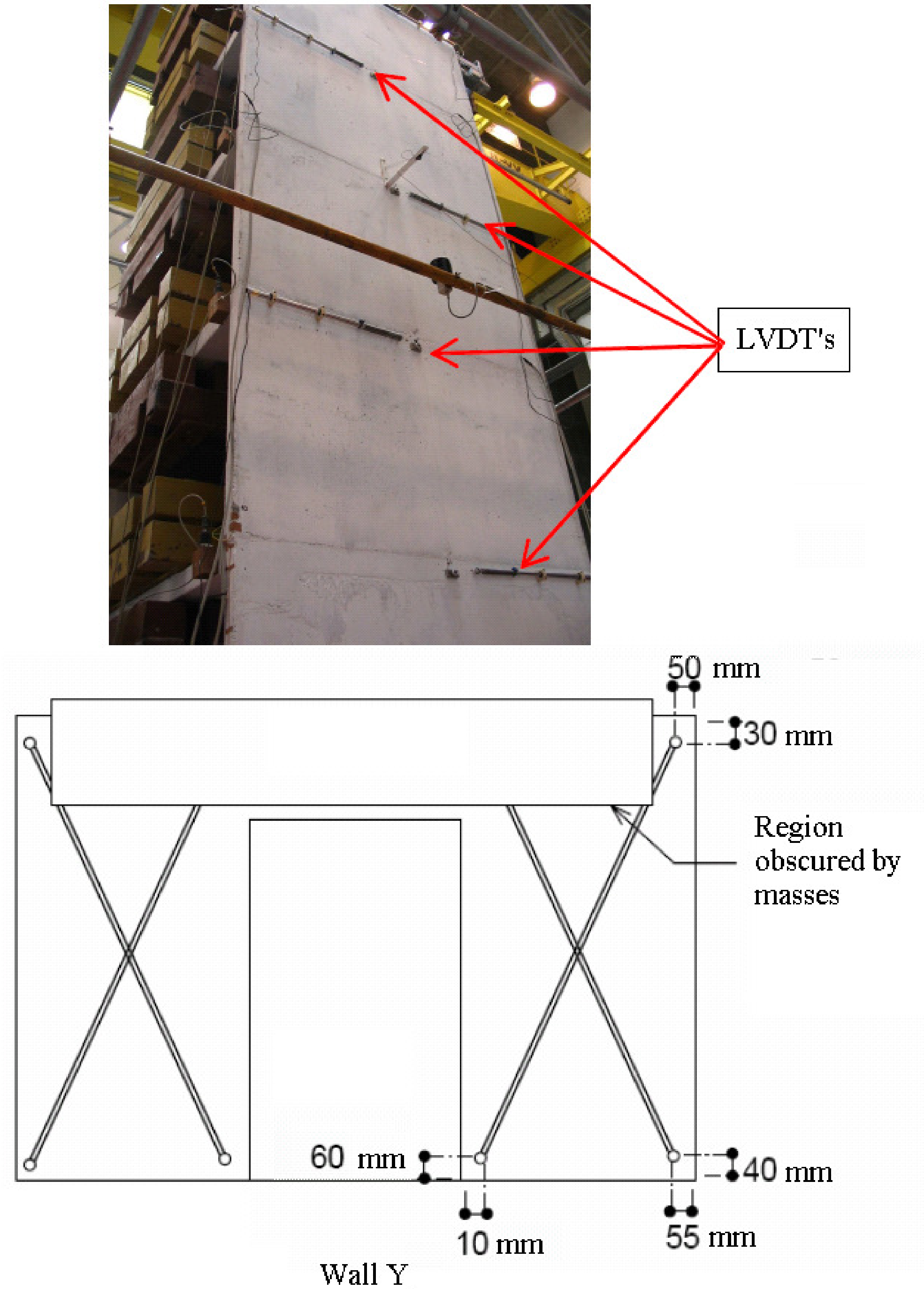

Figure 3-56: Location of LVDT's (Nguyen, 2006)

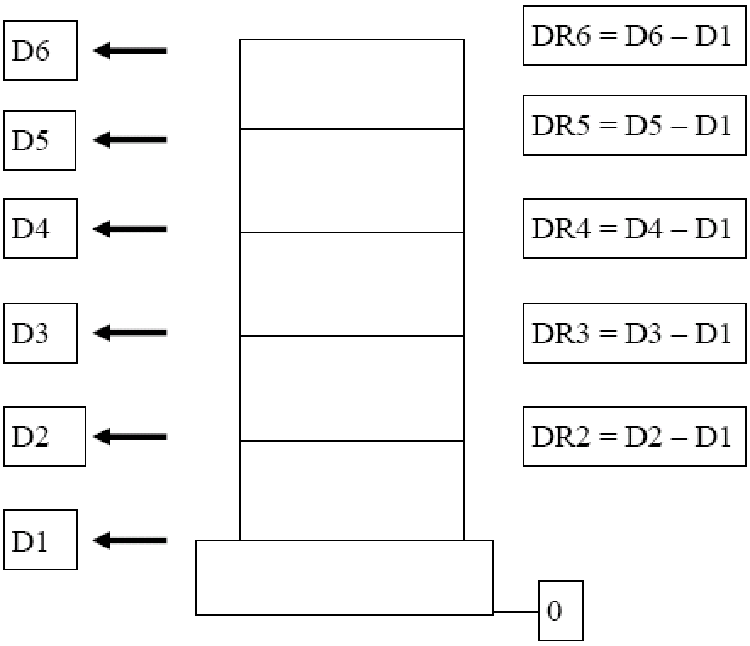

Figure 3-57: Absolute and Relative Displacements Measured by Optical Systems (Nguyen, 2006)

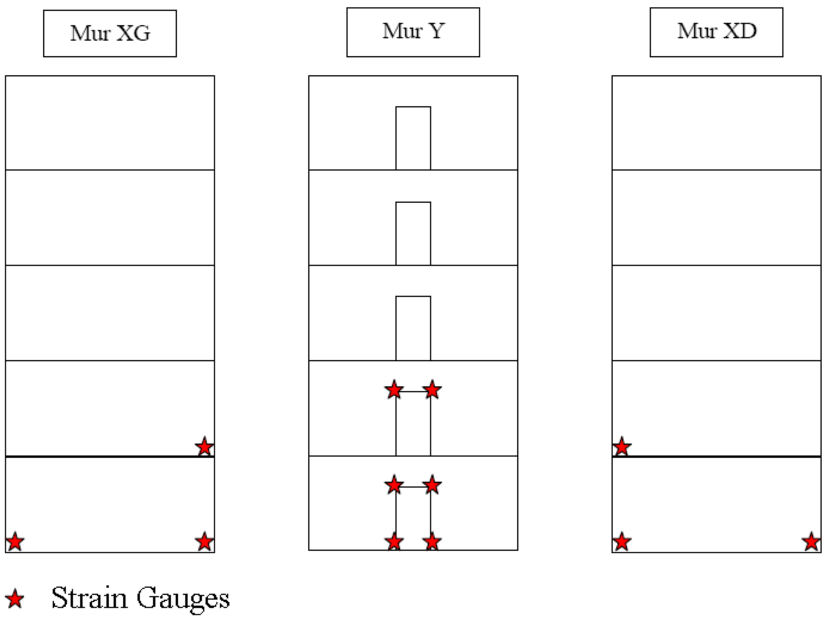

Figure 3-58: Location of Strain Gauges (Nguyen, 2006)

3.4.7 Applied Earthquake Excitation

The specimen was excited in the X and Y directions (as defined in Figure 3-48). The peak ground accelerations for the applied earthquake excitations can be seen in Table 3-42. The response spectrum for the applied ground motions for the X and Y directions can be seen in Figure 3-59 and Figure 3-60, respectively. The acceleration history for the strong motion period of excitation can be seen in Appendix E. This motion however was the target input motion and not the motion measured at the table surface.

Table 3-42: Peak Ground Accelerations for Ecoleader Specimen

Test	Peak Ground Acceleration (g)	
	Direction X	Direction Y
T0	0.30	0.00
T1	0.00	0.14
T2	0.24	0.13
T3	0.45	0.27
T4	0.55	0.30
T5	0.74	0.36
T6	0.85	0.50

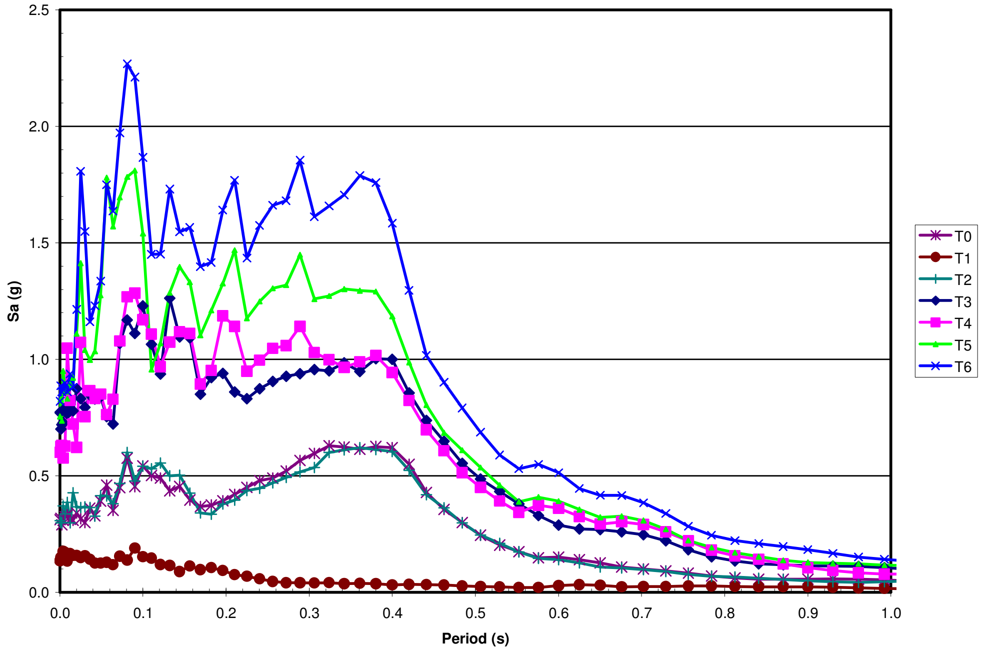

Figure 3-59: CAMUS Ecoleader Response Spectrum – 5% Damping, X Direction

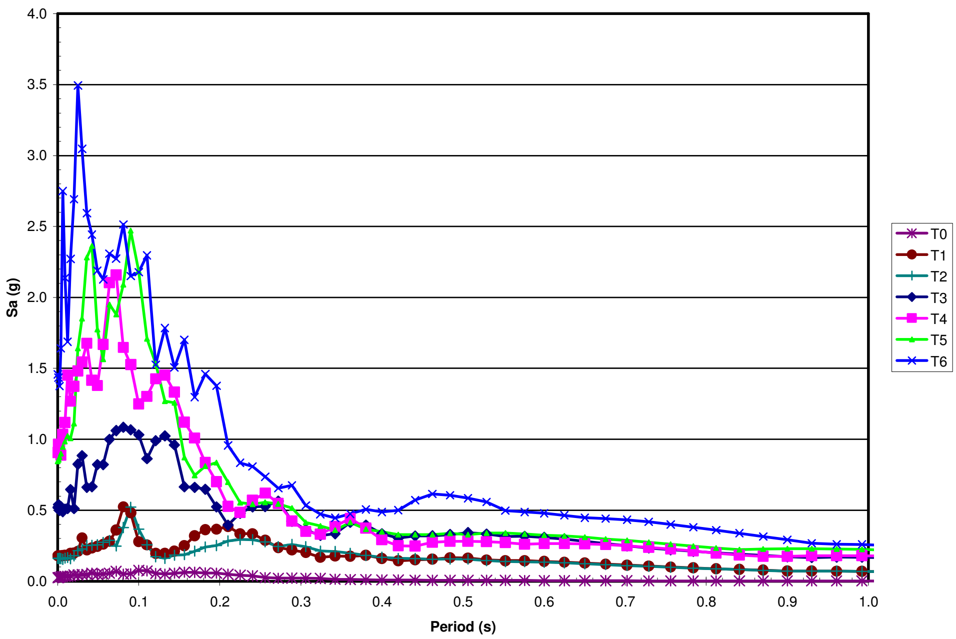

Figure 3-60: CAMUS Ecoleader Response Spectrum – 5% Damping, X Direction

3.4.8 Wall Performance

The behavior of the CAMUS Ecoleader specimen was characterized by flexural cracking. Later runs also saw spalling, fracture of reinforcement as well as the development of non-flexural cracking. In addition to this response, there was significant cracking at the wall-footing interface as well as in the footings themselves. A synopsis of the response data provided by Nguyen follows. Crack spacing and widths as well as strain gauge data were not provided.

Run T0 was excited only in the direction of the flange walls (X direction). The peak roof drift in the X direction was 0.360%. Despite assumptions by the experimenters of a rigid foundation, following the run, cracks were seen in the flange walls at the interface with the footing. Cracking propagated into the footing as well. This can be seen in Figure 3-61.

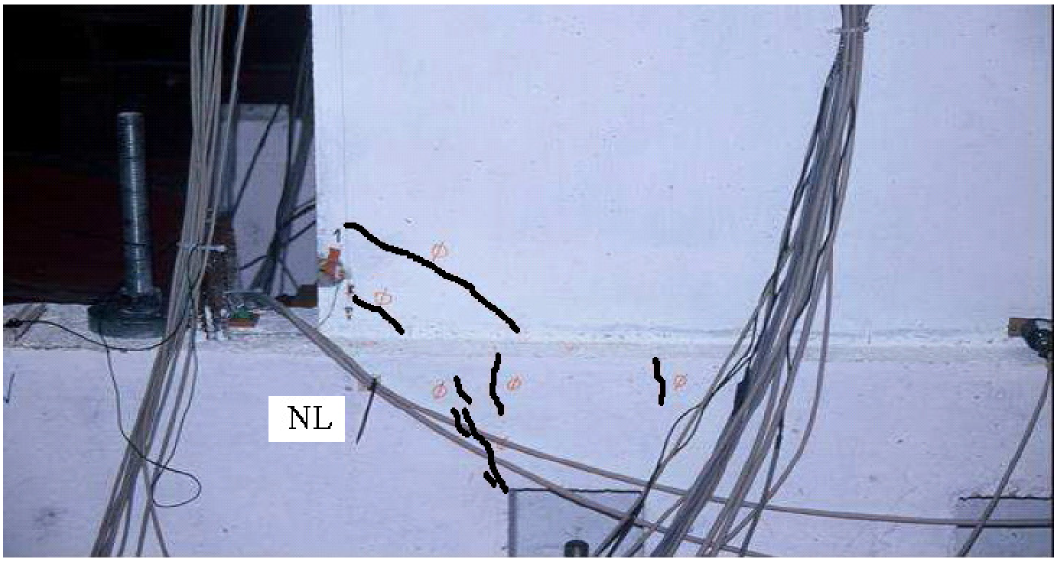

Figure 3-61: North Flange Wall/Footing Interface Following T0 (Nguyen, 2006, with cracks darkened by author)

Run T1 was excited only in the direction of the coupled web wall (Y direction). The peak roof drift in the Y direction was 0.231%. Cracking in the footing continued, although no additional cracking was seen in the flange walls.

Run T2 was excited in the X and Y direction. The peak roof drift in the X direction was 0.385%, the peak roof drift in the Y direction was 0.217%. Cracking initiated in the web wall. The flange walls saw cracking occurring at 45^{o} as can be seen in Figure 3-62.

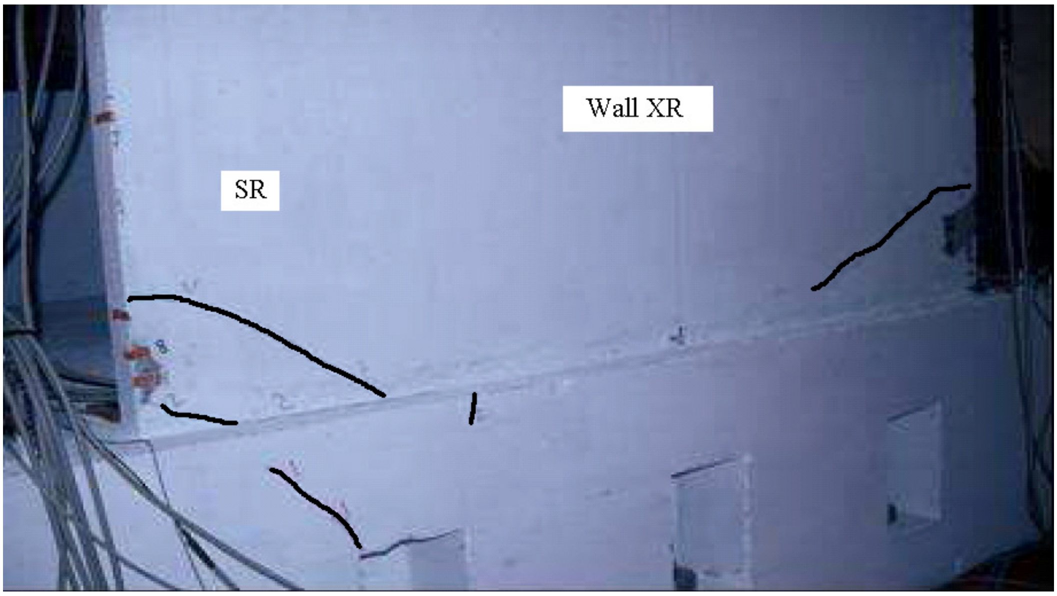

Figure 3-62: Damage in Specimen Following Run T2 (Nguyen, 2006, with cracks darkened by author)

Run T3 was excited in the X and Y direction. The peak roof drift in the X direction was 0.821%. The peak roof drift in the Y direction was 0.438%. Run T3 saw spalling occurring at the ends of the flange as well as buckling of reinforcement and in one isolated case fracture of one of the reinforcing bars. Crack propagation in the X and Y walls can be seen in Figure 3-63.

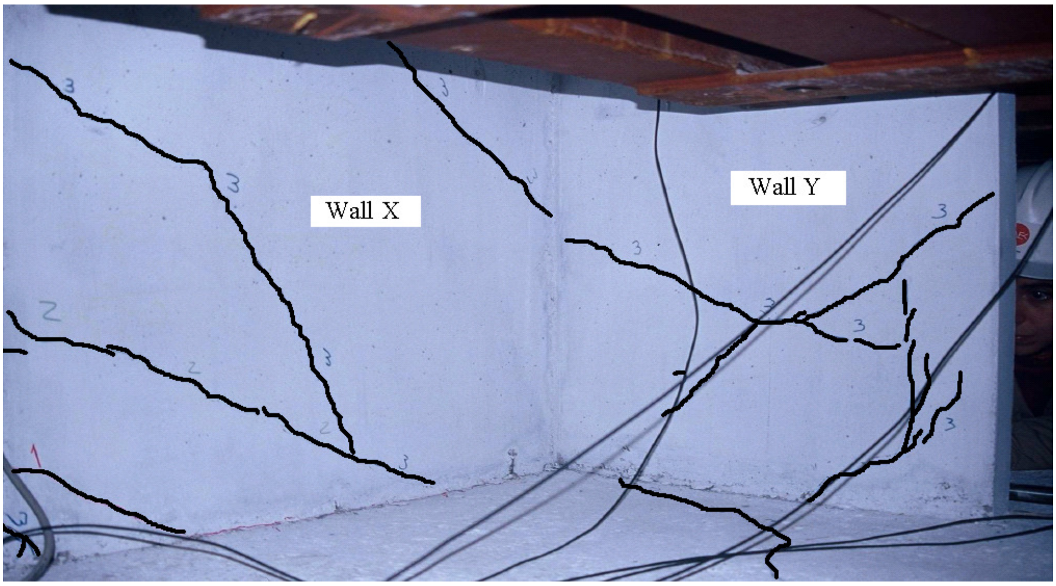

Figure 3-63: Wall X and Y at Level 1 Following T3 (Nguyen, 2006, with cracks darkened by author)

Run T4 was excited in the X and Y direction. The peak roof drift in the X direction was 0.928%. The peak roof drift in the Y direction was 0.634%. Run T4 saw propagation of diagonal 45° cracks as well as the existence of a vertical crack occurring in the right flange wall 14 cm from its edge. This crack pattern can be seen in Figure 3-64.

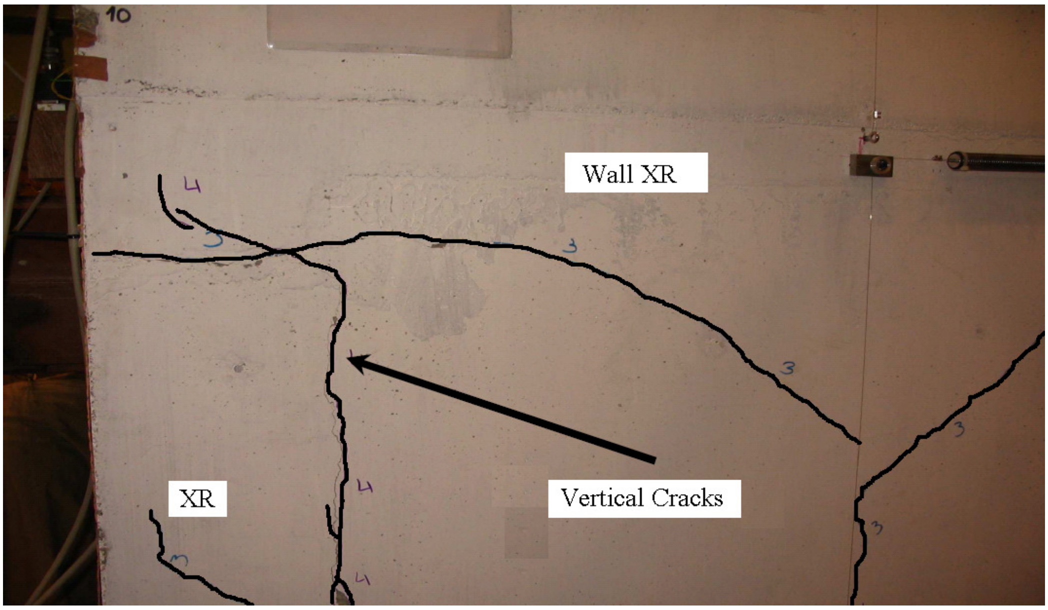

Figure 3-64: Vertical Crack Forming in Wall XR Following T4 (Nguyen, 2006, with cracks darkened by author)

Run T5 was excited in the X and Y direction. The peak roof drift in the X direction was 1.225%. The peak roof drift in the Y direction was 0.705%. Following run 5, no additional reinforcement fractured, although spalling and cracking continued.

Figure 3-65: Crack Patterns in Wall Y Following T5 (Nguyen, 2006, with cracks darkened by author)

Run T6 was excited in the X and Y direction. The peak roof drift in the X direction was 1.279%. The peak roof drift in the Y direction was 0.992%. Run T6 saw additional cracking, as well as the fracture of several additional reinforcing bars in the north side of the left and right flange walls. The reinforcement in the south side of the flange walls did not fracture. Cracking and regions of spalling can be seen in Figure 3-66**Fel! Hittar inte referenskälla.**. In all the tests, there was no indication of yielding of the flexural reinforcement in the coupled web wall. (Nguyen, 2006)

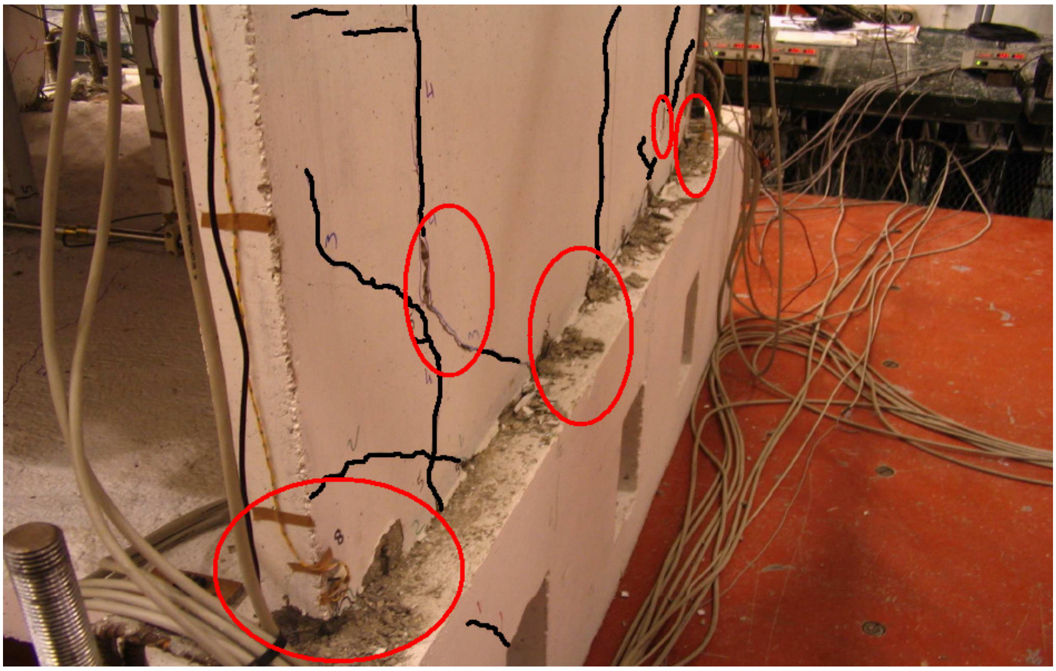

Figure 3-66: Crack Patterns in Wall X Following T6, Areas Circled in Red Denote Regions of Spalling (Nguyen, 2006, with circles added and cracks darkened by author)

3.5 Adjustment of Results Based on Confidence in Test Programs

Many of the runs of the four test programs described in this chapter had issues that caused concerns over the ability of linear elastic analyses in capturing their behavior. In order to ultimately evaluate the methods in Chapter 2, it was desired to weigh each test independently of the others as a way to not penalize methods for not being capable of capturing behavior out of the scope of this study.

A confidence metric using a 0 (lowest potential level of confidence) to 10 (highest potential level of confidence) scale was developed. The goal was to quantify the overall confidence for each run and multiply it by the error values for each run.

Thus, the higher the confidence, the greater weight that particular run would hold. By then adding these weighted errors the tests with more confidence would carry more weight. This is described with the following equation

$$Weighted\_Error_m = \sum_t \left(Error_{m,r} \times Confidence_r \right) \tag{3-1}$$

where:

m = Analysis method

r = Run

The numerical value from this function has no physical meaning; however it allows the methods to be ranked in terms of effectiveness. The method with the lowest weighted error summation from Eq. 3-1 would be ranked as the most effective (#1).

The basis for this ranking system was five different criteria totaling 10 points, each of which will be discussed in detail:

1. Extent of damage not associated with flexure, shear and axial response of the wall (3 points)
2. Table rocking and how it was addressed (2 points)
3. Information provided about the input motion (2 points)
4. Quality of instrumentation (1 points)
5. Uniform stiffness computed to match period is reasonable (2 point)

Thus the confidence term in Eq. 3-1 is defined:

$$\begin{aligned} Confidence_t &= Conf_{damage} + Conf_{rocking} + Conf_{motion} + \ldots \\ &\ldots + Conf_{instrumentation} + Conf_{stiffness} \end{aligned} \tag{3-2}$$

For each test specimen and run, confidence ratings for each criterion and the total confidence rating are listed in Table 3-48. The following subsections discuss these ratings.

3.5.1 Confidence in Damage Mechanisms

The stiffness and damping methods to be evaluated in this study were intended to describe the behavior of concrete walls exhibiting flexural, shear or axial responses to seismic excitation. As such, a run would be given a lower value of confidence if a measured response was affected by damage of the structure other than the wall (e.g. failure of the foundation block, inadequate anchorage of longitudinal reinforcement that resulted in uplift, localized damage due to a connection, etc.) or by damage in the wall that would not typically be associated with flexural, shear or axial response. This issue was deemed as the most likely to result in the limitations associated with capturing the response, and as such it was the most heavily weighted garnering 3 of the 10 points.

Table 3-43: Non-Structural Damage Confidence Key

Little to No Non-Flexural Damage	3
Moderate Non-Flexural Damage	2
Extensive Non-Flexural Damage	1
Non-Flexural Failure	0

Each test program had undesired damage develop in later tests and thus, reduced confidence:

- In the UCSD test, a large splitting crack developed at the longitudinal steel splice at the base of the first floor during EQ 3. As this damage of this type and severity would not be expected in splice regions in a well-detailed, full-scale wall, the confidence for runs EQ 3 and EQ 4 was reduced.
- Combescure, Ragueneau and Mazars provided little information about damage to the CAMUS 2000 specimen, making it difficult to determine if undesired damage affected results for this test program. As a result, confidence was reduced for all runs.
- All of the CAMUS c-shaped specimens exhibited significant damage to the bottom foundation slab in the final run of all three specimens. The confidence value was reduced depending on the severity of this damage.
- CAMUS Ecoleader saw vertical cracking that suggested non-flexural response in run T4.

3.5.2 Table Rocking Confidence

For some test programs, researchers noted that table rocking had a significant impact on the measured response of the wall. In some test programs, table rocking was not discussed. If table rocking that was not addressed or the model recommended by the researchers for modeling table rocking was questionable, the confidence rating for the test program was reduced. Evaluation of simulation data with and without rocking models showed a large difference in response quantities. Thus, this was considered an important issue and confidence was rated from a scale of 0 to 2. The following is the key for the confidence for this criterion.

Table 3-44: Table Rocking Confidence Key

Rocking was measured for and not observed	2
Rocking was measured for, **moderate** rocking was observed and a model was provided to correct for this. (Eg. UCSD)	1.5
Rocking was measured for, **significant** rocking was observed and a model was provided to correct for this. (Eg. CAMUS 2000)	1
Rocking was not considered or instrumented for.	0.5
Significant Rocking was observed but no model was suggested	0

No test used in this study achieved a perfect mark and confidence ratings ranged from 0.5 to 1.5:

- Panagiotou et al. acknowledged that there was moderate rocking of the table for the UCSD test and provided a simple model to capture that portion of the response.
- Combescure et al. also provided a model for simulating table rocking for the CAMUS 2000 test. However, an analysis of displacement output showed that the severity of the rocking was much larger than was observed by UCSD, and thus it was deemed to have had a significant impact on measured wall response.
- For the CAMUS C-shaped and the Ecoleader test programs, table rocking was not discussed in the research reports. Further, table motion was not monitored in the Ecoleader test program. Thus, the lowest confidence ratings were assigned to these tests.

3.5.3 Input Motion Confidence

Accurate information about the actual motion applied to the test specimens was crucial to establishing confidence in the results. Ideally, the measured motion of the table was provided and could be used as the input motion in the numerical simulation. If this was not the case, it was necessary to use the motion input to the table or the motion measured elsewhere, which would not be the same as the actual, measured motion of the table. This could be expected to result in significant differences between simulated and measured wall response, even with a perfect model. Each test program was given a value of confidence for this criterion that ranged from 0 to 2 as described in Table 3-45.

Table 3-45: Input Motion Confidence Key

The motion provided is that which was recorded at the base of the table; in otherwords this is the motion that the specimen is actually subjected to.	2
The motion provided as an input motion was what was intended, but was not confirmed with table instrumentation	1
Information regarding the motion at the table surface was not given. Rather, the only motion that can be used as an input motion in modeling is a floor motion (i.e. this ignores the possible effects of foundation damage/flexibility)	0

Several of the test programs did not provide the motion recorded at the top of the table:

- UCSD and CAMUS 2000 both provided the motion recorded at the top of the table.

- The confidence rating for the CAMUS c-shaped specimen tests were reduced partially as the researchers did not report where the acceleration data were measured.
- For the Ecoleader test program, table accelerations were not measured and only acceleration records at the first floor of the wall were available. Thus, the model of the specimen did not include the foundation elements and any deformation due to foundation flexibility was not simulated.

3.5.4 Instrumentation Confidence

The extent of instrumentation varied for the different test programs. If too few instruments were used, it was difficult to assess wall response. This issue was not considered to be as critical as the previous issues, and each test program was given a confidence rating ranging from 0 to 1 as described in Table 3-46.

Table 3-46: Instrumentation Confidence Key

The specimen and table were well instrumented which provides for an understanding of the global and local response, such as floor displacements, loads, as well as result of yielding.	1
Does not achieve 1, or 0	0.5
Little to no reported information regarding instrumentation of the specimen, reinforcement or table.	0

Most specimens were adequately instrumented:

- The UCSD, CAMUS 2000, and CAMUS Ecoleader specimens were all adequately instrumented to warrant full confidence.

- The data obtained for the c-specimens was rather limited. The limitations and manner the data was presented raised some questions that were difficult to answer regarding the quality of the instrumentation. In addition to this, there was a problem with the data reported for C-2 Stage 1. This raised concerns about all tests in this data set.

3.5.6 Confidence Based on the Uniform Stiffness Required to Match SID Period

The final criterion used to asses confidence in the data was whether the uniform stiffness required to match the measured period was reasonable and did not deviate significantly from what was expected when comparing with other tests. For example, confidence was reduced if the system identification resulted in a period/required uniform stiffness that was far too small or far too large. Confidence was reduced also if stiffness increased with increased drift.

Table 3-47: Uniform Stiffness to Match Period Confidence Key

Uniform Stiffness Key	
Uniform stiffness determined from SAP and System identification seems reasonable	2
Stiffness change is not as high or low as expected	1
The stiffness achieved is erratic and defies reasonable intuition. Ex. The stiffness is low, then increases with increased drift	0

UCSD as well as the C shaped specimens did not exhibit any surprising response with regard to the observed stiffnesses. CAMUS 2000 however saw a significant loss in stiffness despite very low drift demands for the final and ultimate test. CAMUS Ecoleader also saw stiffnesses drop well below $0.05E_cI_g$, which was deemed to be a bottom floor for realistic effective stiffness ratios.

3.5.7 Confidence Metric

Table 3-48 and Table 3-49 show the confidence ratings for each test program and run. Bold values in the "Total Confidence" column represent the average confidence rating for the test program. A review of these data show that the UCSD test program has the highest average confidence rating of 8.5; while the CAMUS Ecoleader test program has the lowest average confidence rating of 5.3.

Table 3-48: Confidence Metric for all Tests (Continued in Table 3-49)

Test Program and Motion Designation	**Damage Description**	**Confidence Points**					
		Total Confidence (10)	Non-Flexural Damage (3)	Table Rocking (2)	Input Motion (2)	Inadequately Instrumented (1)	Stiffness to match response (2)
UCSD		**8.5**	-	-	-	-	-
EQ 1	Minor cracking, M-C suggests @ or near yield	9.5	3	1.5	2	1	2
EQ 2	Yielding of reinforcement at the base	9.5	3	1.5	2	1	2
EQ 3	Limited spalling and unexpected large split crack @ 2nd level	7.5	1	1.5	2	1	2
EQ 4	**Not Run -** lap splice failure and ambiguous geometry change to braces connecting slabs and PT pier	7.5	1	1.5	2	1	2
CAMUS 2000		**7.7**	-	-	-	-	-
Run 1	No damage data reported	8	2	1	2	1	2
Run 2	No damage data reported	8	2	1	2	1	2
Run 3	**Not Run -** Sliding shear failure	7	2	1	2	1	1
CAMUS C-1		**7.0**	-	-	-	-	-
Stage 1	Limited cracking seen near the base	8	3	1	1.5	0.5	2
Stage 2	Nothing reported - likely just further cracking	8	3	1	1.5	0.5	2
Stage 3	Yielding began	7	2	1	1.5	0.5	2
Stage 4	Extensive yielding	6	1	1	1.5	0.5	2
Stage 5	**Not Run -** Fracture of longitudinal reinforcement	6	1	1	1.5	0.5	2

Table 3-49: Confidence Metric for all Tests (Continued from Table 3-48)

Test Program and Motion Designation	**Damage Description**	**Confidence Points**					
		Total Confidence (10)	Non-Flexural Damage (3)	Table Rocking (2)	Input Motion (2)	Inadequately Instrumented (1)	Stiffness to match response (2)
CAMUS C-2		**6.0**	-	-	-	-	-
Stage 1	**Not Run -** insufficient data reported	-	-	-	-	-	-
Stage 2	No significant cracking	7.5	3	1	1.5	0	2
Stage 3	Significant cracking initiated	6.5	2	1	1.5	0	2
Stage 4	Front and back reinforcement yielded	5.5	1	1	1.5	0	2
Stage 5	**Not Run -** Slab failed, confinement yielded	4.5	0	1	1.5	0	2
CAMUS C-3		**7.0**	-	-	-	-	-
Stage 1	Cracking localized at the base	8	3	1	1.5	0.5	2
Stage 2	Cracking localized at the base	8	3	1	1.5	0.5	2
Stage 3	Front and back reinforcement yielded	7	2	1	1.5	0.5	2
Stage 4	Yielding continued	6	1	1	1.5	0.5	2
Stage 5	**Not Run -** Fracture of longitudinal reinforcement	6	1	1	1.5	0.5	2
CAMUS Ecoleader		**5.3**	-	-	-	-	-
T0	Cracks seen at base of the wall and in footing	6.5	3	0.5	0	1	2
T1	**Not Run -** Not excited in the X direction	-	-	-	-	-	-
T2	Additional cracking in wall	6.5	3	0.5	0	1	2
T3	Spalling at ends, buckling of reinforcement and fracture of one bar.	5.5	3	0.5	0	1	1
T4	Propagation of cracks, 45 degree and vertical cracks in wall	4.5	2	0.5	0	1	1
T5	Spalling and cracking continued	4.5	2	0.5	0	1	1
T6	Fracture of additional bars	4.5	2	0.5	0	1	1

3.6 Conclusion

The four test programs discussed in the previous sections were used as the basis for evaluation of the stiffness and damping methods introduced in Chapter 2. These methods were evaluated based on how well they enabled prediction of desired design criteria. These four test programs encompassed specimens in planar, t-shaped, c-shaped and h-shaped configurations; specimens ranging from one to seven stories in height; and of a wide range of drift capacities.

Certain runs of certain tests exhibited responses that were beyond the scope of this research, as such the confidence metric defined in Section 3.5 attempted to correct for undesired responses such as table rocking, foundation damage and other issues. This metric is used in Chapter 5 to provide greater weight to tests that better fit into the scope of this study to improve the ability to draw conclusions on the effectiveness of the methods from Chapter 2.

Chapter 4: Modeling Experimental Tests Using Linear Elastic Time History Software

The methods presented in Chapter 2 for estimating effective stiffness and viscous damping were used to support linear elastic, finite element, time history analyses of the test specimens presented in Chapter 3. These analyses were done using SAP 2000 version 9.2.0, produced by Computers and Structures, Inc. (http://www.csiberkeley.com), but could have been done using any one of a number of commercial and research software. This chapter discusses the assumptions employed in creating numerical models in SAP 2000 of the test specimens presented in Chapter 3. Section 4.1 discusses modeling assumptions employed in creating all of the models, while Sections 4.2 – 4.6 discuss modeling issues unique to each of the test programs.

4.1 Assumptions Used in Creating Numerical Models of the Test Specimens

This section describes aspects of the analysis modeling process that were common to all four of the test specimens including UCSD, CAMUS 2000, CAMUS C, and CAMUS Ecoleader. Linear elastic analysis software was used for the numerical calculations because it is the most common form of finite element analysis due to its ease and speed.

4.1.1 Structural System Model

All structural elements that might impact seismic response were modeled in the structural model. Walls, slabs, and foundations were modeled using thin shell elements. In addition to stiffness modification factors recommended for walls, ACI 318, Section 10.11.1 provides a recommendation for effective stiffness for slabs to be used in an elastic strength design. This was used for all test programs with slabs. This can be seen in Equation 4-1 below.

$$E_c I_{eff} = 0.25 E_c I_g \tag{4-1}$$

Material properties input in the analysis model were equivalent to measured material properties, where available.

4.1.2 Input Variables for Dynamic Analysis

The two parameters investigated in this study were stiffness and damping. The stiffness methods mentioned in Chapter 2 were implemented through the use of direct stiffness modifiers of the shell elements. The damping values were implemented through inputting the appropriate damping value into an analysis case as modal damping. Damping was applied as a single value for all modes.

4.1.3 Input Motion

SAP 2000 supports time history analysis. As such, in the context of modeling the tests introduced in Chapter 3, the accelerations used in the test program were typically the accelerations measured at the top of the shake table. These accelerations were then applied to the underside of the foundation elements. In the case of the Ecoleader specimen, the only acceleration records made available were the records from the first story. This is addressed in Section 4.5.

4.1.4 Extraction of Data

Before comprehensive analyses were done, all models were first validated by performing a modal analysis using the stiffness prescribed by FEMA Cracked. This stiffness was chosen as it was approximately in the middle range of most recommended effective stiffness values. The modal analysis provided a very close approximation of the fundamental period (within 10%) when compared to the fundamental period as reported in the referenced reports.

Displacement and acceleration data were extracted from the model by using plot functions. Plot functions provide the acceleration and displacement experienced by a node of the finite element model over the entirety of the analysis time frame. Acceleration and displacement data were typically taken at locations corresponding to the location of experimental accelerometer and displacement transducer instrument locations. Moment and shear data were obtained by performing section cuts in the analysis model and extracting the time-history loads calculated through the wall.

The following sections will now discuss separate assumptions made for each test program.

4.2 UCSD Modeling Assumptions

The seven-story UCSD wall specimen is presented in detail is Section 3.1. The following describes the analysis approach.

4.2.1 Structural System Model

The specimen comprised two reinforced concrete walls placed in perpendicular directions, reinforced concrete floor slabs, a post-tensioned concrete pier wall, steel tube columns to support gravity loads and steel bracing elements connecting the pier wall to the slab. Flat shell elements were used to model the wall and slabs. Shell elements were approximately 6"x6". The post-tensioned pier, the steel columns, and steel braces were modeled using frame elements. A single element was used for each column, each story of the pier wall and each brace. Figure 4-1 shows the basic model.

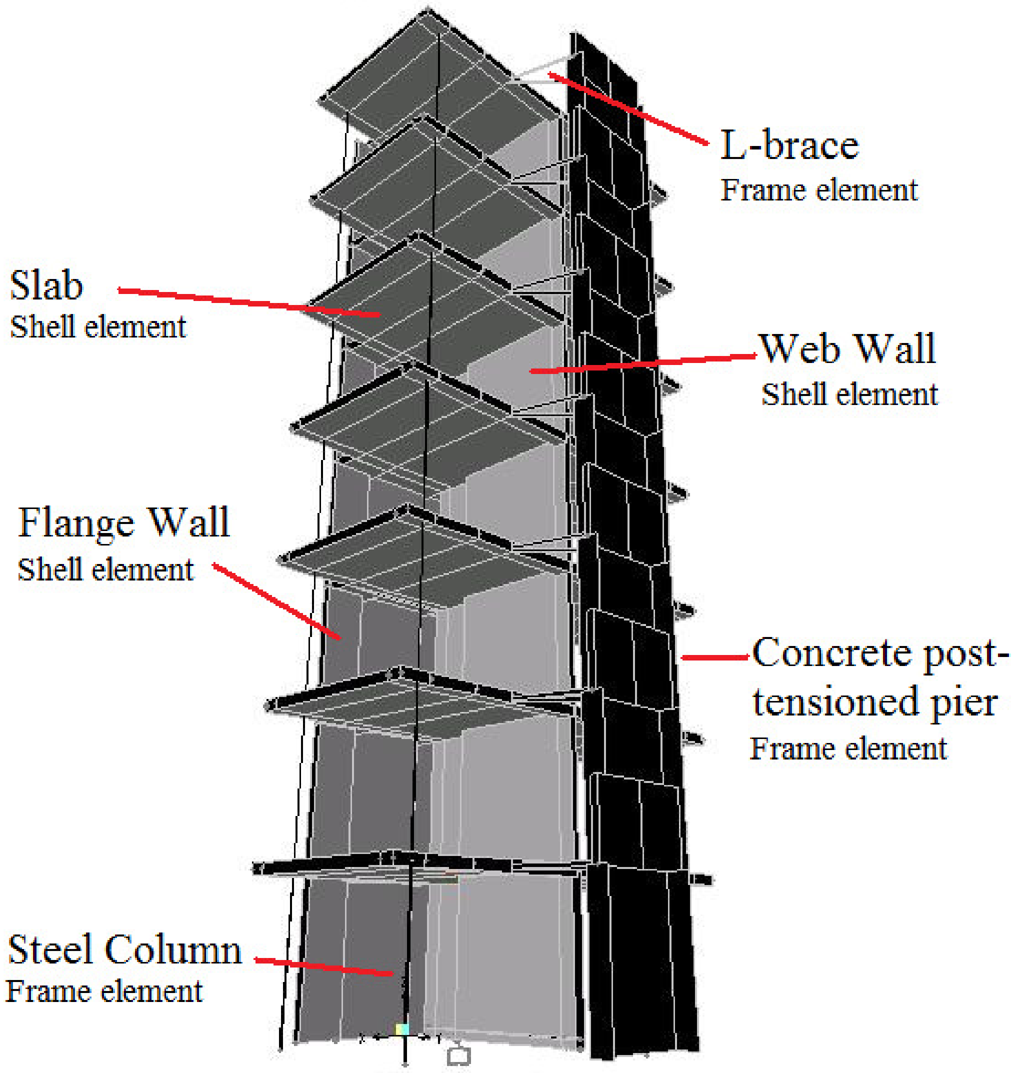

Figure 4-1: Model of UCSD Specimen from SAP 2000

Analyses by Panagiotou et al. ("Model Calibration", 2006) found that all aspects were found to be significant to the response of the structure. Idealizing the test specimen as simply a single wall excited in plane under predicted the total moment for a given displacement. Only by including all components did the model provide satisfactory results. This can be seen graphically in Figure 4-2.

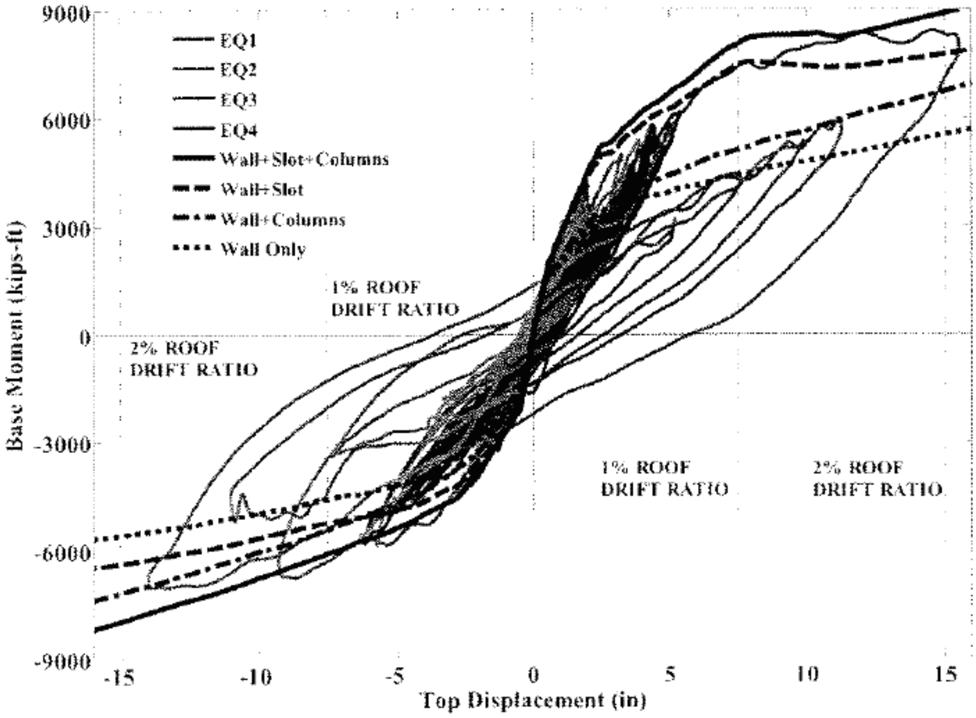

Figure 4-2: Comparison of Measured Hysteretic Response with Computed Envelope of Cyclic Response. Decomposition of Response to Contribution Factors (Panagiotou and Restrepo, "Model Calibration", 2006)

As discussed in Section 3.1, the web and flange of the t-shaped wall are connected only via the floor slab, and to further limit load transfer between the two walls, the slab thickness was reduced to 2 inches in two locations to create a hinge like behavior. This change in thickness was directly modeled by decreasing the thickness of the shell elements in this vicinity. Additionally, it was expected that this region would sustain significantly more damage than would be seen in the rest of the slab; for this reason a $0.1E_cI_g$ effective stiffness modifier was used instead.

As was reported in Section 3.1.5, the referenced report provided a recommendation for flexibility at the base due to table rotation. This was modeled by constraining the base with a diaphragm constraint, which effectively constrained all nodes at the base of the specimen to move in plane. This plane simulated the solid surface of the table, and was then supported using a single link element with all degrees of freedom fixed aside from the rotational stiffness that was prescribed in the literature.

4.2.2 Runs to be Used for Analysis

In the laboratory, the test specimen was subjected to four earthquake ground motions; of these runs EQ1, EQ2, and EQ3 were chosen for extensive analyses. Run EQ4 was not done for several reasons. Panagiotou et al. reported that during the third ground motion, splitting cracks developed at the lap splice at the base of the wall during the third test. While the splice maintained integrity and strength loss was not observed, it is expected that damage in the splice region would have resulted in a substantial increase in wall flexibility that would not be captured by the effective stiffness models. Additionally, prior to application of the fourth ground motion the connection between the braces and the slabs was changed to included a notched connection. No further details of this change were provided. This made the ability to approximate any added flexibility difficult. Given the damage sustained by the wall and the changes in specimen configuration prior to the fourth ground motion, it was decided that the results of analyses of wall response to the fourth ground motion record were not appropriate for use in evaluating the methods presented in Chapter 2.

4.3 CAMUS 2000 Modeling Assumptions

For further details regarding the details of the specimen, refer to Section 3.2. The following describes the analysis approach for the modeling of the CAMUS 2000 specimen.

4.3.1 Structural System Model

The specimen was comprised of two planar walls with concrete slabs. The structure was supported in the transverse direction by steel brace elements. The specimen was modeled using shell elements for the walls, foundation elements and slabs. The steel braces were modeled using frame elements. The foundation elements were modeled using an effective stiffness according to FEMA Cracked. Figure 4-3 shows the basic model.

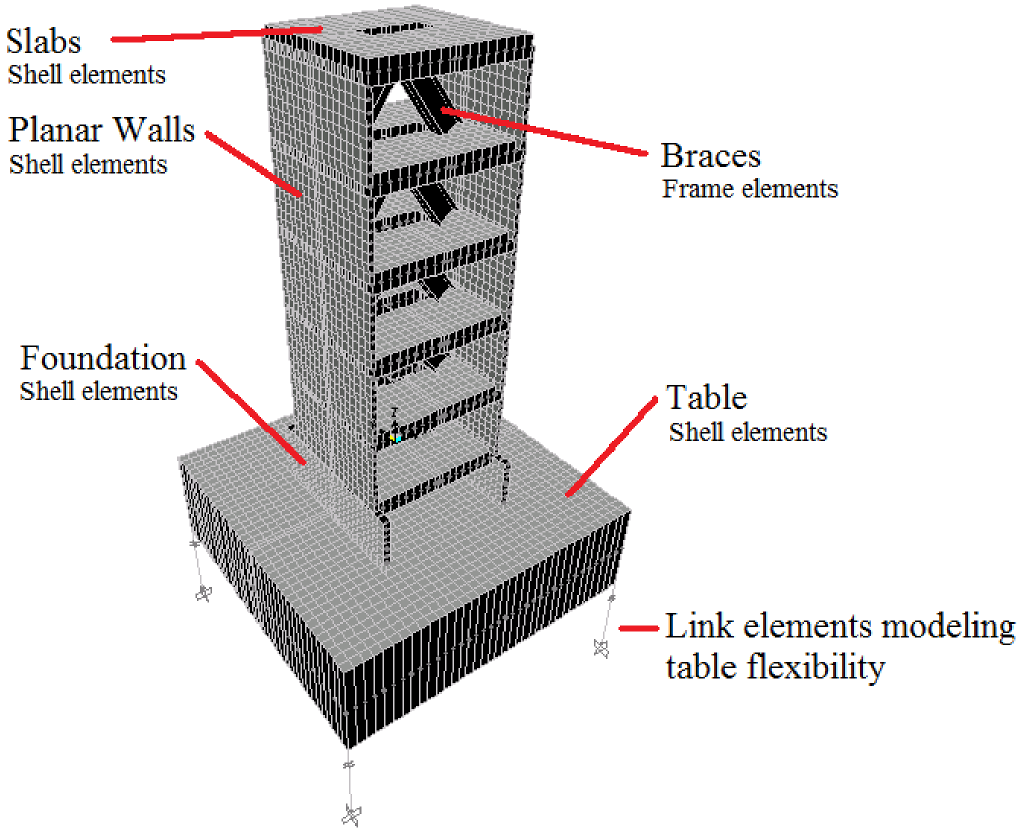

Figure 4-3: Model of CAMUS 2000 Specimen from SAP 2000

The average size of shell elements used for the walls and slabs was approximately 10 cm x 10 cm.

As was reported in Chapter 3, the referenced report provided a recommendation for flexibility at the base due to table rotation. This was modeled by using rigid shell elements with the proper density to model the mass of the table and using four supporting link elements with the suggested axial stiffness.

4.3.2 Runs to be Used for Analysis

The specimen was subjected to a total of three bi-directionally excited runs. The lateral system in the primary direction was two parallel walls. The transverse direction was supported by steel braces, which are outside the scope of this project. Thus, the analytical model was only subjected to accelerations in the direction of the planar walls. As such, the braces had zero stiffness, and were only included so as to provide for a realistic distribution of mass. For Run 2, acceleration data was only available for the roof. The specimen was subjected to three different motions. The third motion saw a sudden sliding shear failure. This test was initially used for analysis, however due to very poor results when compared to period matching stiffness models, it ultimately was dropped from the data set.

4.4 CAMUS C Modeling Assumptions

For further details regarding the specimen refer to Section 3.3. The following describes the analysis approach.

4.4.1 Structural System Model

The specimen was comprised of a C-Shaped specimen with top and bottom slabs. The specimen was modeled using shell elements for the walls and slabs. The additional masses were modeled using evenly distributed rigid frame elements with a rigid diaphragm constraint at the top and bottom to prevent any deformation. Figure 4-4 shows the structural model.

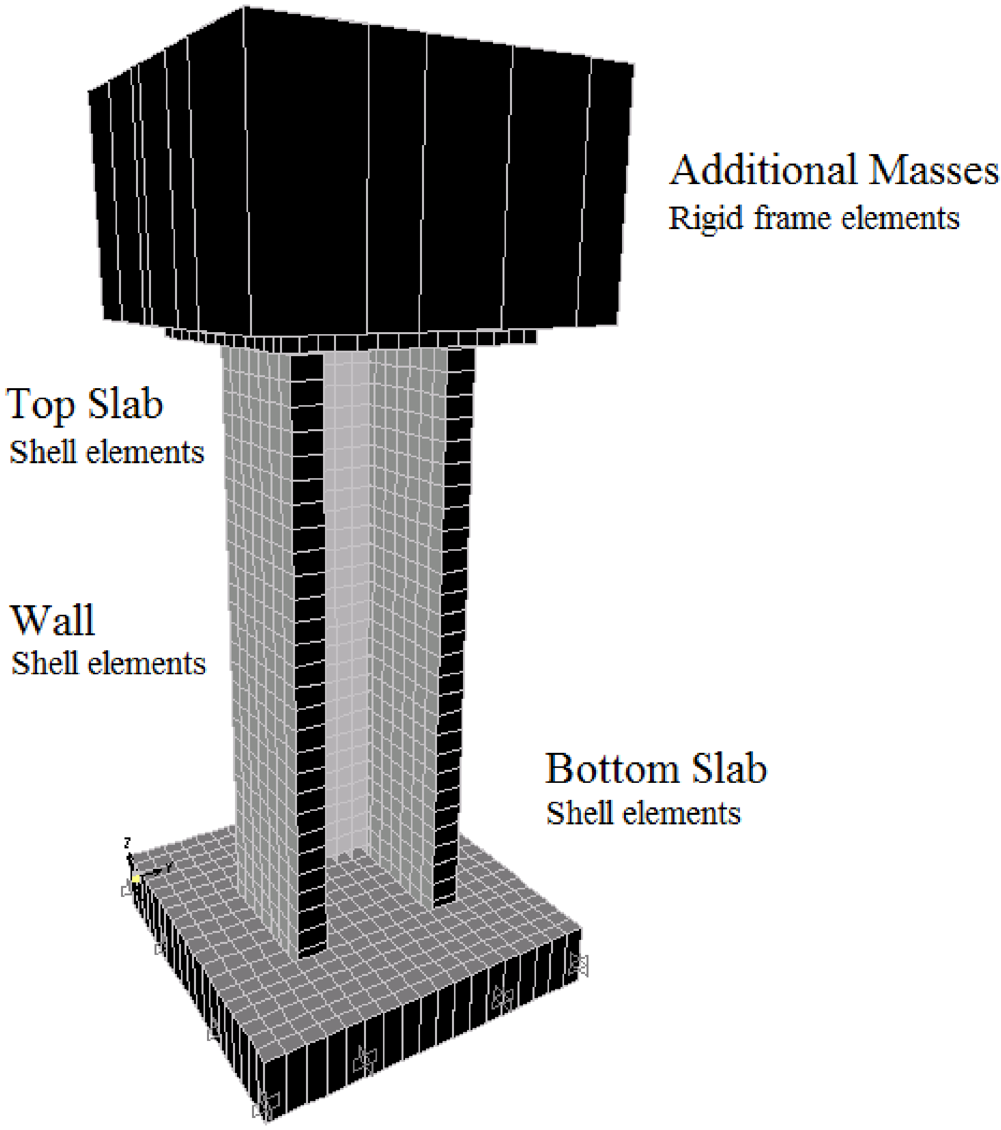

Figure 4-4: Model of CAMUS C Specimens from SAP 2000

The average size of shell elements used for the walls and slabs was approximately 10 cm x 10 cm. Stiffness modifiers were applied for the entire wall and did not vary between flange and web.

4.4.2 Runs to be Used for Analysis

Several runs were not used for analysis. There was no information regarding materials or damage data for specimen C-0. As such, this specimen was not analyzed. Additionally, the ultimate tests for specimens C-1, C-2, and C-3 all saw failure of elements during their respective ultimate runs. C-1 and C-2 saw heavy damage to the bottom slab as well as fracture of longitudinal reinforcement. Researchers reported that C-3 saw failure in the slab. As the extensive damage to the slabs was beyond the scope of this study, these particular runs were not modeled. Upon analyzing error data (to be discussed in Chapter 5), models matching the period of model C-2 test 1 provided drastically different results than what was seen in the channels of output data. As this was the only test to exhibit such complications, it was assumed that there was an unknown problem with either the input motion or the output data provided. For this reason, this particular test was not considered for further analyses.

4.5 CAMUS Ecoleader Modeling Assumptions

Further details regarding the specimen can be found in Section 3.4. The following describes the analysis approach.

4.5.1 Structural System Model

The specimen was comprised of two planar walls in one direction and a coupled wall in the transverse direction. The specimen was modeled using shell elements for the walls and slabs. Figure 4-5 shows the structural model for the CAMUS Ecoleader specimen.

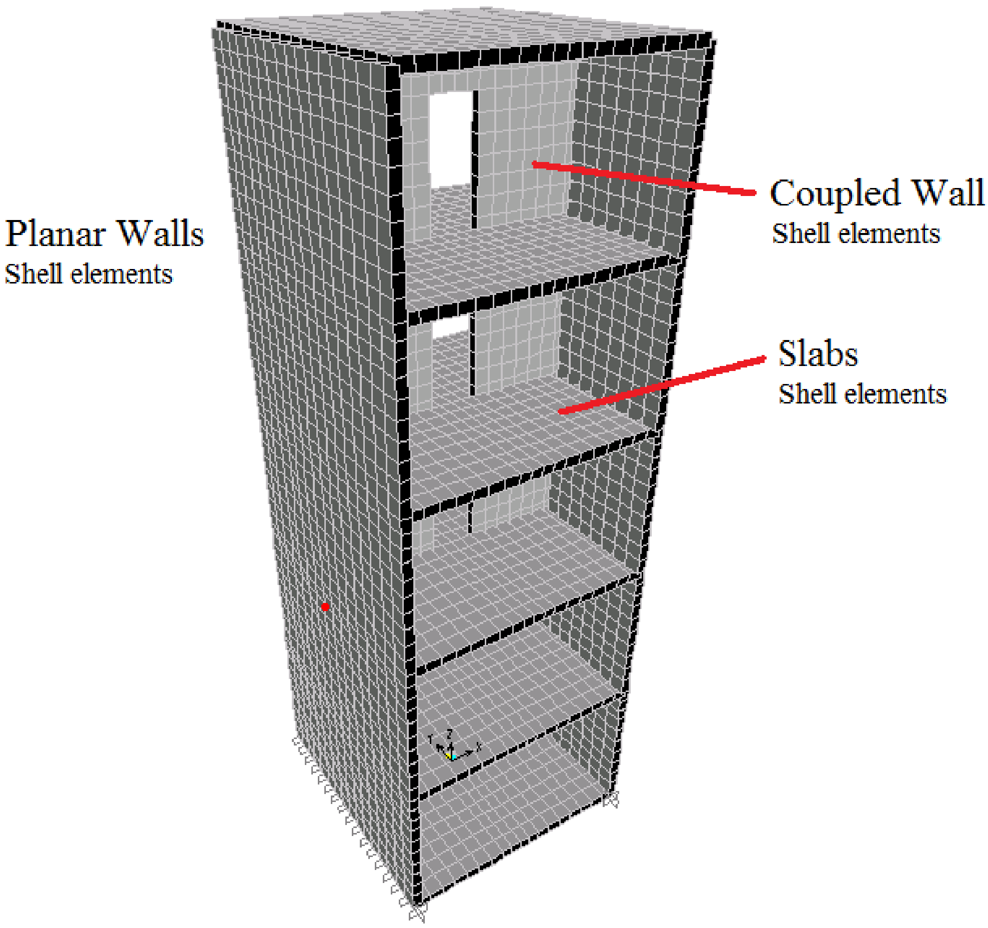

Figure 4-5: Model of CAMUS Ecoleader Specimen from SAP 2000

The average size of shell elements used for the walls and slabs was approximately 10 cm x 10 cm.

4.5.2 Runs to be Used for Analysis

A total of seven runs were performed on the Ecoleader specimen. The first run was excited in the direction of the planar walls. The second run was excited in the direction of the coupled wall, and the five following runs were loaded bi-directionally. As the out of plane coupled wall did not experience significant damage the planar direction was the only considered for analysis. The flexural, shear and axial stiffness used for the coupled wall was the value as prescribed by FEMA for cracked walls.

In the numerical simulation the structure was excited at the base of the wall using the measured acceleration at the top of the foundation. This was done because the actual motion of the table was not available. Accelerometers were not placed on the table to measure this motion because researchers believed the foundation would remain rigid. As discussed in Section 3.4.8, this was not the case and foundation deformation likely introduced errors into the analyses performed here. If the targeted input motion for the table had been provided by the researchers, this might have been a better record for use, however these motions also were not provided.

4.6 Summary of Modeled Specimens and Tests

Table 4-1 and Table 4-2 below provide a representation of the models considered and analyzed. The cells denoted with “NP” were not performed for the reasons discussed in the previous subsections. Some damping methods were used for preliminary analyses and ultimately not used for a comprehensive analysis for all runs. These are described in the cells denoted with “-“.

Table 4-1: Stiffness and Damping Methods to be Used for SAP Analyses ("X" refers to models that have been analyzed, "-" refers to models not run due to ineffectiveness of methods, and "NP" refers to analyses not performed due to laboratory issues) **Continued on next page**

		Existing Methods					Proposed Methods			Period Matching Methods					
										Uniform Stiffness					Variable Stiffness
	Stiffness Model	0.3	FEMA Cracked (0.5)	FEMA Uncracked (0.8)	Adebar Lower Bound	Adebar Upper Bound	Drift based uniform (Brown)	Drift Based Uniform (Doepker)	Drift based variable (Brown)	Sys. ID	3%	7%	FEMA 3%	FEMA 7%	Sys. ID
UCSD	EQ1	X	X	X	X	X	X	X	X	X	X	X	X	X	X
	EQ2	X	X	X	X	X	X	X	X	X	X	X	X	X	X
	EQ3	X	X	X	X	X	X	X	X	X	X	X	X	X	X
	EQ4	NP	NP	NP	NP	NP	NP	NP	NP	NP	NP	NP	NP	NP	NP
CAMUS 2000	Test 1	X	X	X	X	X	X	X	-	X	X	X	-	-	X
	Test 2	X	X	X	X	X	X	X	-	X	X	X	-	-	X
	Test 3	NP	NP	NP	NP	NP	NP	NP	NP	NP	NP	NP	NP	NP	NP
CAMUS C0	Stage 1-5	NP	NP	NP	NP	NP	NP	NP	NP	NP	NP	NP	NP	NP	NP
CAMUS C1	Stage 1	X	X	X	X	X	X	X	-	X	X	X	X	X	X
	Stage 2	X	X	X	X	X	X	X	-	X	X	X	X	X	X
	Stage 3	X	X	X	X	X	X	X	-	X	X	X	X	X	X
	Stage 4	X	X	X	X	X	X	X	-	X	X	X	X	X	X
	Stage 5	NP	NP	NP	NP	NP	NP	NP	NP	NP	NP	NP	NP	NP	NP
CAMUS C2	Stage 1	NP	NP	NP	NP	NP	NP	NP	NP	X	NP	NP	NP	NP	X
	Stage 2	X	X	X	X	X	X	X	-	X	-	-	-	-	X
	Stage 3	X	X	X	X	X	X	X	-	X	-	-	-	-	X
	Stage 4	X	X	X	X	X	X	X	-	X	-	-	-	-	X
	Stage 5	NP	NP	NP	NP	NP	NP	NP	NP	NP	NP	NP	NP	NP	NP
CAMUS C3	Stage 1	X	X	X	X	X	X	X	-	X	-	-	-	-	X
	Stage 2	X	X	X	X	X	X	X	-	X	-	-	-	-	X
	Stage 3	X	X	X	X	X	X	X	-	X	-	-	-	-	X
	Stage 4	X	X	X	X	X	X	X	-	X	-	-	-	-	X
	Stage 5	NP	NP	NP	NP	NP	NP	NP	NP	NP	NP	NP	NP	NP	NP

Table 4-2: Continued from Table 4-1: Stiffness and Damping Methods to be Used for SAP Analyses ("X" refers to models that have been analyzed, "-" refers to models not run due to ineffectiveness of methods, and "NP" refers to analyses not performed due to laboratory issues)

		Existing Methods					**Proposed Methods**			**Period Matching Methods**					
										Uniform Stiffness					Variable Stiffness
	Stiffness Model	0.3	FEMA Cracked (0.5)	FEMA Uncracked (0.8)	Adebar Lower Bound	Adebar Upper Bound	Drift based uniform (Brown)	Drift Based Uniform (Doepker)	Drift based variable (Brown)	Sys. ID	3%	7%	FEMA 3%	FEMA 7%	Sys. ID
CAMUS Ecoleader Planar	Stage 1	**X**	**X**	**X**	**X**	**X**	**X**	**X**	-	**X**	-	-	-	-	-
	Stage 2	NP	NP	NP	NP	NP	NP	NP	NP	NP	NP	NP	NP	NP	NP
	Stage 3	**X**	**X**	**X**	**X**	**X**	**X**	**X**	-	**X**	-	-	-	-	-
	Stage 4	**X**	**X**	**X**	**X**	**X**	**X**	**X**	-	**X**	-	-	-	-	-
	Stage 5	**X**	**X**	**X**	**X**	**X**	**X**	**X**	-	**X**	-	-	-	-	-
	Stage 6	**X**	**X**	**X**	**X**	**X**	**X**	**X**	-	**X**	-	-	-	-	-
	Stage 7	**X**	**X**	**X**	**X**	**X**	**X**	**X**	-	**X**	-	-	-	-	-
CAMUS Ecoleader Coupled	Stage 1-7	NP	NP	NP	NP	NP	NP	NP	NP	NP	NP	NP	NP	NP	NP

Chapter 5: Evaluation of Method

The methods for predicting the effective stiffness, damping and fundamental period of walls presented in Chapter 2 and the modeling techniques presented in Chapter 4 were used to simulate the experimental tests described in Chapter 3. The stiffness, damping and period prediction methods were evaluated through comparison of simulated and measured response quantities. In this chapter, analysis results and the comparison of simulated and measured response quantities are presented. Additionally, conclusions about the effectiveness of the various stiffness, damping and period prediction methods are presented. The chapter is organized as follows:

- 5.1 – Results of the System Identification
- 5.2 – Period Matching Models
- 5.3 – Preliminary Evaluation of Methods
- 5.4 – Methods Evaluated Using Linear Time History Analysis
- 5.5 – Definition of Error Evaluation Functions
- 5.6 – Error Results
- 5.7 – Discussion of Error Results
- 5.8 – Prediction of Response Quantities as a Function of Period Prediction
- 5.9 – Comparison of Doepker and Brown Results
- 5.10 – Sources of Error for Period Matching Models
- 5.11 – Discussion of all Drift Ranges

5.1 Results of System Identification

Ranf and Eberhard (2007) studied the accuracy of system identification methods to determine the dynamic properties of bridge subassemblages subjected to shake table testing. Ranf and Eberhard investigated a number of different system identification methods. For this study, an autoregressive with exogenous excitation (ARX) algorithm was adopted to identify the period of the primary mode of vibration as well as the level of modal damping for each run for each specimen test program. This was chosen as this particular algorithm uses input and output response data and requires no consideration of the structural geometry or other parameters. Ranf also found that using displacement records as input in ARX system identification typically overestimated the damping ratios, particularly in secondary modes when compared to using acceleration records (Ranf 2007). As such, the system identification performed in this study used acceleration records provided at each story level (when available) in each respective study. From this, an estimate of the effective period and the effective modal damping of the primary mode were determined for each run of each test program. In the case of the CAMUS Ecoleader specimen, records were only available for several of the intermediary floors. The CAMUS C specimens were also sparsely instrumented.

The entire acceleration record was used. This in effect resulted in determining the period and damping as an average over the entire time history, and not necessarily at the point of maximum roof drift. In cases in which there was an input motion in the X and Y direction, each was handled independently.

Table 5-1 lists the effective fundamental period and effective damping ratio for each specimen and run computed using the ARX system identification method. Table 5-1 lists also the computed effective fundamental period normalized with respect to the fundamental period as recorded in each tests' corresponding report. The values denoted with an asterisk refer to cases where the drift demands at a subsequent run were less than the run that preceded it. The effective damping as it relates to drift can be seen in Figure 5-1 and the effective period normalized by the fundamental period mentioned in the literature can be seen in Figure 5-2. Both of these plots exclude the data denoted with asterisks as these runs would not be expected to exhibit the same behavior as those seeing progressively increasing levels of roof drift.

Table 5-1: Summary of Period and Modal Damping Found From System Identification (* refers to cases where drift demand is less than the run that preceded it – not used for T and β plots)

	Test	Max Roof Drift	Damping	Teff	Teff/T0
UCSD	EQ 1	0.27%	5.06%	0.65	1.1
	EQ 2	0.76%	8.75%	0.84	1.5
	EQ 3	0.83%	18.01%	0.96	1.7
	EQ 4	2.06%	26.55%	1.23	2.2
CAMUS 2000	Run 1	0.09%	6.90%	0.19	1.2
	Run 2	0.30%	15.00%	0.25	1.6
	Run 3	0.38%	15.00%	0.28	1.8
CAMUS C, Specimen 0	Stage 1	0.85%	7.86%	0.5	1.9
	Stage 2	0.34% *	3.37%	0.58	2.2
	Stage 3	0.75% *	2.91%	0.59	2.3
	Stage 4	2.19%	12.65%	0.68	2.6
	Stage 5	2.05% *	12.65%	0.79	3
CAMUS C, Specimen 1	Stage 1	0.35%	8.36%	0.43	1.6
	Stage 2	0.52%	5.26%	0.47	1.7
	Stage 3	1.31%	6.72%	0.61	2.2
	Stage 4	1.85%	12.88%	0.7	2.6
	Stage 5	3.92%	13.19%	0.85	3.1
CAMUS C, Specimen 2	Stage 1	0.16%	4.14%	0.33	1.1
	Stage 2	0.08% *	2.98%	0.33	1.1
	Stage 3	0.54%	11.56%	0.42	1.5
	Stage 4	1.91%	16.63%	0.61	2.1
	Stage 5	4.06%	36.81%	0.75	2.6
CAMUS C, Specimen 3	Stage 1	0.12%	3.88%	0.3	1.1
	Stage 2	0.35%	9.67%	0.4	1.5
	Stage 3	1.32%	11.77%	0.57	2.1
	Stage 4	2.27%	19.69%	0.74	2.7
	Stage 5	4.08%	27.50%	0.83	3.1
CAMUS, Ecoleader, X Direction	T 0	0.16%	6.18%	0.22	1
	T 1	0.00% *	5.67%	0.2	0.9
	T 2	0.20%	4.06%	0.25	1.1
	T 3	0.62%	14.61%	0.37	1.7
	T 4	0.87%	28.66%	0.4	1.8
	T 5	1.19%	15.70%	0.46	2.1
	T 6	1.30%	10.66%	0.56	2.5

Figure 5-1 shows a trend of an increase in effective damping with increased roof drift demand as expected. For drift ranges of 0.0% to 0.5%, damping ratios range between 3% to as high as 15%. For drift ranges of 0.5% to 1.0% damping ratios range from 8% to 17% with an additional outlier (Ecoleader run T4, roof drift of 0.87% and 28.66% effective damping ratio). For higher drift ranges, the effective damping ratios vary from 10% to almost 40%. The CAMUS Ecoleader specimen shows the least consistent trend. This was the only specimen that had reinforced concrete walls resisting loads in two directions. It also suffered from foundation damage, a scenario that was not anticipated by the researchers. Finally this specimen also saw the greatest number of tests. It could be that yielding was so extensive by test T4 that subsequent tests exhibited little further yielding and thus saw less energy dissipation.

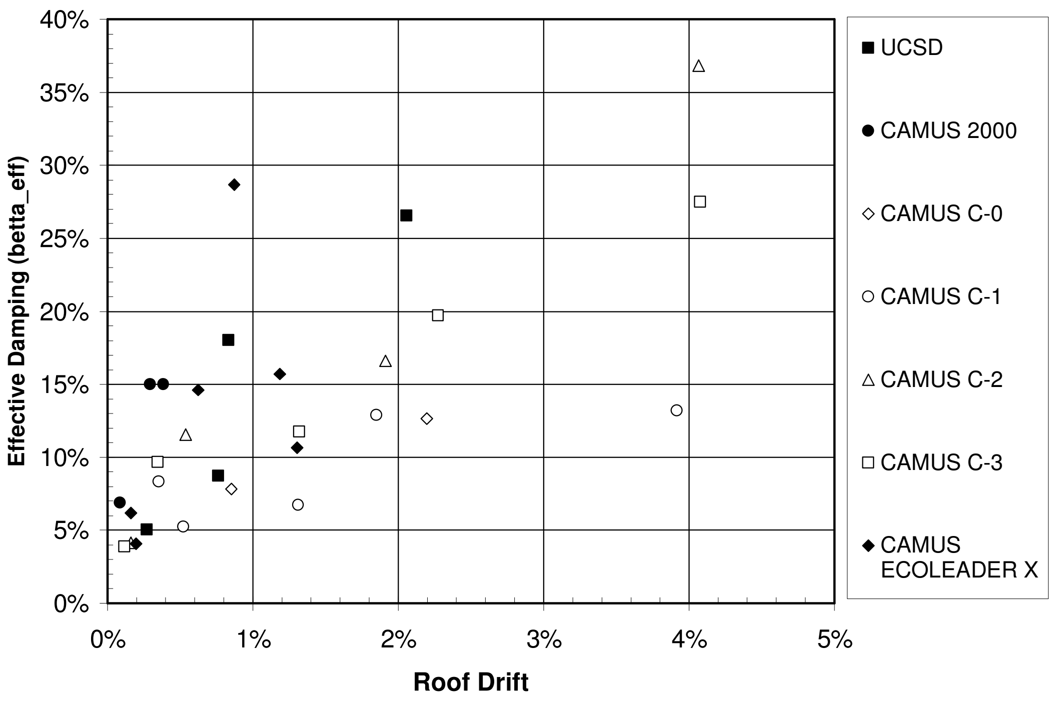

Figure 5-1: Effective Damping as it Relates to Roof Drift Demand for Shake Table Tests

Figure 5-2 shows a trend of increasing period with respect to the roof drift. In the low drift range of 0.0% to 0.5%, the ratio of the effective period to the initial fundamental period recorded in the referenced reports ranges between 1.0 and 1.6. Significant variation depending on the test program is seen for drift ranges between 0.5% and 1.0%. T_{eff}/T_0 ranges from 1.4 to 2.5. For higher drifts, T_{eff}/T_0 varies between 2.1 and 3.6. Ecoleader in particular showed the least clear trend in the data, potentially for reasons as mentioned following Figure 5-1.

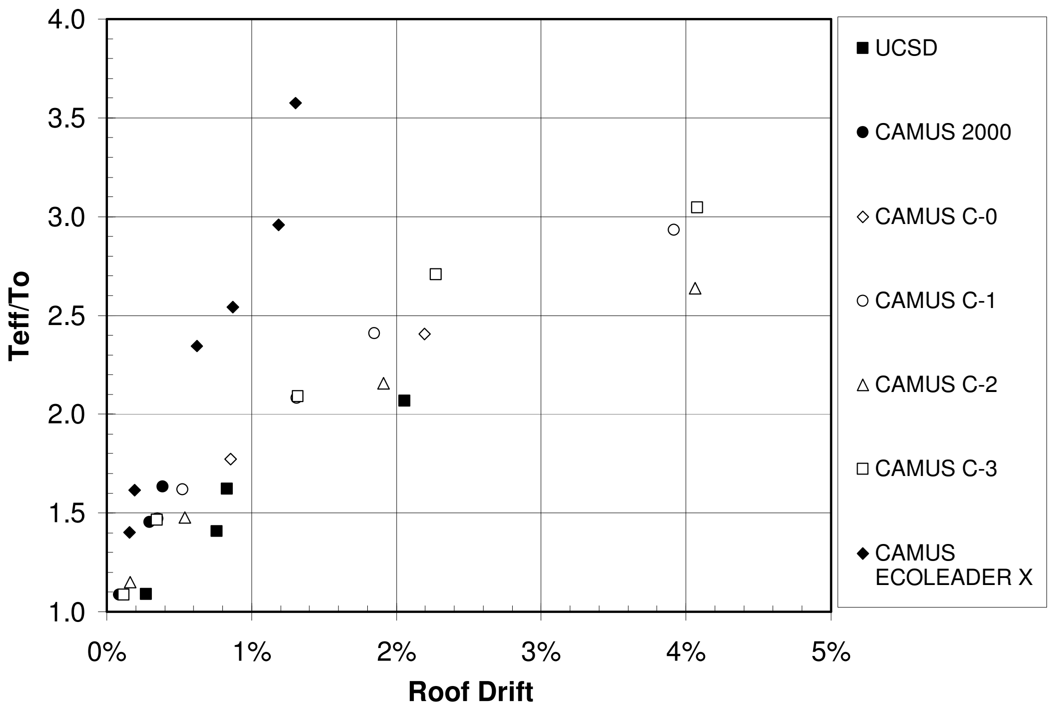

Figure 5-2: Ratio of Effective Period to Fundamental Period as it Relates to Roof Drift Demand for Shake Table Tests

The slope of the trend in the data for each test program tends to behave somewhat independently of the other tests. It is unclear which factors may influence this. The role of aspect ratio, reinforcement ratio, axial load ratio, and other parameters were investigated but there was no strongly consistent trend.

Due to the significant variation in both the damping and period ratios, it is difficult to develop a relationship of T_{eff}/T_0 or β_{eff} as a function of roof drift.

As mentioned in Chapter 3, there are several methods to approximate the initial fundamental period. The effectiveness of these methods will be discussed in section 5.3, however upon looking at the results from Figure 5-2, it is quite clear that there is a significant elongation of the period for even low drift demands, and this stiffness loss must be considered when attempting to predict the response of seismically excited wall buildings. As this degradation in stiffness has a strong correlation to the roof drift demand, a method that accounts for reduction in stiffness with respect to the roof drift has the potential to better predict of the proper period.

5.2 Period Matching Models

In order to evaluate existing and proposed methods, period matching models were determined. Several different methods for matching the period were investigated along with several different values for damping ratios.

5.2.1 Establishing the Stiffness for Period Matching Models

These models used the results of the system identification to match the period. The period matching was achieved using a uniform stiffness and (in some cases) a variation of stiffness over the height. The in plane stiffness for the uniform model was found using an initial estimate that was refined until the period of the primary mode matched the corresponding period determined from the system identification.

The variable stiffness model used the experimental data to establish a moment envelope over the specimen height. By comparing the results of a moment curvature analysis with experimental results, yielded, cracked and uncracked regions were determined. The stiffness values of the uncracked and cracked regions were estimated as $0.8E_cI_g$ and $0.5E_cI_g$ respectively as prescribed by FEMA 356 (ASCE, 2000) where E_cI_g is the gross section stiffness. The stiffness of the post yielded regions were estimated using the same approach as in the uniform stiffness case to match the period. In the cases of runs resulting in a moment less than the yield moment, the stiffness in the cracked regions was adjusted to match the period. An example of moment curvature results and the observed moment envelope are seen in Figure 5-3 and Figure 5-4.

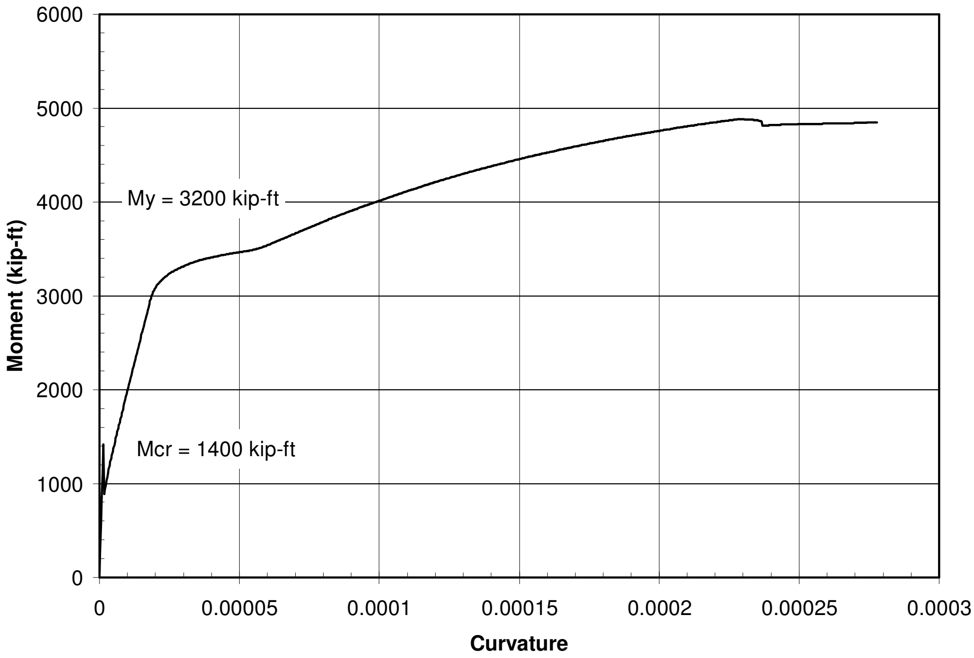

Figure 5-3: Results from Moment Curvature Analysis – UCSD Specimen

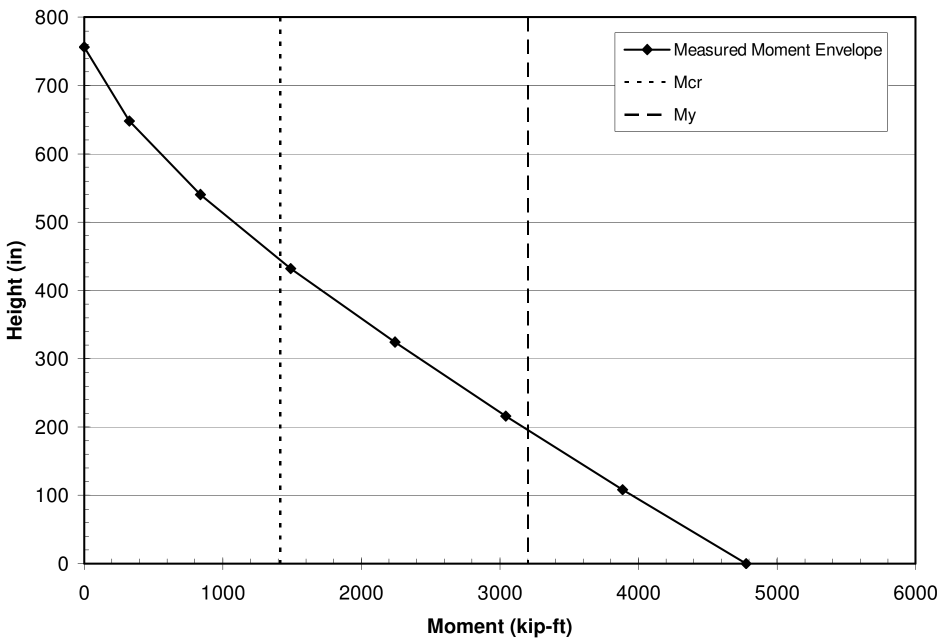

Figure 5-4: Sample Moment Envelope – UCSD EQ 1 Test

The error results of the variable stiffness period matching approach are provided in Appendix A. The result of using a variable stiffness model had a mixed effect, occasionally reducing errors and in other cases having a negligible effect. Furthermore, some test programs did not provide sufficient data to adequately predict which regions were exhibiting cracking, yielding etc. As such this approach was not taken for all specimens and is not discussed in the body of the report.

5.2.2 Damping Value Estimates for Period Matching Models

Different values for damping were used for the period matching stiffness models to investigate its influence. The primary level of damping used in the period matching analyses was the damping determined from the system identification. Additionally, the damping values of 3% and 7% as suggested by Newmark and Hall (1982) as well as the ductility based method described by FEMA 440 (ATC, 2005) were implemented to varying extents. A significant discussion of the period matching results using the values suggested by Newmark and Hall is included in Section 5.10 while further analysis results are found in Appendix A. In the case of the FEMA 440 method, analysis showed that it provided little to no benefit, and the results are thus not included in the body of this document,. The results can be found in Appendix A.

5.2.3 Combination of Stiffness and Damping Values to be Used in Period Matching Models

As mentioned in the previous subsections, two separate stiffness approaches were used and four different damping methods were investigated. Table 5-2 lists the different combinations of stiffness and damping techniques used for the period matching models investigated in this study. In some cases, due to a lack of experimental data, the variable stiffness period matching model was not run. Three percent and 7% modal damping values were also not analyzed for every run of each specimen.

Table 5-2: Analyzed Period Matching Models

Stiffness Models	**Damping Models**
Uniform Period Matching Stiffness	System I.D. Damping
	Newmark and Hall 3%
	Newmark and Hall 7%
	FEMA 440 Ductility Based Damping
Variable Period Matching Stiffness	System I.D. Damping

5.3 Preliminary Evaluation of Methods

An initial evaluation was performed on the methods discussed in Chapter 2 to evaluate how well these methods predict the stiffness, period, and damping as determined from the system identification damping and period matching reference model.

5.3.1 Stiffness Prediction

The various methods of stiffness prediction were compared to the uniform stiffness from the period matching model. As this is the best estimate of the structural stiffness, all other approximations are compared with it. Table 5-3 gives values for effective stiffness for each method.

Table 5-4 provides a value of error computed using a simple percent difference calculation. A positive value of error indicates that the recommended stiffness is greater than the stiffness to match the system identification period. A negative value indicates that the predicted value was less than the SI value.

$$Error_{stiffness} = \left(\frac{\left(\mathrm{E_c} I_{eff}\right)_{estimated} - \left(\mathrm{E_c} I_{eff}\right)_{reference}}{\left(\mathrm{E_c} I_{eff}\right)_{reference}} \right) \quad (5\text{-}1)$$

where:

$\mathrm{Error}_{\mathrm{stiffness}}$ = the percent difference in stiffness,

$(\mathrm{E_c I_{eff}})_{\mathrm{estimated}}$ = the recommended stiffness,

$(\mathrm{E_c I_{eff}})_{\mathrm{reference}}$ = the stiffness to match the system identification period

Table 5-3: Stiffness Modification Factors Predicted from Various Methods

		Period Matching	FEMA 356 Uncracked (Eq. 2-1,2,3)	FEMA 356 Cracked (Eq. 2-4,5,6)	FIB 27 (Eq 2-11)	ACI 318 Uncracked (Eq. 2-8)	ACI 318 Cracked (Eq. 2-9)	Paulay and Priestley (Eq. 2-12)	Adebar Upper Bound (Eq. 2-15)	Adebar Lower Bound (Eq. 2-16)	Brown, 2008 (Eq. 2-18)	Doepker, 2008 (Eq. 2-31)
UCSD	EQ 1	**0.365**	0.8	0.5	0.3	0.7	0.35	0.268	0.65	0.325	0.30	0.27
	EQ 2	**0.16**									0.17	0.17
	EQ 3	**0.1**									0.16	0.16
CAMUS 2000	Test 1	**0.62**	0.8	0.5	0.3	0.7	0.35	0.194	0.643	0.308	0.30	0.37
	Test 2	**0.26**									0.30	0.26
	Test 3	**0.19**									0.27	0.24
CAMUS C-1	Stage 1	**0.23**	0.8	0.5	0.3	0.7	0.35	0.187	0.627	0.268	0.28	0.25
	Stage 2	**0.19**									0.23	0.21
	Stage 3	**0.11**									0.09	0.12
	Stage 4	**0.085**									0.05	0.09
CAMUS C-2	Stage 1	**0.37**	0.8	0.5	0.3	0.7	0.35	0.187	0.627	0.268	0.30	0.32
	Stage 2	**0.37**									0.30	0.38
	Stage 3	**0.23**									0.22	0.2
	Stage 4	**0.11**									0.04	0.08
CAMUS C-3	Stage 1	**0.41**	0.8	0.5	0.3	0.7	0.35	0.187	0.627	0.268	0.30	0.35
	Stage 2	**0.235**									0.28	0.25
	Stage 3	**0.112**									0.09	0.11
	Stage 4	**0.066**									0.03	0.07
CAMUS Ecoleader	T-0	**0.22**	0.8	0.5	0.3	0.7	0.35	0.179	0.618	0.245	0.30	0.32
	T-2	**0.17**									0.30	0.3
	T-3	**0.078**									0.20	0.19
	T-4	**0.067**									0.15	0.15
	T-5	**0.05**									0.10	0.12
	T-6	**0.034**									0.09	0.12

Table 5-4: Percent Difference of Stiffness Prediction Methods with Period Matching Uniform Stiffness

		Period Matching	FEMA 356 Uncracked (Eq 2-1,2,3)	FEMA 356 Cracked (Eq 2-4,5,6)	FIB 27 (Eq. 2-11)	ACI 318 Uncracked (Eq. 2-8)	ACI 318 Cracked (Eq. 2-9)	Paulay and Priestley (Eq. 2-12)	Adebar Upper Bound (Eq. 2-15)	Adebar Lower Bound (Eq. 2-16)	Brown, 2008 (Eq. 2-18)
UCSD	EQ 1	119.2%	37.0%	-17.8%	91.8%	-4.1%	-26.6%	78.1%	-11.0%	-17.8%	-25.6%
	EQ 2	400.0%	212.5%	87.5%	337.5%	118.8%	67.5%	306.3%	103.1%	7.9%	5.2%
	EQ 3	700.0%	400.0%	200.0%	600.0%	250.0%	168.0%	550.0%	225.0%	58.4%	59.3%
CAMUS 2000	Test 1	29.0%	-19.4%	-51.6%	12.9%	-43.5%	-68.8%	3.7%	-50.4%	-51.6%	-39.8%
	Test 2	207.7%	92.3%	15.4%	169.2%	34.6%	-25.5%	147.3%	18.3%	15.4%	1.2%
	Test 3	321.1%	163.2%	57.9%	268.4%	84.2%	1.9%	238.4%	61.8%	42.7%	24.9%
CAMUS C-1	Stage 1	247.8%	117.4%	30.4%	204.3%	52.2%	-18.5%	172.6%	16.3%	22.5%	7.0%
	Stage 2	321.1%	163.2%	57.9%	268.4%	84.2%	-1.4%	230.0%	40.8%	20.9%	8.7%
	Stage 3	627.3%	354.5%	172.7%	536.4%	218.2%	70.3%	470.0%	143.2%	-19.2%	4.6%
	Stage 4	841.2%	488.2%	252.9%	723.5%	311.8%	120.5%	637.6%	214.7%	-45.0%	1.1%
CAMUS C-2	Stage 1	116.2%	35.1%	-18.9%	89.2%	-5.4%	-49.4%	69.5%	-27.7%	-18.9%	-13.2%
	Stage 2	116.2%	35.1%	-18.9%	89.2%	-5.4%	-49.4%	69.5%	-27.7%	-18.9%	2.5%
	Stage 3	247.8%	117.4%	30.4%	204.3%	52.2%	-18.5%	172.6%	16.3%	-2.2%	-11.7%
	Stage 4	627.3%	354.5%	172.7%	536.4%	218.2%	70.3%	470.0%	143.2%	-60.6%	-24.2%
CAMUS C-3	Stage 1	95.1%	22.0%	-26.8%	70.7%	-14.6%	-54.3%	52.9%	-34.8%	-26.8%	-14.8%
	Stage 2	240.4%	112.8%	27.7%	197.9%	48.9%	-20.3%	166.8%	13.8%	20.7%	5.4%
	Stage 3	614.3%	346.4%	167.9%	525.0%	212.5%	67.3%	459.8%	138.8%	-21.1%	2.4%
	Stage 4	1112.1%	657.6%	354.5%	960.6%	430.3%	183.9%	850.0%	305.3%	-57.4%	8.1%
CAMUS Ecoleader	T-0	263.6%	127.3%	36.4%	218.2%	59.1%	-18.7%	180.9%	11.4%	36.4%	46.2%
	T-2	370.6%	194.1%	76.5%	311.8%	105.9%	5.3%	263.5%	44.1%	76.5%	78.3%
	T-3	925.6%	541.0%	284.6%	797.4%	348.7%	129.4%	692.3%	214.1%	161.1%	141.7%
	T-4	1094.0%	646.3%	347.8%	944.8%	422.4%	167.1%	822.4%	265.7%	125.5%	130.7%
	T-5	1500.0%	900.0%	500.0%	1300.0%	600.0%	257.9%	1136.0%	390.0%	106.9%	149.0%
	T-6	2252.9%	1370.6%	782.4%	1958.8%	929.4%	426.3%	1717.6%	620.6%	164.9%	240.7%
Average Error		557.9%	311.2%	146.7%	475.7%	187.8%	57.7%	414.9%	118.1%	21.7%	32.8%
Standard Deviation		525.6%	328.5%	197.1%	459.9%	230.0%	118.7%	405.6%	160.7%	65.1%	68.4%
Maximum Error		2252.9%	1370.6%	782.4%	1958.8%	929.4%	426.3%	1717.6%	620.6%	164.9%	240.7%
Minimum Error		29.0%	-19.4%	15.4%	12.9%	-4.1%	-1.4%	3.7%	-11.0%	-2.2%	1.1%
Average Error in 1st Test		145.2%	53.2%	**-8.1%**	114.5%	**7.3%**	-39.4%	92.9%	-16.0%	**-9.4%**	**-6.7%**
Standard Deviation in 1st Test		91.7%	57.3%	34.4%	80.3%	40.1%	21.0%	69.9%	26.4%	32.7%	30.1%

The errors provided in Table 5-4 used measured material strengths, axial loads, and drift values as opposed to design values. For example, the stiffness values predicted using the expression by Paulay and Priestley (1990) were calculated using the actual yield strength of the reinforcement rather than the design value. The Paulay-Priestley expression and the Adebar expression are a function of the measured axial load. The stiffness values predicted by the Brown 2008 and Doepker 2008 curves used the recorded roof drifts. Thus these estimates indicated a best possible prediction for all methods.

The computed error was plotted as a function of roof drift and is shown in Figure 5-5. To facilitate evaluation of the data Figure 5-6 shows errors for data from methods with lower effective stiffness values such as FEMA Cracked ($0.5EI_g$), FIB 27 ($0.3EI_g$) and the Adebar lower bound stiffness (which is a function of axial load ratio). Figure 5-7 shows the value as predicted by the Doepker and Brown methods.

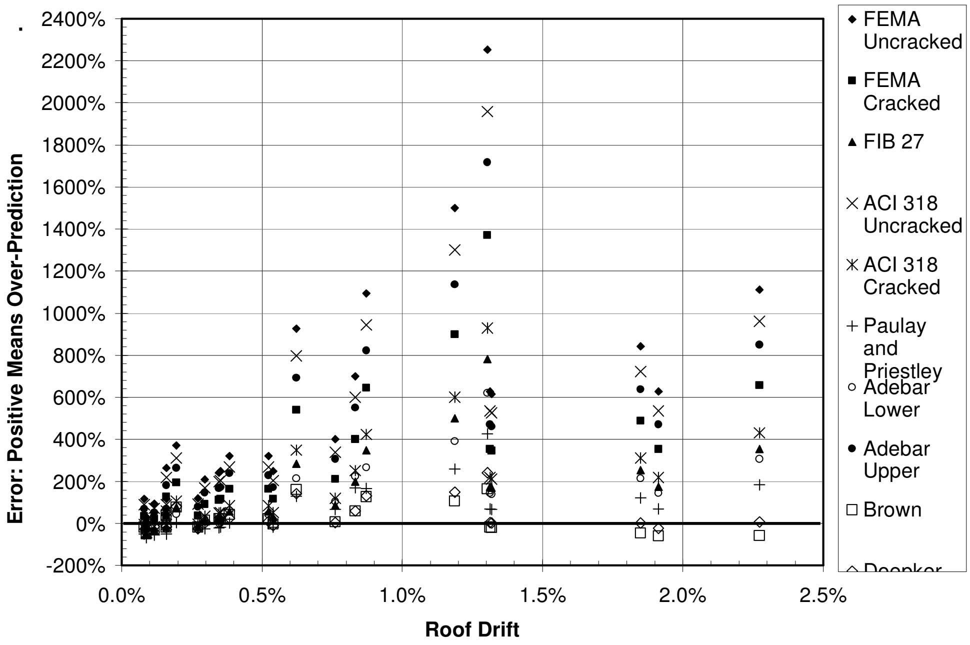

Figure 5-5: Error in Predicted Stiffness with Respect to Drift

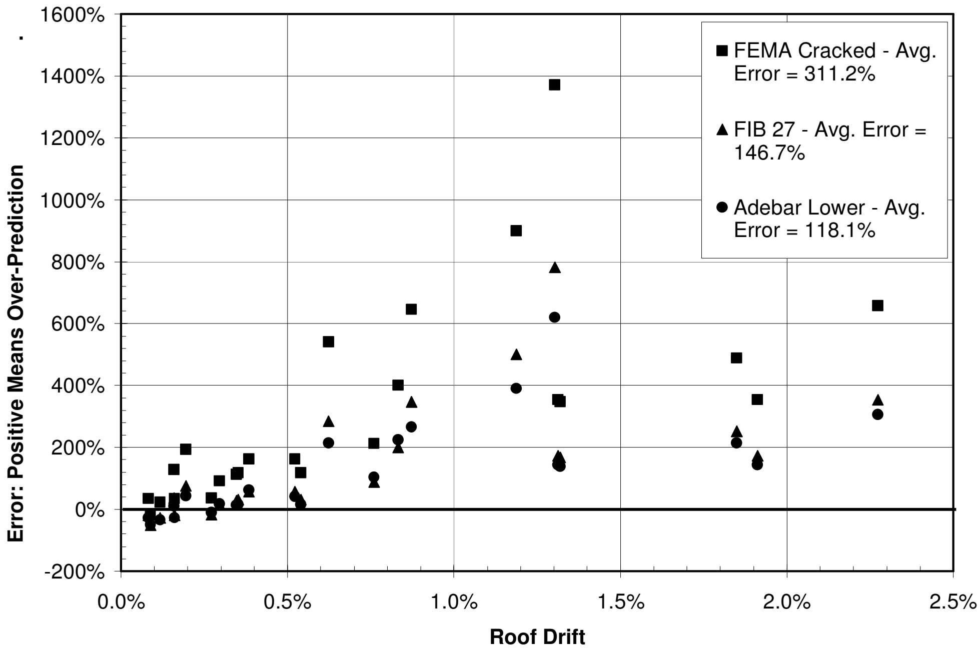

Figure 5-6: Error in Predicted Stiffness with Respect to Drift for Select Existing Methods

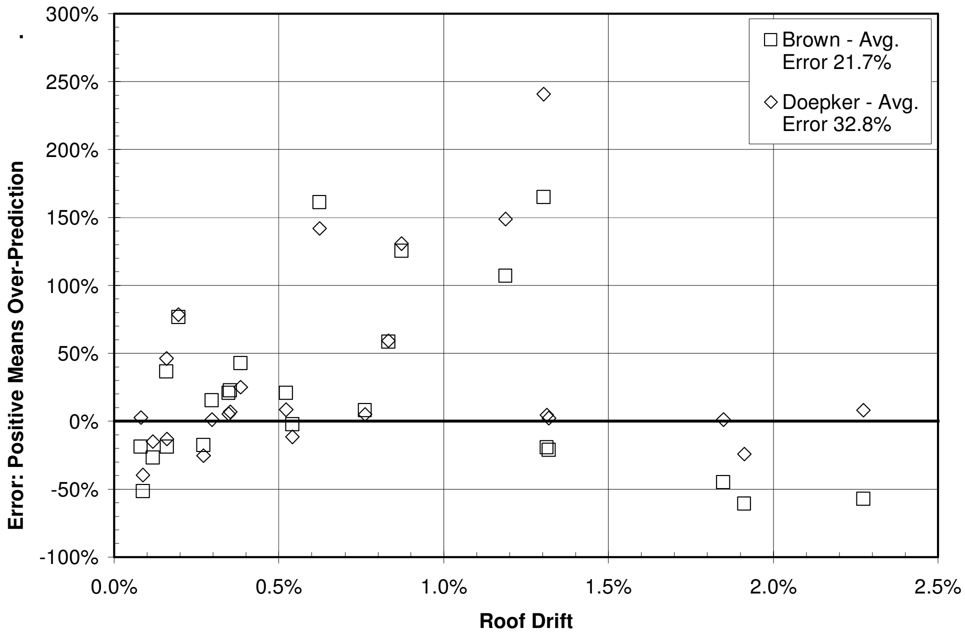

Figure 5-7: Error in Predicted Stiffness with Respect to Drift Proposed Methods

In Table 5-4, a distinction is made between the average error for all runs and the average error for the first run due to the fact that many of the evaluated methods do not account for a reduction in stiffness due to damage. Evaluation of the average error for the first run shows that even knowing measured values such as material properties, axial loads, etc, most methods predict a stiffness that is larger than the period matching stiffness.

The following lists some observations from the results of this preliminary evaluation of methods.

- The FIB 27 ($0.3E_cI_g$) stiffness as well as the ACI 318 recommendation of $0.35E_cI_g$ for cracked walls provide reasonable stiffness estimates for the initial low intensity motions (average error of 10.01% and 28.35% respectively for drifts less than 0.5%), however errors increase in the subsequent runs with drifts greater than 0.5%.

- Paulay-Priestley's expression under-predicts the initial stiffness with an average error of -39.36%. This is largely due to the fact that this stiffness modification factor is sensitive to the inverse of the yield stress of the reinforcement. In the case of the CAMUS 2000, CAMUS C and Ecoleader specimens, the reinforcement yield strength was significantly larger than is typically specified (approximately 90 ksi), resulting in a significant reduction in the prescribed stiffness modification factor.
- The axial load based lower bound function as prescribed by Adebar provides a reasonably small under-prediction of the effective stiffness during the first run with an error of -16.03%; however the upper bound over-predicts the effective stiffness by a significant margin (average error in the first test of 92.95%).

As can be seen, the error for methods using a single uniform stiffness (e.g. FEMA, FIB, and ACI) increases with increasing drift. Methods that account for the axial load ratio such as the Adebar lower bound and the Paulay and Priestley stiffness expression provide a better estimate of the stiffness, however these also see the error increasing with increasing drift.

- The functions as originally described by Brown (2008) and the one introduced in this thesis as Doepker 2008 are the only methods that account for a reduction in stiffness with increasing drift, and provide improved results, particularly in high drift ranges (average error in low drift ranges of 7.28% and 6.55% respectively and overall average error of 21.68% and 32.82% respectively).

5.3.2 Period Prediction

In addition to stiffness estimating methods, methods that evaluate the fundamental period of the tests were studied. Table 5-5 shows the predicted fundamental periods by the FEMA 450 (BSSC, 2003) and Newmark and Hall (1982) methods first referenced in Chapter 2. Table 5-6 provides error values for each run.

$$Error_{period} = \left(\frac{T_{0\_estimated} - T_{0\_literature}}{T_{0\_literature}} \right) \tag{5-2}$$

where:

$Error_{period}$ = the percent difference in the recommended period compared to the fundamental period from the literature.

$T_{0\_estimated}$ = the recommended fundamental period

$T_{0\_literature}$ = the fundamental period as reported in the literature

The simple method from FEMA 450 is a function of the building height, while the Newmark and Hall method considers wall height and length. The methods underestimate or overestimate the period by almost 40%. Furthermore, the methods do not provide an estimate of post damage response. For these reasons, these methods were not considered further in this study.

Table 5-5: Initial Fundamental Periods, Predicted and Actual

	T_0 from Literature	Prediction from NEHRP-FEMA 450	Prediction from Newmark and Hall, 1982
UCSD	0.57	0.447	0.909
CAMUS 2000	0.16	0.151	0.313
CAMUS C-1	0.27	0.111	0.286
CAMUS C-2	0.29	0.111	0.286
CAMUS C-3	0.27	0.111	0.286
CAMUS Ecoleader	0.22	0.151	0.322

Table 5-6: Percent Difference between Period Predicted from Existing Methods

	NEHRP-FEMA 450	Newmark and Hall, 1982
UCSD	-21.54%	59.53%
CAMUS 2000	-5.77%	95.36%
CAMUS C-1	-58.80%	6.07%
CAMUS C-2	-61.64%	-1.24%
CAMUS C-3	-58.80%	6.07%
CAMUS Ecoleader	-31.47%	46.45%
Average Error	-39.67%	35.37%
Standard Deviation	23.50%	38.37%

5.3.3 Damping Prediction

As discussed in Chapter 2, Newmark and Hall (1982) provided three different ranges for the effective damping ratio depending on the damage. These damping ratios are compared with those determined from the system identification. As none of the test specimens included nonstructural elements, the lowest value of the range was used for the comparison. For each specimen and run, an error in damping ratio for the fundamental period is computed:

$$Error_{damping} = \left(\frac{\beta_{eff\_estimated} - \beta_{eff\_System\_ID}}{\beta_{eff\_System\_ID}} \right) \tag{5-3}$$

where:

$Error_{damping}$ = the percent difference in the recommended damping compared to the damping determined from the system identification

$\beta_{eff\_estimated}$ = the recommended effective damping

$\beta_{eff\_System\_ID}$ = the effective damping predicted from the system identification

These error data are presented in Table 5-7 and Figure 5-8.

Table 5-7: Percent Difference in System Identification Damping Values and Those Predicted by Newmark and Hall

		System ID Damping	Percent Difference in Damping Values from Best Fit Damping		
			Newmark and Hall (only slight cracking), βeff = 2%	Newmark and Hall (considerable cracking) βeff = 3%	At or just below the yield point βeff = 7%
UCSD	EQ 1	5.06%	-60.48%	-40.72%	38.32%
	EQ 2	8.75%	-77.16%	-65.73%	-20.04%
	EQ 3	18.01%	-88.89%	-83.34%	-61.12%
CAMUS 2000	Test 1	6.90%	-71.01%	-56.52%	1.45%
	Test 2	15.00%	-86.67%	-80.00%	-53.33%
	Test 3	15.00%	-86.67%	-80.00%	-53.33%
CAMUS C-1	Stage 1	8.36%	-76.08%	-64.11%	-16.27%
	Stage 2	5.26%	-61.98%	-42.97%	33.08%
	Stage 3	6.72%	-70.24%	-55.36%	4.17%
	Stage 4	12.88%	-84.47%	-76.71%	-45.65%
CAMUS C-2	Stage 1	4.14%	-51.73%	-27.59%	68.95%
	Stage 2	2.98%	-32.87%	0.70%	134.96%
	Stage 3	11.56%	-82.70%	-74.06%	-39.46%
	Stage 4	16.63%	-87.97%	-81.96%	-57.90%
CAMUS C-3	Stage 1	3.88%	-48.45%	-22.68%	80.41%
	Stage 2	9.67%	-79.32%	-68.98%	-27.61%
	Stage 3	11.77%	-83.01%	-74.51%	-40.53%
	Stage 4	19.69%	-89.84%	-84.76%	-64.45%
CAMUS Ecoleader	T-0	6.18%	-67.62%	-51.43%	13.33%
	T-2	4.06%	-50.78%	-26.16%	72.29%
	T-3	14.61%	-86.31%	-79.47%	-52.09%
	T-4	28.66%	-93.02%	-89.53%	-75.58%
	T-5	15.70%	-87.26%	-80.89%	-55.41%
	T-6	10.66%	-81.23%	-71.84%	-34.30%
Average Error			-74.41%	-61.61%	-10.42%
Standard Deviation			15.89%	23.83%	55.61%
Maximum Error			-93.02%	-89.53%	134.96%
Minimum Error			-32.87%	0.70%	1.45%
Average Error in 1st Test			-62.56%	-43.84%	31.03%
Standard Deviation in 1st Test			10.96%	16.44%	38.35%

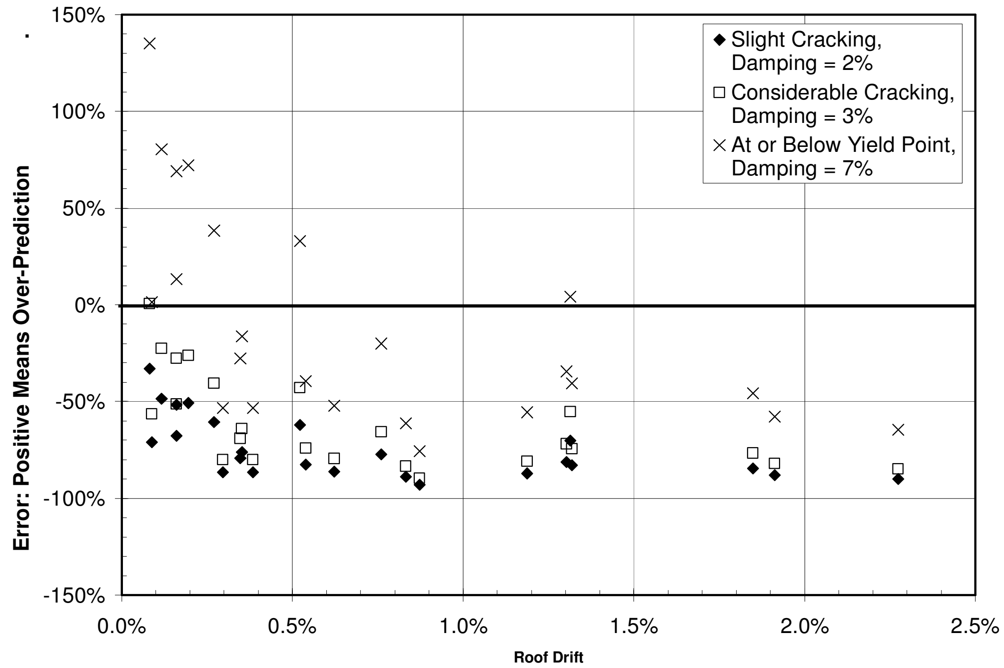

Figure 5-8: Percent Difference in Damping Predicted by Newmark and Hall

The 2% effective damping recommended for slight cracking is consistently lower than the system identification damping ratio (average error of -64.70% for low drift ranges, -74.41% overall). The 3% for considerable cracking provides a closer approximation of the system identification damping, however it too under-predicted the effective damping at low drift ranges (average error of -47.05%). The 7% damping ratio recommended for structures at or below the yield point over-predicts the damping in most cases between 0.0-0.5% drift (average error in low drift ranges of 23.56%), however it provides the closest estimate to the damping overall (-10.42% average error).

Despite these results, the results of period matching models using system identification damping (to be discussed further in Section 5.6 and 5.10) exhibited significant error due to over damping. This makes conclusions difficult to draw and is a subject to be investigated in the future.

5.3.4 Summary of Preliminary Prediction Methods

A preliminary evaluation of available stiffness expressions indicates that the FIB 27 and ACI 318 cracked stiffness expressions provide reasonable stiffness predictions for drifts less than 0.5% (10.01% and 28.35% average error respectively). As the drift increases however the error increases yielding an overall average error of 147% and 475% respectively. The drift based models proposed by Brown (2008) as well as the Doepker (2008) method provide a much better prediction for all drift levels (average errors of 7.28% and 6.55% respectively for low drift ranges and 21.68% 32.82% for all drift ranges).

The FEMA 440 and Newmark and Hall methods provide reasonable estimates for a limited range of response, and were thus not investigated further in this study.

For low drift ranges (0.0%-0.5%), 3% damping under-predicted the system identification damping (-47.05% average error) while 7% over-predicted the system identification damping (23.56% average error). This suggests that effective damping values from 5%-7% would most likely be appropriate in this drift range. Beyond this drift range, values of 7% and greater appear most appropriate for the effective damping of the primary mode.

5.4 Methods Evaluated Using Linear Time History Analysis

The stiffness expressions and damping values were used to estimate the dynamic response of structures using linear elastic time-history analysis methods. To evaluate the accuracy of some of the more common and promising approaches, several of the expressions were used to estimate the dynamic response of the shake table specimens described in Chapter 3 using models described in Chapter 4.

Of the analysis parameters mentioned in Chapter 2, several have been selected as a means to compare the response predicted from typical practice with the actual response. These methods were selected because they were either commonly used in practice (e.g. FEMA Cracked and Uncracked), or they are new methods in the literature (e.g. Adebar, Brown and Doepker). Table 5-8 shows the existing, proposed and period matching methods that will be investigated and compared to experimental data in subsequent analyses.

Table 5-8: Stiffness and Damping Methods to be Used for SAP Analyses ("X" refers to models that have been analyzed, "-" refers to combination not executed)

		Existing Methods					**Proposed Methods**			**Period Matching Methods**					
	Stiffness Model	FIB 27 (0.3)	FEMA Cracked (0.5)	FEMA Uncracked (0.8)	Adebar Lower Bound	Adebar Upper Bound	Drift based uniform (Brown)	Drift Based Uniform (Doepker)	Drift based variable (Brown) **	Uniform Stiffness					Variable Stiffness
										Sys. ID	3% *	7% *	FEMA 3% **	FEMA 7% **	Sys. ID **
UCSD	EQ1-3	X	X	X	X	X	X	X	X	X	X	X	X	X	X
CAMUS 2000	Test 1-2	X	X	X	X	X	X	X	-	X	X	X	-	-	X
CAMUS C1	Stage 1-4	X	X	X	X	X	X	X	-	X	X	X	X	X	X
CAMUS C2	Stage 2-4	X	X	X	X	X	X	X	-	X	-	-	-	-	X
CAMUS C3	Stage 1-4	X	X	X	X	X	X	X	-	X	-	-	-	-	X
CAMUS Ecoleader	Stage 1, 3-7	X	X	X	X	X	X	X	-	X	-	-	-	-	-

* Results will be compared to the system identification damping in Section 5.9

** Results will be found in Appendix A

Some tests were not evaluated due to issues with the test program. Such issues include failure in structural components not in the scope of this study and problems in data provided by the experimenters. Of those methods that were initially evaluated but proven to be ineffective, limited results can be found in Appendix A. Additionally, several damping ratios were evaluated on several methods only and form the basis of a discussion on damping to be found in Section 5.9.

5.5 Definition of Error Evaluation Functions

The following error values correspond to the error in simulated drifts, accelerations, shears and moments during the simulated cycle corresponding to the measured peak cycle. All methods of evaluation are reported in terms of percent. Results of the errors for the period, roof drift, roof acceleration, base shear and base moment are found in Section 5.6.

Error Evaluation Function 1: Period error

$$E_{period} = \frac{T_{estimated} - T_{measured}}{T_{measured}} \tag{5-4}$$

Error Evaluation Function 2: Roof drift error

$$E_{drift} = \left(\frac{\Delta_{roof-estimated} - \Delta_{roof\,\max-measured}}{\Delta_{roof\,\max-measured}} \right) \tag{5-5}$$

Error Evaluation Function 3: Roof acceleration error

$$E_{accel} = \left(\left| \frac{a_{roof-estimated} - a_{roof\,\max-measured}}{a_{roof\,\max-measured}} \right| \right) \tag{5-6}$$

Error Evaluation Function 4: Base shear error

$$E_{shear} = \left(\frac{V_{base-estimated} - V_{base\_\max-measured}}{V_{base\_\max-measured}} \right) \tag{5-7}$$

Error Evaluation Function 5: Base moment error

$$E_{moment} = \left(\frac{M_{base-estimated} - M_{base\_\max-measured}}{M_{base\_\max-measured}} \right) \tag{5-8}$$

Several other error analyses were performed emphasizing story response. These results are found in Appendix A.

5.6 Error Results

The error results for the methods from Section 5.4 have been plotted with respect to drift. The methods were evaluated using the five evaluation methods defined in Section 5.5. The error results for the effective period (5.6.1), roof displacement (5.6.2), roof acceleration (5.6.3), base shear (5.6.4) and the base moment (5.6.5) are reported here. Several methods of evaluation were also derived to investigate the effectiveness at the prediction of story response; these results can be found in the Appendix A.

As some test programs had greater potential sources of error than others, a method was devised to weight each individual run with a level of confidence. This method is described in Section 3.5. The error data is presented in three ways:

i) The complete data set including all analyzed runs.

ii) The complete data set excluding the Ecoleader test program, which is the test program with the lowest confidence.

iii) The data set pertaining to the UCSD runs, which is the test program with the highest confidence.

5.6.1 Error in Effective Period

As expected, error in estimating the fundamental period of the structure results in error in estimating the dynamic response. Thus, modeling methods were evaluated first using the error in simulated effective fundamental period, E_{period}, as defined by Eq. 5-4.

Several different approaches are used to evaluate the accuracy with which the chosen methods simulate the effective fundamental periods of the wall. First, an evaluation is done using plots of error versus maximum roof drift; to facilitate evaluation of different types of methods, symbols are used to emphasize errors associated with single-value methods and with drift-based methods. Second, error data are tabulated. Here error data statistics are compiled for i) the entire data set, ii) the entire data set less the Ecoleader test program, which was given the lowest confidence rating, and iii) only the UCSD test program, which was given the highest confidence rating. Third, methods are ranked using the confidence rating and ranking system described in Section 3.5. Fourth, because some methods are intended for use for a limited range of wall response, data are tabulated for three ranges of maximum roof drift:

1. Roof drifts less than 0.5%
2. Roof drifts between 0.5% and 1.0%
3. Roof drifts greater than 1.0%

Figure 5-9 through Figure 5-11 show the error in effective fundamental period versus maximum measured roof drift for the evaluated methods. In Figure 5-10, colored symbols are used to emphasize results for existing methods. In Figure 5-11, this approach is used to emphasize results for the newly proposed methods and the period-matching method. The data in Figure 5-9 suggest that for very low drifts, approximately 0.1%, the methods on average provide a reasonably accurate estimate of period with a moderate dispersion in the error. However, the data in Figure 5-10 show that as maximum roof drift increases, the single-valued methods increasingly under predict the fundamental period of the structure. The data in Figure 5-11 show that, with the exception of the Ecoleader test data, this trend can be eliminated using updated stiffness methods.

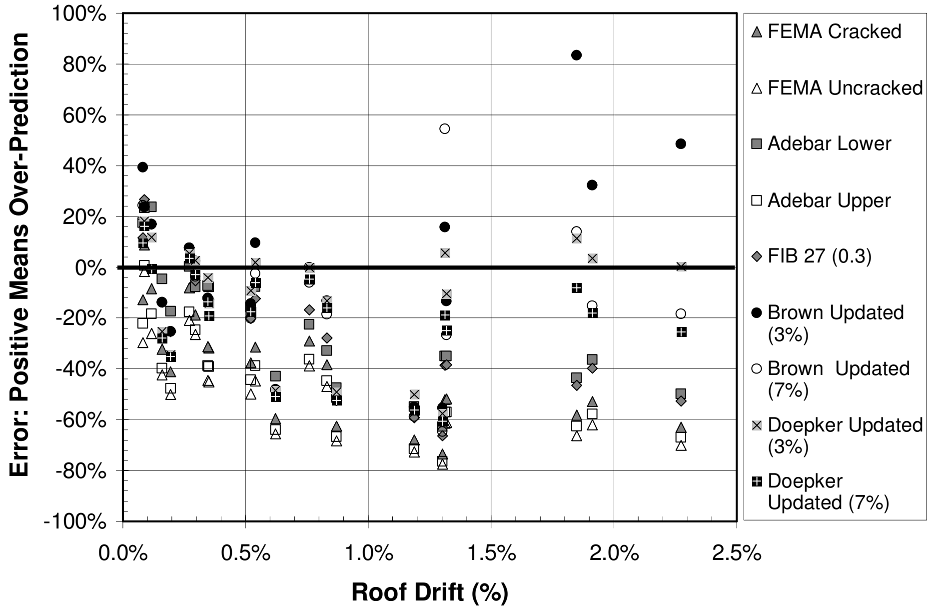

Figure 5-9: Error in Effective Period with Respect to Drift for All Methods

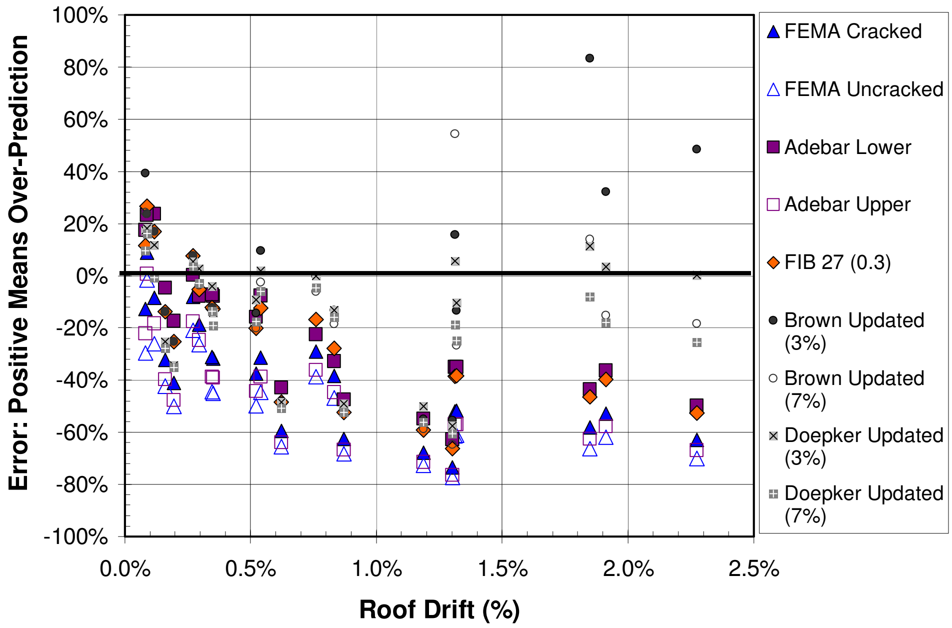

Figure 5-10: Error in Effective Period with Respect to Drift for Existing Methods

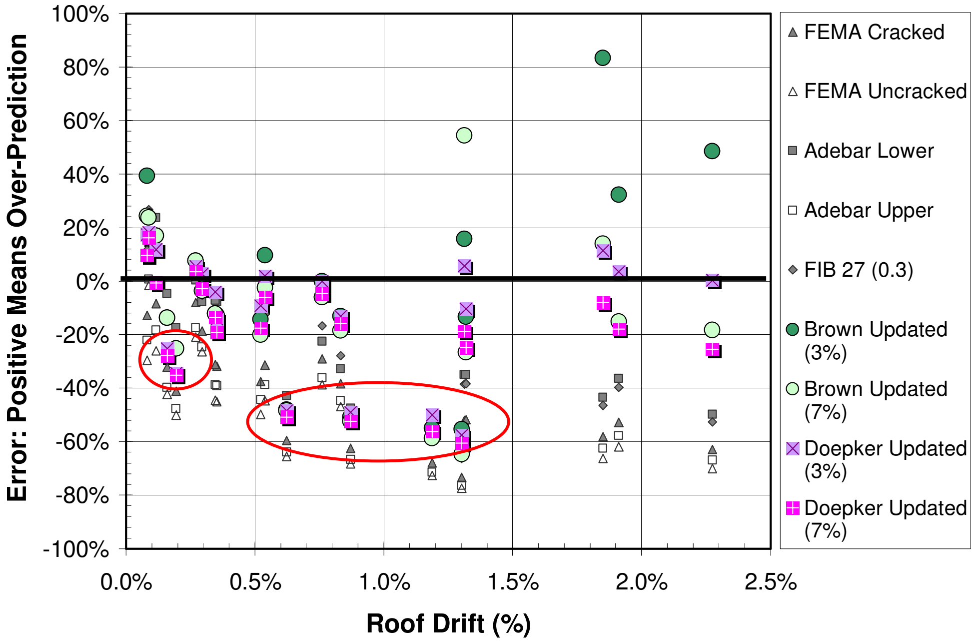

Figure 5-11: Error in Effective Period with Respect to Drift for Proposed Methods (circled points refer to Ecoleader tests)

Error data statistics are presented in Table 5-9 for the evaluated methods for the selected test programs. Table 5-10 provides a ranking of the methods based on the confidence ranking system discussed in Section 3.5. These data support the previous observations. As the drift level increases, existing methods increasingly under predict the roof drift. The updated stiffness methods show significantly improved period prediction potential.

Depending on the data set looked at, the preferred method varies. One thing is clear however that the updated stiffness methods predict the period much better than other existing methods (when excluding Ecoleader, with 3% damping, Doepker 1.7%

and Brown 13.3% error). The only stiffness methods that perform moderately well are the methods that prescribe a lower stiffness such as the FIB 27 (-16.3% error) as well as the Adebar lower bound (-14.8% error). The stiffer methods such as those prescribed by FEMA tend to overestimate the stiffness, which one expects to yield lower roof displacements, and higher forces and accelerations.

Table 5-9: Average Error and Standard Deviation for Effective Period Predictions

	Complete Data Set		Data Set Minus Ecoleader		UCSD Data Set	
Analysis Method	**Mean**	**Standard Deviation**	**Mean**	**Standard Deviation**	**Mean**	**Standard Deviation**
FIB 27 (0.3)	-23.9%	25.7%	-16.3%	23.6%	-12.3%	18.1%
Adebar Upper	-45.1%	20.1%	-39.1%	18.9%	-32.8%	13.9%
Adebar Lower	-21.2%	25.0%	-14.8%	23.3%	-18.3%	16.9%
FEMA Cracked	-38.8%	21.9%	-32.3%	20.5%	-25.1%	15.5%
FEMA Uncracked	-48.7%	19.4%	-43.4%	18.8%	-35.5%	13.3%
Brown Updated Stiffness, 3%	-1.6%	35.0%	13.3%	27.3%	-1.9%	10.5%
Brown Updated Stiffness, 7%	-11.8%	28.9%	0.3%	21.7%	-5.7%	13.0%
Doepker Updated Stiffness, 3%	-10.8%	23.3%	1.7%	10.1%	-2.6%	9.6%
Doepker Updated Stiffness, 7%	-19.5%	21.1%	-9.2%	12.2%	-5.7%	9.8%

Table 5-10: Rank of Effectiveness of Methods of Predicting the Effective Period Considering Test Confidence

Analysis Method	**Conf. Sum**	**Rank All**
FIB 27 (0.3), 3%	30.2	6
Adebar Upper, 3%	63.6	8
Adebar Lower, 3%	26.8	5
FEMA Cracked, 3%	53.6	7
FEMA Uncracked, 3%	69.4	9
Brown Iterated Stiffness, 3%	1.0	1
Brown Iterated Stiffness, 7%	12.5	3
Doepker Iterated Stiffness, (0.8), 3%	11.7	2
Doepker Iterated Stiffness, (0.8), 7%	24.6	4

The error and rankings for low drift ranges are found in Table 5-11 and Table 5-12. Even at low drift levels, relatively low effective stiffness are required to accurately simulate the period. In low drift ranges the updated stiffness methods (Doepker: 5.3% error, Brown: 9.3% error) as well as the FIB 27 (4.6% error) and Adebar lower bound (6.0% error) methods all provide for very good period prediction. By contrast, even at these low drift levels FEMA uncracked and Adebar upper bound (-27.8% and -22.9% error respectively) over predict the stiffness yielding a significant under prediction of the period. These observations are further supported by the ranking in Table 5-12.

Table 5-11: Average Error and Standard Deviation for Effective Period Predictions (drifts between 0.0% and 0.5%)

	Complete Data Set		Data Set Minus Ecoleader		UCSD Data Set	
Analysis Method	**Mean**	**Standard Deviation**	**Mean**	**Standard Deviation**	**Mean**	**Standard Deviation**
FIB 27 (0.3)	-0.7%	17.2%	4.6%	15.2%	7.6%	*
Adebar Upper	-27.5%	15.1%	-22.9%	13.7%	-17.6%	*
Adebar Lower	2.2%	15.3%	6.0%	14.9%	0.2%	*
FEMA Cracked	-19.5%	15.9%	-14.6%	14.3%	-8.1%	*
FEMA Uncracked	-31.8%	15.3%	-27.8%	14.8%	-20.8%	*
Brown Updated Stiffness, 3%	2.9%	21.0%	9.3%	19.0%	7.6%	*
Brown Updated Stiffness, 7%	0.5%	18.2%	6.3%	16.1%	7.6%	*
Doepker Updated Stiffness, 3%	-2.5%	15.6%	5.3%	11.7%	5.5%	*
Doepker Updated Stiffness, 7%	-7.8%	19.3%	-1.0%	12.4%	3.5%	*

* Only one test from UCSD fell in this drift range

Table 5-12: Rank of Effectiveness of Methods of Predicting the Effective Period Considering Test Confidence (drifts between 0.0% and 0.5%)

Analysis Method	Conf. Sum	Rank All
FIB 27 (0.3), 3%	0.1	1
Adebar Upper, 3%	18.6	8
Adebar Lower, 3%	1.8	4
FEMA Cracked, 3%	13.0	7
FEMA Uncracked, 3%	21.7	9
Brown Iterated Stiffness, 3%	2.6	5
Brown Iterated Stiffness, 7%	1.0	3
Doepker Iterated Stiffness, (0.8), 3%	0.9	2
Doepker Iterated Stiffness, (0.8), 7%	4.7	6

The error and rankings for moderate drift ranges are found in Table 5-13 and Table 5-14. The updated stiffness methods perform well (Doepker: -5.1% error, Brown: -4.5% error) when excluding the Ecoleader data, particularly when using 3% damping. FEMA Cracked (-34.1% error) now begins to see significantly increasing errors in this range, and FEMA Uncracked (-45.0% error) continues to struggle. Although FIB 27 seems to fare relatively well, the error in the moderate drift range is larger than it was in the low drift ranges (now at -19.3% error).

Table 5-13: Average Error and Standard Deviation for Effective Period Predictions (drifts between 0.5% and 1.0%)

Analysis Method	Complete Data Set		Data Set Minus Ecoleader		UCSD Data Set	
	Mean	Standard Deviation	Mean	Standard Deviation	Mean	Standard Deviation
FIB 27 (0.3)	-29.7%	16.9%	-19.3%	6.5%	-22.3%	7.8%
Adebar Upper	-49.1%	13.0%	-41.0%	4.1%	-40.4%	5.9%
Adebar Lower	-28.2%	15.6%	-19.6%	10.6%	-27.6%	7.2%
FEMA Cracked	-43.1%	14.4%	-34.1%	4.6%	-33.6%	6.6%
FEMA Uncracked	-52.3%	11.9%	-45.0%	4.7%	-42.8%	5.7%
Brown Updated Stiffness, 3%	-19.5%	24.8%	-4.5%	11.4%	-6.6%	9.3%
Brown Updated Stiffness, 7%	-24.7%	21.2%	-11.8%	8.9%	-12.3%	8.8%
Doepker Updated Stiffness, 3%	-19.6%	23.2%	-5.1%	7.2%	-6.6%	9.3%
Doepker Updated Stiffness, 7%	-24.6%	21.6%	-11.1%	6.6%	-10.4%	8.0%

Table 5-14: Rank of Effectiveness of Methods of Predicting the Effective Period Considering Test Confidence (drifts between 0.5% and 1.0%)

Analysis Method	Conf. Sum	Rank All
FIB 27 (0.3), 3%	11.1	6
Adebar Upper, 3%	19.4	8
Adebar Lower, 3%	10.8	5
FEMA Cracked, 3%	16.8	7
FEMA Uncracked, 3%	20.8	9
Brown Iterated Stiffness, 3%	6.5	1
Brown Iterated Stiffness, 7%	8.8	4
Doepker Iterated Stiffness, (0.8), 3%	6.5	2
Doepker Iterated Stiffness, (0.8), 7%	8.6	3

The error and rankings for high drift ranges are found in Table 5-15 and Table 5-16. At high drift ranges, the updated stiffness methods (Doepker: 2.1% error for 3% damping, Brown: 1.6% error for 7% damping) are the only that provide reasonable results. FIB 27 (-43.1% error) and Adebar lower bound (-39.1% error) cease to provide reasonable estimates for the period at these high drift ranges, and all other methods continue to be much too stiff. These methods were not intended to be used at these high drift levels and thus their respective struggles are expected.

Table 5-15: Average Error and Standard Deviation for Effective Period Predictions (drifts greater than 1.0%)

Analysis Method	Complete Data Set		Data Set Minus Ecoleader		UCSD Data Set	
	Mean	Standard Deviation	Mean	Standard Deviation	Mean	Standard Deviation
FIB 27 (0.3)	-48.7%	11.0%	-43.1%	6.2%	*	*
Adebar Upper	-64.2%	7.7%	-60.3%	4.4%	*	*
Adebar Lower	-45.3%	10.9%	-39.9%	6.6%	*	*
FEMA Cracked	-59.8%	8.6%	-55.5%	4.9%	*	*
FEMA Uncracked	-67.2%	6.4%	-64.1%	3.9%	*	*
Brown Updated Stiffness, 3%	8.0%	52.3%	33.3%	36.1%	*	*
Brown Updated Stiffness, 7%	-16.5%	41.2%	1.6%	33.3%	*	*
Doepker Updated Stiffness, 3%	-13.9%	28.2%	2.1%	8.1%	*	*
Doepker Updated Stiffness, 7%	-30.3%	20.1%	-19.0%	7.0%	*	*

* No UCSD tests were performed in this drift range

Table 5-16: Rank of Effectiveness of Methods of Predicting the Effective Period Considering Test Confidence (drifts greater than 1.0%)

Analysis Method	Conf. Sum	Rank All
FIB 27 (0.3), 3%	19.2	6
Adebar Upper, 3%	25.6	8
Adebar Lower, 3%	17.8	5
FEMA Cracked, 3%	23.8	7
FEMA Uncracked, 3%	26.9	9
Brown Iterated Stiffness, 3%	4.9	3
Brown Iterated Stiffness, 7%	4.7	2
Doepker Iterated Stiffness, (0.8), 3%	4.3	1
Doepker Iterated Stiffness, (0.8), 7%	11.3	4

Upon analysis of the error data, the following was observed:

- In order to estimate the period using a single value effective stiffness, low effective stiffness methods such as FIB 27 and Adebar's lower bound are essential as stiffness values on the order of FEMA Cracked and Uncracked under predict the period.
- For structures subjected to moderate drifts, these lower stiffness methods increasingly under predict the period, before yielding significant error at higher drift ranges.
- Updated stiffness methods out performed existing stiffness recommendations in moderate and high drift demands while yielding comparable results to the lower stiffness single value methods.
- An investigation of the role that accurate prediction of the effective period has in prediction of other response quantities is discussed in Section 5.8.

5.6.2 Error in Roof Displacement

The IBC 2000 limits the maximum roof drift under earthquake loading. Additionally, for performance-based design, maximum roof drift is used commonly to estimate structural and non-structural damage resulting from earthquake loading. Thus, the chosen methods presented in Chapter 2 are evaluated on the basis of the error in simulated maximum roof drift, E_{drift}.

Data are evaluated using the same approach as was used for evaluating the accuracy of the methods for predicting effective fundamental period: plots of error versus maximum measured roof drift as well as tabulated data. To determine maximum roof drift, it is necessary to complete a time-history analysis using both an effective stiffness model and an effective viscous damping ratio. Thus, results are provided for the two chosen damping ratios of 3% and 7%.

Figure 5-12 through Figure 5-17 show error in simulated maximum roof drift, E_{drift} as computed using Eq. 5-5, versus maximum measured roof drift. The full results of the roof drift error analysis for all methods can be seen in Figure 5-12 and Figure 5-13. Results emphasizing the existing methods can be seen in Figure 5-14 and Figure 5-15. Results emphasizing the updated stiffness methods as well as the period matching model (with system identification damping) are seen in Figure 5-16 and Figure 5-17. The data in these figures support the following observations:

- Data in Figure 5-12 and Figure 5-13 show that in general, an effective damping ratio of 7% results in under prediction of maximum roof drift in comparison with 3%.
- Data in Figure 5-14 and Figure 5-15 show that the lower stiffness single-value methods provide reasonably accurate simulation of response for low drift levels.
- Single-value methods under predict drift for moderate and high drifts.

- Data in Figure 5-16 and Figure 5-17 show that updated stiffness methods perform better than single-value methods at high drifts.

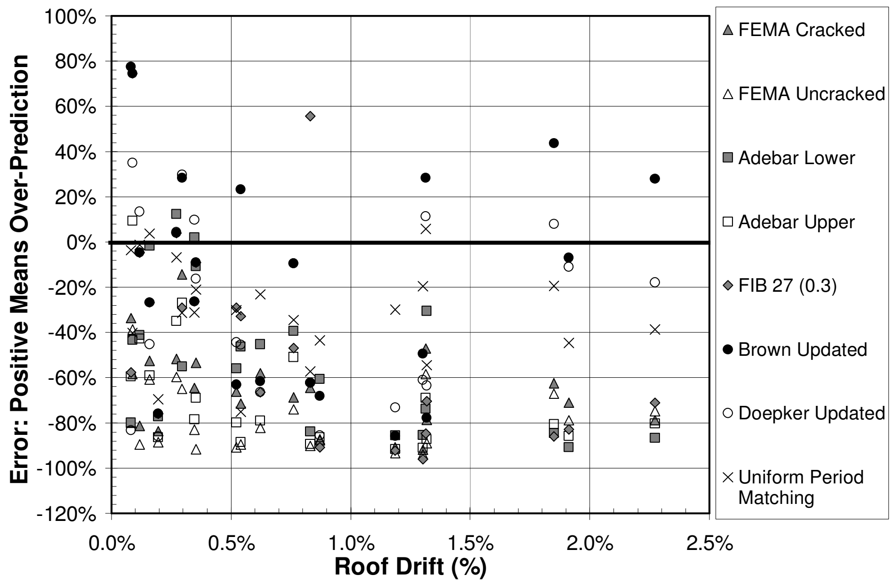

Figure 5-12: Error in Roof Drift with Respect to Drift for All Methods - 3% Damping

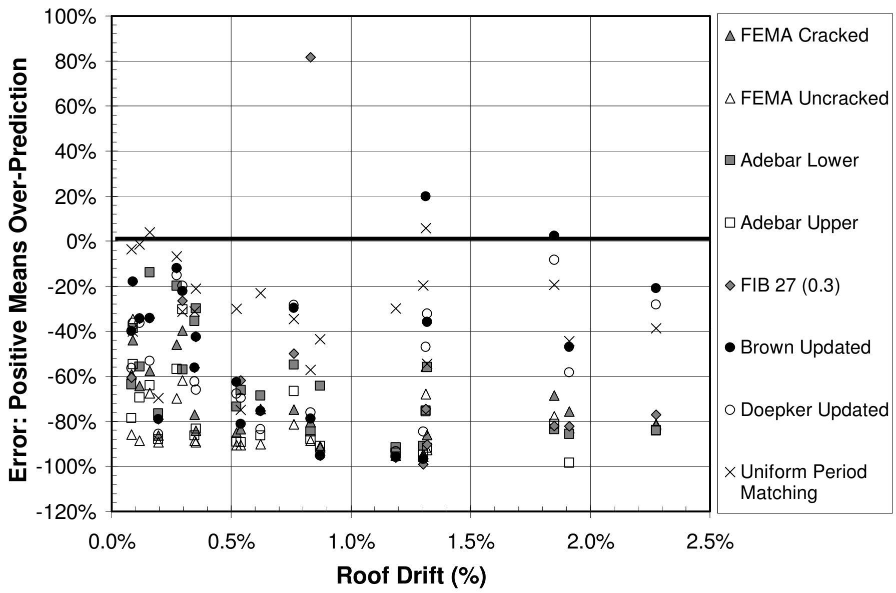

Figure 5-13: Error in Roof Drift with Respect to Drift for All Methods - 7% Damping

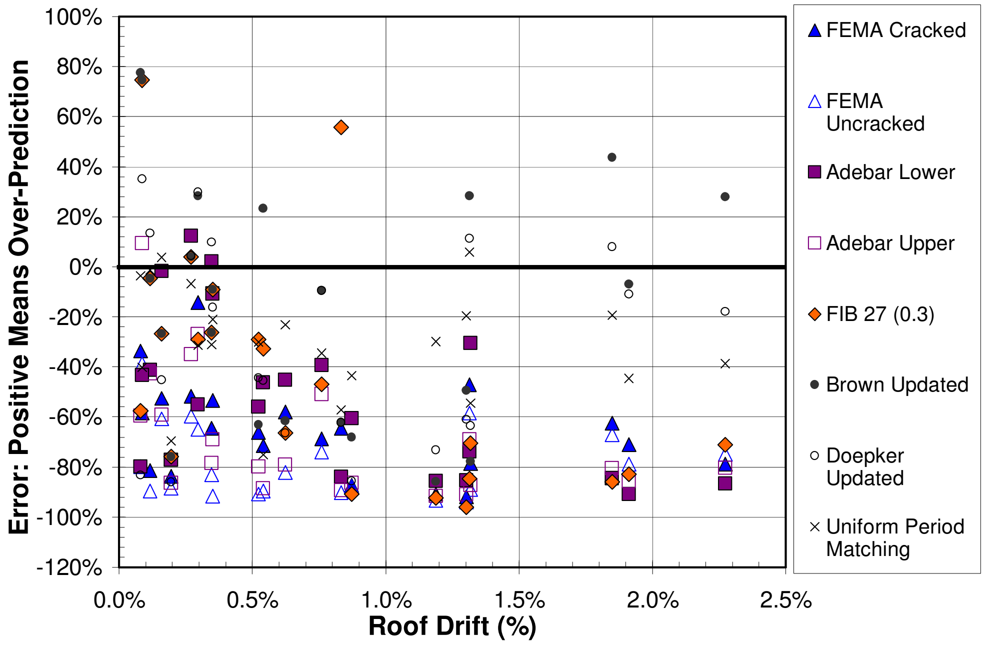

Figure 5-14: Error in Roof Drift with Respect to Drift for Existing Methods - 3% Damping

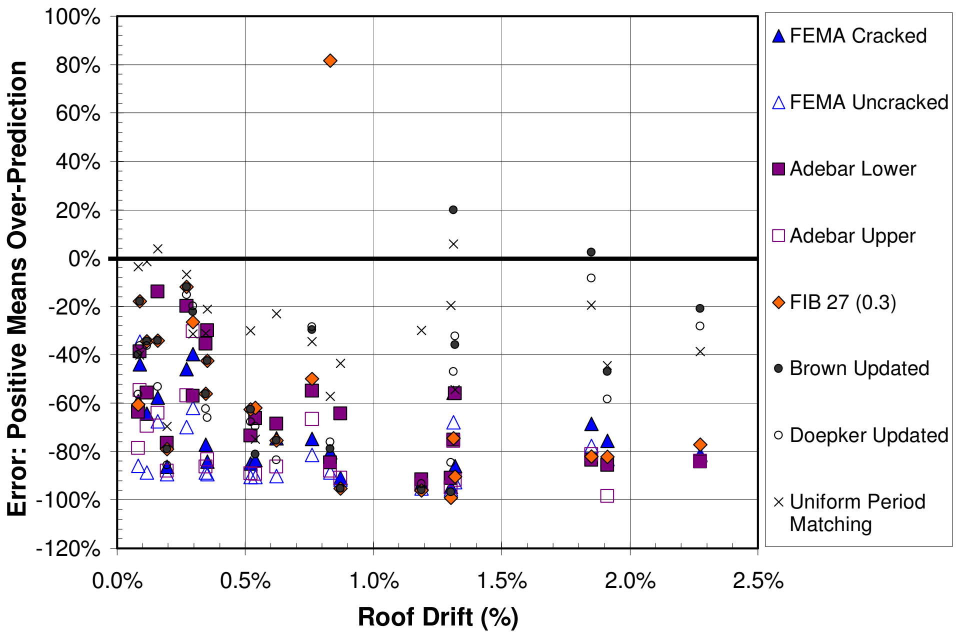

Figure 5-15: Error in Roof Drift with Respect to Drift for Existing Methods - 7% Damping

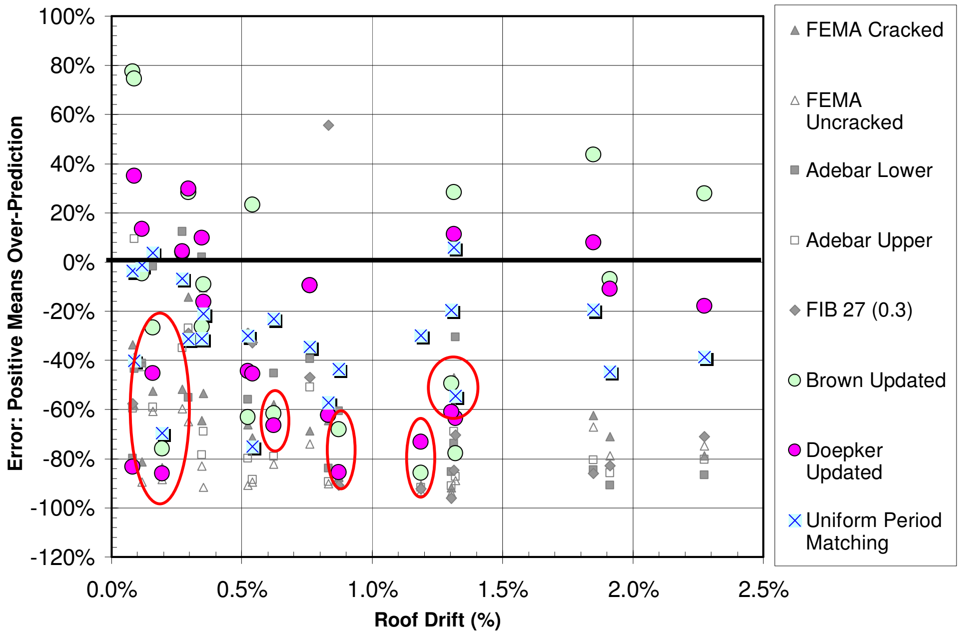

Figure 5-16: Error in Roof Drift with Respect to Drift for Proposed and Period Matching Methods - 3% Damping (circled points refer to Ecoleader tests)

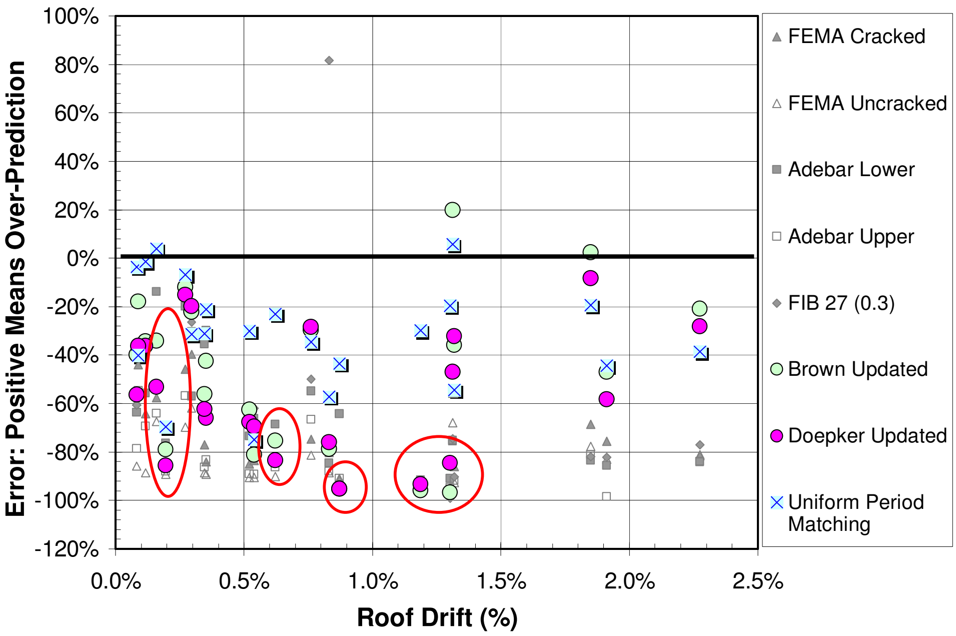

Figure 5-17: Error in Roof Drift with Respect to Drift for Proposed and Period Matching Methods - 7% Damping (circled points refer to Ecoleader tests)

Table 5-17 provides statistics for error in maximum roof drift and a ranking of the methods on the basis of these data as well as the confidence data in Table 3-48 and Table 3-49 is provided in Table 5-18. The data in these tables support the previous observations. On average a 3% effective viscous damping ratio provides more accurate simulation than does 7%. The low-stiffness value methods (FIB 27 and Adebar lower bound) when paired with 3%, and especially 7% effective damping under predict maximum roof drift. The updated stiffness methods provide an improved means of predicting the roof drift for the range of roof drifts. When paired with a 3% effective damping ratio, the Brown (3.0% error) and Doepker (-15.1% error) Updated Stiffness methods provide the best results. The period matching methods under predict the roof drift, possibly in part due to over damping of the system. Of the methods that use a single non-updated uniform stiffness, FIB 27 (-31.0% error) is the only that is in the top tier.

Table 5-17: Average Error and Standard Deviation for Roof Drift Predictions

Analysis Method	Complete Data Set		Data Set Minus Ecoleader		UCSD Data Set	
	Mean	Standard Deviation	Mean	Standard Deviation	Mean	Standard Deviation
FIB 27 (0.3), 3%	-42.9%	46.6%	-31.0%	47.5%	4.3%	51.3%
FIB 27 (0.3), 7%	-55.8%	40.0%	-46.8%	41.6%	6.6%	67.7%
Adebar Upper, 3%	-68.5%	25.7%	-63.3%	27.8%	-58.4%	27.9%
Adebar Upper, 7%	-79.1%	16.3%	-76.4%	17.4%	-70.4%	15.9%
Adebar Lower, 3%	-52.8%	31.7%	-50.4%	32.3%	-36.9%	48.2%
Adebar Lower, 7%	-62.2%	22.7%	-60.2%	20.8%	-53.0%	32.5%
FEMA Cracked, 3%	-65.0%	18.8%	-60.4%	17.6%	-61.7%	8.9%
FEMA Cracked, 7%	-72.8%	16.3%	-69.1%	15.8%	-67.0%	18.5%
FEMA Uncracked, 3%	-78.5%	14.6%	-76.3%	15.2%	-74.6%	15.3%
FEMA Uncracked, 7%	-81.9%	14.3%	-79.5%	15.0%	-79.9%	9.5%
Brown Updated Stiffness, 3%	-14.5%	49.4%	3.0%	45.5%	-22.6%	35.0%
Brown Updated Stiffness, 7%	-47.0%	32.8%	-34.9%	27.2%	-40.1%	34.6%
Doepker Updated Stiffness, 3%	-29.9%	39.5%	-15.1%	35.3%	-22.5%	35.2%
Doepker Updated Stiffness, 7%	-54.7%	26.2%	-44.2%	21.4%	-39.8%	32.0%
Uniform Period Matching	-30.2%	22.2%	-30.2%	22.1%	-32.9%	25.2%

Table 5-18: Rank of Effectiveness of Methods of Predicting the Roof Drift Considering Test Confidence

Analysis Method	Conf. Sum	Rank All	Rank 3%	Rank 7%
FIB 27 (0.3), 3%	56.0	4	4	
FIB 27 (0.3), 7%	77.7	7		3
Adebar Upper, 3%	99.3	11	7	
Adebar Upper, 7%	117.3	13		7
Adebar Lower, 3%	74.7	6	5	
Adebar Lower, 7%	90.4	9		5
FEMA Cracked, 3%	95.9	10	6	
FEMA Cracked, 7%	107.9	12		6
FEMA Uncracked, 3%	117.7	14	8	
FEMA Uncracked, 7%	122.8	15		8
Brown Iterated Stiffness, 3%	16.6	**1**	**1**	
Brown Iterated Stiffness, 7%	66.2	5		**2**
Doepker Iterated Stiffness, (0.8), 3%	39.1	**2**	**2**	
Doepker Iterated Stiffness, (0.8), 7%	78.5	8		**4**
Uniform Best Fit	44.8	**3**	**3**	**1**

Table 5-19 provides error data statistics for runs with maximum roof drifts less than 0.5%; Table 5-20 ranks the evaluated methods on the basis of these data and the confidence data in Table 3-48 and Table 3-49. The data in these tables show that in the low drift range the Doepker (-1.0% when excluding Ecoleader), Brown (20.6% error) and FIB 27 (-6.9% error) all perform well when paired with a 3% damping ratio. Stiffer methods significantly under predict the roof drift, with mean errors ranging from -43.1% (Adebar upper bound with 3% damping) to -72.5% (FEMA Uncracked with 3% damping).

Table 5-19: Average Error and Standard Deviation for Roof Drift Predictions (drifts between 0.0% and 0.5%)

Analysis Method	Complete Data Set		Data Set Minus Ecoleader		UCSD Data Set	
	Mean	Standard Deviation	Mean	Standard Deviation	Mean	Standard Deviation
FIB 27 (0.3), 3%	-16.7%	42.6%	-6.9%	41.2%	4.0%	*
FIB 27 (0.3), 7%	-40.3%	21.6%	-35.7%	18.5%	-11.9%	*
Adebar Upper, 3%	-49.7%	29.6%	-43.1%	29.7%	-34.9%	*
Adebar Upper, 7%	-67.9%	18.7%	-65.6%	19.8%	-56.8%	*
Adebar Lower, 3%	-32.7%	34.5%	-30.8%	33.1%	12.4%	*
Adebar Lower, 7%	-43.4%	21.1%	-42.9%	16.2%	-19.7%	*
FEMA Cracked, 3%	-54.8%	21.7%	-51.0%	21.7%	-51.8%	*
FEMA Cracked, 7%	-62.0%	17.4%	-59.1%	17.1%	-45.8%	*
FEMA Uncracked, 3%	-72.9%	18.0%	-72.5%	19.1%	-59.7%	*
FEMA Uncracked, 7%	-75.0%	18.7%	-74.1%	20.5%	-69.8%	*
Brown Updated Stiffness, 3%	4.6%	49.3%	20.6%	41.2%	4.0%	*
Brown Updated Stiffness, 7%	-37.6%	20.6%	-32.1%	15.6%	-11.9%	*
Doepker Updated Stiffness, 3%	-15.4%	46.0%	-1.0%	40.0%	4.4%	*
Doepker Updated Stiffness, 7%	-47.9%	22.9%	-41.7%	20.3%	-15.1%	*
Uniform Period Matching	-22.3%	23.5%	-19.3%	15.5%	-6.8%	*

* Only one test from UCSD fell in this drift range

Table 5-20: Rank of Effectiveness of Methods of Predicting the Roof Drift Considering Test Confidence (drifts between 0.0% and 0.5%)

Analysis Method	Conf. Sum	Rank All	Rank 3%	Rank 7%
FIB 27 (0.3), 3%	10.2	3	3	
FIB 27 (0.3), 7%	27.2	7		3
Adebar Upper, 3%	33.8	10	6	
Adebar Upper, 7%	47.1	13		7
Adebar Lower, 3%	21.8	5	5	
Adebar Lower, 7%	29.8	8		4
FEMA Cracked, 3%	38.1	11	7	
FEMA Cracked, 7%	42.9	12		6
FEMA Uncracked, 3%	50.8	14	8	
FEMA Uncracked, 7%	52.3	15		8
Brown Iterated Stiffness, 3%	4.6	1	1	
Brown Iterated Stiffness, 7%	25.3	6		2
Doepker Iterated Stiffness, (0.8), 3%	8.6	2	2	
Doepker Iterated Stiffness, (0.8), 7%	32.3	9		5
Uniform Best Fit	15.2	4	4	1

Table 5-21 and Table 5-22 provide statistics for error in maximum roof drift in the moderate roof drift range as well as a ranking of the methods on the basis of these data and the confidence data in Table 3-48 and Table 3-49. All of the methods provide poor simulation of maximum roof drift for this range. This could possibly be due to the fact that this range likely sees a high level of damage and thus the changes in stiffness and damping are large. For the single-value stiffness methods excluding the Ecoleader data, errors range from -56.3% (for Adebar lower bound with 3% damping) to -87.8% (for FEMA Uncracked with 7% damping). The Doepker method yields errors of -40.4% for 3% damping and -60.4% for 7% damping. The best results for the data set excluding Ecoleader are observed in the FIB 27 stiffness with -13.3% error and the Brown Updated Stiffness method with -27.9%. The updated stiffness methods along with FIB 27 perform significantly better than the single-value stiffness methods when exclusively looking at the UCSD data set. These large errors are attributed to the fact that structures subjected to this level of roof drift are typically seeing the onset of extensive yielding. Further, the functions that form the basis of the updated stiffness methods fit the data most poorly in this drift range. These potential issues as well as other are discussed in detail in Section 5.6.7.

Table 5-21: Average Error and Standard Deviation for Roof Drift Predictions (drifts between 0.5% and 1.0%)

Analysis Method	Complete Data Set		Data Set Minus Ecoleader		UCSD Data Set	
	Mean	Standard Deviation	Mean	Standard Deviation	Mean	Standard Deviation
FIB 27 (0.3), 3%	-35.1%	50.0%	-13.3%	46.6%	4.4%	72.6%
FIB 27 (0.3), 7%	-43.9%	63.4%	-23.2%	70.1%	15.8%	93.0%
Adebar Upper, 3%	-79.0%	14.4%	-77.2%	18.0%	-70.1%	27.1%
Adebar Upper, 7%	-85.0%	9.2%	-83.2%	11.1%	-77.2%	15.1%
Adebar Lower, 3%	-55.2%	16.0%	-56.3%	19.6%	-61.5%	31.5%
Adebar Lower, 7%	-68.6%	9.9%	-69.8%	12.5%	-69.7%	21.0%
FEMA Cracked, 3%	-69.4%	9.9%	-67.8%	3.1%	-66.7%	3.0%
FEMA Cracked, 7%	-81.5%	6.3%	-80.9%	4.6%	-77.5%	4.0%
FEMA Uncracked, 3%	-85.7%	6.6%	-86.2%	8.1%	-82.1%	11.5%
FEMA Uncracked, 7%	-88.8%	3.8%	-87.8%	4.4%	-84.9%	5.2%
Brown Updated Stiffness, 3%	-40.2%	37.9%	-27.9%	42.3%	-35.9%	37.3%
Brown Updated Stiffness, 7%	-70.4%	22.6%	-63.0%	23.7%	-54.2%	34.7%
Doepker Updated Stiffness, 3%	-52.3%	25.9%	-40.4%	22.1%	-35.9%	37.3%
Doepker Updated Stiffness, 7%	-70.1%	22.8%	-60.4%	21.7%	-52.1%	33.7%
Uniform Period Matching	-43.9%	19.3%	-49.2%	20.9%	-45.9%	16.0%

Table 5-22: Rank of Effectiveness of Methods of Predicting the Roof Drift Considering Test Confidence (drifts between 0.5% and 1.0%)

Analysis Method	Conf. Sum	Rank All	Rank 3%	Rank 7%
FIB 27 (0.3), 3%	12.5	1	1	
FIB 27 (0.3), 7%	16.1	3		1
Adebar Upper, 3%	31.9	11	7	
Adebar Upper, 7%	34.7	13		7
Adebar Lower, 3%	22.7	6	5	
Adebar Lower, 7%	28.4	9		5
FEMA Cracked, 3%	28.4	10	6	
FEMA Cracked, 7%	33.5	12		6
FEMA Uncracked, 3%	35.3	14	8	
FEMA Uncracked, 7%	36.6	15		8
Brown Iterated Stiffness, 3%	15.6	2	2	
Brown Iterated Stiffness, 7%	27.4	8		4
Doepker Iterated Stiffness, (0.8), 3%	19.6	5	4	
Doepker Iterated Stiffness, (0.8), 7%	27.2	7		3
Uniform Best Fit	18.1	4	3	2

Table 5-23 and Table 5-24 provide statistics for error in maximum roof drift in the high roof drift range as well as a ranking of the methods on the basis of these data and the confidence data in Table 3-48 and Table 3-49. Updated stiffness methods performed very well (-14.6% for Doepker and 3.0% for Brown) in this drift range, with 3% damping being the preferred level of damping. The uniform period matching model out performed all existing methods yet did not perform as well as the updated stiffness methods (error in roof drift of -30.2%). The uniform period matching models tended to under predict the roof drift suggesting that over damping may be occurring. All existing methods have unacceptably large errors, ranging from -67.6% for FEMA Cracked with 3% damping and 86.2% for Adebar's upper bound with 7% damping. Even FIB 27 struggled significantly with an average error of -79.0% for 3% damping.

Table 5-23: Average Error and Standard Deviation for Roof Drift Predictions (drifts greater than 1.0%)

Analysis Method	Complete Data Set		Data Set Minus Ecoleader		UCSD Data Set	
	Mean	Standard Deviation	Mean	Standard Deviation	Mean	Standard Deviation
FIB 27 (0.3), 3%	-83.4%	9.7%	-79.0%	7.7%	*	*
FIB 27 (0.3), 7%	-85.9%	9.4%	-81.2%	6.0%	*	*
Adebar Upper, 3%	-83.6%	7.8%	-80.6%	7.1%	*	*
Adebar Upper, 7%	-88.5%	8.3%	-86.2%	9.0%	*	*
Adebar Lower, 3%	-76.7%	21.0%	-73.2%	24.7%	*	*
Adebar Lower, 7%	-81.0%	12.3%	-76.8%	12.3%	*	*
FEMA Cracked, 3%	-74.4%	15.9%	-67.6%	13.3%	*	*
FEMA Cracked, 7%	-79.3%	13.9%	-73.5%	11.9%	*	*
FEMA Uncracked, 3%	-79.3%	13.6%	-73.6%	11.6%	*	*
FEMA Uncracked, 7%	-84.8%	10.3%	-80.5%	9.0%	*	*
Brown Updated Stiffness, 3%	-17.1%	53.7%	3.0%	48.8%	*	*
Brown Updated Stiffness, 7%	-39.1%	45.0%	-16.3%	27.4%	*	*
Doepker Updated Stiffness, 3%	-29.6%	35.6%	-14.6%	30.0%	*	*
Doepker Updated Stiffness, 7%	-50.3%	30.8%	-34.8%	19.1%	*	*
Uniform Period Matching	-28.7%	19.9%	-30.2%	23.9%	*	*

* No UCSD tests were performed in this drift range

Table 5-24: Rank of Effectiveness of Methods of Predicting the Roof Drift Considering Test Confidence (drifts greater than 1.0%)

Analysis Method	Conf. Sum	Rank All	Rank 3%	Rank 7%
FIB 27 (0.3), 3%	33.3	11	7	
FIB 27 (0.3), 7%	34.4	14		7
Adebar Upper, 3%	33.5	12	8	
Adebar Upper, 7%	35.5	15		8
Adebar Lower, 3%	30.2	7	5	
Adebar Lower, 7%	32.2	10		5
FEMA Cracked, 3%	29.4	6	4	
FEMA Cracked, 7%	31.5	8		4
FEMA Uncracked, 3%	31.6	9	6	
FEMA Uncracked, 7%	33.9	13		6
Brown Iterated Stiffness, 3%	5.6	1	1	
Brown Iterated Stiffness, 7%	13.5	4		2
Doepker Iterated Stiffness, (0.8), 3%	10.9	2	2	
Doepker Iterated Stiffness, (0.8), 7%	18.9	5		3
Uniform Best Fit	11.6	3	3	1

Upon analysis of the error data, the following was observed for roof drift prediction:

- Models implementing a single value effective stiffness routinely under predicted the roof drift in all drift ranges. The exception was FIB 27 which performed well in low and moderate drift ranges. FIB 27 saw unacceptably high error values for high drift ranges.
- Updated stiffness models performed well in low drift ranges. Moderate drift ranges saw poor results which may be due to the onset of extensive yielding, the tendency of the derived functions to over predict the stiffness in this range, as well as a slightly limited data set. The updated stiffness models ultimately out performed all models in the high drift ranges on average yielding a slight under prediction.
- The uniform period matching models routinely under predicted the roof drift for all drift levels. This indicates that the system identification damping used for these analyses was likely too high.

5.6.3 Error in Roof Acceleration

To predict the scope and degree of nonstructural damage, prediction of acceleration is extremely important. Accurate prediction of story accelerations is in particular very important in regions of low drift. In this drift range, structural damage is likely minimal however significant nonstructural damage could be inflicted on acceleration sensitive equipment. Thus, the chosen methods presented in Chapter 2 are evaluated on the basis of the error in simulated maximum roof acceleration, E_{accel}.

Data are evaluated using the same approach as was used for evaluating the accuracy of the methods for predicting the effective fundamental period: plots of error versus maximum measured roof drift as well as tabulated data. To determine the roof acceleration, it is necessary to complete a time-history analysis using both an effective stiffness model and an effective viscous damping ratio. Thus, results are provided for the two chosen damping ratios of 3% and 7%.

Figure 5-18 through Figure 5-23 show error in simulated roof acceleration at the point of maximum roof drift, E_{accel} as computed using Eq. 5-6, versus maximum measured roof drift. The full results of the roof acceleration error analysis for all methods can be seen in Figure 5-18 and Figure 5-19. Results emphasizing the existing methods can be seen in Figure 5-20 and Figure 5-21, and results emphasizing the updated stiffness methods as well as the period matching model (with system identification damping) are seen in Figure 5-22 and Figure 5-23. The data in these figures support the following observations:

- The scale of the errors in Figure 5-18 and Figure 5-19 show that acceleration is a much more difficult parameter to predict than the effective period or the roof drift. Most methods appear to on average under predict the roof acceleration in this range for both 3% and 7% damping.

- Data in Figure 5-20 and Figure 5-21 show that the single-value methods exhibit a steep trend of increasing error with increasing drift.
- Most single-value methods over predict roof acceleration for moderate and high drifts. FIB 27 and Adebar's lower bound perform better in these drift ranges.
- Data in Figure 5-22 and Figure 5-23 show that updated stiffness methods suffer a similar increasing level of error as was exhibited by the existing methods, although the trend is less severe. The scatter is quite large in the low drift ranges, and the error increases for high drift ranges. The updated stiffness methods perform better than stiffer single value methods although they yield similar behavior to the FIB 27 stiffness.

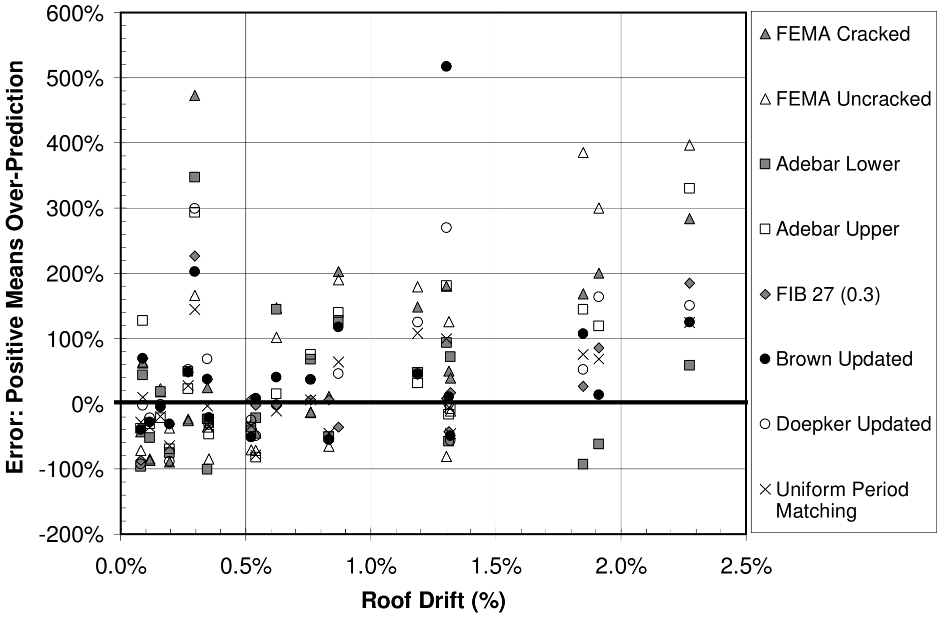

Figure 5-18: Error in Roof Acceleration with Respect to Drift for All Methods - 3% Damping

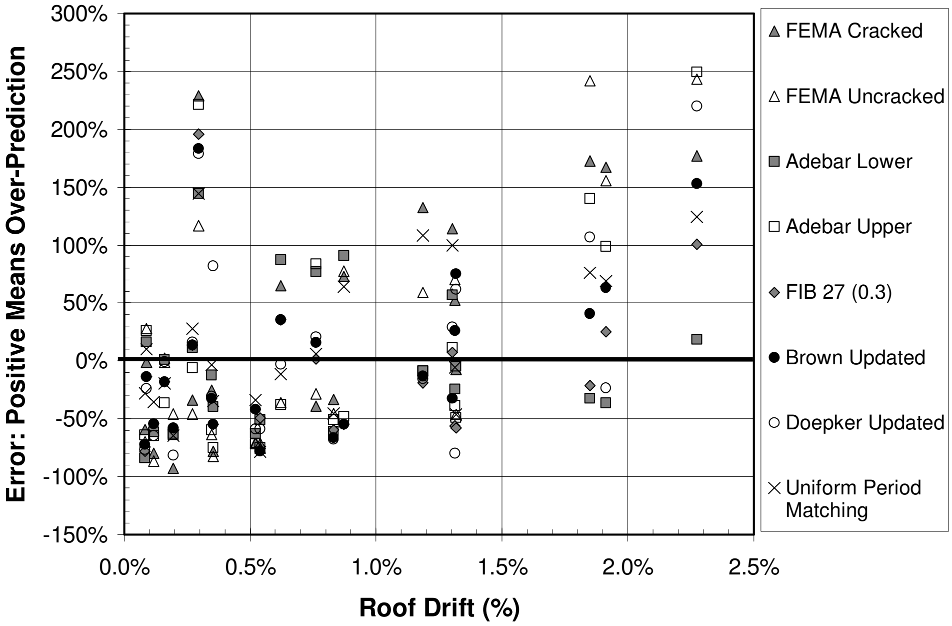

Figure 5-19: Error in Roof Acceleration with Respect to Drift for All Methods - 7% Damping

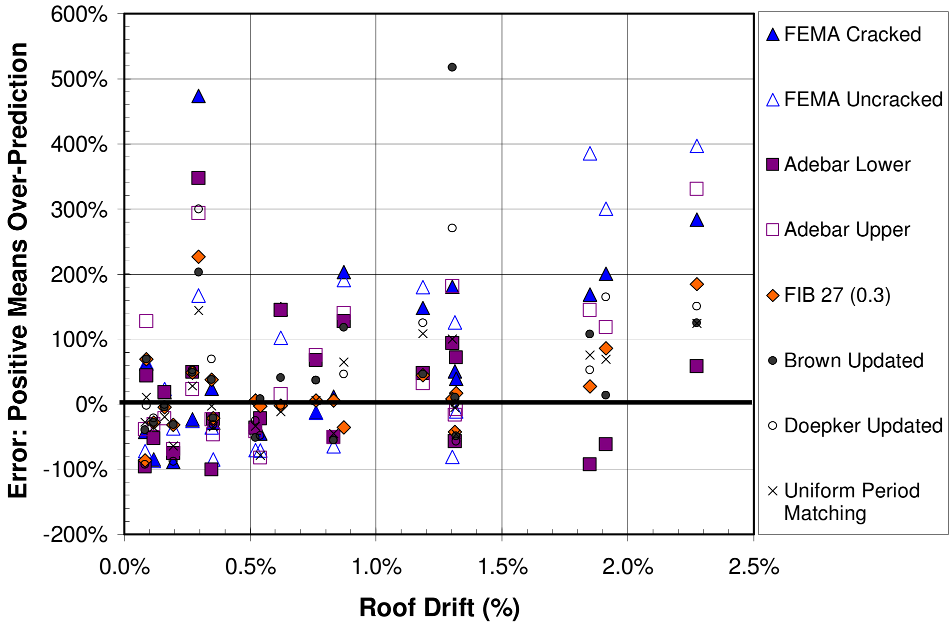

Figure 5-20: Error in Roof Acceleration with Respect to Drift for Existing Methods - 3% Damping

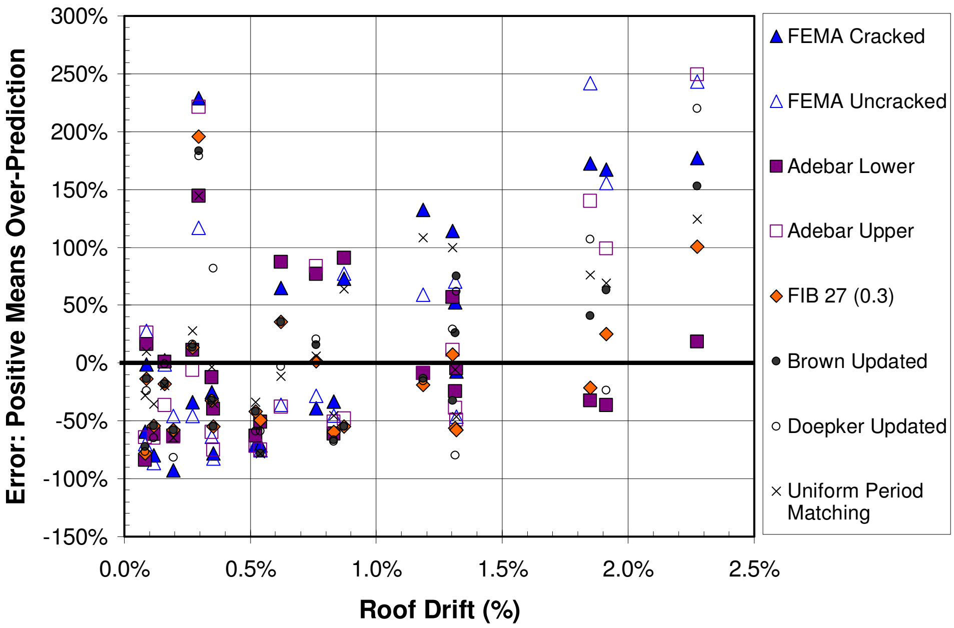

Figure 5-21: Error in Roof Acceleration with Respect to Drift for Existing Methods - 7% Damping

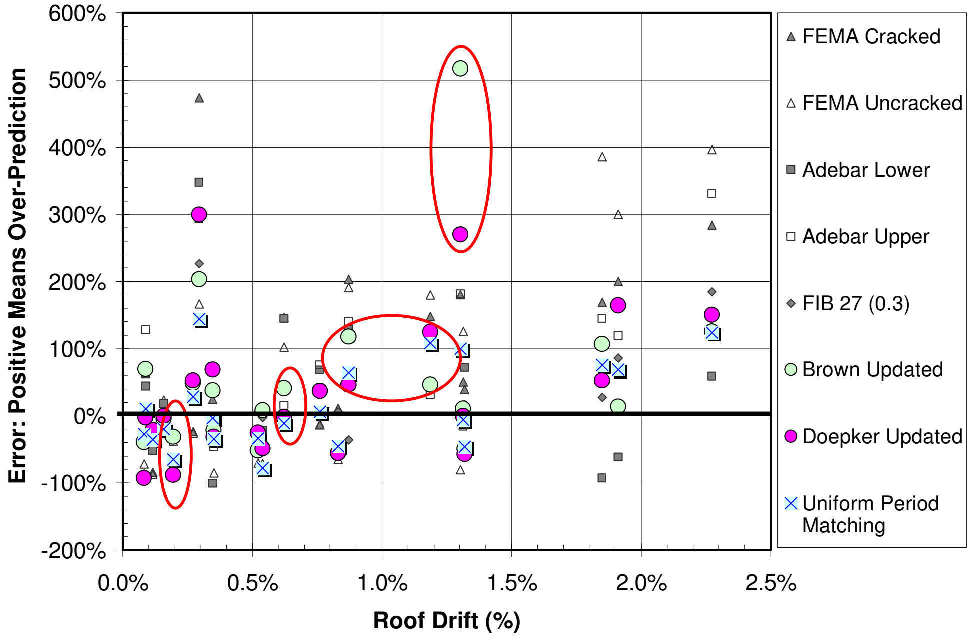

Figure 5-22: Error in Roof Acceleration with Respect to Drift for Proposed and Period Matching Methods - 3% Damping (circled points refer to Ecoleader tests)

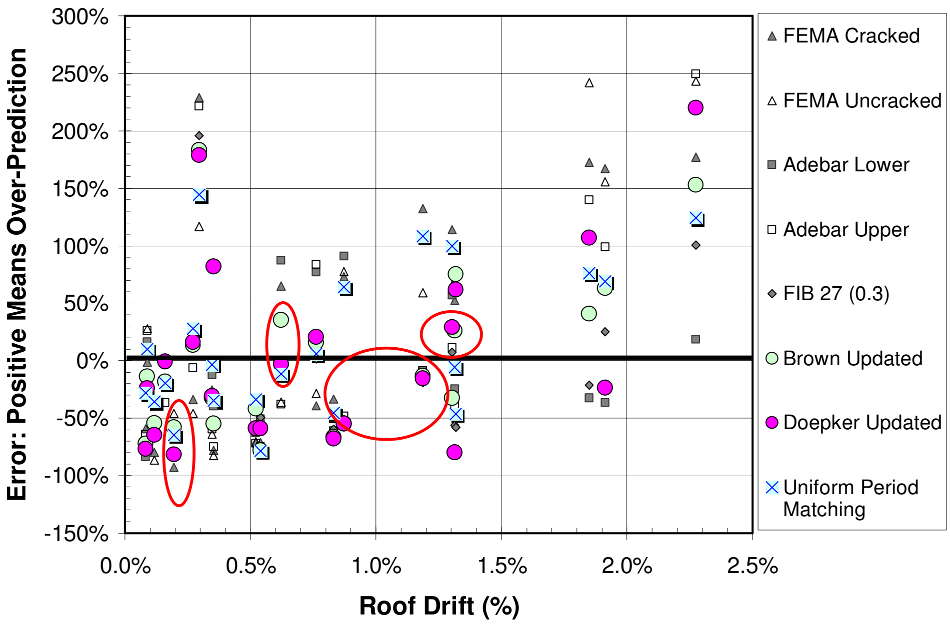

Figure 5-23: Error in Roof Acceleration with Respect to Drift for Proposed and Period Matching Methods - 7% Damping (circled points refer to Ecoleader tests)

Table 5-25 provides statistics for error in roof acceleration and a ranking of the methods on the basis of these data as well as the confidence data in Table 3-48 and Table 3-49 is provided in Table 5-26. Unlike most of the criteria looked at following analysis, the best results came when using a 7% effective viscous damping ratio. In using this level of damping, the updated stiffness methods performed quite well on average (12.6% error for Doepker and 9.8% error for Brown). Numerous methods had low average errors, with FIB 27 at -11.4% error, Adebar lower bound at -12.7%, Adebar upper bound at 16.5%, FEMA Cracked at 18.7%, and FEMA Uncracked at 15.1%. These methods however all exhibited extremely large values for standard deviation, ranging from 60% to well over 100% in some cases.

Table 5-25: Average Error and Standard Deviation for Roof Acceleration Predictions

Analysis Method	Complete Data Set		Data Set Minus Ecoleader		UCSD Data Set	
	Mean	Standard Deviation	Mean	Standard Deviation	Mean	Standard Deviation
FIB 27 (0.3), 3%	23.2%	70.9%	33.2%	79.7%	20.1%	24.5%
FIB 27 (0.3), 7%	-13.2%	62.4%	-11.4%	70.8%	-15.0%	39.2%
Adebar Upper, 3%	47.8%	115.1%	48.4%	124.3%	15.9%	63.4%
Adebar Upper, 7%	3.7%	95.6%	16.5%	109.1%	8.8%	68.5%
Adebar Lower, 3%	18.3%	104.2%	2.8%	109.8%	22.2%	63.9%
Adebar Lower, 7%	-1.8%	60.3%	-12.7%	58.1%	9.1%	69.0%
FEMA Cracked, 3%	75.2%	137.4%	65.4%	147.6%	-8.2%	17.7%
FEMA Cracked, 7%	26.9%	99.5%	18.7%	106.3%	-35.5%	3.1%
FEMA Uncracked, 3%	58.2%	153.3%	56.4%	169.2%	-34.8%	27.0%
FEMA Uncracked, 7%	16.0%	100.7%	15.1%	115.1%	-39.9%	10.1%
Brown Updated Stiffness, 3%	50.1%	123.5%	26.0%	72.5%	9.9%	56.9%
Brown Updated Stiffness, 7%	0.7%	70.1%	9.8%	78.5%	-12.4%	46.8%
Doepker Updated Stiffness, 3%	38.3%	106.1%	30.7%	101.8%	11.4%	58.4%
Doepker Updated Stiffness, 7%	3.4%	82.7%	12.6%	93.2%	-10.2%	49.8%
Uniform Period Matching	14.7%	64.8%	9.2%	63.8%	-3.7%	37.6%

Table 5-26: Rank of Effectiveness of Methods of Predicting the Roof Acceleration

Analysis Method	Conf. Sum	Rank All	Rank 3%	Rank 7%
FIB 27 (0.3), 3%	36.0	10	3	
FIB 27 (0.3), 7%	20.1	7		7
Adebar Upper, 3%	63.6	13	6	
Adebar Upper, 7%	4.0	2		2
Adebar Lower, 3%	24.9	9	2	
Adebar Lower, 7%	4.9	3		3
FEMA Cracked, 3%	96.5	15	8	
FEMA Cracked, 7%	24.8	8		8
FEMA Uncracked, 3%	66.8	14	7	
FEMA Uncracked, 7%	9.8	5		5
Brown Iterated Stiffness, 3%	60.8	12	5	
Brown Iterated Stiffness, 7%	0.9	1		1
Doepker Iterated Stiffness, (0.8), 3%	48.5	11	4	
Doepker Iterated Stiffness, (0.8), 7%	5.2	4		4
Uniform Best Fit	14.7	6	1	6

Table 5-27 provides error data statistics for runs with maximum roof drifts less than 0.5%; Table 5-28 ranks the evaluated methods on the basis of these data and the confidence data in Table 3-48 and Table 3-49.

The interests in predicting story accelerations is most significant in the low drift ranges where it is desired to keep nonstructural damage to a minimum in low intensity shaking. Although many methods have very low average errors with regards to roof acceleration prediction, the standard deviations are very high (ranging from at best 75% to as much as 190%). Furthermore, the accelerations were best predicted using 7% damping while drifts were best predicted using 3% damping. These various issues raise the concern of whether a linear elastic analysis is capable of reliably predicting story accelerations.

When neglecting the Ecoleader data set, the average error in the roof acceleration prediction for the single value effective stiffness models ranged from as low as -3.2% (Adebar upper bound with 7% damping, standard deviation of 105.7%) to as high as 54.4% (FEMA Cracked with 3% damping, standard deviation of 190.6%). The updated stiffness methods had errors ranging from -4.4% (Brown updated stiffness method with 7% damping, standard deviation of 87.5%) to 39.0% (Doepker updated stiffness method with 3% damping, standard deviation of 126.9%).

Even using a period matching model with the effective viscous damping ratio obtained from system identification had mixed results as it yielded an 11.6% error however with a standard deviation of 63.3%.

Table 5-27: Average Error and Standard Deviation for Roof Acceleration Predictions (drifts between 0.0% and 0.5%)

Analysis Method	Complete Data Set		Data Set Minus Ecoleader		UCSD Data Set	
	Mean	Standard Deviation	Mean	Standard Deviation	Mean	Standard Deviation
FIB 27 (0.3), 3%	23.3%	89.9%	35.1%	100.0%	48.3%	*
FIB 27 (0.3), 7%	-11.2%	82.4%	-3.5%	92.8%	13.4%	*
Adebar Upper, 3%	23.6%	116.2%	43.4%	125.5%	22.8%	*
Adebar Upper, 7%	-13.6%	94.1%	-3.2%	105.7%	-6.3%	*
Adebar Lower, 3%	12.5%	138.0%	24.1%	154.8%	49.6%	*
Adebar Lower, 7%	-9.7%	67.9%	-3.6%	74.9%	11.4%	*
FEMA Cracked, 3%	34.5%	171.9%	54.4%	190.6%	-23.5%	*
FEMA Cracked, 7%	-15.4%	97.9%	-6.9%	107.9%	-33.8%	*
FEMA Uncracked, 3%	-9.9%	82.8%	-10.7%	94.0%	-26.0%	*
FEMA Uncracked, 7%	-27.9%	66.0%	-29.2%	75.0%	-46.0%	*
Brown Updated Stiffness, 3%	25.9%	77.1%	38.5%	83.9%	48.3%	*
Brown Updated Stiffness, 7%	-11.9%	77.9%	-4.4%	87.5%	13.4%	*
Doepker Updated Stiffness, 3%	20.5%	117.9%	39.0%	126.9%	52.8%	*
Doepker Updated Stiffness, 7%	-0.1%	84.6%	11.6%	90.9%	16.1%	*
Uniform Period Matching	-0.3%	60.8%	11.6%	63.3%	28.1%	*

* Only one test from UCSD fell in this drift range

Table 5-28: Rank of Effectiveness of Methods of Predicting the Roof Acceleration (drifts between 0.0% and 0.5%)

Analysis Method	Conf. Sum	Rank All	Rank 3%	Rank 7%
FIB 27 (0.3), 3%	18.5	11	5	
FIB 27 (0.3), 7%	6.3	4		4
Adebar Upper, 3%	18.9	12	6	
Adebar Upper, 7%	8.1	7		6
Adebar Lower, 3%	11.0	9	3	
Adebar Lower, 7%	5.4	3		3
FEMA Cracked, 3%	25.8	15	8	
FEMA Cracked, 7%	10.0	8		7
FEMA Uncracked, 3%	6.9	6	2	
FEMA Uncracked, 7%	19.7	13		8
Brown Iterated Stiffness, 3%	20.1	14	7	
Brown Iterated Stiffness, 7%	6.8	5		5
Doepker Iterated Stiffness, (0.8), 3%	17.3	10	4	
Doepker Iterated Stiffness, (0.8), 7%	1.8	2		2
Uniform Best Fit	1.6	1	1	1

Table 5-29 and Table 5-30 provide statistics for error in roof acceleration in the moderate roof drift range (between 0.5% and 1.0%) as well as a ranking of the methods on the basis of these data and the confidence data in Table 3-48 and Table 3-49.

In moderate drift ranges, using 3% damping appears to outperform 7% unlike in the low drift ranges. FIB 27 performs the best for acceleration prediction with an average error of 3.7% and a standard deviation of only 4.3%. The updated stiffness methods perform reasonably, with errors of -15.5% for Brown and -23% for Doepker (standard deviations of 45.5% and 42.0%). All methods with the exception of FEMA Uncracked have moderate errors of less than 30%, although some are plagued with very large standard deviations. The uniform period matching model under predicts the acceleration averaging -37.9% error.

Table 5-29: Average Error and Standard Deviation for Roof Acceleration Predictions (drifts between 0.5% and 1.0%)

Analysis Method	Complete Data Set		Data Set Minus Ecoleader		UCSD Data Set	
	Mean	Standard Deviation	Mean	Standard Deviation	Mean	Standard Deviation
FIB 27 (0.3), 3%	-3.8%	16.2%	3.7%	4.3%	5.9%	0.2%
FIB 27 (0.3), 7%	-28.2%	38.1%	-37.4%	26.8%	-29.2%	43.2%
Adebar Upper, 3%	9.3%	85.2%	-24.9%	69.2%	12.5%	89.3%
Adebar Upper, 7%	-33.3%	59.0%	-28.4%	75.4%	16.3%	95.1%
Adebar Lower, 3%	38.5%	86.4%	-10.3%	53.3%	8.4%	83.8%
Adebar Lower, 7%	13.4%	78.6%	-24.4%	67.7%	7.9%	97.5%
FEMA Cracked, 3%	45.5%	103.5%	-19.2%	24.4%	-0.5%	16.6%
FEMA Cracked, 7%	-12.9%	65.4%	-53.8%	20.3%	-36.3%	3.9%
FEMA Uncracked, 3%	12.1%	109.8%	-55.0%	27.9%	-39.2%	36.6%
FEMA Uncracked, 7%	-29.6%	55.6%	-54.8%	21.9%	-36.9%	12.2%
Brown Updated Stiffness, 3%	16.1%	65.0%	-15.5%	45.5%	-9.3%	65.3%
Brown Updated Stiffness, 7%	-31.6%	46.4%	-42.6%	41.8%	-25.2%	58.2%
Doepker Updated Stiffness, 3%	-8.0%	42.9%	-23.0%	42.0%	-9.3%	65.3%
Doepker Updated Stiffness, 7%	-37.1%	36.6%	-41.1%	41.5%	-23.4%	62.6%
Uniform Period Matching	-16.5%	49.0%	-37.9%	34.8%	-19.7%	36.2%

Table 5-30: Rank of Effectiveness of Methods of Predicting the Roof Acceleration (drifts between 0.5% and 1.0%)

Analysis Method	Conf. Sum	Rank All	Rank 3%	Rank 7%
FIB 27 (0.3), 3%	0.4	1	1	
FIB 27 (0.3), 7%	11.4	10		5
Adebar Upper, 3%	1.8	2	2	
Adebar Upper, 7%	10.7	9		4
Adebar Lower, 3%	12.0	12	8	
Adebar Lower, 7%	3.3	4		1
FEMA Cracked, 3%	11.5	11	7	
FEMA Cracked, 7%	9.7	8		3
FEMA Uncracked, 3%	2.2	3	3	
FEMA Uncracked, 7%	15.1	15		8
Brown Iterated Stiffness, 3%	3.3	5	4	
Brown Iterated Stiffness, 7%	12.4	13		6
Doepker Iterated Stiffness, (0.8), 3%	3.8	6	5	
Doepker Iterated Stiffness, (0.8), 7%	14.3	14		7
Uniform Best Fit	8.4	7	6	2

Table 5-31 and Table 5-32 provide statistics for error in roof acceleration in the high roof drift range as well as a ranking of the methods on the basis of these data and the confidence data in Table 3-48 and Table 3-49. In the high drift range (greater than 1.0% drift), all methods saw a significant amount of scatter. With regards to damping, some methods performed best with 3% damping while others performed better with 7% damping. FIB 27 and Adebar lower bound with 7% damping were the only existing methods to provide acceptable results, with an average error of -1.9% and -16.0% respectively. Other existing methods had results that varied from 54.3% for FIB 27 with 3% damping to 239.4% for FEMA Cracked stiffness with 3% damping. The updated stiffness methods also struggled with an average error ranging from 41.6% for Brown's updated stiffness with 3% damping up to 71.7% for Brown's stiffness with 7% damping. The uniform period matching model in this drift range, as in others struggles with an average error of 43.4%.

Table 5-31: Average Error and Standard Deviation for Roof Acceleration Predictions (drifts greater than 1.0%)

Analysis Method	Complete Data Set		Data Set Minus Ecoleader		UCSD Data Set	
	Mean	Standard Deviation	Mean	Standard Deviation	Mean	Standard Deviation
FIB 27 (0.3), 3%	46.3%	72.3%	54.3%	86.0%	*	*
FIB 27 (0.3), 7%	-3.1%	54.9%	-1.9%	66.5%	*	*
Adebar Upper, 3%	111.8%	123.1%	114.0%	141.2%	*	*
Adebar Upper, 7%	57.6%	109.9%	80.2%	125.8%	*	*
Adebar Lower, 3%	8.5%	76.3%	-16.4%	75.8%	*	*
Adebar Lower, 7%	-4.6%	32.9%	-16.0%	22.9%	*	*
FEMA Cracked, 3%	152.9%	85.5%	148.4%	103.7%	*	*
FEMA Cracked, 7%	115.5%	69.7%	112.5%	84.8%	*	*
FEMA Uncracked, 3%	185.2%	187.5%	239.4%	177.2%	*	*
FEMA Uncracked, 7%	111.7%	106.9%	133.0%	123.1%	*	*
Brown Updated Stiffness, 3%	110.2%	189.0%	41.6%	72.8%	*	*
Brown Updated Stiffness, 7%	44.7%	61.4%	71.7%	49.2%	*	*
Doepker Updated Stiffness, 3%	100.7%	110.4%	62.1%	95.4%	*	*
Doepker Updated Stiffness, 7%	42.7%	99.0%	57.1%	116.4%	*	*
Uniform Period Matching	60.8%	63.2%	43.4%	68.3%	*	*

* No UCSD tests were performed in this drift range

Table 5-32: Rank of Effectiveness of Methods of Predicting the Roof Acceleration (drifts greater than 1.0%)

Analysis Method	Conf. Sum	Rank All	Rank 3%	Rank 7%
FIB 27 (0.3), 3%	18.0	5	2	
FIB 27 (0.3), 7%	2.4	2		1
Adebar Upper, 3%	42.9	11	6	
Adebar Upper, 7%	22.8	8		6
Adebar Lower, 3%	1.9	1	1	
Adebar Lower, 7%	2.7	3		2
FEMA Cracked, 3%	59.2	14	7	
FEMA Cracked, 7%	44.4	12		7
FEMA Uncracked, 3%	75.9	15	8	
FEMA Uncracked, 7%	44.6	13		8
Brown Iterated Stiffness, 3%	37.4	10	5	
Brown Iterated Stiffness, 7%	20.1	6		4
Doepker Iterated Stiffness, (0.8), 3%	35.0	9	4	
Doepker Iterated Stiffness, (0.8), 7%	17.7	4		3
Uniform Best Fit	21.5	7	3	5

Upon analysis of the error data, the following was observed for roof acceleration prediction:

- In most cases the methods are over predicting the acceleration. This is to be expected as most existing methods over predict the stiffness.
- In general, all methods resulted in large standard deviations including period matching models suggesting the limitation of using a linear elastic analysis to predict accelerations at all drift ranges.
- In low drift ranges, where a more accurate estimate may be required, using lower stiffness methods such as FIB 27 and Adebar lower bound as well as the Doepker and Brown updated stiffness methods provide the most accurate results. These methods however still tend to result in prohibitively high levels of error with large standard deviations.

- For the low drift range, the most effective methods performed best with 7% damping. Acceleration was the only analysis quantity that exhibited this behavior.
- Poor response as well as the fact that 7% damping performed better than 3% damping suggest the limitations in capturing the acceleration response. Further research in methods to accurately predict acceleration would be a worthwhile topic for future studies.

The following subsection discusses the error in base shear. A discussion of the errors in roof drift, roof acceleration, base shear and base moment are discussed with respect to the drift range beginning in Section 5.7.

5.6.4 Error in Base Shear

Accurate prediction of the expected base shear arising from seismic excitation is essential for economical placement of reinforcement as well as damage prediction. Data are evaluated using the same approach as was used for evaluating the accuracy of the methods for predicting effective fundamental period: plots of error versus maximum measured roof drift as well as tabulated data. To determine the base shear at the point of maximum roof drift, it is necessary to complete a time-history analysis using both an effective stiffness model and an effective viscous damping ratio. Thus, results are provided for the two chosen damping ratios of 3% and 7%.

Figure 5-24 through Figure 5-29 show error in simulated base shear, E_{shear} as computed using Eq. 5-7, versus maximum measured roof drift. The full results of the base shear error analysis for all methods can be seen in Figure 5-24 and Figure 5-25. Results emphasizing the existing methods can be seen in Figure 5-26 and Figure 5-27, and results emphasizing the updated stiffness methods as well as the period matching model (with system identification damping) are seen in Figure 5-28 and Figure 5-29. The data in these figures support the following observations:

- Data in Figure 5-24 and Figure 5-25 show that at low drift ranges an effective damping ratio of 3% appears to provide better prediction.
- Data in Figure 5-26 and Figure 5-27 show that existing single-value methods over predict the base shear for moderate and high drifts.
- Data in Figure 5-28 and Figure 5-29 show that proposed methods (particularly when excluding Ecoleader test results) outperform existing methods for moderate and high drift ranges.
- Data in Figure 5-28 and Figure 5-29 further show that the uniform period matching methods on average have very low errors for all drift ranges. It however on average appears to under predict the base shear potentially due to over damping.

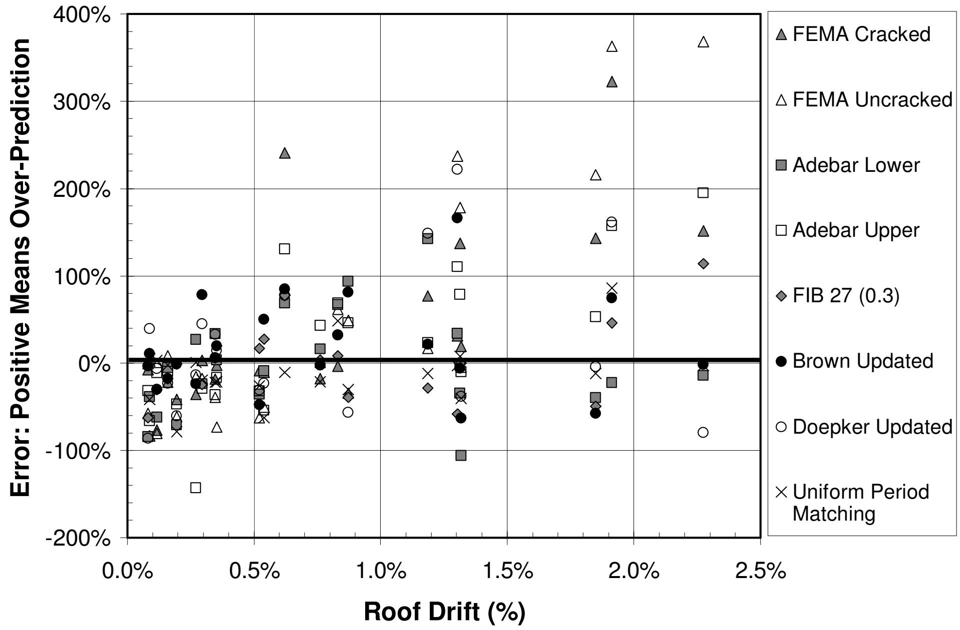

Figure 5-24: Error in Base Shear with Respect to Drift for All Methods - 3% Damping

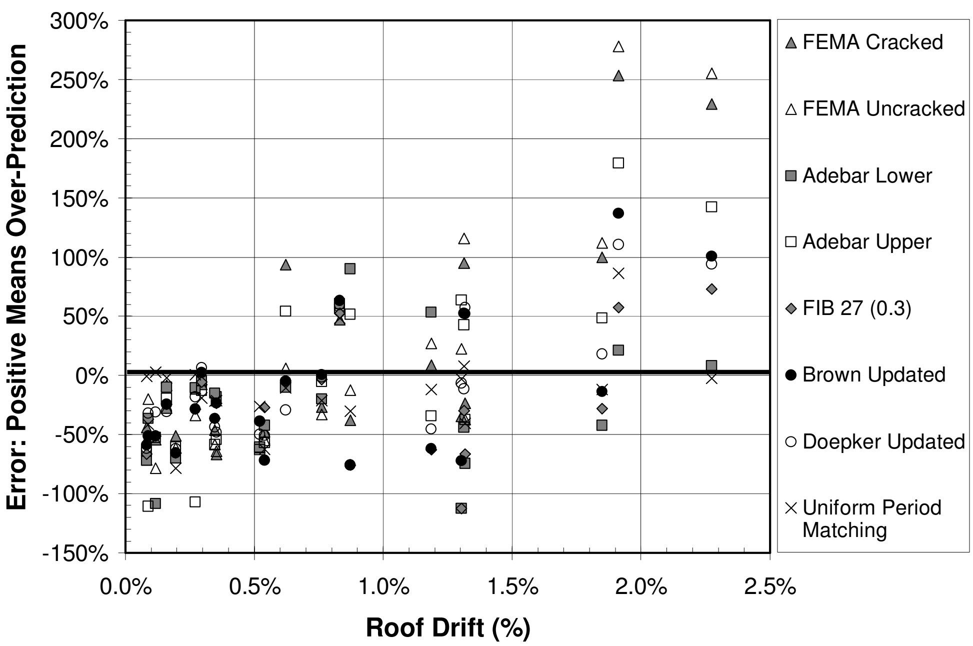

Figure 5-25: Error in Base Shear with Respect to Drift for All Methods - 7% Damping

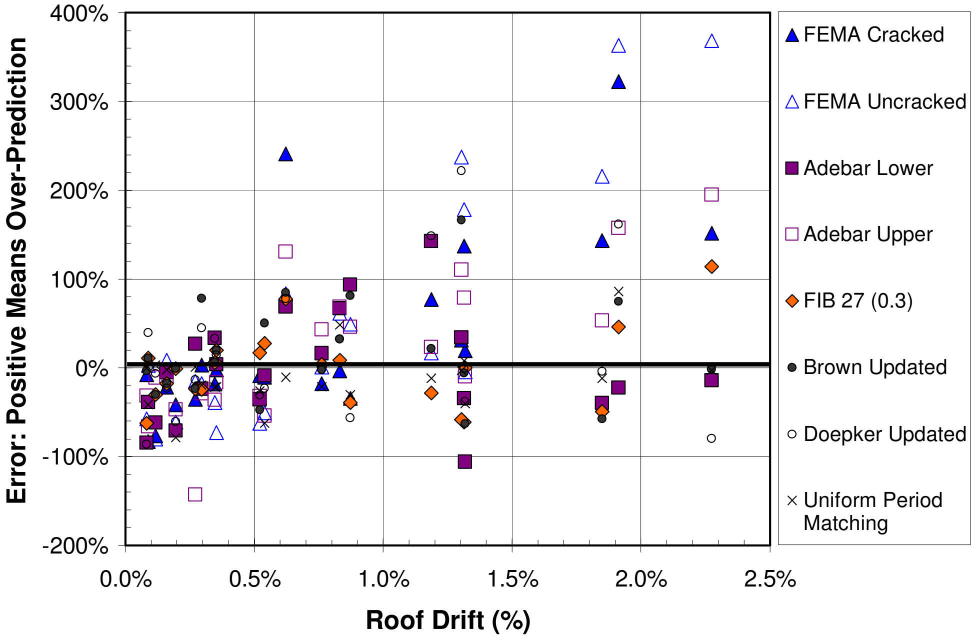

Figure 5-26: Error in Base Shear with Respect to Drift for Existing Methods - 3% Damping

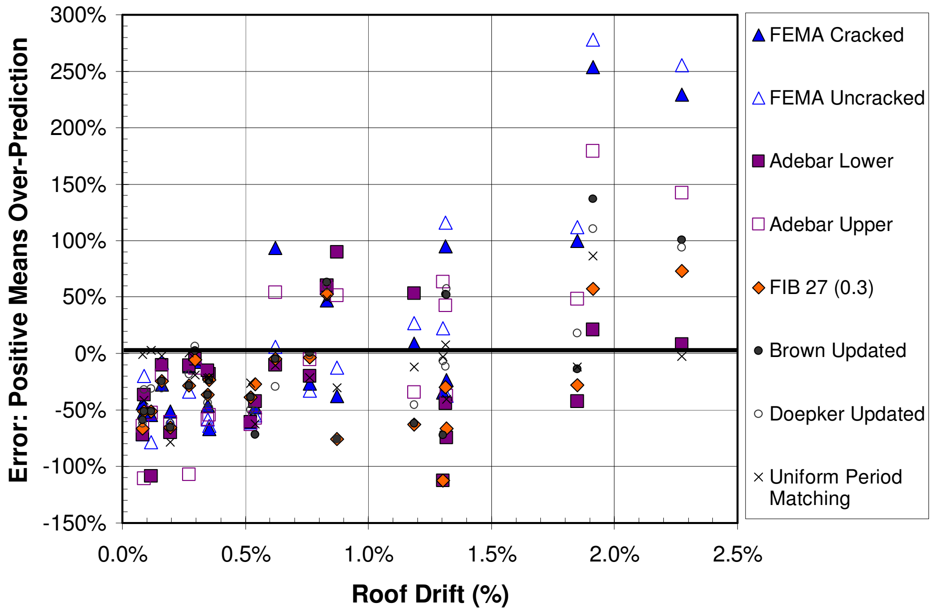

Figure 5-27: Error in Base Shear with Respect to Drift for Existing Methods - 7% Damping

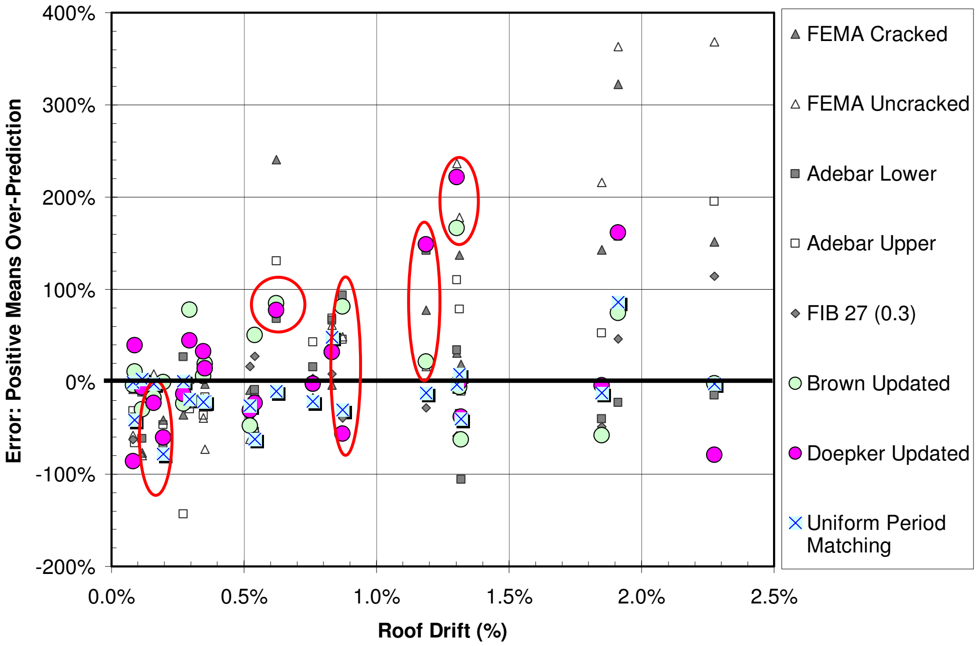

Figure 5-28: Error in Base Shear with Respect to Drift for Proposed and Period Matching Methods - 3% Damping (circled points refer to Ecoleader tests)

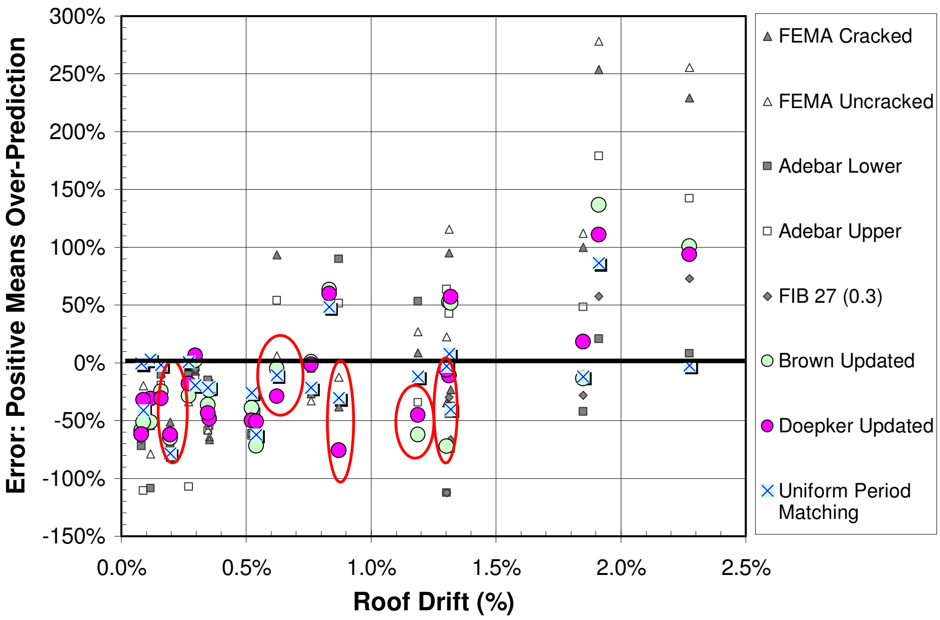

Figure 5-29: Error in Base Shear with Respect to Drift for Proposed and Period Matching Methods - 7% Damping (circled points refer to Ecoleader tests)

Table 5-33 provides statistics for error in maximum base shear at the point of maximum roof drift and a ranking of the methods on the basis of these data as well as the confidence data in Table 3-48 and Table 3-49 is provided in Table 5-34. The data in these tables support the previous observations. When excluding the Ecoleader test results, on average, the stiffer single value existing methods using 3% damping over predict the base shear (32.0% and 49.4% for FEMA Cracked and Uncracked respectively). Using 7% damping on these stiff methods improves the response with regards to base shear (17.8% and 19.0% for FEMA Cracked and Uncracked respectively) however the base shear is still over predicted on average.

The lower stiffness single value methods see an improvement in using 3% viscous damping as opposed to 7% (e.g. FIB 27 yielded average errors of 0.3% and -17.1% for 3% and 7% viscous damping ratios respectively).

The updated stiffness methods outperform most methods, and seem to have similar results independent of viscous damping ratio on average over the entire data set. Brown averaged 2.3% and 2.1% error for a damping ratio of 3% and 7% while Doepker averaged 2.6% and -0.1% for 3% and 7% damping. The uniform period matching models on average performed well, however with a slight under prediction in base shear on average (-7.6%).

Table 5-33: Average Error and Standard Deviation for Base Shear Predictions

Analysis Method	Complete Data Set		Data Set Minus Ecoleader		UCSD Data Set	
	Mean	Standard Deviation	Mean	Standard Deviation	Mean	Standard Deviation
FIB 27 (0.3), 3%	-2.8%	44.1%	0.3%	43.9%	-3.8%	17.5%
FIB 27 (0.3), 7%	-28.2%	44.7%	-17.1%	42.8%	6.9%	41.4%
Adebar Upper, 3%	19.1%	80.8%	10.4%	85.3%	-10.3%	115.7%
Adebar Upper, 7%	-4.4%	75.6%	-9.5%	83.3%	-18.2%	83.0%
Adebar Lower, 3%	-2.7%	59.9%	-20.2%	44.0%	36.6%	26.6%
Adebar Lower, 7%	-23.6%	51.0%	-28.7%	40.9%	10.0%	44.1%
FEMA Cracked, 3%	34.8%	103.2%	32.0%	105.0%	-18.8%	16.0%
FEMA Cracked, 7%	10.7%	90.5%	17.8%	101.5%	2.8%	39.0%
FEMA Uncracked, 3%	51.2%	135.5%	49.4%	149.3%	15.8%	40.4%
FEMA Uncracked, 7%	12.6%	98.4%	19.0%	114.2%	-2.5%	53.2%
Brown Updated Stiffness, 3%	17.0%	54.7%	2.3%	42.2%	2.2%	28.3%
Brown Updated Stiffness, 7%	-12.3%	58.9%	2.1%	61.4%	11.7%	46.8%
Doepker Updated Stiffness, 3%	15.9%	78.1%	2.6%	57.0%	5.6%	23.9%
Doepker Updated Stiffness, 7%	-11.4%	50.9%	-0.1%	54.1%	13.4%	41.0%
Uniform Period Matching	-11.8%	33.8%	-7.6%	35.3%	9.3%	35.8%

Table 5-34: Rank of Effectiveness of Methods of Predicting the Base Shear

Analysis Method	Conf. Sum	Rank All	Rank 3%	Rank 7%
FIB 27 (0.3), 3%	4.6	1	1	
FIB 27 (0.3), 7%	40.7	14		8
Adebar Upper, 3%	14.5	5	3	
Adebar Upper, 7%	19.9	11		6
Adebar Lower, 3%	10.9	4	2	
Adebar Lower, 7%	39.6	13		7
FEMA Cracked, 3%	37.4	12	7	
FEMA Cracked, 7%	6.4	2		1
FEMA Uncracked, 3%	56.1	15	8	
FEMA Uncracked, 7%	6.6	3		2
Brown Iterated Stiffness, 3%	17.3	7	5	
Brown Iterated Stiffness, 7%	18.4	8		3
Doepker Iterated Stiffness, (0.8), 3%	14.6	6	4	
Doepker Iterated Stiffness, (0.8), 7%	18.5	9		4
Uniform Best Fit	18.8	10	6	5

Table 5-35 provides error data statistics for runs with maximum roof drifts less than 0.5%; Table 5-36 ranks the evaluated methods on the basis of these data and the confidence data in Table 3-48 and Table 3-49. The data in these tables show that when neglecting the contributions of Ecoleader, the updated stiffness methods perform extremely well in low drift ranges. Methods using 3% damping out performed 7%. Doepker had an average error of only 3.6%, while Brown yielded an error of 8.2%. The uniform period matching method consistently under predicts with an error of -14.3%, however it has a much lower value of standard deviation than any of the other leading methods. This under prediction of the error is further indication of possible over damping from using the damping obtained from the system identification. FIB 27 performs well for 3% damping with an error of -14.8% however all other existing methods have much greater errors ranging from -20.6% (for Adebar's lower bound with 3% damping) to -65.7% (for Adebar's upper bound with 7% damping).

Table 5-35: Average Error and Standard Deviation for Base Shear Predictions (drifts between 0.0% and 0.5%)

Analysis Method	Complete Data Set		Data Set Minus Ecoleader		UCSD Data Set	
	Mean	Standard Deviation	Mean	Standard Deviation	Mean	Standard Deviation
FIB 27 (0.3), 3%	-13.5%	25.3%	-14.8%	28.7%	-23.7%	*
FIB 27 (0.3), 7%	-39.2%	20.7%	-37.6%	20.5%	-28.5%	*
Adebar Upper, 3%	-43.3%	41.5%	-47.7%	45.5%	-143.1%	*
Adebar Upper, 7%	-60.0%	33.1%	-65.7%	33.9%	-107.1%	*
Adebar Lower, 3%	-24.4%	42.6%	-20.6%	44.5%	27.1%	*
Adebar Lower, 7%	-38.4%	36.6%	-37.9%	38.6%	-10.6%	*
FEMA Cracked, 3%	-31.5%	31.0%	-31.5%	35.4%	-35.4%	*
FEMA Cracked, 7%	-40.2%	20.3%	-40.4%	22.4%	-11.6%	*
FEMA Uncracked, 3%	-36.9%	32.9%	-40.0%	31.4%	-15.0%	*
FEMA Uncracked, 7%	-44.4%	28.4%	-47.1%	28.4%	-33.6%	*
Brown Updated Stiffness, 3%	4.4%	32.1%	8.2%	35.6%	-23.7%	*
Brown Updated Stiffness, 7%	-37.5%	21.3%	-35.4%	21.0%	-28.5%	*
Doepker Updated Stiffness, 3%	-6.5%	45.2%	3.6%	45.5%	-13.4%	*
Doepker Updated Stiffness, 7%	-35.7%	21.6%	-32.6%	22.1%	-18.2%	*
Uniform Period Matching	-20.1%	26.3%	-14.3%	16.2%	0.8%	*

* Only one test from UCSD fell in this drift range

Table 5-36: Rank of Effectiveness of Methods of Predicting the Base Shear (drifts between 0.0% and 0.5%)

Analysis Method	Conf. Sum	Rank All	Rank 3%	Rank 7%
FIB 27 (0.3), 3%	9.5	3	3	
FIB 27 (0.3), 7%	27.0	11		5
Adebar Upper, 3%	32.3	14	8	
Adebar Upper, 7%	43.3	15		8
Adebar Lower, 3%	15.6	5	5	
Adebar Lower, 7%	26.2	10		4
FEMA Cracked, 3%	22.2	6	6	
FEMA Cracked, 7%	27.7	12		6
FEMA Uncracked, 3%	25.7	8	7	
FEMA Uncracked, 7%	31.1	13		7
Brown Iterated Stiffness, 3%	3.1	1	1	
Brown Iterated Stiffness, 7%	25.8	9		3
Doepker Iterated Stiffness, (0.8), 3%	3.2	2	2	
Doepker Iterated Stiffness, (0.8), 7%	24.3	7		2
Uniform Best Fit	13.2	4	4	1

Table 5-37 and Table 5-38 provide statistics for error in maximum roof drift in the moderate roof drift range as well as a ranking of the methods on the basis of these data and the confidence data in Table 3-48 and Table 3-49. In this drift range the uniform period matching models continued to under predict the base shear on average (-15.3% error), further reinforcing the theory of over damping when using the damping determined from the system identification. The updated stiffness methods performed extremely well, with the Doepker method averaging -5.8% error and the Brown method averaging 8.2% error. Both methods performed better with 3% damping. FIB 27 by contrast performed better with 7% damping, and had an error of -4.1%. Many of the existing methods performed quite well in this drift range (less than 20% average error), however many were plagued by larger standard deviations than the updated stiffness methods or FIB 27.

Table 5-37: Average Error and Standard Deviation for Base Shear Predictions (drifts between 0.5% and 1.0%)

Analysis Method	Complete Data Set		Data Set Minus Ecoleader		UCSD Data Set	
	Mean	Standard Deviation	Mean	Standard Deviation	Mean	Standard Deviation
FIB 27 (0.3), 3%	15.9%	37.9%	14.2%	10.5%	6.2%	3.7%
FIB 27 (0.3), 7%	-16.2%	42.9%	-4.1%	40.6%	24.6%	39.4%
Adebar Upper, 3%	33.8%	67.7%	6.5%	58.8%	56.0%	18.2%
Adebar Upper, 7%	6.4%	56.3%	-16.8%	55.9%	26.2%	44.2%
Adebar Lower, 3%	33.4%	50.5%	9.6%	43.4%	41.3%	35.8%
Adebar Lower, 7%	2.8%	59.5%	-15.7%	53.5%	20.2%	57.0%
FEMA Cracked, 3%	27.7%	105.0%	-10.2%	5.7%	-10.4%	9.8%
FEMA Cracked, 7%	-5.2%	61.2%	-21.7%	47.7%	10.0%	52.2%
FEMA Uncracked, 3%	13.7%	60.8%	-12.6%	56.4%	31.1%	42.9%
FEMA Uncracked, 7%	-16.0%	44.7%	-22.5%	55.7%	13.1%	64.9%
Brown Updated Stiffness, 3%	33.2%	51.1%	8.2%	43.2%	15.1%	24.4%
Brown Updated Stiffness, 7%	-21.2%	52.3%	-11.7%	58.0%	31.8%	44.3%
Doepker Updated Stiffness, 3%	-0.4%	48.5%	-5.8%	28.2%	15.1%	24.4%
Doepker Updated Stiffness, 7%	-24.6%	48.2%	-10.6%	52.2%	29.1%	43.3%
Uniform Period Matching	-17.0%	36.5%	-15.3%	46.3%	13.5%	49.5%

Table 5-38: Rank of Effectiveness of Methods of Predicting the Base Shear (drifts between 0.5% and 1.0%)

Analysis Method	Conf. Sum	Rank All	Rank 3%	Rank 7%
FIB 27 (0.3), 3%	6.7	8	4	
FIB 27 (0.3), 7%	4.9	6		4
Adebar Upper, 3%	12.5	15	8	
Adebar Upper, 7%	0.4	2		1
Adebar Lower, 3%	11.1	14	7	
Adebar Lower, 7%	1.5	3		2
FEMA Cracked, 3%	8.4	12	5	
FEMA Cracked, 7%	3.4	5		3
FEMA Uncracked, 3%	3.2	4	2	
FEMA Uncracked, 7%	7.4	10		7
Brown Iterated Stiffness, 3%	10.0	13	6	
Brown Iterated Stiffness, 7%	6.7	9		6
Doepker Iterated Stiffness, (0.8), 3%	0.0	1	1	
Doepker Iterated Stiffness, (0.8), 7%	8.0	11		8
Uniform Best Fit	6.5	7	3	5

Table 5-39 and Table 5-40 provide statistics for error in maximum roof drift in the high roof drift range as well as a ranking of the methods on the basis of these data and the confidence data in Table 3-48 and Table 3-49. All methods in this drift range exhibited very large variation in the accuracy of the results.

Unlike the low and moderate drift ranges, the period matching model slightly over predicted the base shear in high drift ranges with an average error of 7.9%. These models resulted in a lower standard deviation than the other well performing methods. The Doepker updated stiffness (7.8% error) and the Brown updated stiffness (-10.6%) both performed well with 3% damping, although the errors when using 7% damping were both extremely high. FIB 27 performed well with both levels of damping, however 7% damping performed best (1.2% error as opposed to 10.2% error with 3% damping).

Existing methods behaved as expected in this drift range. Their significant over prediction in the stiffness resulted in an enormous over prediction of the base shear. The error in base shear ranged from 75.0% for Adebar's upper bound with 7% damping all the way to 224.3% for FEMA Uncracked with 3% damping.

Table 5-39: Average Error and Standard Deviation for Base Shear Predictions (drifts greater than 1.0%)

Analysis Method	Complete Data Set		Data Set Minus Ecoleader		UCSD Data Set	
	Mean	Standard Deviation	Mean	Standard Deviation	Mean	Standard Deviation
FIB 27 (0.3), 3%	-5.1%	65.0%	10.2%	72.1%	*	*
FIB 27 (0.3), 7%	-24.2%	67.4%	1.2%	60.6%	*	*
Adebar Upper, 3%	86.9%	73.0%	94.9%	82.1%	*	*
Adebar Upper, 7%	57.8%	81.3%	75.0%	86.2%	*	*
Adebar Lower, 3%	-5.8%	77.4%	-43.4%	36.4%	*	*
Adebar Lower, 7%	-27.2%	57.8%	-26.3%	39.7%	*	*
FEMA Cracked, 3%	126.0%	102.1%	154.8%	108.4%	*	*
FEMA Cracked, 7%	89.7%	116.4%	130.8%	112.7%	*	*
FEMA Uncracked, 3%	196.5%	148.6%	224.3%	153.9%	*	*
FEMA Uncracked, 7%	110.5%	119.4%	144.8%	127.5%	*	*
Brown Updated Stiffness, 3%	19.3%	80.1%	-10.6%	55.5%	*	*
Brown Updated Stiffness, 7%	27.7%	79.8%	65.7%	56.9%	*	*
Doepker Updated Stiffness, 3%	58.5%	116.3%	7.8%	91.5%	*	*
Doepker Updated Stiffness, 7%	31.0%	57.9%	53.8%	50.9%	*	*
Uniform Period Matching	3.5%	39.5%	7.9%	47.4%	*	*

* No UCSD tests were performed in this drift range

Table 5-40: Rank of Effectiveness of Methods of Predicting the Base Shear (drifts greater than 1.0%)

Analysis Method	Conf. Sum	Rank All	Rank 3%	Rank 7%
FIB 27 (0.3), 3%	1.7	2	2	
FIB 27 (0.3), 7%	8.8	5		2
Adebar Upper, 3%	34.4	11	6	
Adebar Upper, 7%	23.0	10		6
Adebar Lower, 3%	6.4	4	4	
Adebar Lower, 7%	11.8	6		3
FEMA Cracked, 3%	51.3	14	7	
FEMA Cracked, 7%	37.5	12		7
FEMA Uncracked, 3%	78.6	15	8	
FEMA Uncracked, 7%	45.1	13		8
Brown Iterated Stiffness, 3%	4.2	3	3	
Brown Iterated Stiffness, 7%	14.0	8		5
Doepker Iterated Stiffness, (0.8), 3%	17.8	9	5	
Doepker Iterated Stiffness, (0.8), 7%	13.7	7		4
Uniform Best Fit	0.9	1	1	1

Upon analysis of the error data, the following was observed for base shear prediction:

- Larger single value stiffness methods over predict the base shear for high roof drift demands.
- More flexible single value stiffness methods such as FIB 27 and Adebar's lower bound yield closer results, although variability in the results was high resulting in high standard deviations. A value of 3% effective viscous damping was most effective in low drift ranges while 7% performed better for moderate and high drift ranges.
- In high drift ranges, all methods exhibited very large variation in the accuracy of the results. It might be concluded that in high drift ranges, a single linear elastic analysis might be limited in its ability to predict base shears.
- On average, updated stiffness methods improved the prediction of the shear response. 3% viscous damping on average provided the best results.

5.6.5 Error in Base Moment

Prediction of the expected base moment arising from seismic excitation is essential for economical placement of reinforcement as well as damage prediction. Data are evaluated using the same approach as was used for evaluating the accuracy of the methods for predicting effective fundamental period: plots of error in predicted base moment versus maximum measured roof drift as well as tabulated data. To determine the base moment at the point of maximum roof drift, it is necessary to complete a time-history analysis using both an effective stiffness model and an effective viscous damping ratio. Thus, results are provided for the two chosen damping ratios of 3% and 7%.

Figure 5-30 through Figure 5-35 show error in simulated base shear, E_{moment} as computed using Eq. 5-8, versus maximum measured roof drift. The full results of the base moment error analysis for all methods can be seen in Figure 5-30 and Figure 5-31. Results emphasizing the existing methods can be seen in Figure 5-32 and Figure 5-33, and results emphasizing the updated stiffness methods as well as the period matching model (with system identification damping) are seen in Figure 5-34 and Figure 5-35. The data in these figures support the following observations:

- Data in Figure 5-30 and Figure 5-31 show that most single-value stiffness methods tend to under predict the base moment at low drift ranges and over predict the base moment at high drift ranges.
- Data in Figure 5-26 and Figure 5-27 show that Adebar lower bound and FIB 27 stiffness methods outperform stiffer single-value stiffness methods.
- Data in Figure 5-32 and Figure 5-33 show that proposed methods (particularly when excluding Ecoleader test results) outperform most existing methods especially for moderate and high drift ranges.
- Data in Figure 5-34 and Figure 5-35 further show that the uniform period matching methods on average have low errors for all drift ranges. It however

on average appears to under predict the base shear potentially due to over damping.

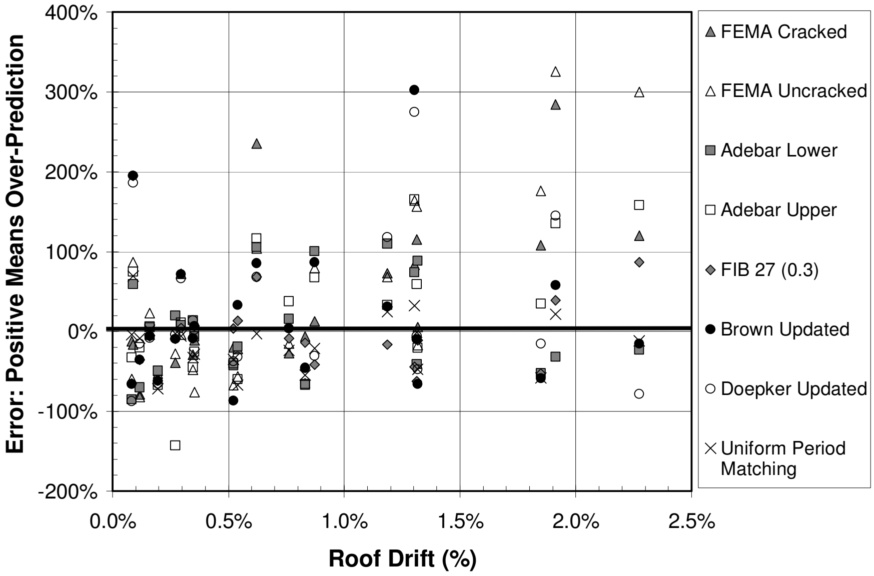

Figure 5-30: Error in Base Moment with Respect to Drift for All Methods - 3% Damping

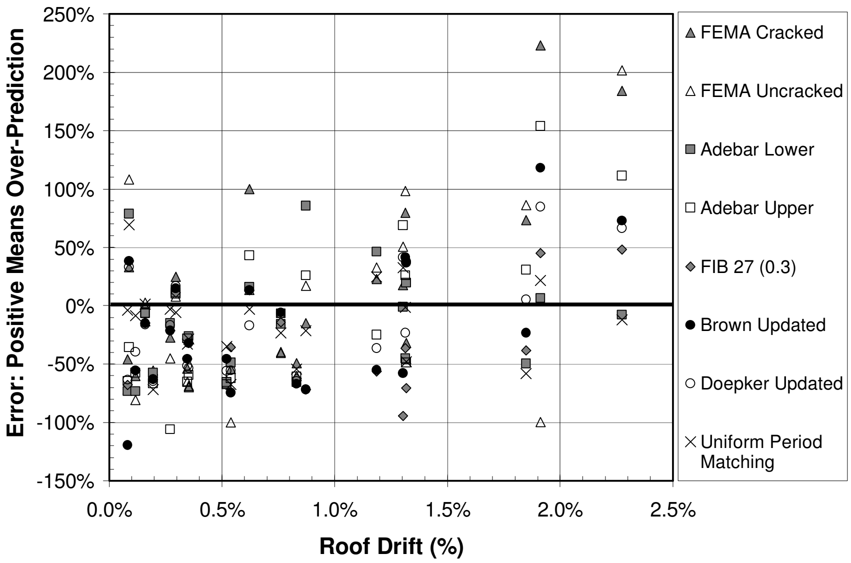

Figure 5-31: Error in Base Moment with Respect to Drift for All Methods - 7% Damping

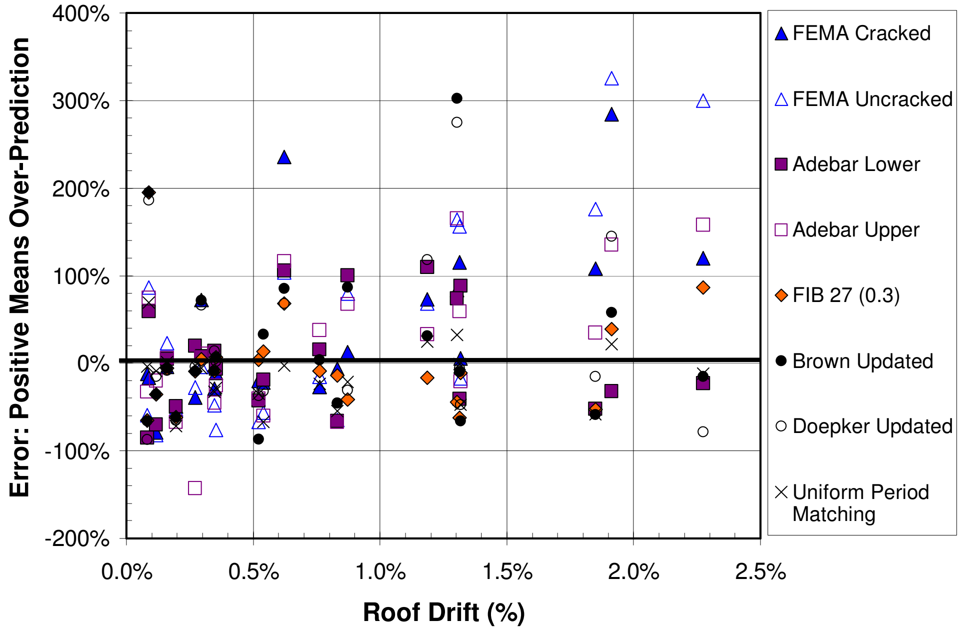

Figure 5-32: Error in Base Moment with Respect to Drift for Existing Methods - 3% Damping

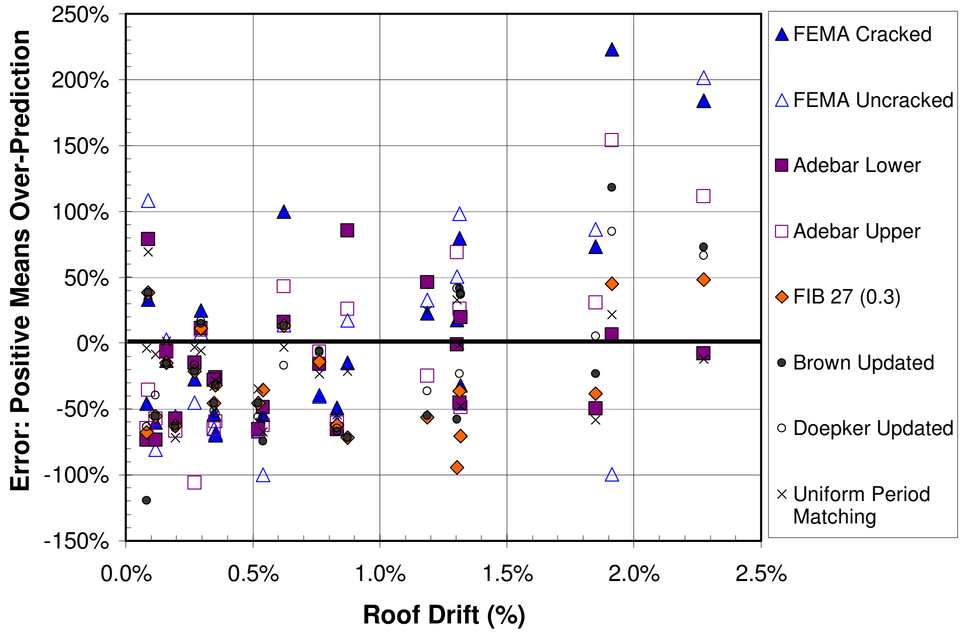

Figure 5-33: Error in Base Moment with Respect to Drift for Existing Methods - 7% Damping

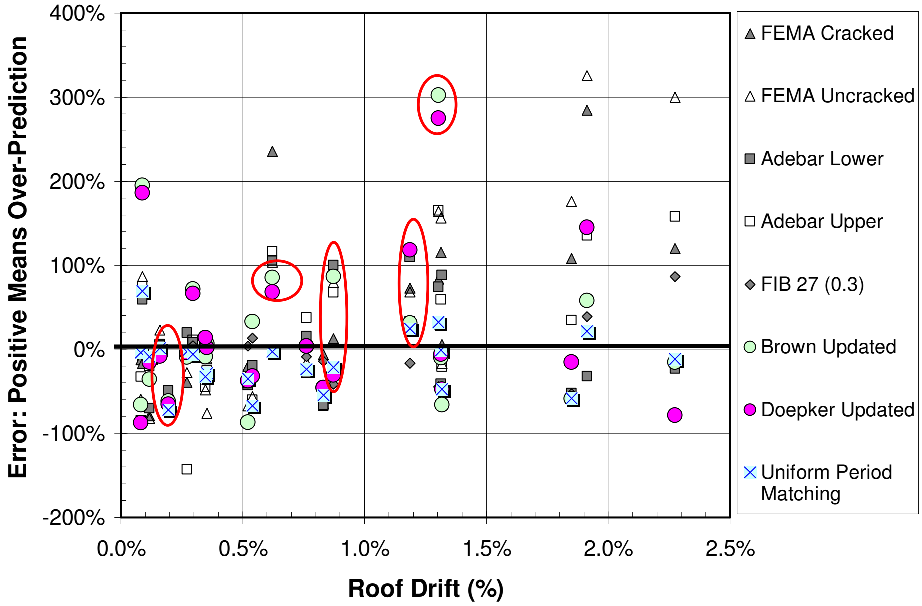

Figure 5-34: Error in Base Moment with Respect to Drift for Proposed and Period Matching Methods - 3% Damping (circled points refer to Ecoleader tests)

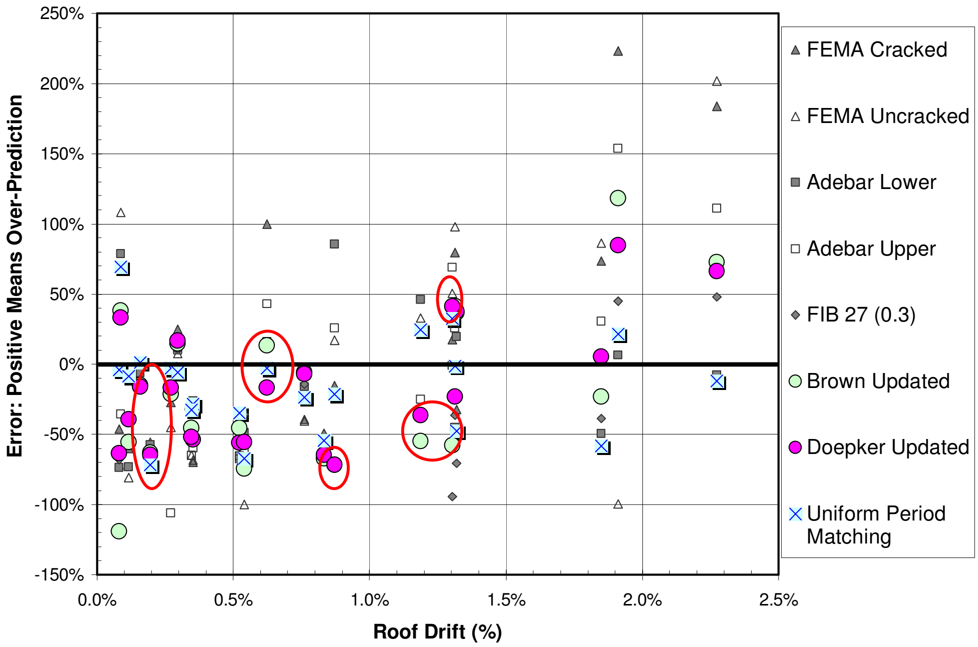

Figure 5-35: Error in Base Moment with Respect to Drift for Proposed and Period Matching Methods - 7% Damping (circled points refer to Ecoleader tests)

Table 5-41 provides statistics for error in base moment and a ranking of the methods on the basis of these data as well as the confidence data in Table 3-48 and Table 3-49 is provided in Table 5-42. The data in these tables support the previous observations. The best performing methods in terms of average error in base moment prediction were from models using the FIB 27 stiffness (5.1% average error) or the updated stiffness approaches (-2.0% for Brown and 3.0% for Doepker). For these, 3% damping was most effective. The period matching model appears to be in general under predicting the base moment as exhibited by its relatively significant average error (-18.2%) with a lower standard deviation (33.7%). This appears to be indicative of over damping.

Table 5-41: Average Error and Standard Deviation for Base Moment Predictions

Analysis Method	Complete Data Set		Data Set Minus Ecoleader		UCSD Data Set	
	Mean	Standard Deviation	Mean	Standard Deviation	Mean	Standard Deviation
FIB 27 (0.3), 3%	-0.9%	58.8%	5.1%	63.1%	-10.6%	3.1%
FIB 27 (0.3), 7%	-30.5%	40.0%	-23.9%	39.3%	-32.5%	26.0%
Adebar Upper, 3%	17.2%	80.0%	3.6%	77.3%	-57.2%	90.6%
Adebar Upper, 7%	-11.9%	65.2%	-18.9%	70.4%	-57.8%	49.7%
Adebar Lower, 3%	5.1%	60.7%	-14.5%	47.3%	-10.1%	48.2%
Adebar Lower, 7%	-14.3%	45.5%	-24.8%	40.9%	-32.0%	28.8%
FEMA Cracked, 3%	36.2%	92.1%	27.7%	90.9%	-24.2%	16.5%
FEMA Cracked, 7%	8.0%	80.6%	7.6%	90.4%	-38.6%	11.1%
FEMA Uncracked, 3%	41.5%	120.4%	32.9%	134.9%	-35.9%	25.8%
FEMA Uncracked, 7%	-8.2%	78.5%	-15.1%	89.5%	-48.6%	10.4%
Brown Updated Stiffness, 3%	18.5%	91.3%	-2.0%	68.9%	-17.1%	25.8%
Brown Updated Stiffness, 7%	-19.0%	55.9%	-10.5%	61.0%	-31.4%	31.9%
Doepker Updated Stiffness, 3%	18.4%	91.0%	3.0%	73.7%	-15.3%	26.8%
Doepker Updated Stiffness, 7%	-16.0%	45.8%	-11.7%	48.0%	-29.4%	30.8%
Uniform Period Matching	-14.9%	34.3%	-18.2%	33.7%	-26.9%	25.9%

Table 5-42: Rank of Effectiveness of Methods of Predicting the Base Moment

Analysis Method	Conf. Sum	Rank All	Rank 3%	Rank 7%
FIB 27 (0.3), 3%	0.3	1	1	
FIB 27 (0.3), 7%	44.6	15		8
Adebar Upper, 3%	11.1	4	3	
Adebar Upper, 7%	30.0	12		7
Adebar Lower, 3%	0.5	2	2	
Adebar Lower, 7%	26.9	10		5
FEMA Cracked, 3%	39.1	13	7	
FEMA Cracked, 7%	0.9	3		1
FEMA Uncracked, 3%	41.7	14	8	
FEMA Uncracked, 7%	20.4	7		2
Brown Iterated Stiffness, 3%	17.4	5	4	
Brown Iterated Stiffness, 7%	29.1	11		6
Doepker Iterated Stiffness, (0.8), 3%	19.1	6	5	
Doepker Iterated Stiffness, (0.8), 7%	26.7	9		4
Uniform Best Fit	24.2	8	6	3

Table 5-43 provides error data statistics for runs with maximum roof drifts less than 0.5%; Table 5-44 ranks the evaluated methods on the basis of these data and the confidence data in Table 3-48 and Table 3-49. The data in these tables show that in the low drift range the updated stiffness methods exhibit higher average error when excluding the Ecoleader test program. In this case 3% damping slightly outperforms 7% for these methods. With errors of 23.1% for Brown and 22.2% for Doepker, the updated stiffness methods perform worse than many of the existing methods (ex. FEMA Cracked with -16.3% error). The most effective methods in this range are the less stiff uniform methods: FIB 27 (12.6% error) and Adebar lower bound (-8.7% error).

The uniform stiffness period matching model performs very well on average with only a -1.9% average error and a low standard deviation (33.6%) when compared to other methods.

Table 5-43: Average Error and Standard Deviation for Base Moment Predictions (drifts between 0.0% and 0.5%)

Analysis Method	Complete Data Set		Data Set Minus Ecoleader		UCSD Data Set	
	Mean	Standard Deviation	Mean	Standard Deviation	Mean	Standard Deviation
FIB 27 (0.3), 3%	2.2%	77.2%	12.6%	84.4%	-9.3%	*
FIB 27 (0.3), 7%	-27.9%	35.4%	-24.7%	37.8%	-21.3%	*
Adebar Upper, 3%	-26.8%	59.4%	-25.8%	65.2%	-142.5%	*
Adebar Upper, 7%	-50.1%	34.8%	-54.0%	35.1%	-105.9%	*
Adebar Lower, 3%	-11.7%	46.9%	-8.7%	51.5%	20.0%	*
Adebar Lower, 7%	-21.0%	47.6%	-17.9%	52.5%	-14.8%	*
FEMA Cracked, 3%	-18.6%	41.4%	-16.3%	45.8%	-39.0%	*
FEMA Cracked, 7%	-29.9%	37.7%	-28.4%	41.5%	-27.2%	*
FEMA Uncracked, 3%	-26.7%	54.3%	-30.1%	58.3%	-27.7%	*
FEMA Uncracked, 7%	-29.8%	60.7%	-30.7%	68.1%	-45.1%	*
Brown Updated Stiffness, 3%	9.7%	80.7%	22.2%	87.2%	-9.3%	*
Brown Updated Stiffness, 7%	-33.3%	45.8%	-31.6%	50.9%	-21.3%	*
Doepker Updated Stiffness, 3%	9.8%	79.6%	23.1%	85.2%	-3.9%	*
Doepker Updated Stiffness, 7%	-28.4%	35.3%	-25.0%	37.4%	-16.7%	*
Uniform Period Matching	-9.3%	37.3%	-1.9%	33.6%	-3.0%	*

* Only one test from UCSD fell in this drift range

Table 5-44: Rank of Effectiveness of Methods of Predicting the Base Moment (drifts between 0.0% and 0.5%)

Analysis Method	Conf. Sum	Rank All	Rank 3%	Rank 7%
FIB 27 (0.3), 3%	2.8	1	1	
FIB 27 (0.3), 7%	18.9	9		3
Adebar Upper, 3%	20.4	11	8	
Adebar Upper, 7%	36.3	15		8
Adebar Lower, 3%	7.0	3	3	
Adebar Lower, 7%	14.0	7		2
FEMA Cracked, 3%	13.1	6	6	
FEMA Cracked, 7%	20.7	12		5
FEMA Uncracked, 3%	18.9	8	7	
FEMA Uncracked, 7%	21.0	13		6
Brown Iterated Stiffness, 3%	8.2	4	4	
Brown Iterated Stiffness, 7%	22.5	14		7
Doepker Iterated Stiffness, (0.8), 3%	8.6	5	5	
Doepker Iterated Stiffness, (0.8), 7%	19.2	10		4
Uniform Best Fit	5.7	2	2	1

Table 5-45 and Table 5-46 provide statistics for error in maximum base moment in the moderate roof drift range as well as a ranking of the methods on the basis of these data and the confidence data in Table 3-48 and Table 3-49. In the moderate drift range, the stiffer methods such as Adebar upper and FEMA uncracked result in prohibitively high errors (ranging from -32.3% for Adebar upper with 3% damping to -66.7% for FEMA Uncracked with 7% damping). In this range the FIB 27 stiffness provides exceptional results with only -1.4% error. FEMA cracked performs well with -18.8% error. The update stiffness methods struggle slightly in this range with -27.9% average error for Doepker and -23.8% for Brown. The uniform stiffness period matching model significantly under predicts the base moment.

Table 5-45: Average Error and Standard Deviation for Base Moment Predictions (drifts between 0.5% and 1.0%)

Analysis Method	Complete Data Set		Data Set Minus Ecoleader		UCSD Data Set	
	Mean	Standard Deviation	Mean	Standard Deviation	Mean	Standard Deviation
FIB 27 (0.3), 3%	3.5%	36.8%	-1.4%	12.3%	-11.3%	4.1%
FIB 27 (0.3), 7%	-36.0%	31.6%	-39.3%	20.2%	-38.1%	34.2%
Adebar Upper, 3%	9.1%	75.8%	-32.3%	48.2%	-14.5%	74.2%
Adebar Upper, 7%	-21.4%	48.9%	-49.3%	28.6%	-33.7%	38.3%
Adebar Lower, 3%	15.7%	72.7%	-27.9%	34.6%	-25.1%	57.3%
Adebar Lower, 7%	-15.6%	58.8%	-48.8%	23.3%	-40.6%	34.9%
FEMA Cracked, 3%	28.9%	102.4%	-18.8%	8.9%	-16.7%	14.7%
FEMA Cracked, 7%	-20.5%	61.2%	-51.9%	10.4%	-44.4%	7.0%
FEMA Uncracked, 3%	-3.3%	76.4%	-50.9%	24.2%	-40.0%	35.1%
FEMA Uncracked, 7%	-39.3%	46.6%	-66.7%	24.8%	-50.4%	14.1%
Brown Updated Stiffness, 3%	12.8%	70.1%	-23.8%	53.0%	-21.0%	35.2%
Brown Updated Stiffness, 7%	-41.8%	37.3%	-48.1%	30.8%	-36.4%	43.4%
Doepker Updated Stiffness, 3%	-12.3%	43.1%	-27.9%	22.0%	-21.0%	35.2%
Doepker Updated Stiffness, 7%	-45.3%	26.7%	-45.8%	26.2%	-35.7%	40.7%
Uniform Period Matching	-34.1%	23.5%	-45.0%	19.6%	-38.9%	21.9%

Table 5-46: Rank of Effectiveness of Methods of Predicting the Base Moment (drifts between 0.5% and 1.0%)

Analysis Method	Conf. Sum	Rank All	Rank 3%	Rank 7%
FIB 27 (0.3), 3%	1.2	3	3	
FIB 27 (0.3), 7%	14.4	11		4
Adebar Upper, 3%	0.9	2	2	
Adebar Upper, 7%	11.1	9		2
Adebar Lower, 3%	2.2	4	4	
Adebar Lower, 7%	10.1	8		1
FEMA Cracked, 3%	7.5	7	7	
FEMA Cracked, 7%	11.3	10		3
FEMA Uncracked, 3%	6.0	6	6	
FEMA Uncracked, 7%	18.6	15		8
Brown Iterated Stiffness, 3%	0.8	1	1	
Brown Iterated Stiffness, 7%	16.5	13		6
Doepker Iterated Stiffness, (0.8), 3%	5.8	5	5	
Doepker Iterated Stiffness, (0.8), 7%	17.7	14		7
Uniform Best Fit	14.6	12	8	5

Table 5-47 and Table 5-48 provide statistics for error in maximum roof drift in the high roof drift range as well as a ranking of the methods on the basis of these data and the confidence data in Table 3-48 and Table 3-49.

In the high drift range the higher stiffness methods exhibit an unacceptably high value of average error (ranging from 54.5% for Adebar upper bound with 7% damping to 188.1% for FEMA Uncracked with 3% damping). The Adebar lower bound and FIB 27 continue to perform well with errors of -12.0% and -0.2% respectively. The updated stiffness methods perform very well in this range with Doepker yielding an average error of -0.5% and Brown with -18.5% for 3% damping.

The uniform stiffness period matching model sees again an under prediction in the base moment yielding an average error of -19.6%. This suggests the system identification damping is over damping the system.

Table 5-47: Average Error and Standard Deviation for Base Moment Predictions (drifts greater than 1.0%)

Analysis Method	Complete Data Set		Data Set Minus Ecoleader		UCSD Data Set	
	Mean	Standard Deviation	Mean	Standard Deviation	Mean	Standard Deviation
FIB 27 (0.3), 3%	-8.8%	54.0%	-0.2%	62.8%	*	*
FIB 27 (0.3), 7%	-29.0%	55.2%	-10.5%	53.8%	*	*
Adebar Upper, 3%	80.7%	72.2%	73.4%	73.5%	*	*
Adebar Upper, 7%	45.2%	71.9%	54.5%	79.3%	*	*
Adebar Lower, 3%	17.7%	69.7%	-12.0%	57.2%	*	*
Adebar Lower, 7%	-4.5%	34.1%	-15.3%	30.9%	*	*
FEMA Cracked, 3%	112.7%	85.2%	126.5%	100.2%	*	*
FEMA Cracked, 7%	81.2%	92.2%	105.6%	100.8%	*	*
FEMA Uncracked, 3%	167.5%	120.2%	188.1%	136.5%	*	*
FEMA Uncracked, 7%	46.3%	98.6%	48.1%	120.6%	*	*
Brown Updated Stiffness, 3%	34.5%	126.3%	-18.5%	49.6%	*	*
Brown Updated Stiffness, 7%	19.1%	66.8%	49.2%	52.0%	*	*
Doepker Updated Stiffness, 3%	55.9%	127.5%	-0.5%	86.3%	*	*
Doepker Updated Stiffness, 7%	25.1%	45.1%	34.2%	44.0%	*	*
Uniform Period Matching	-5.8%	35.9%	-19.6%	33.1%	*	*

* No UCSD tests were performed in this drift range

Table 5-48: Rank of Effectiveness of Methods of Predicting the Base Moment (drifts greater than 1.0%)

Analysis Method	Conf. Sum	Rank All	Rank 3%	Rank 7%
FIB 27 (0.3), 3%	3.7	2	1	
FIB 27 (0.3), 7%	11.2	8		5
Adebar Upper, 3%	30.6	12	6	
Adebar Upper, 7%	17.3	10		6
Adebar Lower, 3%	5.3	4	3	
Adebar Lower, 7%	2.8	1		1
FEMA Cracked, 3%	44.8	14	7	
FEMA Cracked, 7%	32.9	13		8
FEMA Uncracked, 3%	66.6	15	8	
FEMA Uncracked, 7%	19.2	11		7
Brown Iterated Stiffness, 3%	8.4	5	4	
Brown Iterated Stiffness, 7%	9.9	6		3
Doepker Iterated Stiffness, (0.8), 3%	16.3	9	5	
Doepker Iterated Stiffness, (0.8), 7%	10.2	7		4
Uniform Period Matching	3.9	3	2	2

Upon analysis of the error data, the following was observed for base moment prediction:

- Updated stiffness methods as well as FIB 27 all provided low average errors. FIB 27 on average fared the best. For all three methods, using 3% damping was preferred.
- Stiffer single value methods performed to varying degrees in the low and moderate drift range. The errors for these methods however increased significantly in the high drift range.
- The period matching models consistently under predict the moment in the low and moderate drift ranges. This appears to be symptomatic of over damping. The extent of the under prediction in the moderate drift range however suggests that the over damping that has been observed in most of the discussed criteria does not address the entire problem. The struggles of the period matching model in this drift range are discussed in Section 5.10 and some conclusions have bearing on the struggles of the updated stiffness models as well.

5.7 Discussion of Error Results

The following subsections discuss the error results for the three different drift ranges: low (less than 0.5% roof drift), moderate (between 0.5% and 1.0% roof drift) and high (greater than 1.0% roof drift). Each section presents observations made from the error results presented in Section 5.6 for select methods and provides recommendations on which methods proved to be most effective.

5.7.1 Review of Error Data for the Low Drift Range (<0.5% Roof Drift)

Application of elastic, effective stiffness modeling is most valuable for use in predicting response for low maximum drifts. In this response range, inelastic structural response is a minimum and elastic analysis is most appropriate. Additionally, analysis for design typically seeks to model the structure in this range because for service level loading, maximum drift will be small and because seismic design procedures have been developed on the basis of the "equal displacement" assumption in which it is assumed that for single-degree-of-freedom oscillators that have relatively long fundamental periods, as is the case for the fundamental mode of many buildings, the maximum displacement of an elastic-plastic oscillator will be approximately the same as that of an elastic oscillator with the same initial stiffness.

A review of the error data for low drift ranges (maximum roof drift of less than 0.5%) results in the following observations:

1. Use of uniform effective stiffness of $0.5E_cI_g$ or larger with 3% effective viscous damping result in large errors in predicted response quantities including max drift, roof acceleration, base shear and base moment. For example FEMA Cracked on average saw:

    - Error in Effective Period: -14.6%
    - Error in Roof Drift: -51.0%

- Error in Roof Acceleration: 54.4% (-6.9% for 7% damping)
- Error in Base Shear: -31.5%
- Error in Base Moment: -16.3%

2. Use of a uniform effective stiffness value of $0.3E_cI_g$ as prescribed by FIB 27 with 3% effective viscous damping result in relatively small errors in most response quantities. The average errors in these quantities were:

   - Error in Effective Period: 4.6%
   - Error in Roof Drift: -6.9%
   - Error in Roof Acceleration: 35.1% (-3.5% for 7% damping)
   - Error in Base Shear: -14.8%
   - Error in Base Moment: 12.6%

3. A single update of the effective stiffness using the Brown model with 3% effective viscous damping resulted in average errors in response quantities that were typically lower than stiffer methods. Average errors in some response quantities were larger than those resulting from the use of $0.3E_cI_g$.

   - Error in Effective Period: 9.3%
   - Error in Roof Drift: 20.6%
   - Error in Roof Acceleration: 38.5% (-4.4% for 7% damping)
   - Error in Base Shear: 8.2%
   - Error in Base Moment: 22.2%

4. Updating the stiffness using the Doepker model with 3% effective viscous damping resulted in average errors in response quantities that were typically lower than Brown's and in many cases lower than those resulting from the use of $0.3E_cI_g$.

   - Error in Effective Period: 5.3%
   - Error in Roof Drift: -1.0%
   - Error in Roof Acceleration: 39.0% (11.6% for 7% damping)

- Error in Base Shear: 3.6%
- Error in Base Moment: 23.1%

5. Using an effective stiffness to match the period from the system identification as well as the system identification effective damping ratio in general saw an under prediction in roof drift as well as forces and shears. This is likely symptomatic of over damping.

    - Error in Roof Drift: -19.3%
    - Error in Roof Acceleration: 11.6%
    - Error in Base Shear: -14.3%
    - Error in Base Moment: -1.9%

6. Most methods performed best in this drift range by using a 3% effective damping ratio. This level of damping provided a better prediction for roof drift, base shear and base moment than models using a 7% effective damping ratio. For prediction of the roof acceleration at the point of maximum roof drift, use of a viscous damping ratio of 7% resulted in smaller errors than the use of 3%. For example:

    - FIB 27 Roof Acceleration Error: 35.1% for 3% damping and -3.5% for 7% damping
    - Doepker Roof Acceleration Error: 39.0% for 3% damping and 11.6% for 7% damping

On the basis of the above observations, use of the FEMA Cracked model ($0.5E_cI_g$) is not recommended. Instead, use of either the FIB method ($0.3E_cI_g$) or the Doepker method is recommended. The former provides better prediction of the effective period and the base moment while the later provides better prediction of the roof drift, acceleration and base shear.

5.7.2 Review of Error Data for the Moderate Drift Range (Between 0.5% and 1.0% Roof Drift)

Response prediction for the moderate drift range (roof drifts between 0.5% and 1.0%) proved the most difficult. It is not clear if this is due to the test data or the fact that in this drift range response likely oscillates between yielding and elastic unloading and reloading.

A review of the error data for moderate drift ranges results in the following observations:

1. Use of uniform effective stiffness of $0.5E_cI_g$ or larger with 3% effective viscous damping result in large errors in predicted response quantities, particularly maximum roof drift. The roof drift errors in general increased from the low drift range, however the base shear and base moment prediction were closer. For example FEMA Cracked on average saw:

    - Error in Effective Period: -34.1%
    - Error in Roof Drift: -67.8%
    - Error in Roof Acceleration: -19.2% (-53.8% for 7% damping)
    - Error in Base Shear: -10.2%
    - Error in Base Moment: -18.8%

2. Use of a uniform effective stiffness value of $0.3E_cI_g$ as prescribed by FIB 27 with 3% effective viscous damping result in relatively small errors in most response quantities. The average errors in these quantities were:

    - Error in Effective Period: -19.3%
    - Error in Roof Drift: -13.3%
    - Error in Roof Acceleration: 3.7% (-37.4 % for 7% damping)
    - Error in Base Shear: 14.2%

- Error in Base Moment: -1.4%

3. A single update of the effective stiffness using the Brown model with 3% effective viscous damping resulted in average errors in response quantities that were typically lower than most stiffer methods; however average errors (with the exception of the error in base shear) were larger than those resulting from the use of $0.3E_cI_g$.

    - Error in Effective Period: -4.5%
    - Error in Roof Drift: -27.9%
    - Error in Roof Acceleration: -15.5% (-42.6% for 7% damping)
    - Error in Base Shear: 8.2%
    - Error in Base Moment: -23.8%

4. Updating the stiffness using the Doepker model with 3% effective viscous damping resulted in average errors in response quantities that were typically higher than those resulting from the use of $0.3E_cI_g$ and Brown's (with the exception of the base shear).

    - Error in Effective Period: -5.1%
    - Error in Roof Drift: -40.4%
    - Error in Roof Acceleration: -23.0% (-41.1% for 7% damping)
    - Error in Base Shear: -5.8%
    - Error in Base Moment: -27.9%

5. Using an effective stiffness to match the period from the system identification as well as the system identification effective damping ratio in general saw a significant under prediction of all response quantities. This is likely symptomatic of over damping as well as potentially other deleterious effects.

    - Error in Roof Drift: -49.2%
    - Error in Roof Acceleration: -37.9%

- Error in Base Shear: -15.3%
- Error in Base Moment: -45.0%

6. Unlike the low drift case, all response quantities were typically better predicted by using a 3% effective damping ratio.

7. As can be seen in observations 3 and 4, average errors in response predicted using the Brown and Doepker updated stiffness methods were much larger in the moderate drift range than any other. This could be due to the fact that these stiffness models do not do a particularly good job of fitting the experimental stiffness values in this range. Figure 5-36 highlights the updated stiffness models and data in the moderate drift range. Thus there is a tendency to over predict the stiffness.

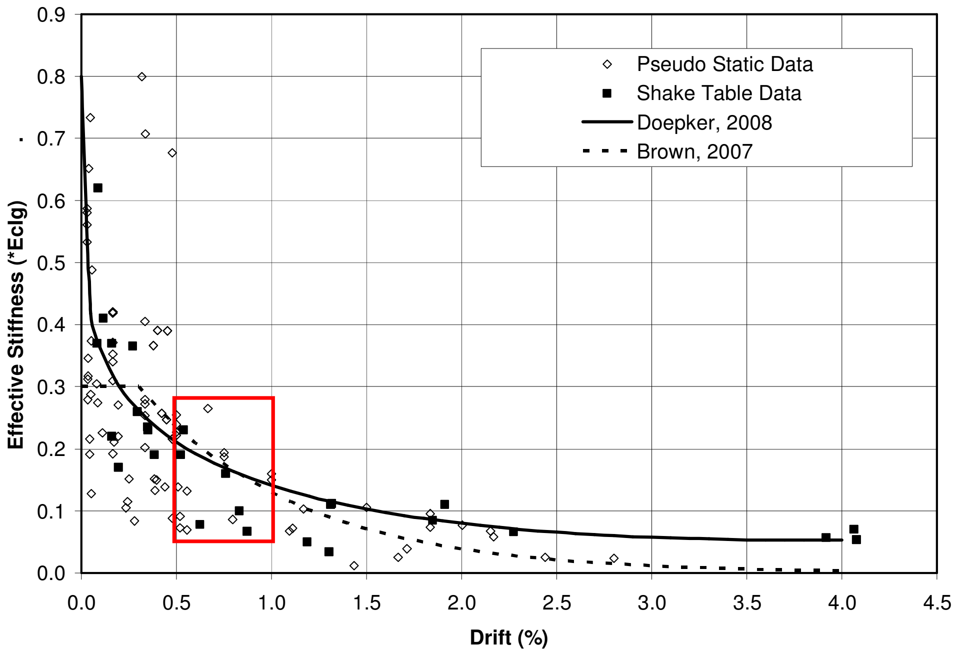

Figure 5-36: Doepker and Brown Stiffness Regressions, Entire Drift Range

As Figure 5-36 shows, in the moderate drift range there are three shake table tests whose stiffness fits well with both regressions and three that do not. When looking at these three points, the average error for roof drift for the three closest to the curves (at 0.522%, 0.540% and 0.761% roof drift) is -33.1% for Doepker and -16.5% for Brown. By contrast, the average error for roof drift for the three furthest to the curves (0.623%, 0.832% and 0.872% roof drift) is -63.9% for Brown and -71.5% for Doepker.

The following are several overarching conclusions of the various methods in the moderate drift range.

- Updated stiffness methods as well as period matching methods struggle to capture the roof drift in moderate drift ranges. FIB with 3% damping out performed all other methods with a -13.3% roof drift error.
- FIB continues to perform better for acceleration prediction (3.7% compared to -19.2% for FEMA Cracked), although updated stiffness methods perform reasonably, with errors in and around 20% (-15.5% for Brown and -23% for Doepker). While in low drift ranges the acceleration values were better captured using 7% damping, in this drift range 3% damping performs best.
- Period matching models consistently under predict the value of design quantities suggesting the possibility that using the system identification damping over damps the system.

- Updating the stiffness provides good prediction of the base shear (-5.8% for Doepker and 8.2% for Brown) and moment (-23.3% for Brown and -27.9% for Doepker), however FIB 27 performs well also (14.2% for shear and -1.4% for moment). It appears as if both updated stiffness methods struggle in this range for some design parameters. Further refinement of both equations may improve this however. This may be a topic for future work.

On the basis of the above observations, use of the FEMA Cracked model ($0.5E_cI_g$) is not recommended. The Doepker and Brown method did not perform well in this drift range. Refinement of the equations making up these methods potentially could alleviate struggles in this drift range. FIB 27 ($0.3E_cI_g$) with a 3% viscous damping ratio by contrast performs well in the moderate drift range yielding low average errors in roof drift (-13.3%), roof acceleration (3.7%), base shear (14.2%), and base moment (-1.4%).

5.7.3 Review of Error Data for the High Drift Range (>1.0% Roof Drift)

In the high drift range it is possible to estimate response quantities with acceptable accuracy using elastic effective stiffness models. After review of the data in Section 5.6, the following observations can be made:

1. Use of uniform effective stiffness of $0.5E_cI_g$ or larger with 3% effective viscous damping results in extremely large errors in all predicted response quantities. For example FEMA Cracked on average saw:

   - Error in Effective Period: -55.5%
   - Error in Roof Drift: -67.6%
   - Error in Roof Acceleration: 148.4% (112.5% for 7% damping)
   - Error in Base Shear: 154.8%
   - Error in Base Moment: 126.5%

2. Use of a uniform effective stiffness value of $0.3E_cI_g$ as prescribed by FIB 27 with 3% damping saw unacceptably large errors in roof drift and roof acceleration prediction. The model on average however still was able to predict the base shear and base moment with low average error. The average error in the high drift range was as follows:

   - Error in Effective Period: -43.1%
   - Error in Roof Drift: -79.0%
   - Error in Roof Acceleration: 54.3% (-1.9% for 7% damping)
   - Error in Base Shear: 10.2%
   - Error in Base Moment: -0.2%

3. A single update of the effective stiffness using the Brown model with 3% effective viscous damping resulted in significant improvement in roof drift prediction over $0.3E_cI_g$. This method saw low errors, though slightly larger than $0.3E_cI_g$ for base shear and base moment.

   - Error in Effective Period: 33.3%
   - Error in Roof Drift: 3.0%
   - Error in Roof Acceleration: 41.6% (71.7% for 7% damping)
   - Error in Base Shear: -10.6%
   - Error in Base Moment: -18.5%

4. Updating the stiffness using the Doepker model with 3% effective viscous damping resulted in a low average error in roof drift (though higher than Brown) and low average errors in base shear and moment. The error values in the various predicted response quantities can be seen below:

   - Error in Effective Period: 2.1%
   - Error in Roof Drift: -14.6%
   - Error in Roof Acceleration: 62.1% (57.1% for 7% damping)
   - Error in Base Shear: 7.8%
   - Error in Base Moment: -0.5%

5. Using an effective stiffness to match the period from the system identification as well as the system identification effective damping ratio in general saw an error in the roof drift higher than the updated stiffness methods. The errors in shear and moment were low, though both were higher than the two errors from the Doepker updated stiffness method. The under prediction in the roof drift is potentially due to over damping by using the system identification damping:

   - Error in Roof Drift: -30.2%
   - Error in Roof Acceleration: 43.4%
   - Error in Base Shear: 7.9%
   - Error in Base Moment: -19.6%

6. For the more effective methods, there 3% damping better predicted the acceleration for Brown's updated stiffness (41.6% versus 71.7% error). For the Doepker updated stiffness method, 7% damping performed better for acceleration prediction (62.1% versus 57.1% error). Regardless of damping ratio used, in both cases the error in acceleration was very large.

On the basis of the above observations, use of the FEMA Cracked model ($0.5E_cI_g$) is not recommended. Although FIB 27 ($0.3E_cI_g$) proved to be an accurate predictor of shear and moment, its inability to capture the roof drift at high measured roof drift demands limits its applications and is thus not recommended. All methods struggled with the roof acceleration in this drift range, which may suggest that using linear elastic analysis tools limit the ability to determine accurate story accelerations at high drift levels. The Doepker and Brown updated stiffness methods both performed well in roof drift prediction (-14.6% for Doepker and 3.0% for Brown), base shear prediction (7.8% for Doepker and -10.6% for Brown) and base moment prediction (-0.5% for Doepker and -18.5% for Brown). It is for this reason that for structures subjected to drift demands greater than 1.0% the Brown and Doepker updated stiffness methods are both recommended.

5.7.4 Recommendation by Drift Range Conclusions

The following summarizes the methods recommended for the three drift ranges:

- Low Drift Ranges: Use of either the FIB 27 method ($0.3E_cI_g$) or the Doepker method is recommended. FIB 27 provides better prediction of the effective period and the base moment while the later provides better prediction of the roof drift, acceleration and base shear.

- Moderate Drift Ranges: Updated stiffness methods struggle in the moderate drift range. Use of the FIB 27 method saw the best prediction of response quantities
- High Drift Ranges: Updated stiffness methods provide the best overall prediction of response quantities. Doepker method is recommended. The FIB 27 method provides prohibitively high errors in the roof drift.

5.8 Prediction of Response Quantities as a Function of Period Prediction

Error in estimating the fundamental period of the structure results in error in estimating other dynamic response quantities. Figure 5-37 through Figure 5-45 show the error in the roof drift, roof acceleration and base shear as a function of the error in the predicted period. This is performed for the entire data set with emphasis placed on the Doepker method. The plots correspond to a data set of all drift ranges, those points in the low drift range (less than 0.5% roof drift), and errors resulting in runs from the moderate and high drift ranges (0.5% roof drift and greater).

Figure 5-37 shows the error in the roof drift for the entire set of error data, Figure 5-38 shows the error for low drift ranges and Figure 5-39 shows error data for the moderate and high drift ranges. In looking at the data in these three plots, there appears to be a near linear correlation between the error in roof drift and the error in the predicted period. For the most part, the analyses that had a low error in the predicted period exhibited a low error in the roof drift. When looking at the low drift range data set, an error in the period prediction of +/- 10% results in a range in roof drift errors between 4.4% and 29.9%. Looking at the moderate and high drift ranges however, this range becomes larger, ranging from -45.5% to 11.4%.

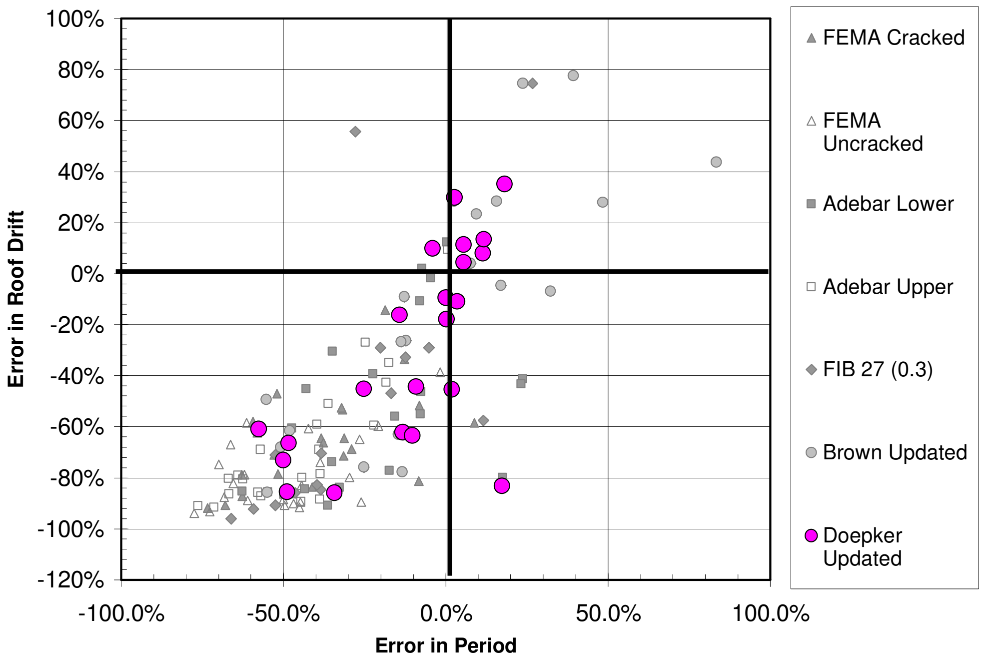

Figure 5-37: Error in Roof Drift as it Relates to Error in Period (All Drift Ranges)

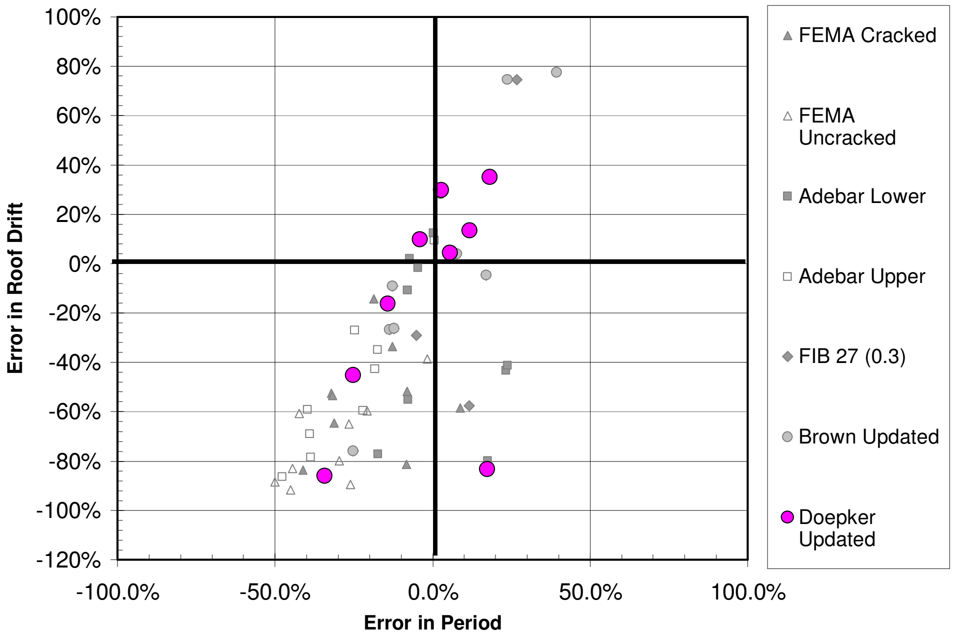

Figure 5-38: Error in Roof Drift as it Relates to Error in Period (Low Drift Range)

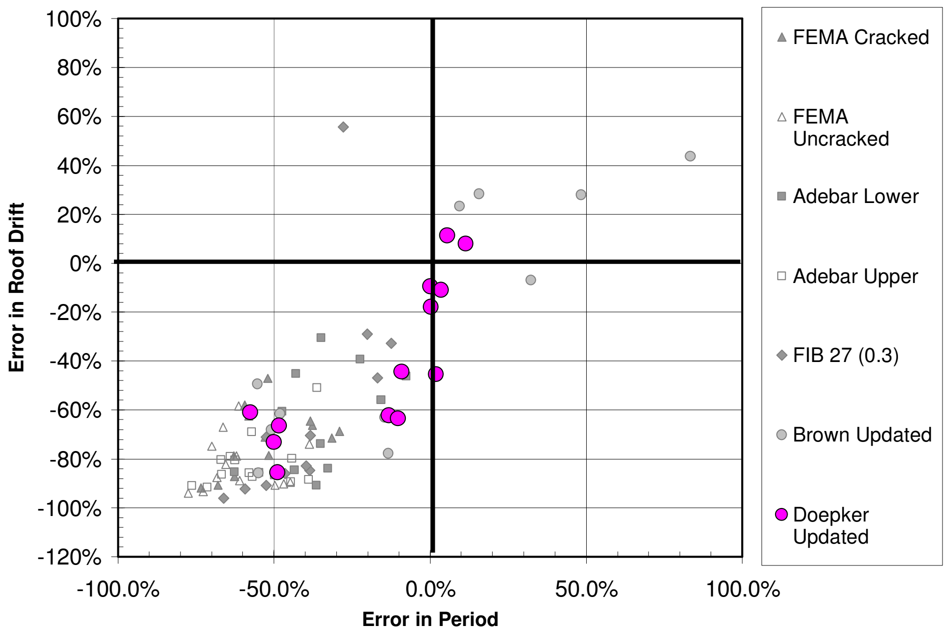

Figure 5-39: Error in Roof Drift as it Relates to Error in Period (Moderate and High Drift Ranges)

Figure 5-40 shows the error in the roof acceleration for the entire set of error data, Figure 5-41 shows the error for low drift range and Figure 5-42 shows error data for the moderate and high drift ranges. Unlike the roof drift plots, there is no linear correlation between the roof acceleration prediction and the period prediction. The plots do appear to exhibit lower errors in roof acceleration for lower errors in the predicted period, however some points perform very poorly even with good period prediction (e.g. 299.5% error in roof acceleration for 2.6% error in period).

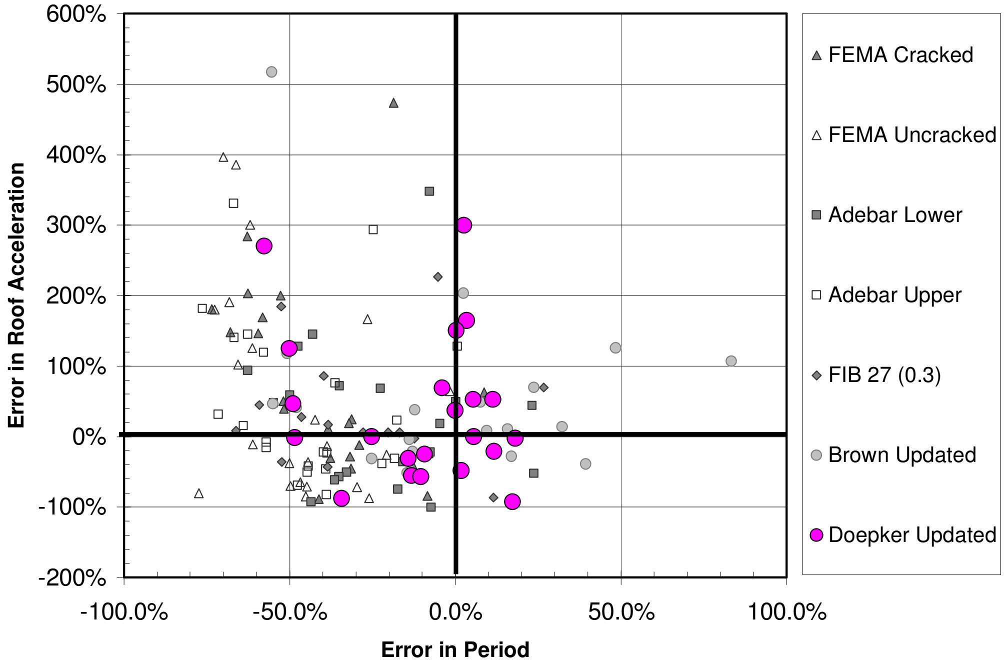

Figure 5-40: Error in Roof Acceleration as it Relates to Error in Period (All Drift Ranges)

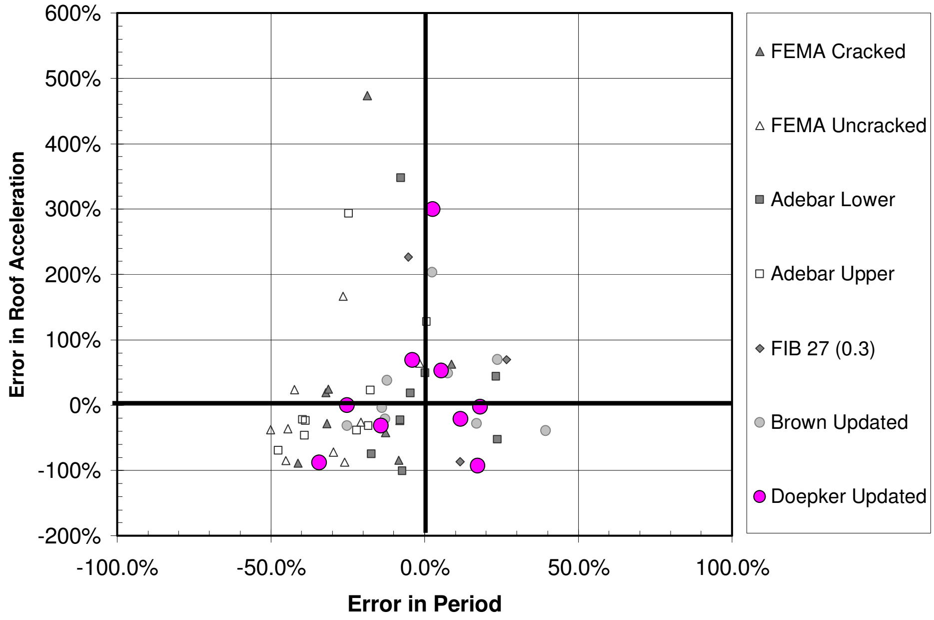

Figure 5-41: Error in Roof Acceleration as it Relates to Error in Period (Low Drift Range)

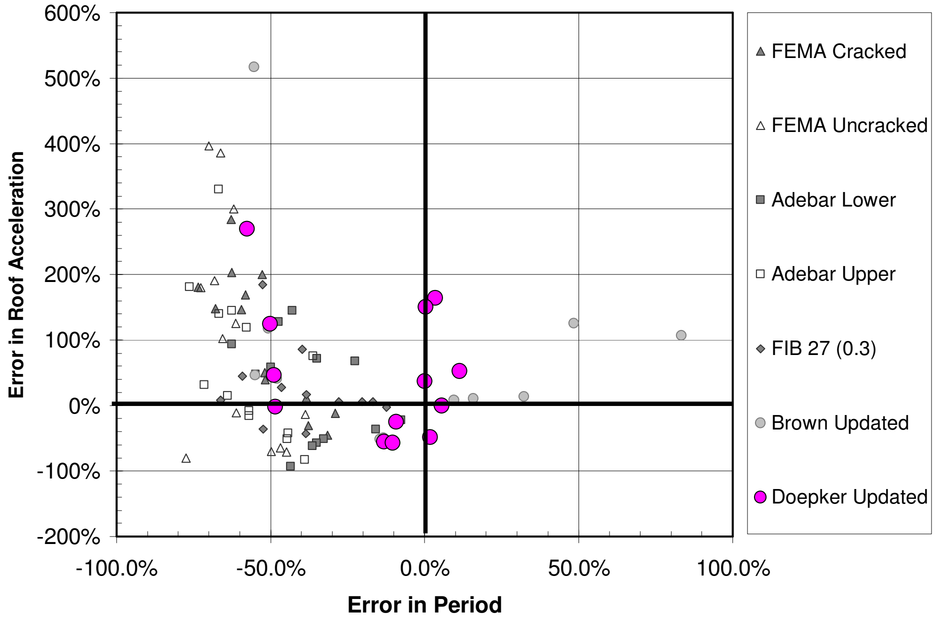

Figure 5-42: Error in Roof Acceleration as it Relates to Error in Period (Moderate and High Drift Ranges)

Figure 5-43 shows the error in the base shear for the entire set of error data, Figure 5-44 shows the error for low drift ranges and Figure 5-45 shows error data for the moderate and high drift ranges. The trend in the data closely resembles that seen in the roof acceleration errors. There is no strong correlation between the error in base shear and the error in the period. Error in the base shear is near zero for low values of error in the predicted period. For error in the predicted period of +/- 10% the error in the base shear for the low drift range ranges from -13.4% to 44.7%. For the moderate and high drift ranges, the range in error for the base shear increases to be between -79.5% and 161.4%.

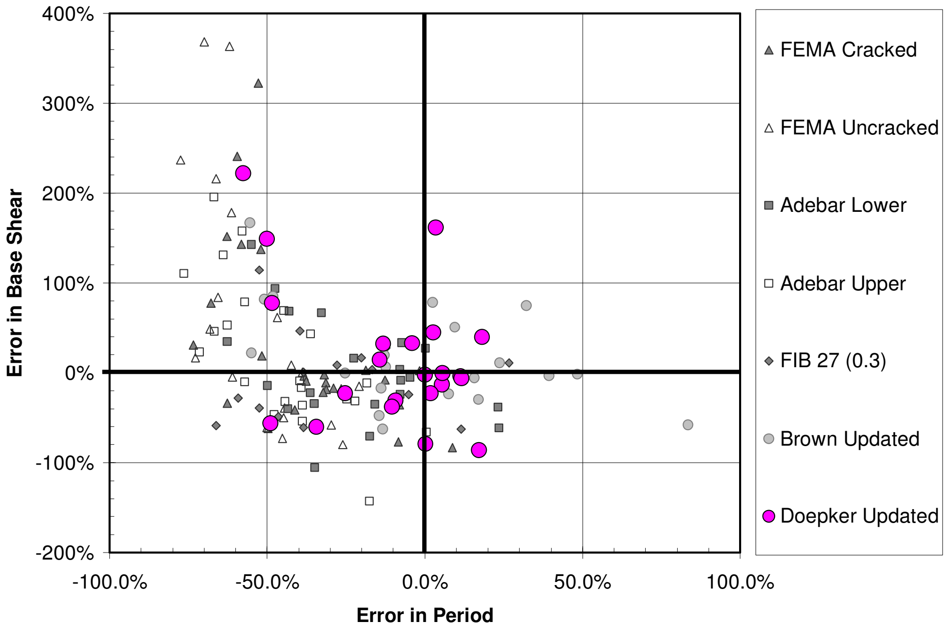

Figure 5-43: Error in Base Shear as it Relates to Error in Period (All Drift Ranges)

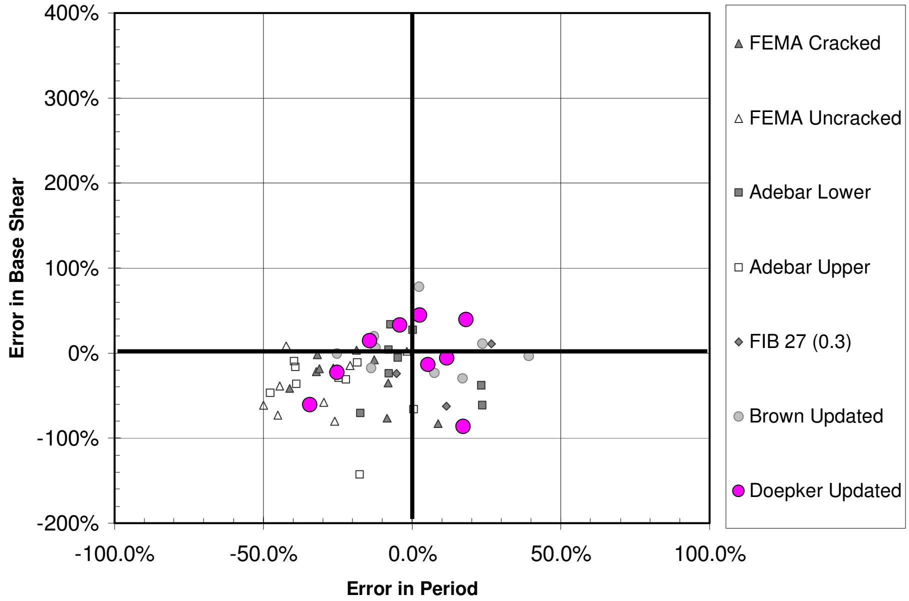

Figure 5-44: Error in Base Shear as it Relates to Error in Period (Low Drift Range)

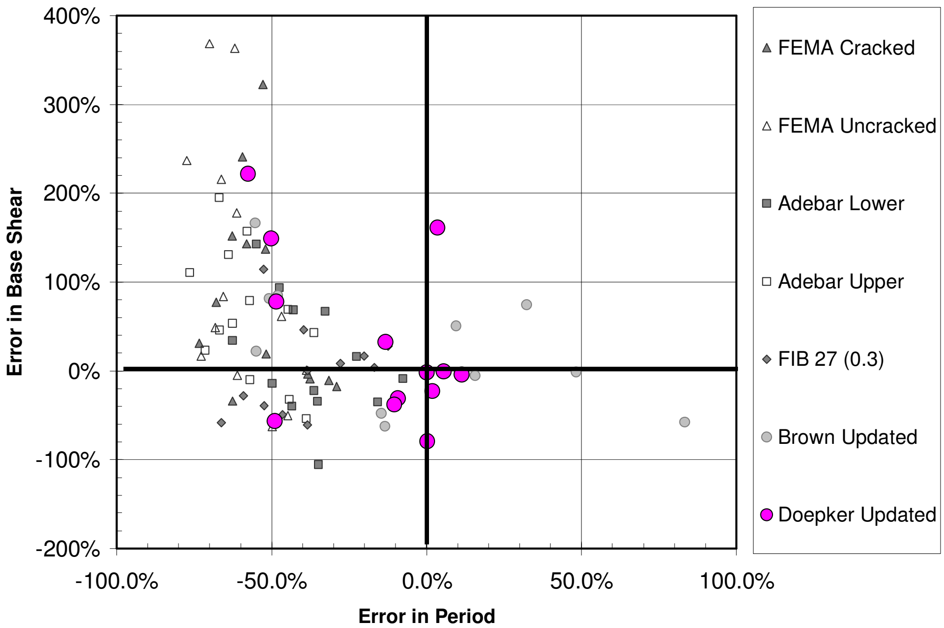

Figure 5-45: Error in Base Shear as it Relates to Error in Period (Moderate and High Drift Ranges)

From the observations made from the error plots presented above, the following conclusions may be drawn:

- Low errors in the period prediction often result in lower errors in response quantities. The error in the period is much more correlated to the error in the roof drift than other response quantities.
- Very close prediction of the period of the primary mode is not a guarantee that all response quantities will be accurately predicted. Other contributing factors include poor prediction of the effective damping, as well as damage and other factors not captured in a linear model.
- Close prediction of the period tends to result in better results in the low drift data set than in the higher drift levels. This may be due to the significant inelastic action occurring at higher drifts.

5.9 Comparison of Doepker and Brown Results

Two methods in which stiffness is a function of drift were considered as part of this research: the Brown and Doepker Updated Stiffness methods. The stiffness-drift model employed in the Doepker method was developed as part of this study by expanding the data set used by Brown to include shake table data and to produce improved prediction response. The following subsections use the previously presented error to compare these two methods.

5.9.1 Comparison of Doepker and Brown Results for Low Drift Ranges

As discussed in Chapter 2, one of the primary reasons for establishing an additional function using the same data set was the potential of Brown's function to significantly under predict the stiffness for stiffer systems. The Doepker method has a maximum stiffness of $0.8E_cI_g$ while the Brown method has a maximum stiffness of $0.3E_cI_g$. Of the tests included in the data set, there were relatively few tests that had effective stiffness (computed with the aid of the system identification) of greater than $0.3E_cI_g$. These tests were UCSD EQ 1, CAMUS 2000 Run 1, and CAMUS C-3 Stage 1. The stiffness modification factor as predicted by the two methods along with the corresponding roof drift error can be seen in Table 5-49 (stiffness predicted with 3% damping models) and Table 5-50 (stiffness predicted with 7% damping models).

The Doepker method, using 3% damping, provides a slightly better prediction for effective stiffness for the three tests. This, however, does not translate into significantly better results for prediction of the maximum roof drift.

Table 5-49: Predicted Keff for Iterative Methods and Roof Drift Errors, 3% Damping

Test	**Determined Keff**	**Brown Keff**	**Doepker Keff**	**Brown Drift Error**	**Doepker Drift Error**
UCSD: EQ 1	0.36	0.30	0.32	4.0%	4.4%
CAMUS 2000: Run 1	0.62	0.30	0.37	74.6%	35.1%
CAMUS C-3: Run 1	0.41	0.30	0.33	-4.7%	13.4%
Average Error	-	-	-	**24.6%**	**17.6%**

Table 5-50: Predicted Keff for Iterative Methods and Roof Drift Errors, 7% Damping

Test	Determined Keff	Brown Keff	Doepker Keff	Brown Drift Error	Doepker Drift Error
UCSD: EQ 1	0.36	0.30	0.34	-11.9%	-15.1%
CAMUS 2000: Run 1	0.62	0.30	0.39	-17.8%	-36.4%
CAMUS C-3: Run 1	0.41	0.30	0.42	-34.4%	-36.3%
CAMUS C-3: Run 1	0.41	0.30	0.33	-4.7%	13.4%
Average Error	-	-	-	**-21.4%**	**-29.3%**

Table 5-51, Table 5-52, Table 5-53, Table 5-54 and Table 5-55 compare the average error in the effective period, roof drift, roof acceleration, base shear and base moment for the Brown and Doepker updated stiffness methods using 3% and 7% damping for the entire data set in the low drift range.

These data show that the Doepker method provide slightly smaller errors and standard deviations if the data from the Ecoleader test program are not considered. For both, 3% damping appears to perform better for the roof drift, base shear and base moment while 7% performs better for the period and acceleration.

Table 5-51: Average Error in Effective Period for Doepker and Brown Updated Stiffness Methods, Low Drift Range

Analysis Method	Complete Data Set		Data Set Minus Ecoleader		UCSD Data Set	
	Mean	Standard Deviation	Mean	Standard Deviation	Mean	Standard Deviation
Brown Updated Stiffness, 3%	2.9%	21.0%	9.3%	19.0%	7.6%	*
Brown Updated Stiffness, 7%	0.5%	18.2%	6.3%	16.1%	7.6%	*
Doepker Updated Stiffness, 3%	-2.5%	15.6%	5.3%	11.7%	5.5%	*
Doepker Updated Stiffness, 7%	-7.8%	19.3%	-1.0%	12.4%	3.5%	*

* Standard deviation not reported because there is only one test in this range

Table 5-52: Average Error in Roof Drift for Doepker and Brown Updated Stiffness Methods, Low Drift Range

Analysis Method	Complete Data Set		Data Set Minus Ecoleader		UCSD Data Set	
	Mean	Standard Deviation	Mean	Standard Deviation	Mean	Standard Deviation
Brown Updated Stiffness, 3%	4.6%	49.3%	20.6%	41.2%	4.0%	*
Brown Updated Stiffness, 7%	-37.6%	20.6%	-32.1%	15.6%	-11.9%	*
Doepker Updated Stiffness, 3%	-15.4%	46.0%	-1.0%	40.0%	4.4%	*
Doepker Updated Stiffness, 7%	-47.9%	22.9%	-41.7%	20.3%	-15.1%	*

* Standard deviation not reported because there is only one test in this range

Table 5-53: Average Error in Roof Acceleration for Doepker and Brown Updated Stiffness Methods, Low Drift Range

Analysis Method	Complete Data Set		Data Set Minus Ecoleader		UCSD Data Set	
	Mean	Standard Deviation	Mean	Standard Deviation	Mean	Standard Deviation
Brown Updated Stiffness, 3%	25.9%	77.1%	38.5%	83.9%	48.3%	*
Brown Updated Stiffness, 7%	-11.9%	77.9%	-4.4%	87.5%	13.4%	*
Doepker Updated Stiffness, 3%	20.5%	117.9%	39.0%	126.9%	52.8%	*
Doepker Updated Stiffness, 7%	-0.1%	84.6%	11.6%	90.9%	16.1%	*

* Standard deviation not reported because there is only one test in this range

Table 5-54: Average Error in Base Shear for Doepker and Brown Updated Stiffness Methods, Low Drift Range

Analysis Method	Complete Data Set		Data Set Minus Ecoleader		UCSD Data Set	
	Mean	Standard Deviation	Mean	Standard Deviation	Mean	Standard Deviation
Brown Updated Stiffness, 3%	4.4%	32.1%	8.2%	35.6%	-23.7%	*
Brown Updated Stiffness, 7%	-37.5%	21.3%	-35.4%	21.0%	-28.5%	*
Doepker Updated Stiffness, 3%	-6.5%	45.2%	3.6%	45.5%	-13.4%	*
Doepker Updated Stiffness, 7%	-35.7%	21.6%	-32.6%	22.1%	-18.2%	*

* Standard deviation not reported because there is only one test in this range

Table 5-55: Average Error in Base Moment for Doepker and Brown Updated Stiffness Methods, Low Drift Range

Analysis Method	Complete Data Set		Data Set Minus Ecoleader		UCSD Data Set	
	Mean	Standard Deviation	Mean	Standard Deviation	Mean	Standard Deviation
Brown Updated Stiffness, 3%	9.7%	80.7%	22.2%	87.2%	-9.3%	*
Brown Updated Stiffness, 7%	-33.3%	45.8%	-31.6%	50.9%	-21.3%	*
Doepker Updated Stiffness, 3%	9.8%	79.6%	23.1%	85.2%	-3.9%	*
Doepker Updated Stiffness, 7%	-28.4%	35.3%	-25.0%	37.4%	-16.7%	*

* Standard deviation not reported because there is only one test in this range

Given the limited data set, and the closeness of these results, it is inconclusive as to whether the method introduced in this thesis provides much of an advantage for low drift ranges.

5.9.2 Comparison of Doepker and Brown Results for Moderate Drift Ranges

Table 5-56, Table 5-57, Table 5-58, Table 5-59 and Table 5-60 compare the average error in the effective period, roof drift, roof acceleration, base shear and base moment for the Brown and Doepker updated stiffness methods in the moderate drift range.

The results in the moderate drift range are again varied, and in many cases both updated stiffness methods struggled in this range for reasons as discussed when this was first introduced in Section 5.6 and elaborated upon in 5.7.2. In this case, the updated stiffness methods performed best with 3% damping for all investigated parameters.

The Doepker method out performs Brown for only the base shear, while Brown performs slightly better at predicting the effective period, roof drift, roof acceleration and base moment.

Table 5-56: Average Error in Effective Period for Doepker and Brown Updated Stiffness Methods, Moderate Drift Range

Analysis Method	Complete Data Set		Data Set Minus Ecoleader		UCSD Data Set	
	Mean	Standard Deviation	Mean	Standard Deviation	Mean	Standard Deviation
Brown Updated Stiffness, 3%	-19.5%	24.8%	-4.5%	11.4%	-6.6%	9.3%
Brown Updated Stiffness, 7%	-24.7%	21.2%	-11.8%	8.9%	-12.3%	8.8%
Doepker Updated Stiffness, 3%	-19.6%	23.2%	-5.1%	7.2%	-6.6%	9.3%
Doepker Updated Stiffness, 7%	-24.6%	21.6%	-11.1%	6.6%	-10.4%	8.0%

Table 5-57: Average Error in Roof Drift for Doepker and Brown Updated Stiffness Methods, Moderate Drift Range

Analysis Method	Complete Data Set		Data Set Minus Ecoleader		UCSD Data Set	
	Mean	Standard Deviation	Mean	Standard Deviation	Mean	Standard Deviation
Brown Updated Stiffness, 3%	-40.2%	37.9%	-27.9%	42.3%	-35.9%	37.3%
Brown Updated Stiffness, 7%	-70.4%	22.6%	-63.0%	23.7%	-54.2%	34.7%
Doepker Updated Stiffness, 3%	-52.3%	25.9%	-40.4%	22.1%	-35.9%	37.3%
Doepker Updated Stiffness, 7%	-70.1%	22.8%	-60.4%	21.7%	-52.1%	33.7%

Table 5-58: Average Error in Roof Acceleration for Doepker and Brown Updated Stiffness Methods, Moderate Drift Range

Analysis Method	Complete Data Set		Data Set Minus Ecoleader		UCSD Data Set	
	Mean	Standard Deviation	Mean	Standard Deviation	Mean	Standard Deviation
Brown Updated Stiffness, 3%	16.1%	65.0%	-15.5%	45.5%	-9.3%	65.3%
Brown Updated Stiffness, 7%	-31.6%	46.4%	-42.6%	41.8%	-25.2%	58.2%
Doepker Updated Stiffness, 3%	-8.0%	42.9%	-23.0%	42.0%	-9.3%	65.3%
Doepker Updated Stiffness, 7%	-37.1%	36.6%	-41.1%	41.5%	-23.4%	62.6%

Table 5-59: Average Error in Base Shear for Doepker and Brown Updated Stiffness Methods, Moderate Drift Range

Analysis Method	Complete Data Set		Data Set Minus Ecoleader		UCSD Data Set	
	Mean	Standard Deviation	Mean	Standard Deviation	Mean	Standard Deviation
Brown Updated Stiffness, 3%	33.2%	51.1%	8.2%	43.2%	15.1%	24.4%
Brown Updated Stiffness, 7%	-21.2%	52.3%	-11.7%	58.0%	31.8%	44.3%
Doepker Updated Stiffness, 3%	-0.4%	48.5%	-5.8%	28.2%	15.1%	24.4%
Doepker Updated Stiffness, 7%	-24.6%	48.2%	-10.6%	52.2%	29.1%	43.3%

Table 5-60: Average Error in Base Moment for Doepker and Brown Updated Stiffness Methods, Moderate Drift Range

Analysis Method	Complete Data Set		Data Set Minus Ecoleader		UCSD Data Set	
	Mean	Standard Deviation	Mean	Standard Deviation	Mean	Standard Deviation
Brown Updated Stiffness, 3%	12.8%	70.1%	-23.8%	53.0%	-21.0%	35.2%
Brown Updated Stiffness, 7%	-41.8%	37.3%	-48.1%	30.8%	-36.4%	43.4%
Doepker Updated Stiffness, 3%	-12.3%	43.1%	-27.9%	22.0%	-21.0%	35.2%
Doepker Updated Stiffness, 7%	-45.3%	26.7%	-45.8%	26.2%	-35.7%	40.7%

Given the overall difficulties for both methods in the moderate drift range, it is hard to generalize these results; however it appears as if Brown is the superior method for expected levels of excitation of between 0.5% and 1.0%.

5.9.3 Comparison of Doepker and Brown Results for High Drift Ranges

Table 5-61, Table 5-62, Table 5-63, Table 5-64 and Table 5-65 compare the average error in the effective period, roof drift, roof acceleration, base shear and base moment for the Brown and Doepker updated stiffness methods for the data set in the high drift range.

Again, the results in this drift range appear split. When looking at the data set that subtracts the Ecoleader results, 3% continues to be the damping value of choice. The Doepker method better predicts the period, the base shear and the base moment, while Brown's equation better predicts the roof drift and acceleration. A portion of why Brown's method appears to slightly out perform Doepker is the absence of a bottom cap for the Brown method. Several of these models exhibited extremely low stiffnesses (less than $0.5E_cI_g$) that may be unrealistic in a full scale building complete with stiffening non structural elements.

Table 5-61: Average Error in Effective Period for Doepker and Brown Updated Stiffness Methods, High Drift Range

Analysis Method	Complete Data Set		Data Set Minus Ecoleader		UCSD Data Set	
	Mean	Standard Deviation	Mean	Standard Deviation	Mean	Standard Deviation
Brown Updated Stiffness, 3%	8.0%	52.3%	33.3%	36.1%	*	*
Brown Updated Stiffness, 7%	-16.5%	41.2%	1.6%	33.3%	*	*
Doepker Updated Stiffness, 3%	-13.9%	28.2%	2.1%	8.1%	*	*
Doepker Updated Stiffness, 7%	-30.3%	20.1%	-19.0%	7.0%	*	*

Table 5-62: Average Error in Roof Drift for Doepker and Brown Updated Stiffness Methods, High Drift Range

Analysis Method	Complete Data Set		Data Set Minus Ecoleader		UCSD Data Set	
	Mean	Standard Deviation	Mean	Standard Deviation	Mean	Standard Deviation
Brown Updated Stiffness, 3%	-17.1%	53.7%	3.0%	48.8%	*	*
Brown Updated Stiffness, 7%	-39.1%	45.0%	-16.3%	27.4%	*	*
Doepker Updated Stiffness, 3%	-29.6%	35.6%	-14.6%	30.0%	*	*
Doepker Updated Stiffness, 7%	-50.3%	30.8%	-34.8%	19.1%	*	*

Table 5-63: Average Error in Roof Acceleration for Doepker and Brown Updated Stiffness Methods, High Drift Range

Analysis Method	Complete Data Set		Data Set Minus Ecoleader		UCSD Data Set	
	Mean	Standard Deviation	Mean	Standard Deviation	Mean	Standard Deviation
Brown Updated Stiffness, 3%	110.2%	189.0%	41.6%	72.8%	*	*
Brown Updated Stiffness, 7%	44.7%	61.4%	71.7%	49.2%	*	*
Doepker Updated Stiffness, 3%	100.7%	110.4%	62.1%	95.4%	*	*
Doepker Updated Stiffness, 7%	42.7%	99.0%	57.1%	116.4%	*	*

Table 5-64: Average Error in Base Shear for Doepker and Brown Updated Stiffness Methods, High Drift Range

Analysis Method	Complete Data Set		Data Set Minus Ecoleader		UCSD Data Set	
	Mean	Standard Deviation	Mean	Standard Deviation	Mean	Standard Deviation
Brown Updated Stiffness, 3%	19.3%	80.1%	-10.6%	55.5%	*	*
Brown Updated Stiffness, 7%	27.7%	79.8%	65.7%	56.9%	*	*
Doepker Updated Stiffness, 3%	58.5%	116.3%	7.8%	91.5%	*	*
Doepker Updated Stiffness, 7%	31.0%	57.9%	53.8%	50.9%	*	*

Table 5-65: Average Error in Base Moment for Doepker and Brown Updated Stiffness Methods, High Drift Range

Analysis Method	Complete Data Set		Data Set Minus Ecoleader		UCSD Data Set	
	Mean	Standard Deviation	Mean	Standard Deviation	Mean	Standard Deviation
Brown Updated Stiffness, 3%	34.5%	126.3%	-18.5%	49.6%	*	*
Brown Updated Stiffness, 7%	19.1%	66.8%	49.2%	52.0%	*	*
Doepker Updated Stiffness, 3%	55.9%	127.5%	-0.5%	86.3%	*	*
Doepker Updated Stiffness, 7%	25.1%	45.1%	34.2%	44.0%	*	*

5.9.4 Doepker and Brown Comparison Conclusions

In directly comparing the two updated stiffness methods, both methods perform comparably. As such, both methods would be recommended for use in practice.

5.10 Sources of Error for Period Matching Models

One would expect that the period matching models would provide the most accurate prediction of response in comparison with other methods. However, as was repeatedly seen in Section 5.6 and 5.7, that was not the case. It was hypothesized that this was due to the fact that the system identification provided the period and damping ratio to best fit the entire record and not the true point of maximum roof drift. Furthermore, upon looking at comparisons of simulated roof displacement time histories with measured roof displacement time histories, it appears as if the damping determined for the system identification was often greater than what occurred in reality.

In particular, system identification appeared to result in damping values that were too large to provide accurate prediction of response quantities. For some tests, the period matching stiffness models were analyzed using 3% and 7% damping in addition to the damping obtained from the system identification. Error results from these analyses suggested that in some cases using 3% or 7% would improve results. The following sections investigated different values of damping for use with system identification stiffness.

5.10.1 Comparison of System Identification Damping with 3% and 7% Damping

In order to evaluate the role damping plays in enabling accurate prediction of response using the stiffness of the period matching models, several test programs were analyzed using the period matching stiffness with 3% and 7% modal damping in addition to the damping value obtained from the system identification. UCSD, CAMUS C Specimen 1 and CAMUS 2000 were selected as suitable specimens to focus on because these three specimens had the highest confidence ratings.

The average resulting errors in response quantities are summarized in Table 5-66, Table 5-67, Table 5-68 and Table 5-69.

Table 5-66: Average Error in Roof Drift for Uniform Period Matching Models with Different Damping, UCSD, CAMUS C-1, and CAMUS 2000, All Drift Ranges

Analysis Method	Mean Error	Standard Deviation
Uniform Period Matching	-26.1%	18.5%
Uniform Period Matching, 3%	-0.1%	21.1%
Uniform Period Matching, 7%	-21.9%	16.8%

Table 5-67: Average Error in Roof Acceleration for Uniform Period Matching Models with Different Damping, UCSD, CAMUS C-1, and CAMUS 2000, All Drift Ranges

Analysis Method	Mean Error	Standard Deviation
Uniform Period Matching	16.1%	60.8%
Uniform Period Matching, 3%	51.0%	64.2%
Uniform Period Matching, 7%	26.4%	87.6%

Table 5-68: Average Error in Base Shear for Uniform Period Matching Models with Different Damping, UCSD, CAMUS C-1, and CAMUS 2000, All Drift Ranges

Analysis Method	Mean Error	Standard Deviation
Uniform Period Matching	-9.3%	26.1%
Uniform Period Matching, 3%	8.0%	23.5%
Uniform Period Matching, 7%	-10.5%	22.6%

Table 5-69: Average Error in Base Moment for Uniform Period Matching Models with Different Damping, UCSD, CAMUS C-1, and CAMUS 2000, All Drift Ranges

Analysis Method	Mean Error	Standard Deviation
Uniform Period Matching	-15.6%	38.0%
Uniform Period Matching, 3%	14.9%	25.8%
Uniform Period Matching, 7%	-6.7%	34.5%

These data support several conclusions:

- The damping ratio has a significant impact on the predicted response. Choosing the correct damping ratio is essential to minimize error in predicted response quantities.
- The system identification damping is not the best damping to use for prediction of all response quantities. Using this for the damping ratio typically under predicted the roof drift, base shear, base moment, all of which indicated that the system identification damping is too large. This is supported by the following observations
    - Using a lower damping ratio reduces the error in the maximum roof drift.
    - Using a lower damping ratio reduces the error in the base shear and moment, yet by a less significant effect.

The hypothesis that the system identification damping over damps the system is discussed in the following subsections, first the investigation in potential higher mode effects (5.10.2) as well as investigation in the so called “Zero Error Damping” (5.10.3).

5.10.2 Investigation into Higher Order Mode Effects

The system identification damping provides the period and damping experienced for the primary mode. For lack of better information, this damping value was applied for all modes. However, this could potentially result in over damping of the secondary modes of vibration. To test this hypothesis, an analysis was performed using the period matching stiffness, the system identification damping applied only to the primary mode, and a damping ratio of 3% for all other modes.

This approach was used to analyze the UCSD wall because higher mode effects were expected to be most significant for this wall due to its slenderness as well as the high number of slabs and other complicating structural features. The EQ 3 motion was selected because the system identification damping of 18.01% was extremely high and thus application of this damping ratio in all modes was most likely to result in over damping of higher modes. The error results for the system identification damping and reduced higher mode damping approaches are show in Table 5-70.

Table 5-70: Difference in Errors for UCSD EQ 3 Run with System I.D. Damping versus System I.D. Damping for Primary Mode and 3% for All Others

	System I.D. Damping	**System I.D. Damping for Primary Mode, 3% All Others**
Error in Roof Drift	-57.2%	-57.4%
Error in Roof Acceleration	-45.2%	-49.4%
Error in Base Shear	48.5%	45.6%
Error in Base Moment	-54.4%	-53.9%

As can be seen, there was no significant change in the response quantity errors. Thus, over damping of higher modes is not the cause of the large errors resulting from the use of the system identification damping.

5.10.3 Investigation into "Zero Error" Damping

For several of the specimens (UCSD, CAMUS 2000, and CAMUS C-1), analyses were run using the system identification damping, as well as the common values of 3% and 7%. These results were used to predict a damping value that would result in zero error in maximum drift. The linear fit to the drift error data for UCSD EQ 1 shows how this was done. The point of intersection at zero error was termed as the "Zero Error" value of damping.

In some cases this methodology resulted in negative values for damping as seen in Figure 5-47. The "Zero Error" damping values are summarized alongside those from the original system identification damping in Table 5-71. Further regression plots in the "Zero Error" analysis can be seen in Appendix B. In all of the cases, the zero error damping was determined to be less than the damping determined from the system identification. This agrees with the trend seen in the error results first discussed in section 5.6 where the simulated results appeared to be over damped. It is interesting to note however that the zero error damping for UCSD appears to decrease with demand, while the damping increases for CAMUS 2000 and there is no clear trend for CAMUS C-1.

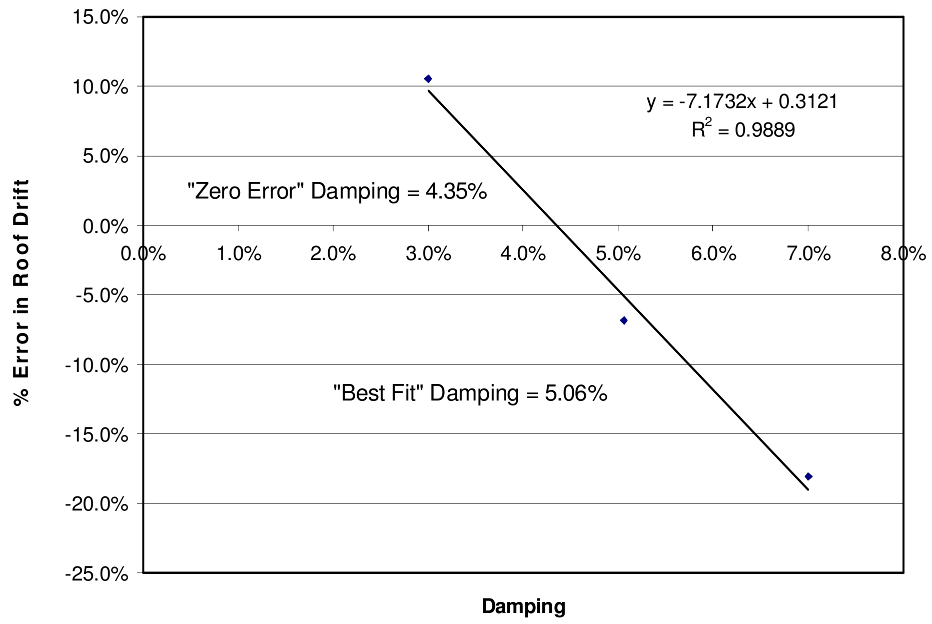

Figure 5-46: UCSD EQ 1 – Error in Roof Drift with Respect to Damping

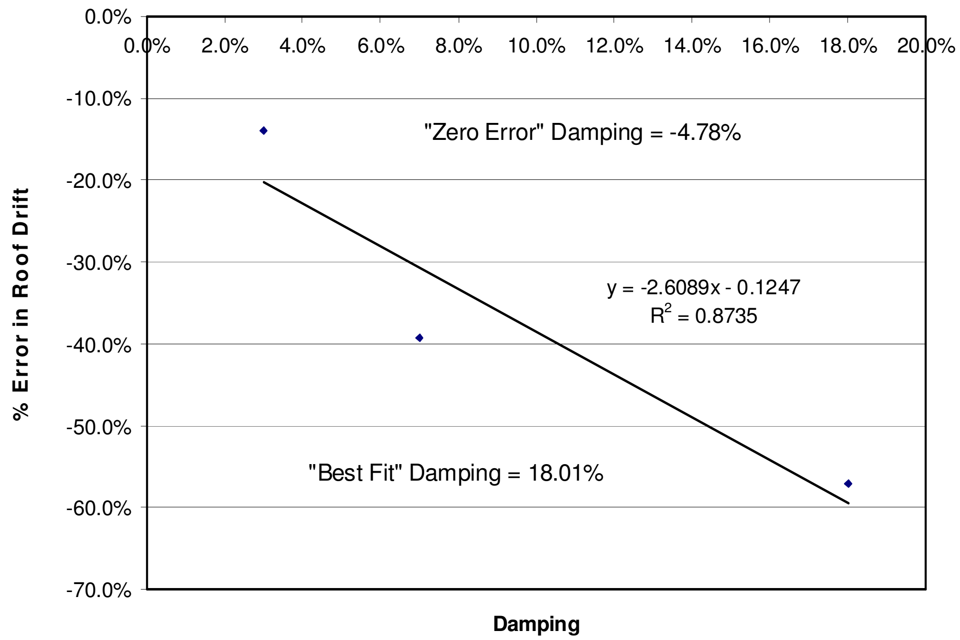

Figure 5-47: UCSD EQ 3 – Error with Respect to Damping

Table 5-71: Zero Error Damping As Determined for UCSD, CAMUS 2000 and CAMUS C-1 Tests

Test	Drift	System I.D. Damping	Zero Error Damping
UCSD EQ 1 *	0.271%	5.06%	4.35%
UCSD EQ 2	0.761%	8.75%	0.74%
UCSD EQ 3	0.832%	18.01%	-4.78%
CAMUS 2000 Run 1	0.088%	6.90%	-46.61%
CAMUS 2000 Run 2	0.296%	15.00%	3.45%
CAMUS 2000 Run 3	0.384%	15.00%	11.48%
CAMUS C-1 Stage 1 *	0.352%	8.36%	6.15%
CAMUS C-1 Stage 2	0.522%	5.26%	2.86%
CAMUS C-1 Stage 3 *	1.313%	6.72%	7.90%
CAMUS C-1 Stage 4	1.849%	13.19%	-5.61%

* Refers to tests selected for analysis with the “zero error damping”

UCSD EQ 1, CAMUS C-1 Stage 1 and CAMUS C-1 Stage 3 were selected for additional analysis using the zero error damping. These were selected because the resulting damping value was a sensible positive integer that was sufficiently different from the system identification damping as well as from 3% and 7%. Table 5-72, Table 5-73 and Table 5-74 show the change in the errors in roof drift, roof acceleration, base shear and base moment when using the zero error damping.

In all cases, the absolute value of the error in roof drift decreases. However, the change in the errors for the other response data is mixed. Ultimately, these results suggest that the damping obtained from the system identification may not be a fair representation of the damping experienced at the point of maximum roof drift.

Table 5-72: Comparison in Errors for UCSD EQ 1, System I.D. Damping versus Zero Error Damping

	System I.D. Damping	Zero Error Damping
Error in Roof Drift	-6.8%	-1.6%
Error in Roof Acceleration	28.1%	35.1%
Error in Base Shear	0.8%	6.0%
Error in Base Moment	-3.0%	2.3%

Table 5-73: Comparison in Errors for CAMUS C-1 Stage 1, System I.D. Damping versus Zero Error Damping

	System I.D. Damping	**Zero Error Damping**
Error in Roof Drift	-21.0%	-3.6%
Error in Roof Acceleration	-34.7%	-28.8%
Error in Base Shear	-21.2%	-3.8%
Error in Base Moment	-28.5%	-12.8%

Table 5-74: Comparison in Errors for CAMUS C-1 Stage 3, System I.D. Damping versus Zero Error Damping

	System I.D. Damping	**Zero Error Damping**
Error in Roof Drift	5.8%	1.1%
Error in Roof Acceleration	-5.7%	-10.1%
Error in Base Shear	7.9%	3.0%
Error in Base Moment	-1.3%	-5.7%

5.10.4 Investigation into "Zero Error" Damping

Analysis of the results suggest that using the damping obtained from the system identification is resulting in an over damping of the system. This could be due to the methodology in the system identification.

5.11 Discussion of All Drift Ranges

The following summarizes observations made about the various methods investigated in this study and presents conclusions and recommendations regarding their use in practice.

Most existing methods over predict the stiffness. FEMA Cracked ($0.5E_cI_g$) was identified as the stiffness most commonly used in an informal survey of consulting engineers, and even after subtracting out the Ecoleader results, this study found this method to provide unacceptably large errors in many response quantities, particularly roof drifts. As such, this stiffness is not recommended. More specifically, using a 3% viscous damping ratio, this study found this method:

- Does a poor job at predicting the roof acceleration for all drift levels. In all cases the standard deviation of the data was extremely high suggesting a difficulty in accurate prediction of the acceleration.
- Does a poor job overall at predicting roof displacements in all drift ranges (errors of -51.0%, -67.8%, and -67.6% for low, moderate and high drift ranges respectively).
- Does a moderate to good job in low and moderate drift ranges at predicting base shear forces (errors of -31.5% and -10.2% respectively) and base moments (-16.3% and -18.8%).
- Does a very poor job in high drift ranges at predicting the base shear and the base moment (154.8% and 126.5% respectively).
- **Conclusion:** The stiffness of $0.5E_cI_g$ or higher is not recommended.

FIB 27 prescribes the use of $0.3E_cI_g$, which is significantly lower than the $0.5E_cI_g$ commonly used. This drastically improved the results, and was able to provide acceptable average errors (absolute value of error less than 20%) for low (less than 0.5% roof drift) and moderate (between 0.5% and 1.0% roof drift) drift levels. This method however struggled for drifts greater than 1.0%. Were a single method to be used, and the building in question was not expected to be subjected to drifts greater than 1.0%, this stiffness method seems a quick and simple prediction. Upon eliminating the Ecoleader data, and using a 3% viscous damping ratio, this study found this effective stiffness:

- Does a poor job at predicting the roof acceleration for all drift levels. In all cases the standard deviation of the data was extremely high suggesting a difficulty in accurate prediction of the acceleration.
- Does a good job at predicting the design quantities in low and moderate drift ranges:
    - Roof drift: errors of -6.9% and -13.3% respectively
    - Base shear: errors of -14.8% and 14.2% respectively
    - Base moment: errors of 12.6% and -1.4% respectively
- Does a poor job at predicting the roof drift in the high drift range (-79.0% error)
- Does a good job in high drift ranges at predicting the base shear (10.2%) and base moment (-0.2%).

- **Conclusion:** Use of $0.3E_cI_g$ for the effective stiffness is recommended for low and moderate drift ranges. It however yields unacceptably large errors in the roof drift for roof drift demands greater than 1.0%.

A single update of the stiffness using the Brown and Doepker regressions yielded results of similar accuracy as the FIB 27 stiffness for low drift ranges (less than 0.5% roof drift). The methods struggled with roof drift in the moderate drift range (between 0.5% and 1.0% roof drift), yet proved the most effective methods in the high drift range (greater than 1.0% roof drift). Upon eliminating the Ecoleader data, and using a 3% viscous damping ratio, this study found this effective stiffness:

- Does a poor job at predicting the roof acceleration for all drift levels. In all cases the standard deviation of the data was extremely high suggesting a difficulty in accurate prediction of the acceleration.
- Provides a good prediction of analysis quantities for low drift ranges:
    - Roof drift: -1.0% error for Doepker and 20.6% for Brown
    - Base shear: 3.6% error for Doepker and 8.2% for Brown
    - Base moment: 23.1% error for Doepker and 22.2% for Brown
- Provides for a poor prediction of roof drift and modest prediction of base shear and base moment in moderate drift ranges
    - Roof drift: -40.4% error for Doepker and -27.9% for Brown
    - Base shear: -5.8% error for Doepker and 8.2% for Brown

    - Base moment: -27.9% error for Doepker and -23.8% for Brown
- **Conclusion:** Struggles of updated stiffness methods in intermediate range suggest a need to revise the two functions to perform better in this range.
- Provides for a good prediction of analysis quantities for high drift ranges
    - Roof drift: -14.6% error for Doepker and 3.0% for Brown
    - Base shear: 7.8% error for Doepker and -10.6% for Brown
    - Base moment: -0.5% error for Doepker and -18.5% for Brown
- **Conclusion:** Use of the updated stiffness methods is recommended as an alternative for using $0.3E_cI_g$ in low drift ranges. It is the only recommended stiffness method in high drift ranges. Revision of the functions to better fit experimental data in the moderate drift range is recommended before this method is recommended for all roof drift demands.

Models using a period matching stiffness with a viscous damping ratio obtained from a system identification often times under predict design quantities for all drift ranges.

- For low, moderate and high drift ranges, the method in general under predicted analysis quantities. The following levels of error were observed:
    - Roof drift: errors of -19.3%, -49.2% and -30.2% respectively
    - Base shear: errors of -14.3%, -15.5% and 7.9% respectively
    - Base moment: errors of -1.9%, -45.0% and -19.6% respectively

- **Conclusion:** The viscous damping ratio obtained from the system identification over damps the system resulting in a decrease in the simulated roof drift, base shear and base moment.

Chapter 6: Summary, Conclusions and Recommendations

An on-going research project sponsored by the National Science Foundation and led by researchers at the University of Washington is investigating the behavior, analysis and design of slender reinforced concrete walls with complex configurations. These types of walls are the lateral load resisting systems in most mid- to high-rise buildings constructed on the West Coast. The results of elastic analysis provide the basis for the design of most of these walls.

The study documented in this thesis was undertaken as part of the on-going project to investigate the accuracy of previously proposed and newly developed methods for predicting the fundamental period of walled buildings and the effective stiffness and viscous damping ratio used in elastic, dynamic analysis of walls. The results of shake table tests of concrete walls were used as a basis for evaluating the methods. The results of this study include improved understanding of the error resulting from the use of these methods in building response quantities used typically in design, such as maximum roof drift, roof acceleration, base shear and base moment. The results of this study also include recommendations for modeling walls for dynamic, elastic analysis to support seismic design.

6.1 Summary of Research Activities

The following summarizes the research process that culminated in a set of recommendations for modeling walls for dynamic, elastic analysis to support seismic design.

Chapter 2 presents the results of an initial review of previous research to indentify methods for defining the fundamental period of walled buildings as well as the effective stiffness and the viscous damping ratio used for elastic dynamic analysis of concrete walls. A total of three methods for defining the fundamental period, ten methods for defining effective stiffness and three methods for defining effective viscous damping ratio were identified. The approach of the methods defining the period, effective stiffness and effective viscous damping ratio varied. Stiffness methods such as those prescribed in FEMA 356 provided recommendations regardless of performance. Methods such as that described by Newmark and Hall as well as FEMA 450, provided estimates of the fundamental period based on wall geometry. Other methods such as the FEMA 440 methods for predicting period and viscous damping along with the Brown stiffness method used performance based approaches.

Previous research conducted at the University of Washington as part of the on-going NSF-sponsored research project used data from pseudo-static laboratory tests to develop a dataset defining the effective flexural stiffness of a concrete wall as a function of maximum roof drift demand. As part of the study documented here, these data were extended using shake-table data and a new model defining effective stiffness as a function of roof drift was developed. Additionally, a method for employing this model to define the effective stiffness of a concrete wall was developed in which the results of an initial elastic, dynamic analysis are used to estimate the maximum roof drift demand. This demand is then used to update the model and to determine an effective stiffness. Based on a preliminary review of the methods, a reduced set of six stiffness methods were used. These used one selected method for estimating the viscous damping ratio. No period estimating methods were extensively investigated.

Chapter 3 presents the concrete wall, shake table test data used in this study. A review of the literature resulted in identification of four test programs conducted at three sites around the world. It is believed that the literature review was comprehensive and that additional shake table data for concrete walls do not exist. The tests included H-, C- and T-shaped walls ranging in height from 1 to 7-stories. Wall specimens ranged from 1:3 to 1:1 in scale. Walls were subjected to uni- and bi-directional earthquake motions. For many specimens, response was determined by flexural action or flexure-shear action; however, for some specimens, response was determined by damage to foundation elements, bond slip in walls splices and rocking of the shaking table. Many specimens were well instrumented and multiple measured acceleration, displacement, deformation and strain histories were provided by the researchers for use in characterizing wall response; however, this was not the case for all specimens. Since table rocking may affect measured response quantities, in many cases research also provided information for modeling this rocking; again, this was not the case for all test programs. Ultimately, each run was assigned a confidence score on the basis of i) the type of damage mechanism determining response, ii) the presence of table rocking and how it was addressed, iii) the quality of information provided about the input motion, iv) the quantity and quality of data and v) whether or not a reasonable degradation in specimen stiffness was observed.

Chapter 4 presents the approach for the elastic, dynamic analyses of the wall test specimens. All were elastic time-history analyses done using SAP 2000 version 9.2.0. Models of the concrete wall test specimens were created using shell elements, with an average element size of 4"x4" to 6"x6". Effective stiffness models were implemented by reducing shell element flexural and shear stiffnesses from the gross-section stiffness. Effective viscous damping models were implemented by applying modal damping for all modes. The shake table was modeled using the recommendations provided by the researchers.

Chapter 5 presents the evaluation of the methods and recommendations for modeling wall buildings for design. Methods were evaluated on the basis of the accuracy with which maximum roof drift, roof acceleration, base shear and base moment were simulated. These are response quantities used typically in design, and, thus, provide an appropriate basis for method evaluation. Methods were evaluated for three different ranges of measured maximum roof drift: less than 0.5%, 0.5% to 1.0% and greater than 1%. Within these drift ranges, varying levels of accuracy could be expected and desired for the response quantities of interest. Methods were ranked on the basis of a weighted error score, where the error in the predicted response quantities for each run was weighted by the confidence score of the run. Ultimately, using the results of the evaluation, recommendations were made for modeling walls for seismic design.

6.2 Conclusions and Observations about Simulation Methods

Comparison of simulated and measured response quantities for concrete walls subjected to simulated earthquake loading supports a number of conclusions of interest to researchers and designers. Perhaps, the most significant results of this study, is the observation that linear elastic analysis using an effective stiffness equal to 50% or more of the gross section stiffness significantly over predicts the stiffness of the structure. This results in under prediction of maximum roof drifts and over prediction of forces and accelerations. This is true for low demand levels, resulting in maximum roof drifts of less than 0.5%, and is especially true for moderate and high demand levels resulting in maximum roof drifts of more than 0.5%.

If a lower effective stiffness is used, such as $0.30E_cI_g$ as recommended in FIB 27 for equivalent monolithic pre-cast elements, response quantities can be predicted with an acceptable level of accuracy and precision for low (maximum roof drift < 0.5%) and moderate (maximum roof drift between 0.5% and 1.0%) demand levels. Specifically, use of $0.30E_cI_g$ with a viscous damping ratio of 3% in this drift range resulted in errors in critical response quantities of less than 15%. The errors and corresponding standard deviations for critical response quantities in low drift levels are as follows:

- Roof drift: -6.9% (standard deviation of 41.2%)
- Base shear: -14.8% (standard deviation of 28.7%)
- Base moment: 12.6% (standard deviation of 84.4%)

The errors and corresponding standard deviations for critical response quantities in moderate drift levels are as follows:

- Roof drift: -13.3% (standard deviation of 46.6%)
- Base shear: 14.2% (standard deviation of 10.5%)
- Base moment: -1.4% (standard deviation of 12.3%)

However, as demands increase, use of a single, predetermined effective stiffness results in substantial error and use of drift-based methods is required for accurate prediction of response. For example, for maximum roof drifts in excess of 1.0% drift, use of an effective stiffness of $0.30E_cI_g$ with a viscous damping ratio of 3% resulted in errors in the predicted roof drift of -79% (standard deviation of 7.7%). Use of the proposed Doepker drift-based update method enables prediction of response quantities for high drift demands:

- Roof drift: -14.6% (standard deviation of 30.0%)
- Base shear: 7.8% (standard deviation of 91.5%)
- Base moment: -0.5% (standard deviation of 86.3%)

Acceleration proved to be the most difficult response quantity to capture for all methods. In low drift ranges, acceleration was better predicted with models using a 7% viscous damping ratio than models using 3%. For example, in low drift ranges the

Doepker method yielded an average error of 39.0% (standard deviation of %) in the roof acceleration with a 3% viscous damping ratio and 11.6% (standard deviation of 90.9%) with a 7% viscous damping ratio. The high value of standard deviation was seen in all methods, and suggests limitations in consistent, accurate prediction of the floor accelerations.

With the exception of the acceleration prediction in the low and high drift ranges, the errors in the simulated response quantities for all drift ranges were lowest when using a viscous damping ratio of 3%. This damping ratio was chosen following the recommendation of Newmark and Hall, which suggested using a level of damping between 3% and 5% for reinforced concrete structures with considerable cracking. The lower value of this range was chosen as the evaluated shake table specimens had no nonstructural elements to provide additional damping. Thus, for use in design, a recommendation of 3% damping based on these results would likely suggest a damping in the range of 3-5% depending on the non-structural characteristics of the structure in question.

In addition to the existing and proposed methods, models were run using a uniform stiffness to match the period obtained from a system identification. These models also used a viscous damping ratio that was determined from the system identification. The results of these tests seem to suggest that using this damping effectively over damped the system.

6.3 Recommendations for Practice

The results of this study support the following recommendations for dynamic analysis of concrete walls for design. For low seismic demands, resulting in low to moderate roof drifts (less than 1.0%), an effective stiffness for wall elements equal to 30% of the gross-section stiffness and a viscous damping ratio for the structural system of 3% for all modes should be used. This could be expected to result in errors in the maximum roof drift, base shear and base moment of less than 15%. For high seismic demands, resulting in maximum roof drifts in excess of 1%, the effective stiffness for wall elements should be defined using the Doepker updated stiffness method and a viscous damping ratio for structural elements of 3% should be used. This could be expected to result in errors in the maximum roof drift, base shear and base moment of less than 15%.

6.4 Recommendations for Future Research

The results of this study suggest several topics to be investigated in future research. First, the Doepker updated stiffness method resulted in low errors in analysis quantities in the low and high drift ranges. However, analysis using this method resulted in prohibitively high errors in the moderate (between 0.5% and 1.0%) roof drift range. Revising the Doepker updated stiffness method to better fit experimental stiffness data in this drift range may result in improved prediction of response quantities. This would support recommendation of the use of the Doepker updated stiffness method for all levels of roof drift demand.

Second, when the effective viscous damping ratios computed from a system identification analysis of test specimen acceleration records were used in the period matching models, the simulated response histories appeared to be over-damped in comparison with the measured histories. Thus, additional research is warranted to address calculation of appropriate damping values from experimental response histories to enable more accurate prediction of maximum response quantities. The use of system identification algorithms other than that used in this study may be more appropriate, or it may be necessary to perform the system identification in a small time frame around the point of maximum roof drift.

Third, theoretically nonlinear models could provide more accurate simulation of wall response, especially for walls experiencing moderate to high drift demands and exhibiting flexural or flexure-shear yield mechanisms. However, the results of previous research suggest that nonlinear models can provide highly inaccurate simulation of response and highly inaccurate prediction of response quantities such as maximum drift and acceleration. To investigate the accuracy of nonlinear response models and further assess the accuracy of the elastic analysis methods considered here, it is recommended that the current study be essentially repeated using several commonly employed nonlinear response models.

Fourth, the dataset used for evaluation of the methods was small and included data from several tests with quite low confidence scores. Thus, it is recommended that additional shake table tests be conducted using test specimens that are near full scale, represent common configurations, and are designed in accordance with current codes to ensure response is determined by flexural yielding of the wall. These test specimens should be well instrumented to facilitate assessment of response and use of the data for model evaluation.

BIBLIOGRAPHY

American Concrete Institute (ACI). (2002). "Building Code Requirements for Structural Concrete and Commentary". ACI 318-2002. Farmington Hills, Michigan.

Adebar, P., Ibrahim, A. M. M., Bryson, Michael (2007). "Test of High-Rise Core Wall: Effective Stiffness for Seismic Analysis". ACI Structural Journal, Farmington Hills, Michigan.

American Society of Civil Engineers (ASCE) (2000). "Prestandard and Commentary for the Seismic Rehabilitation of Buildings". Federal Emergency Management Agency (FEMA) 356. Reston, Virginia.

Applied Technology Council (ATC) (2005). "Improvement of Nonlinear Static Seismic Analysis Procedure". Federal Emergency Management Agency (FEMA) 440. Redwood City, California

Brown, P. (2008). "Probabilistic Earthquake Damage Prediction for Reinforced Concrete Building Components". Masters Thesis. Department of Civil and Environmental Engineering, University of Washington, Seattle.

Building Seismic Safety Council (BSSC) (2003). "NEHRP Recommended Provisions for Seismic Regulations for New Buildings and Other Structures". Federal Emergency Management Agency (FEMA) 450. Washington D.C.

Chopra, A. K. (2004). "*Dynamics of Structures: Theory and Applications to Earthquake Engineering. 2nd Ed.*". H. Guirda Publishing Co, Athens, Greece.

Combescure D., F. Ragueneau and J. Mazars (2002). "CAMUS 2000 Benchmark. Experimental results and specifications to the participants". Commissariat a L'Energie Atomique, Saclay, France.

Computers and Structures Inc. (CSI). 07/22/2008. "CSI Berkeley". 08/21/2008. [http://www.csiberkeley.com].

Federation Internationale du Beton (FIB). (2003). *Displacement-based seismic design of reinforced concrete buildings*. FIB Bulletin Number 25, Lausanne, Switzerland.

Federation Internationale du Beton (FIB). (2003). *Seismic design of precast concrete building structures*. FIB Bulletin Number 27, Lausanne, Switzerland.

Ile N. and J. M. Reynouard (2003). “Lightly Reinforced Walls Subjected to Multi-Directional Seismic Excitations: Interpretation of CAMUS 2000-1 Dynamic Tests”. ISET Journal of Earthquake Technology. Roorkee, India.

Gulkan, P. and M. A. Sozen (1974). “Inelastic Responses of Reinforced Concrete Structures to Earthquake Motions”. ACI Journal, Vol. 71, No. 12, 604-610.

Lestuzzi, Pierino (2002). Effective Stiffness of RC Walls in Dynamic Tests. “12th European Conference on Earthquake Engineering Proceedings”. London, UK

“NEES@UCSD”. 12/16/2006. Network for Earthquake Engineering Simulation (NEES) @ UCSD. 5/31/2007. [http://nees.ucsd.edu/7Story.html].

“7 Story Building”. 06/28/06. NEES Central. 05/31/2007. [http://central.nees.org].

Newmark, N. M. and W. J. Hall (1982). “*Earthquake Spectra and Design”*. Earthquake Engineering Research Institute, Berkeley, California.

Nguyen X. H. (2006). “Vulnerabilities of Reinforced Concrete Structural Walls Submitted to Seismic Loadings”. L’Ecole Doctorale Terres, Univers, Environmental, Institut National Polytechnique de Grenoble, Grenoble, France.

Oyen, P. E. (2006). “Evaluation of Analytical Tools for Determining the Seismic Response of Reinforced Concrete Shear Walls”. Masters Thesis. Department of Civil and Environmental Engineering, University of Washington, Seattle.

Panagiotou, M. and J. Restrepo (2006). “Model Calibration for the UCSD 7-Story Building Slice”. NEES/UCSD Seminar on Analytical Modeling of Reinforced Concrete Walls for Earthquake Resistance, San Diego, California.

Panagiotou, M., J. Restrepo, J. Conte and R. Englekirk (2006). “Seismic Response of Reinforced Concrete Wall Buildings”. Proceedings of the 8th U.S. National Conference on Earthquake Engineering, San Francisco, California.

Panagiotou, M., J. Restrepo, J. Conte and R. Englekirk (2006) "Shake Table Response of a Full Scale Reinforced Concrete Wall Building Slice". Structural Engineers Association of California 75th Annual Proceedings, Long Beach, California.

Panagiotou, M., J. Restrepo, and J. Conte (2007) "Shake Table Test of a 7-Story Full Scale Reinforced Concrete Structural Wall Building Slice Phase I: Rectangular Wall Section". Report No. SSRP-07-07 Draft, University of California, San Diego.

Paulay, T. and M. J. N. Priestley (1990). *Seismic Design of Reinforced Concrete and Masonry Buildings*. Jon Wiley and Sons, New York, N.Y.

Ranf, R. T. (2007). "Model Selection for Performance-Based Earthquake Engineering of Bridges". Ph. D. Thesis. Department of Civil and Environmental Engineering, University of Washington.

Reynouard J. and M. N. Fardis (2001). "*Shear Walls Structures*". Laboratorio Nacional de Engenharia Civil (LNEC), Lisboa, Portugal.

Appendix A: Complete Error Results

A.1 Definition of Error Evaluation Functions

The following lists the equations used to evaluate the effectiveness of the methods introduced in Chapter 2. These expand upon those introduced in Section 5.5.

Error Evaluation Function 1: Period error

$$E_{period} = \frac{T_{estimated} - T_{measured}}{T_{measured}} \tag{5-4}$$

Error Evaluation Function 2: Roof drift error

$$E_{drift} = \left(\frac{\Delta_{roof-estimated} - \Delta_{roof\ \max-measured}}{\Delta_{roof\ \max-measured}} \right) \tag{5-5}$$

Error Evaluation Function 2-2: Average story drift error

$$E_{drift-2} = \frac{1}{n} \sum_{n=1}^{n} \left| \frac{(\Delta_{n+1} - \Delta_{n})_{estimated} - (\Delta_{n+1} - \Delta_{n})_{measured}}{(\Delta_{n+1} - \Delta_{n})_{measured}} \right| \tag{A-1}$$

Error Evaluation Function 2-3: Maximum story drift error

$$E_{drift-3} = \max_{n} \left(\left| \frac{(\Delta_{n+1} - \Delta_{n})_{estimated} - (\Delta_{n+1} - \Delta_{n})_{measured}}{(\Delta_{n+1} - \Delta_{n})_{measured}} \right| \right) \tag{A-2}$$

Error Evaluation Function 3: Roof acceleration error

$$E_{accel} = \left(\left| \frac{a_{roof-estimated} - a_{roof\ \max-measured}}{a_{roof\ \max-measured}} \right| \right) \tag{5-6}$$

Error Evaluation Function 3-2: Total acceleration error normalized with respect to max roof acceleration

$$E_{accel-2} = \frac{1}{n}\frac{\sum_{n=1}^{n}\left|a_{estimated} - a_{measured}\right|}{a_{\max\_measured}} \tag{A-3}$$

Error Evaluation Function 3-3: Maximum story acceleration error

$$E_{accel-3} = \frac{\max_n\left(\left|a_{estimated} - a_{measured}\right|\right)}{\left|a_{\max\_measured}\right|} \tag{A-4}$$

Error Evaluation Function 4: Base shear error

$$E_{shear} = \left(\frac{V_{base-estimated} - V_{base\_\max-measured}}{V_{base\_\max-measured}}\right) \tag{5-7}$$

Error Evaluation Function 4-2: Average error in imposed inertial loads

$$E_{shear-2} = \frac{1}{n}\frac{\sum_{n=1}^{n}\left|F_{estimated} - F_{measured}\right|}{F_{\max\_measured}} \tag{A-5}$$

Error Evaluation Function 4-3: Maximum story error in imposed inertial loads

$$E_{shear-3} = \frac{\max_n\left(\left|F_{estimated} - F_{measured}\right|\right)}{\left|F_{\max\_measured}\right|} \tag{A-6}$$

Error Evaluation Function 5: Base moment error

$$E_{moment} = \left(\frac{M_{base-estimated} - M_{base\_\max-measured}}{M_{base\_\max-measured}}\right) \tag{5-8}$$

where:

n = the number of stories or data records available.

A.2 Complete Average Error Results

The tables below include the average error data for all the tests using the evaluated methods. Cells denoted with "N/A" refer to cases where no error was determined because the evaluation method was not evaluated on this particular test, and cells denoted with "NO DATA" refer to cases that were not evaluated because the necessary experimental data was not made available (e.g. No story records were available).

Table A- 1: Error in Period Prediction (Evaluation Method 1) for UCSD Test Specimen

Specimen	**UCSD**		
Test	**EQ1**	**EQ2**	**EQ3**
Period (s)	0.65	0.84	0.96
Drifts	0.271%	0.761%	0.832%
Analysis Method	**Error**		
FIB 27 (0.3), 3%	7.6%	-16.8%	-27.8%
FIB 27 (0.3), 7%	7.6%	-16.8%	-27.8%
Adebar Upper, 3%	-17.6%	-36.2%	-44.7%
Adebar Upper, 7%	-17.6%	-36.2%	-44.7%
Adebar Lower, 3%	0.2%	-22.5%	-32.7%
Adebar Lower, 7%	0.2%	-22.5%	-32.7%
FEMA Cracked, 3%	-8.1%	-28.9%	-38.3%
FEMA Cracked, 7%	-8.1%	-28.9%	-38.3%
FEMA Uncracked, 3%	-20.8%	-38.8%	-46.8%
FEMA Uncracked, 7%	-20.8%	-38.8%	-46.8%
Brown Iterated Stiffness, 3%	7.6%	0.0%	-13.2%
Brown Iterated Stiffness, 7%	7.6%	-6.1%	-18.5%
Iterated Stiffness, (0.4), 3%	N/A	N/A	N/A
Iterated Stiffness, (0.4), 7%	N/A	N/A	N/A
Doepker Iterated Stiffness, (0.8), 3%	5.5%	0.0%	-13.2%
Doepker Iterated Stiffness, (0.8), 7%	3.5%	-4.7%	-16.0%

Table A- 2: Error in Period Prediction (Evaluation Method 1) for CAMUS C-1 Test Specimen

Specimen	**CAMUS C - 1**			
Test	**Stage 1**	**Stage 2**	**Stage 3**	**Stage 4**
Period (s)	0.43	0.47	0.61	0.70
Drifts	0.352%	0.522%	1.313%	1.849%
Analysis Method	**Error**			
FIB 27 (0.3), 3%	-12.8%	-20.2%	-38.5%	-46.4%
FIB 27 (0.3), 7%	-12.8%	-20.2%	-38.5%	-46.4%
Adebar Upper, 3%	-39.1%	-44.3%	-57.0%	-62.6%
Adebar Upper, 7%	-39.1%	-44.3%	-57.0%	-62.6%
Adebar Lower, 3%	-7.9%	-15.7%	-35.1%	-43.4%
Adebar Lower, 7%	-7.9%	-15.7%	-35.1%	-43.4%
FEMA Cracked, 3%	-31.9%	-37.7%	-52.0%	-58.1%
FEMA Cracked, 7%	-31.9%	-37.7%	-52.0%	-58.1%
FEMA Uncracked, 3%	-45.1%	-49.8%	-61.3%	-66.3%
FEMA Uncracked, 7%	-45.1%	-49.8%	-61.3%	-66.3%
Brown Iterated Stiffness, 3%	-12.8%	-14.5%	15.7%	83.4%
Brown Iterated Stiffness, 7%	-12.8%	-20.2%	54.5%	14.0%
Iterated Stiffness, (0.4), 3%	N/A	N/A	N/A	N/A
Iterated Stiffness, (0.4), 7%	N/A	N/A	N/A	N/A
Doepker Iterated Stiffness, (0.8), 3%	-14.2%	-9.2%	5.6%	11.4%
Doepker Iterated Stiffness, (0.8), 7%	-19.2%	-17.5%	-18.8%	-8.0%

Table A- 3: Error in Period Prediction (Evaluation Method 1) for CAMUS C-2 Test Specimen

Specimen	**CAMUS C - 2**		
Test	**Stage 2**	**Stage 3**	**Stage 4**
Period (s)	0.33	0.42	0.61
Drifts	0.082%	0.540%	1.912%
Analysis Method	**Error**		
FIB 27 (0.3), 3%	11.5%	-12.4%	-39.7%
FIB 27 (0.3), 7%	11.5%	-12.4%	-39.7%
Adebar Upper, 3%	-22.1%	-38.8%	-57.9%
Adebar Upper, 7%	-22.1%	-38.8%	-57.9%
Adebar Lower, 3%	17.6%	-7.6%	-36.4%
Adebar Lower, 7%	17.6%	-7.6%	-36.4%
FEMA Cracked, 3%	-12.7%	-31.4%	-52.8%
FEMA Cracked, 7%	-12.7%	-31.4%	-52.8%
FEMA Uncracked, 3%	-29.7%	-44.8%	-62.0%
FEMA Uncracked, 7%	-29.7%	-44.8%	-62.0%
Brown Iterated Stiffness, 3%	39.4%	9.5%	32.3%
Brown Iterated Stiffness, 7%	24.2%	-2.4%	-15.2%
Iterated Stiffness, (0.4), 3%	N/A	N/A	N/A
Iterated Stiffness, (0.4), 7%	N/A	N/A	N/A
Doepker Iterated Stiffness, (0.8), 3%	17.3%	1.9%	3.5%
Doepker Iterated Stiffness, (0.8), 7%	9.6%	-6.1%	-17.9%

Table A- 4: Error in Period Prediction (Evaluation Method 1) for CAMUS C-3 Test Specimen

Specimen	CAMUS C - 3			
Test	Stage 1	Stage 2	Stage 3	Stage 4
Period (s)	0.30	0.40	0.57	0.74
Drifts	0.117%	0.347%	1.318%	2.274%
Analysis Method	Error			
FIB 27 (0.3), 3%	17.0%	-12.3%	-38.4%	-52.6%
FIB 27 (0.3), 7%	17.0%	-12.3%	-38.4%	-52.6%
Adebar Upper, 3%	-18.3%	-38.8%	-57.0%	-66.9%
Adebar Upper, 7%	-18.3%	-38.8%	-57.0%	-66.9%
Adebar Lower, 3%	23.7%	-7.3%	-34.9%	-49.9%
Adebar Lower, 7%	23.7%	-7.3%	-34.9%	-49.9%
FEMA Cracked, 3%	-8.3%	-31.3%	-51.8%	-62.8%
FEMA Cracked, 7%	-8.3%	-31.3%	-51.8%	-62.8%
FEMA Uncracked, 3%	-26.0%	-44.5%	-61.1%	-70.0%
FEMA Uncracked, 7%	-26.0%	-44.5%	-61.1%	-70.0%
Brown Iterated Stiffness, 3%	17.0%	-12.3%	-13.3%	48.4%
Brown Iterated Stiffness, 7%	17.0%	-12.3%	-26.7%	-18.4%
Iterated Stiffness, (0.4), 3%	N/A	N/A	N/A	N/A
Iterated Stiffness, (0.4), 7%	N/A	N/A	N/A	N/A
Doepker Iterated Stiffness, (0.8), 3%	11.7%	-4.0%	-10.4%	0.3%
Doepker Iterated Stiffness, (0.8), 7%	-0.7%	-13.6%	-24.8%	-25.5%

Table A- 5: Error in Period Prediction (Evaluation Method 1) for CAMUS 2000 Test Specimen

Specimen	CAMUS 2000		
Test	Run 1	Run 2	Run 3
Period (s)	0.187	0.25	0.281
Drifts	0.088%	0.296%	0.384%
Analysis Method	Error		
FIB 27 (0.3), 3%	26.7%	-5.2%	-15.7%
FIB 27 (0.3), 7%	26.7%	-5.2%	-15.7%
Adebar Upper, 3%	0.6%	-24.7%	-33.0%
Adebar Upper, 7%	0.6%	-24.7%	-33.0%
Adebar Lower, 3%	23.3%	-7.8%	-17.9%
Adebar Lower, 7%	23.3%	-7.8%	-17.9%
FEMA Cracked, 3%	8.8%	-18.6%	-27.6%
FEMA Cracked, 7%	8.8%	-18.6%	-27.6%
FEMA Uncracked, 3%	-1.7%	-26.5%	-34.6%
FEMA Uncracked, 7%	-1.7%	-26.5%	-34.6%
Brown Iterated Stiffness, 3%	23.7%	2.5%	-3.5%
Brown Iterated Stiffness, 7%	23.7%	-3.6%	-9.0%
Iterated Stiffness, (0.4), 3%	22.5%	0.5%	-1.0%
Iterated Stiffness, (0.4), 7%	22.0%	-5.2%	-9.4%
Doepker Iterated Stiffness, (0.8), 3%	18.2%	2.6%	-2.2%
Doepker Iterated Stiffness, (0.8), 7%	16.2%	-2.9%	-5.7%

Table A- 6: Error in Period Prediction (Evaluation Method 1) for Ecoleader Test Specimen

Specimen	CAMUS Ecoleader					
Test	**Run 1**	**Run 3**	**Run 4**	**Run 5**	**Run 6**	**Run 7**
Period (s)	0.22	0.25	0.37	0.40	0.46	0.56
Drifts	0.159%	0.195%	0.623%	0.872%	1.187%	1.303%
Analysis Method	**Error**					
FIB 27 (0.3), 3%	-13.8%	-25.2%	-48.5%	-52.5%	-59.2%	-66.2%
FIB 27 (0.3), 7%	-13.8%	-25.2%	-48.5%	-52.5%	-59.2%	-66.2%
Adebar Upper, 3%	-39.7%	-47.7%	-63.9%	-66.7%	-71.4%	-76.4%
Adebar Upper, 7%	-39.7%	-47.7%	-63.9%	-66.7%	-71.4%	-76.4%
Adebar Lower, 3%	-4.7%	-17.3%	-43.0%	-47.4%	-54.9%	-62.6%
Adebar Lower, 7%	-4.7%	-17.3%	-43.0%	-47.4%	-54.9%	-62.6%
FEMA Cracked, 3%	-32.2%	-41.2%	-59.5%	-62.6%	-67.9%	-73.4%
FEMA Cracked, 7%	-32.2%	-41.2%	-59.5%	-62.6%	-67.9%	-73.4%
FEMA Uncracked, 3%	-42.3%	-50.0%	-65.5%	-68.2%	-72.7%	-77.4%
FEMA Uncracked, 7%	-42.3%	-50.0%	-65.5%	-68.2%	-72.7%	-77.4%
Brown Iterated Stiffness, 3%	-13.8%	-25.2%	-48.0%	-50.8%	-55.0%	-55.3%
Brown Iterated Stiffness, 7%	-13.8%	-25.2%	-48.5%	-52.5%	-58.8%	-64.7%
Iterated Stiffness, (0.4), 3%	N/A	N/A	N/A	N/A	N/A	N/A
Iterated Stiffness, (0.4), 7%	N/A	N/A	N/A	N/A	N/A	N/A
Doepker Iterated Stiffness, (0.8), 3%	-25.2%	-34.3%	-48.5%	-49.0%	-50.1%	-57.6%
Doepker Iterated Stiffness, (0.8), 7%	-27.8%	-35.2%	-50.8%	-52.5%	-56.2%	-60.6%

Table A- 7: Error in Roof Drift Prediction (Evaluation Method 2) for UCSD Test Specimen

Specimen	UCSD		
Test	EQ1	EQ2	EQ3
Period (s)	0.65	0.84	0.96
Drifts	0.271%	0.761%	0.832%
FIB 27 (0.3), 3%	4.0%	-46.9%	55.7%
FIB 27 (0.3), 7%	-11.9%	-49.9%	81.5%
Adebar Upper, 3%	-34.9%	-51.0%	-89.3%
Adebar Upper, 7%	-56.8%	-66.5%	-87.9%
Adebar Lower, 3%	12.4%	-39.2%	-83.8%
Adebar Lower, 7%	-19.7%	-54.8%	-84.5%
FEMA Cracked, 3%	-51.8%	-68.8%	-64.5%
FEMA Cracked, 7%	-45.8%	-74.7%	-80.4%
FEMA Uncracked, 3%	-59.7%	-74.0%	-90.3%
FEMA Uncracked, 7%	-69.8%	-81.2%	-88.6%
Brown Iterated Stiffness, 3%	4.0%	-9.6%	-62.3%
Brown Iterated Stiffness, 7%	-11.9%	-29.6%	-78.7%
Iterated Stiffness, (0.4), 3%	N/A	N/A	N/A
Iterated Stiffness, (0.4), 7%	N/A	N/A	N/A
Doepker Iterated Stiffness, (0.8), 3%	4.4%	-9.6%	-62.3%
Doepker Iterated Stiffness, (0.8), 7%	-15.1%	-28.3%	-75.9%
Uniform Best Fit	-6.8%	-34.6%	-57.2%
Uniform Best Fit, 3%	10.5%	-9.6%	-14.0%
Uniform Best Fit, 7%	-18.1%	-29.3%	-39.3%
Uniform Best Fit, 3% FEMA	10.5%	-41.3%	-51.4%
Uniform Best Fit, 7% FEMA	10.5%	-30.7%	-44.4%
Variable Best Fit	-6.9%	-35.4%	-56.0%

Table A- 8: Error in Roof Drift Prediction (Evaluation Method 2) for CAMUS C-1 Test Specimen

Specimen	CAMUS C - 1			
Test	Stage 1	Stage 2	Stage 3	Stage 4
Period (s)	0.43	0.47	0.61	0.70
Drifts	0.352%	0.522%	1.313%	1.849%
FIB 27 (0.3), 3%	-9.0%	-28.9%	-84.8%	-86.0%
FIB 27 (0.3), 7%	-42.5%	-62.5%	-74.6%	-81.9%
Adebar Upper, 3%	-68.9%	-79.9%	-69.0%	-80.6%
Adebar Upper, 7%	-83.2%	-89.1%	-75.6%	-81.2%
Adebar Lower, 3%	-10.8%	-55.9%	-73.8%	-84.6%
Adebar Lower, 7%	-29.8%	-73.4%	-75.2%	-83.4%
FEMA Cracked, 3%	-53.3%	-66.2%	-47.1%	-62.5%
FEMA Cracked, 7%	-84.1%	-85.0%	-55.8%	-68.6%
FEMA Uncracked, 3%	-91.7%	-90.8%	-58.4%	-67.1%
FEMA Uncracked, 7%	-89.1%	-90.6%	-67.9%	-77.8%
Brown Iterated Stiffness, 3%	-9.0%	-63.1%	28.3%	43.6%
Brown Iterated Stiffness, 7%	-42.5%	-62.5%	19.9%	2.5%
Iterated Stiffness, (0.4), 3%	N/A	N/A	N/A	N/A
Iterated Stiffness, (0.4), 7%	N/A	N/A	N/A	N/A
Doepker Iterated Stiffness, (0.8), 3%	-16.3%	-44.3%	11.4%	8.1%
Doepker Iterated Stiffness, (0.8), 7%	-66.0%	-67.8%	-47.0%	-8.3%
Uniform Best Fit	-21.0%	-30.1%	5.8%	-19.4%
Uniform Best Fit, 3%	32.9%	0.2%	24.7%	-9.3%
Uniform Best Fit, 7%	-11.0%	-43.3%	4.7%	-11.6%
Uniform Best Fit, 3% FEMA	32.9%	0.2%	-4.1%	-19.7%
Uniform Best Fit, 7% FEMA	32.9%	0.2%	10.3%	-16.2%
Variable Best Fit	-17.8%	-28.6%	11.7%	-13.6%

Table A- 9: Error in Roof Drift Prediction (Evaluation Method 2) for CAMUS C-2 Test Specimen

Specimen	CAMUS C - 2		
Test	Stage 2	Stage 3	Stage 4
Period (s)	0.33	0.42	0.61
Drifts	0.082%	0.540%	1.912%
FIB 27 (0.3), 3%	-57.7%	-32.9%	-82.8%
FIB 27 (0.3), 7%	-60.6%	-61.9%	-82.2%
Adebar Upper, 3%	-59.5%	-88.5%	-85.8%
Adebar Upper, 7%	-78.6%	-89.1%	-98.4%
Adebar Lower, 3%	-79.8%	-46.3%	-90.7%
Adebar Lower, 7%	-63.7%	-66.2%	-85.5%
FEMA Cracked, 3%	-33.6%	-71.6%	-71.0%
FEMA Cracked, 7%	-59.1%	-83.5%	-75.6%
FEMA Uncracked, 3%	-79.9%	-89.6%	-78.8%
FEMA Uncracked, 7%	-85.9%	-90.6%	-83.1%
Brown Iterated Stiffness, 3%	77.5%	23.2%	-6.9%
Brown Iterated Stiffness, 7%	-39.9%	-81.1%	-47.0%
Iterated Stiffness, (0.4), 3%	N/A	N/A	N/A
Iterated Stiffness, (0.4), 7%	N/A	N/A	N/A
Doepker Iterated Stiffness, (0.8), 3%	-83.3%	-45.5%	-10.9%
Doepker Iterated Stiffness, (0.8), 7%	-56.3%	-69.7%	-58.3%
Uniform Best Fit	-3.5%	-75.0%	-44.5%
Uniform Best Fit, 3%	N/A	N/A	N/A
Uniform Best Fit, 7%	N/A	N/A	N/A
Uniform Best Fit, 3% FEMA	N/A	N/A	N/A
Uniform Best Fit, 7% FEMA	N/A	N/A	N/A
Variable Best Fit	0.7%	-71.0%	-40.3%

Table A- 10: Error in Roof Drift Prediction (Evaluation Method 2) for CAMUS C-3 Test Specimen

Specimen	CAMUS C - 3			
Test	Stage 1	Stage 2	Stage 3	Stage 4
Period (s)	0.30	0.40	0.57	0.74
Drifts	0.117%	0.347%	1.318%	2.274%
FIB 27 (0.3), 3%	-4.7%	-26.3%	-70.5%	-71.0%
FIB 27 (0.3), 7%	-34.4%	-56.2%	-90.3%	-77.0%
Adebar Upper, 3%	-42.6%	-78.4%	-87.2%	-80.4%
Adebar Upper, 7%	-69.4%	-86.2%	-91.7%	-83.9%
Adebar Lower, 3%	-41.1%	2.0%	-30.5%	-86.5%
Adebar Lower, 7%	-55.8%	-35.3%	-56.0%	-84.1%
FEMA Cracked, 3%	-81.4%	-64.6%	-78.5%	-78.9%
FEMA Cracked, 7%	-64.2%	-77.0%	-86.1%	-81.6%
FEMA Uncracked, 3%	-89.5%	-83.0%	-88.9%	-74.9%
FEMA Uncracked, 7%	-88.7%	-88.6%	-92.7%	-81.1%
Brown Iterated Stiffness, 3%	-4.7%	-26.3%	-77.7%	27.9%
Brown Iterated Stiffness, 7%	-34.4%	-56.2%	-35.8%	-20.9%
Iterated Stiffness, (0.4), 3%	N/A	N/A	N/A	N/A
Iterated Stiffness, (0.4), 7%	N/A	N/A	N/A	N/A
Doepker Iterated Stiffness, (0.8), 3%	13.4%	9.8%	-63.5%	-17.9%
Doepker Iterated Stiffness, (0.8), 7%	-36.3%	-62.3%	-32.2%	-28.1%
Uniform Best Fit	-1.4%	-31.1%	-54.4%	-38.7%
Uniform Best Fit, 3%	N/A	N/A	N/A	N/A
Uniform Best Fit, 7%	N/A	N/A	N/A	N/A
Uniform Best Fit, 3% FEMA	N/A	N/A	N/A	N/A
Uniform Best Fit, 7% FEMA	N/A	N/A	N/A	N/A
Variable Best Fit	2.0%	-26.0%	-51.3%	-34.2%

Table A- 11: Error in Roof Drift Prediction (Evaluation Method 2) for CAMUS 2000 Test Specimen

Specimen	CAMUS 2000		
Test	Run 1	Run 2	Run 3
Period (s)	0.187	0.25	0.281
Drifts	0.088%	0.296%	0.384%
FIB 27 (0.3), 3%	74.6%	-29.0%	-53.5%
FIB 27 (0.3), 7%	-17.8%	-26.4%	-43.9%
Adebar Upper, 3%	9.5%	-27.0%	-52.3%
Adebar Upper, 7%	-54.7%	-30.4%	-47.5%
Adebar Lower, 3%	-43.3%	-55.0%	-51.0%
Adebar Lower, 7%	-38.7%	-57.1%	-65.8%
FEMA Cracked, 3%	-58.4%	-14.2%	-38.3%
FEMA Cracked, 7%	-43.9%	-39.8%	-58.6%
FEMA Uncracked, 3%	-38.7%	-64.8%	-62.0%
FEMA Uncracked, 7%	-34.5%	-61.9%	-69.3%
Brown Iterated Stiffness, 3%	74.6%	28.4%	48.0%
Brown Iterated Stiffness, 7%	-17.8%	-22.2%	-12.7%
Iterated Stiffness, (0.4), 3%	35.3%	9.1%	58.4%
Iterated Stiffness, (0.4), 7%	-41.2%	-26.4%	-15.0%
Doepker Iterated Stiffness, (0.8), 3%	35.1%	29.9%	53.9%
Doepker Iterated Stiffness, (0.8), 7%	-36.4%	-19.8%	3.9%
Uniform Best Fit	-40.2%	-31.3%	-20.1%
Uniform Best Fit, 3%	-37.2%	0.8%	60.5%
Uniform Best Fit, 7%	-40.2%	-8.9%	20.8%
Uniform Best Fit, 3% FEMA	N/A	N/A	N/A
Uniform Best Fit, 7% FEMA	N/A	N/A	N/A
Variable Best Fit	-43.4%	-30.5%	-21.3%

Table A- 12: Error in Roof Drift Prediction (Evaluation Method 2) for Ecoleader Test Specimen

Specimen	**CAMUS Ecoleader**					
Test	**Run 1**	**Run 3**	**Run 4**	**Run 5**	**Run 6**	**Run 7**
Period (s)	0.22	0.25	0.37	0.40	0.46	0.56
Drifts	0.159%	0.195%	0.623%	0.872%	1.187%	1.303%
FIB 27 (0.3), 3%	-26.8%	-75.9%	-66.5%	-90.9%	-92.3%	-96.1%
FIB 27 (0.3), 7%	-34.1%	-79.0%	-75.3%	-95.3%	-96.0%	-99.1%
Adebar Upper, 3%	-59.1%	-86.4%	-79.1%	-86.3%	-91.5%	-91.0%
Adebar Upper, 7%	-64.0%	-88.0%	-86.2%	-91.0%	-93.9%	-94.7%
Adebar Lower, 3%	-1.7%	-77.0%	-45.3%	-60.6%	-85.5%	-85.2%
Adebar Lower, 7%	-13.8%	-76.5%	-68.6%	-64.2%	-91.6%	-90.9%
FEMA Cracked, 3%	-52.6%	-83.6%	-58.1%	-87.3%	-90.8%	-91.9%
FEMA Cracked, 7%	-57.5%	-86.3%	-74.6%	-90.9%	-93.1%	-94.5%
FEMA Uncracked, 3%	-60.7%	-88.4%	-82.2%	-87.6%	-93.4%	-93.9%
FEMA Uncracked, 7%	-67.4%	-89.2%	-90.2%	-91.7%	-95.2%	-95.8%
Brown Iterated Stiffness, 3%	-26.8%	-75.9%	-61.5%	-68.0%	-85.7%	-49.4%
Brown Iterated Stiffness, 7%	-34.1%	-79.0%	-75.3%	-95.3%	-95.8%	-96.7%
Iterated Stiffness, (0.4), 3%	N/A	N/A	N/A	N/A	N/A	N/A
Iterated Stiffness, (0.4), 7%	N/A	N/A	N/A	N/A	N/A	N/A
Doepker Iterated Stiffness, (0.8), 3%	-45.3%	-85.9%	-66.5%	-85.6%	-73.0%	-61.0%
Doepker Iterated Stiffness, (0.8), 7%	-53.1%	-85.7%	-83.6%	-95.3%	-93.3%	-84.6%
Uniform Best Fit	3.8%	-69.6%	-23.1%	-43.5%	-29.8%	-19.7%
Uniform Best Fit, 3%	N/A	N/A	N/A	N/A	N/A	N/A
Uniform Best Fit, 7%	N/A	N/A	N/A	N/A	N/A	N/A
Uniform Best Fit, 3% FEMA	N/A	N/A	N/A	N/A	N/A	N/A
Uniform Best Fit, 7% FEMA	N/A	N/A	N/A	N/A	N/A	N/A
Variable Best Fit	N/A	N/A	N/A	N/A	N/A	N/A

Table A- 13: Average Story Drift Error (Evaluation Method 3) for UCSD Test Specimen

Specimen	**UCSD**		
Test	**EQ1**	**EQ2**	**EQ3**
Period (s)	0.65	0.84	0.96
Drifts	0.271%	0.761%	0.832%
FIB 27 (0.3), 3%	21.0%	48.1%	55.7%
FIB 27 (0.3), 7%	22.3%	51.0%	81.5%
Adebar Upper, 3%	36.1%	52.4%	89.5%
Adebar Upper, 7%	57.6%	67.5%	88.0%
Adebar Lower, 3%	22.0%	40.9%	84.1%
Adebar Lower, 7%	26.4%	56.1%	84.7%
FEMA Cracked, 3%	52.3%	69.6%	64.9%
FEMA Cracked, 7%	46.0%	75.5%	80.6%
FEMA Uncracked, 3%	59.8%	74.5%	90.4%
FEMA Uncracked, 7%	69.9%	81.7%	88.8%
Brown Iterated Stiffness, 3%	21.0%	17.2%	62.2%
Brown Iterated Stiffness, 7%	22.3%	31.0%	78.9%
Iterated Stiffness, (0.4), 3%	N/A	N/A	N/A
Iterated Stiffness, (0.4), 7%	N/A	N/A	N/A
Doepker Iterated Stiffness, (0.8), 3%	20.5%	17.2%	62.2%
Doepker Iterated Stiffness, (0.8), 7%	24.0%	29.7%	76.0%
Uniform Best Fit	19.1%	35.8%	57.0%
Uniform Best Fit, 3%	21.2%	17.2%	18.5%
Uniform Best Fit, 7%	25.4%	30.8%	39.3%
Uniform Best Fit, 3% FEMA	21.2%	42.4%	51.3%
Uniform Best Fit, 7% FEMA	21.2%	32.0%	44.4%
Variable Best Fit	17.1%	36.2%	55.4%

Table A- 14: Average Story Drift Error (Evaluation Method 3) for CAMUS C-1 Test Specimen

Specimen	CAMUS C - 1			
Test	Stage 1	Stage 2	Stage 3	Stage 4
Period (s)	0.43	0.47	0.61	0.70
Drifts	0.352%	0.522%	1.313%	1.849%
FIB 27 (0.3), 3%	27.6%	36.5%	86.5%	87.8%
FIB 27 (0.3), 7%	49.8%	66.5%	77.3%	84.2%
Adebar Upper, 3%	72.8%	81.9%	72.2%	82.9%
Adebar Upper, 7%	85.3%	90.2%	78.0%	83.4%
Adebar Lower, 3%	27.9%	60.6%	76.6%	86.4%
Adebar Lower, 7%	38.9%	76.3%	78.0%	85.5%
FEMA Cracked, 3%	59.1%	69.6%	52.5%	66.9%
FEMA Cracked, 7%	86.1%	86.5%	60.3%	72.3%
FEMA Uncracked, 3%	92.7%	91.6%	62.2%	70.7%
FEMA Uncracked, 7%	90.4%	91.4%	70.8%	80.2%
Brown Iterated Stiffness, 3%	27.6%	67.1%	28.9%	40.5%
Brown Iterated Stiffness, 7%	49.8%	66.5%	24.5%	25.4%
Iterated Stiffness, (0.4), 3%	N/A	N/A	N/A	N/A
Iterated Stiffness, (0.4), 7%	N/A	N/A	N/A	N/A
Doepker Iterated Stiffness, (0.8), 3%	28.0%	50.3%	20.6%	24.9%
Doepker Iterated Stiffness, (0.8), 7%	70.3%	71.2%	52.7%	26.1%
Uniform Best Fit	31.3%	37.6%	19.2%	29.8%
Uniform Best Fit, 3%	36.5%	19.5%	26.9%	26.4%
Uniform Best Fit, 7%	28.0%	49.4%	19.4%	26.6%
Uniform Best Fit, 3% FEMA	36.5%	19.5%	20.5%	30.1%
Uniform Best Fit, 7% FEMA	36.5%	19.5%	20.0%	27.0%
Variable Best Fit	27.2%	34.9%	12.3%	17.0%

Table A- 15: Average Story Drift Error (Evaluation Method 3) for CAMUS C-2 Test Specimen

Specimen	**CAMUS C - 2**		
Test	**Stage 2**	**Stage 3**	**Stage 4**
Period (s)	0.33	0.42	0.61
Drifts	0.082%	0.540%	1.912%
FIB 27 (0.3), 3%	52.8%	No Data	85.0%
FIB 27 (0.3), 7%	56.2%	No Data	84.4%
Adebar Upper, 3%	62.9%	No Data	87.6%
Adebar Upper, 7%	80.4%	No Data	95.0%
Adebar Lower, 3%	81.6%	No Data	91.9%
Adebar Lower, 7%	66.8%	No Data	87.3%
FEMA Cracked, 3%	39.0%	No Data	74.5%
FEMA Cracked, 7%	62.5%	No Data	78.5%
FEMA Uncracked, 3%	81.4%	No Data	81.2%
FEMA Uncracked, 7%	110.5%	No Data	85.0%
Brown Iterated Stiffness, 3%	73.4%	No Data	30.9%
Brown Iterated Stiffness, 7%	45.1%	No Data	53.7%
Iterated Stiffness, (0.4), 3%	N/A	No Data	N/A
Iterated Stiffness, (0.4), 7%	N/A	No Data	N/A
Doepker Iterated Stiffness, (0.8), 3%	84.7%	No Data	31.2%
Doepker Iterated Stiffness, (0.8), 7%	60.1%	No Data	63.5%
Uniform Best Fit	24.4%	No Data	51.5%
Uniform Best Fit, 3%	N/A	No Data	N/A
Uniform Best Fit, 7%	N/A	No Data	N/A
Uniform Best Fit, 3% FEMA	N/A	No Data	N/A
Uniform Best Fit, 7% FEMA	N/A	No Data	N/A
Variable Best Fit	27.3%	No Data	44.7%

Table A- 16: Average Story Drift Error (Evaluation Method 3) for CAMUS C-3 Test Specimen

Specimen	**CAMUS C - 3**			
Test	**Stage 1**	**Stage 2**	**Stage 3**	**Stage 4**
Period (s)	0.30	0.40	0.57	0.74
Drifts	0.117%	0.347%	1.318%	2.274%
FIB 27 (0.3), 3%	24.5%	35.9%	73.8%	74.5%
FIB 27 (0.3), 7%	42.4%	61.9%	91.4%	79.8%
Adebar Upper, 3%	49.3%	81.1%	88.5%	82.7%
Adebar Upper, 7%	73.0%	87.9%	92.6%	85.8%
Adebar Lower, 3%	48.4%	26.5%	38.4%	88.2%
Adebar Lower, 7%	61.3%	43.7%	60.9%	86.0%
FEMA Cracked, 3%	83.5%	69.1%	80.8%	81.4%
FEMA Cracked, 7%	68.3%	79.9%	87.6%	83.7%
FEMA Uncracked, 3%	90.6%	85.0%	90.0%	77.6%
FEMA Uncracked, 7%	89.9%	89.9%	93.4%	83.1%
Brown Iterated Stiffness, 3%	24.5%	35.9%	73.8%	39.3%
Brown Iterated Stiffness, 7%	42.4%	61.9%	91.4%	30.7%
Iterated Stiffness, (0.4), 3%	N/A	N/A	N/A	N/A
Iterated Stiffness, (0.4), 7%	N/A	N/A	N/A	N/A
Doepker Iterated Stiffness, (0.8), 3%	24.3%	26.2%	67.6%	29.4%
Doepker Iterated Stiffness, (0.8), 7%	43.9%	67.2%	40.0%	37.1%
Uniform Best Fit	23.4%	40.1%	59.7%	46.5%
Uniform Best Fit, 3%	N/A	N/A	N/A	N/A
Uniform Best Fit, 7%	N/A	N/A	N/A	N/A
Uniform Best Fit, 3% FEMA	N/A	N/A	N/A	N/A
Uniform Best Fit, 7% FEMA	N/A	N/A	N/A	N/A
Variable Best Fit	16.7%	34.5%	52.8%	37.7%

Table A- 17: Average Story Drift Error (Evaluation Method 3) for CAMUS 2000 Test Specimen

Specimen	**CAMUS 2000**		
Test	**Run 1**	**Run 2**	**Run 3**
Period (s)	0.187	0.25	0.281
Drifts	0.088%	0.296%	0.384%
FIB 27 (0.3), 3%	114.8%	34.5%	53.0%
FIB 27 (0.3), 7%	33.9%	31.2%	43.1%
Adebar Upper, 3%	74.5%	33.6%	51.6%
Adebar Upper, 7%	51.3%	35.4%	46.8%
Adebar Lower, 3%	40.3%	60.2%	56.8%
Adebar Lower, 7%	36.3%	59.3%	64.9%
FEMA Cracked, 3%	54.7%	30.2%	57.2%
FEMA Cracked, 7%	41.3%	44.9%	57.9%
FEMA Uncracked, 3%	37.7%	67.1%	60.8%
FEMA Uncracked, 7%	32.2%	63.4%	68.5%
Brown Iterated Stiffness, 3%	114.8%	45.0%	83.9%
Brown Iterated Stiffness, 7%	33.9%	26.9%	32.5%
Iterated Stiffness, (0.4), 3%	81.4%	29.4%	92.5%
Iterated Stiffness, (0.4), 7%	38.8%	31.2%	31.0%
Doepker Iterated Stiffness, (0.8), 3%	63.4%	46.7%	89.8%
Doepker Iterated Stiffness, (0.8), 7%	36.7%	24.5%	43.8%
Uniform Best Fit	37.8%	35.4%	33.1%
Uniform Best Fit, 3%	38.7%	22.6%	94.9%
Uniform Best Fit, 7%	37.9%	20.8%	57.1%
Uniform Best Fit, 3% FEMA	N/A	N/A	N/A
Uniform Best Fit, 7% FEMA	N/A	N/A	N/A
Variable Best Fit	42.1%	34.0%	22.4%

Table A- 18: Average Story Drift Error (Evaluation Method 3) for Ecoleader Test Specimen

Specimen	**CAMUS Ecoleader**					
Test	**Run 1**	**Run 3**	**Run 4**	**Run 5**	**Run 6**	**Run 7**
Period (s)	0.22	0.25	0.37	0.40	0.46	0.56
Drifts	0.159%	0.195%	0.623%	0.872%	1.187%	1.303%
FIB 27 (0.3), 3%	No Data	No Data	No Data	No Data	No Data	No Data
FIB 27 (0.3), 7%	No Data	No Data	No Data	No Data	No Data	No Data
Adebar Upper, 3%	No Data	No Data	No Data	No Data	No Data	No Data
Adebar Upper, 7%	No Data	No Data	No Data	No Data	No Data	No Data
Adebar Lower, 3%	No Data	No Data	No Data	No Data	No Data	No Data
Adebar Lower, 7%	No Data	No Data	No Data	No Data	No Data	No Data
FEMA Cracked, 3%	No Data	No Data	No Data	No Data	No Data	No Data
FEMA Cracked, 7%	No Data	No Data	No Data	No Data	No Data	No Data
FEMA Uncracked, 3%	No Data	No Data	No Data	No Data	No Data	No Data
FEMA Uncracked, 7%	No Data	No Data	No Data	No Data	No Data	No Data
Brown Iterated Stiffness, 3%	No Data	No Data	No Data	No Data	No Data	No Data
Brown Iterated Stiffness, 7%	No Data	No Data	No Data	No Data	No Data	No Data
Iterated Stiffness, (0.4), 3%	No Data	No Data	No Data	No Data	No Data	No Data
Iterated Stiffness, (0.4), 7%	No Data	No Data	No Data	No Data	No Data	No Data
Doepker Iterated Stiffness, (0.8), 3%	No Data	No Data	No Data	No Data	No Data	No Data
Doepker Iterated Stiffness, (0.8), 7%	No Data	No Data	No Data	No Data	No Data	No Data
Uniform Best Fit	No Data	No Data	No Data	No Data	No Data	No Data
Uniform Best Fit, 3%	No Data	No Data	No Data	No Data	No Data	No Data
Uniform Best Fit, 7%	No Data	No Data	No Data	No Data	No Data	No Data
Uniform Best Fit, 3% FEMA	No Data	No Data	No Data	No Data	No Data	No Data
Uniform Best Fit, 7% FEMA	No Data	No Data	No Data	No Data	No Data	No Data
Variable Best Fit	No Data	No Data	No Data	No Data	No Data	No Data

Table A- 19: Maximum Story Drift Error (Evaluation Method 4) for UCSD Test Specimen

Specimen	**UCSD**		
Test	**EQ1**	**EQ2**	**EQ3**
Period (s)	0.65	0.84	0.96
Drifts	0.271%	0.761%	0.832%
FIB 27 (0.3), 3%	59.1%	68.5%	75.2%
FIB 27 (0.3), 7%	44.7%	70.4%	88.5%
Adebar Upper, 3%	60.7%	75.7%	95.1%
Adebar Upper, 7%	75.8%	83.6%	94.1%
Adebar Lower, 3%	67.7%	67.7%	91.9%
Adebar Lower, 7%	47.7%	76.8%	91.4%
FEMA Cracked, 3%	68.7%	82.5%	80.9%
FEMA Cracked, 7%	61.1%	85.2%	89.8%
FEMA Uncracked, 3%	71.1%	84.3%	94.6%
FEMA Uncracked, 7%	77.9%	89.2%	94.0%
Brown Iterated Stiffness, 3%	59.1%	44.9%	72.7%
Brown Iterated Stiffness, 7%	44.7%	56.2%	86.7%
Iterated Stiffness, (0.4), 3%	N/A	N/A	N/A
Iterated Stiffness, (0.4), 7%	N/A	N/A	N/A
Doepker Iterated Stiffness, (0.8), 3%	59.4%	44.9%	72.7%
Doepker Iterated Stiffness, (0.8), 7%	45.8%	29.7%	84.3%
Uniform Best Fit	39.6%	58.4%	68.6%
Uniform Best Fit, 3%	65.9%	44.9%	39.1%
Uniform Best Fit, 7%	46.4%	56.4%	56.8%
Uniform Best Fit, 3% FEMA	65.9%	62.5%	65.1%
Uniform Best Fit, 7% FEMA	65.9%	56.1%	60.5%
Variable Best Fit	35.5%	55.9%	63.7%

Table A- 20: Maximum Story Drift Error (Evaluation Method 4) for CAMUS C-1 Test Specimen

Specimen	CAMUS C - 1			
Test	Stage 1	Stage 2	Stage 3	Stage 4
Period (s)	0.43	0.47	0.61	0.70
Drifts	0.352%	0.522%	1.313%	1.849%
FIB 27 (0.3), 3%	52.4%	57.8%	90.6%	92.3%
FIB 27 (0.3), 7%	69.8%	77.8%	84.1%	89.8%
Adebar Upper, 3%	83.3%	87.7%	80.0%	88.8%
Adebar Upper, 7%	91.0%	93.3%	84.2%	89.2%
Adebar Lower, 3%	53.6%	73.9%	83.7%	91.2%
Adebar Lower, 7%	63.5%	84.3%	84.9%	90.8%
FEMA Cracked, 3%	74.9%	79.3%	66.0%	78.2%
FEMA Cracked, 7%	91.5%	90.8%	71.6%	81.8%
FEMA Uncracked, 3%	95.3%	94.0%	71.8%	79.9%
FEMA Uncracked, 7%	93.8%	93.9%	78.2%	86.4%
Brown Iterated Stiffness, 3%	52.4%	78.2%	45.8%	71.7%
Brown Iterated Stiffness, 7%	69.8%	77.8%	35.7%	44.6%
Iterated Stiffness, (0.4), 3%	N/A	N/A	N/A	N/A
Iterated Stiffness, (0.4), 7%	N/A	N/A	N/A	N/A
Doepker Iterated Stiffness, (0.8), 3%	56.1%	67.3%	32.9%	41.4%
Doepker Iterated Stiffness, (0.8), 7%	82.1%	80.9%	67.0%	50.1%
Uniform Best Fit	59.1%	58.9%	35.6%	56.3%
Uniform Best Fit, 3%	61.6%	41.3%	41.4%	51.0%
Uniform Best Fit, 7%	54.0%	66.6%	36.3%	52.3%
Uniform Best Fit, 3% FEMA	61.6%	41.3%	41.6%	56.5%
Uniform Best Fit, 7% FEMA	61.6%	41.3%	33.2%	54.5%
Variable Best Fit	55.2%	55.8%	15.9%	29.1%

Table A- 21: Maximum Story Drift Error (Evaluation Method 4) for CAMUS C-2 Test Specimen

Specimen	CAMUS C - 2		
Test	Stage 2	Stage 3	Stage 4
Period (s)	0.33	0.42	0.61
Drifts	0.082%	0.540%	1.912%
FIB 27 (0.3), 3%	79.9%	No Data	92.4%
FIB 27 (0.3), 7%	81.5%	No Data	92.0%
Adebar Upper, 3%	80.5%	No Data	93.5%
Adebar Upper, 7%	89.7%	No Data	146.5%
Adebar Lower, 3%	90.5%	No Data	95.8%
Adebar Lower, 7%	82.9%	No Data	93.5%
FEMA Cracked, 3%	67.7%	No Data	86.5%
FEMA Cracked, 7%	80.2%	No Data	88.7%
FEMA Uncracked, 3%	89.7%	No Data	89.6%
FEMA Uncracked, 7%	112.8%	No Data	91.7%
Brown Iterated Stiffness, 3%	106.0%	No Data	59.2%
Brown Iterated Stiffness, 7%	71.8%	No Data	76.7%
Iterated Stiffness, (0.4), 3%	N/A	No Data	N/A
Iterated Stiffness, (0.4), 7%	N/A	No Data	N/A
Doepker Iterated Stiffness, (0.8), 3%	92.1%	No Data	61.2%
Doepker Iterated Stiffness, (0.8), 7%	79.4%	No Data	81.3%
Uniform Best Fit	54.4%	No Data	75.6%
Uniform Best Fit, 3%	N/A	No Data	N/A
Uniform Best Fit, 7%	N/A	No Data	N/A
Uniform Best Fit, 3% FEMA	N/A	No Data	N/A
Uniform Best Fit, 7% FEMA	N/A	No Data	N/A
Variable Best Fit	47.5%	No Data	61.1%

Table A- 22: Maximum Story Drift Error (Evaluation Method 4) for CAMUS C-3 Test Specimen

Specimen	CAMUS C - 3			
Test	Stage 1	Stage 2	Stage 3	Stage 4
Period (s)	0.30	0.40	0.57	0.74
Drifts	0.117%	0.347%	1.318%	2.274%
FIB 27 (0.3), 3%	47.4%	58.0%	82.6%	86.3%
FIB 27 (0.3), 7%	63.7%	75.0%	94.2%	89.1%
Adebar Upper, 3%	67.2%	87.4%	92.2%	90.5%
Adebar Upper, 7%	82.5%	91.9%	94.9%	92.2%
Adebar Lower, 3%	67.6%	41.9%	58.8%	93.7%
Adebar Lower, 7%	75.8%	63.1%	73.8%	92.4%
FEMA Cracked, 3%	89.3%	79.3%	86.9%	89.7%
FEMA Cracked, 7%	79.3%	86.5%	91.5%	91.0%
FEMA Uncracked, 3%	93.6%	89.4%	92.8%	87.0%
FEMA Uncracked, 7%	93.1%	92.9%	95.3%	90.2%
Brown Iterated Stiffness, 3%	47.4%	58.0%	82.6%	57.8%
Brown Iterated Stiffness, 7%	63.7%	75.0%	94.2%	63.3%
Iterated Stiffness, (0.4), 3%	N/A	N/A	N/A	N/A
Iterated Stiffness, (0.4), 7%	N/A	N/A	N/A	N/A
Doepker Iterated Stiffness, (0.8), 3%	36.9%	37.7%	78.5%	62.6%
Doepker Iterated Stiffness, (0.8), 7%	64.0%	78.5%	60.2%	66.6%
Uniform Best Fit	44.4%	61.0%	73.6%	72.1%
Uniform Best Fit, 3%	N/A	N/A	N/A	N/A
Uniform Best Fit, 7%	N/A	N/A	N/A	N/A
Uniform Best Fit, 3% FEMA	N/A	N/A	N/A	N/A
Uniform Best Fit, 7% FEMA	N/A	N/A	N/A	N/A
Variable Best Fit	33.0%	56.0%	59.3%	55.2%

Table A- 23: Maximum Story Drift Error (Evaluation Method 4) for CAMUS 2000 Test Specimen

Specimen	CAMUS 2000		
Test	Run 1	Run 2	Run 3
Period (s)	0.187	0.25	0.281
Drifts	0.088%	0.296%	0.384%
FIB 27 (0.3), 3%	174.9%	86.3%	85.3%
FIB 27 (0.3), 7%	92.6%	80.9%	91.4%
Adebar Upper, 3%	123.4%	92.2%	97.9%
Adebar Upper, 7%	112.8%	84.9%	92.1%
Adebar Lower, 3%	103.3%	106.0%	145.1%
Adebar Lower, 7%	88.3%	87.6%	116.8%
FEMA Cracked, 3%	116.1%	106.0%	119.8%
FEMA Cracked, 7%	94.8%	95.6%	93.5%
FEMA Uncracked, 3%	93.1%	89.1%	124.1%
FEMA Uncracked, 7%	84.4%	85.3%	113.8%
Brown Iterated Stiffness, 3%	174.9%	56.7%	107.3%
Brown Iterated Stiffness, 7%	92.6%	77.9%	89.1%
Iterated Stiffness, (0.4), 3%	140.6%	64.7%	122.2%
Iterated Stiffness, (0.4), 7%	79.8%	80.9%	89.2%
Doepker Iterated Stiffness, (0.8), 3%	82.9%	61.9%	114.2%
Doepker Iterated Stiffness, (0.8), 7%	85.4%	76.4%	90.1%
Uniform Best Fit	89.3%	81.6%	91.2%
Uniform Best Fit, 3%	108.0%	68.1%	126.4%
Uniform Best Fit, 7%	89.3%	77.0%	86.2%
Uniform Best Fit, 3% FEMA	N/A	N/A	N/A
Uniform Best Fit, 7% FEMA	N/A	N/A	N/A
Variable Best Fit	78.0%	86.5%	90.6%

Table A- 24: Maximum Story Drift Error (Evaluation Method 4) for Ecoleader Test Specimen

Specimen	CAMUS Ecoleader					
Test	Run 1	Run 3	Run 4	Run 5	Run 6	Run 7
Period (s)	0.22	0.25	0.37	0.40	0.46	0.56
Drifts	0.159%	0.195%	0.623%	0.872%	1.187%	1.303%
FIB 27 (0.3), 3%	No Data	No Data	No Data	No Data	No Data	No Data
FIB 27 (0.3), 7%	No Data	No Data	No Data	No Data	No Data	No Data
Adebar Upper, 3%	No Data	No Data	No Data	No Data	No Data	No Data
Adebar Upper, 7%	No Data	No Data	No Data	No Data	No Data	No Data
Adebar Lower, 3%	No Data	No Data	No Data	No Data	No Data	No Data
Adebar Lower, 7%	No Data	No Data	No Data	No Data	No Data	No Data
FEMA Cracked, 3%	No Data	No Data	No Data	No Data	No Data	No Data
FEMA Cracked, 7%	No Data	No Data	No Data	No Data	No Data	No Data
FEMA Uncracked, 3%	No Data	No Data	No Data	No Data	No Data	No Data
FEMA Uncracked, 7%	No Data	No Data	No Data	No Data	No Data	No Data
Brown Iterated Stiffness, 3%	No Data	No Data	No Data	No Data	No Data	No Data
Brown Iterated Stiffness, 7%	No Data	No Data	No Data	No Data	No Data	No Data
Iterated Stiffness, (0.4), 3%	No Data	No Data	No Data	No Data	No Data	No Data
Iterated Stiffness, (0.4), 7%	No Data	No Data	No Data	No Data	No Data	No Data
Doepker Iterated Stiffness, (0.8), 3%	No Data	No Data	No Data	No Data	No Data	No Data
Doepker Iterated Stiffness, (0.8), 7%	No Data	No Data	No Data	No Data	No Data	No Data
Uniform Best Fit	No Data	No Data	No Data	No Data	No Data	No Data
Uniform Best Fit, 3%	No Data	No Data	No Data	No Data	No Data	No Data
Uniform Best Fit, 7%	No Data	No Data	No Data	No Data	No Data	No Data
Uniform Best Fit, 3% FEMA	No Data	No Data	No Data	No Data	No Data	No Data
Uniform Best Fit, 7% FEMA	No Data	No Data	No Data	No Data	No Data	No Data
Variable Best Fit	No Data	No Data	No Data	No Data	No Data	No Data

Table A- 25: Error in Roof Acceleration Prediction (Evaluation Method 5) for UCSD Test Specimen

Specimen	UCSD		
Test	EQ1	EQ2	EQ3
Period (s)	0.65	0.84	0.96
Drifts	0.271%	0.761%	0.832%
FIB 27 (0.3), 3%	48.3%	5.8%	6.1%
FIB 27 (0.3), 7%	13.4%	1.3%	-59.8%
Adebar Upper, 3%	22.8%	75.7%	-50.7%
Adebar Upper, 7%	-6.3%	83.6%	-50.9%
Adebar Lower, 3%	49.6%	67.7%	-50.8%
Adebar Lower, 7%	11.4%	76.8%	-61.0%
FEMA Cracked, 3%	-23.5%	-12.2%	11.3%
FEMA Cracked, 7%	-33.8%	-39.1%	-33.6%
FEMA Uncracked, 3%	-26.0%	-13.3%	-65.0%
FEMA Uncracked, 7%	-46.0%	-28.3%	-45.5%
Brown Iterated Stiffness, 3%	48.3%	36.9%	-55.4%
Brown Iterated Stiffness, 7%	13.4%	15.9%	-66.4%
Iterated Stiffness, (0.4), 3%	N/A	N/A	N/A
Iterated Stiffness, (0.4), 7%	N/A	N/A	N/A
Doepker Iterated Stiffness, (0.8), 3%	52.8%	36.9%	-55.4%
Doepker Iterated Stiffness, (0.8), 7%	16.1%	20.8%	-67.7%
Uniform Best Fit	28.1%	5.9%	-45.2%
Uniform Best Fit, 3%	52.3%	36.9%	16.5%
Uniform Best Fit, 7%	12.9%	6.5%	-24.5%
Uniform Best Fit, 3% FEMA	52.3%	-6.6%	-37.7%
Uniform Best Fit, 7% FEMA	52.3%	12.9%	-32.5%
Variable Best Fit	32.3%	-2.9%	-46.8%

Table A- 26: Error in Roof Acceleration Prediction (Evaluation Method 5) for CAMUS C-1 Test Specimen

Specimen	**CAMUS C - 1**			
Test	**Stage 1**	**Stage 2**	**Stage 3**	**Stage 4**
Period (s)	0.43	0.47	0.61	0.70
Drifts	0.352%	0.522%	1.313%	1.849%
FIB 27 (0.3), 3%	-21.3%	5.7%	-43.0%	27.2%
FIB 27 (0.3), 7%	-54.6%	-41.7%	-55.9%	-21.3%
Adebar Upper, 3%	-46.5%	-42.2%	-16.2%	144.6%
Adebar Upper, 7%	-74.8%	-71.6%	-38.6%	139.8%
Adebar Lower, 3%	-23.2%	-36.2%	-57.3%	-93.1%
Adebar Lower, 7%	-39.6%	-62.9%	-24.6%	-32.4%
FEMA Cracked, 3%	-28.4%	-30.3%	50.4%	168.6%
FEMA Cracked, 7%	-78.1%	-71.3%	52.6%	172.7%
FEMA Uncracked, 3%	-84.7%	-70.4%	125.7%	385.7%
FEMA Uncracked, 7%	-82.5%	-70.3%	70.2%	242.1%
Brown Iterated Stiffness, 3%	-21.3%	-51.6%	10.9%	107.1%
Brown Iterated Stiffness, 7%	-54.6%	-41.7%	26.1%	41.0%
Iterated Stiffness, (0.4), 3%	N/A	N/A	N/A	N/A
Iterated Stiffness, (0.4), 7%	N/A	N/A	N/A	N/A
Doepker Iterated Stiffness, (0.8), 3%	-31.8%	-24.9%	-0.1%	52.7%
Doepker Iterated Stiffness, (0.8), 7%	82.1%	-58.8%	-79.8%	107.0%
Uniform Best Fit	-34.7%	-33.8%	-5.7%	75.9%
Uniform Best Fit, 3%	-1.3%	-7.4%	0.2%	90.9%
Uniform Best Fit, 7%	-34.5%	-47.3%	-6.8%	83.8%
Uniform Best Fit, 3% FEMA	-1.3%	-7.4%	-38.1%	75.3%
Uniform Best Fit, 7% FEMA	-1.3%	-7.4%	-10.1%	82.6%
Variable Best Fit	-29.5%	-37.0%	-4.8%	84.1%

Table A- 27: Error in Roof Acceleration Prediction (Evaluation Method 5) for CAMUS C-2 Test Specimen

Specimen	**CAMUS C - 2**		
Test	**Stage 2**	**Stage 3**	**Stage 4**
Period (s)	0.33	0.42	0.61
Drifts	0.082%	0.540%	1.912%
FIB 27 (0.3), 3%	-86.6%	-2.7%	85.9%
FIB 27 (0.3), 7%	-78.2%	-49.4%	25.3%
Adebar Upper, 3%	-38.4%	-82.4%	118.9%
Adebar Upper, 7%	-64.3%	-74.7%	98.8%
Adebar Lower, 3%	-96.0%	-22.1%	-61.9%
Adebar Lower, 7%	-83.9%	-50.6%	-36.6%
FEMA Cracked, 3%	-42.4%	-45.4%	200.4%
FEMA Cracked, 7%	-59.2%	-71.2%	167.4%
FEMA Uncracked, 3%	-71.7%	-71.2%	300.1%
FEMA Uncracked, 7%	-69.9%	-75.2%	155.6%
Brown Iterated Stiffness, 3%	-39.4%	8.3%	13.9%
Brown Iterated Stiffness, 7%	-72.1%	-78.1%	63.2%
Iterated Stiffness, (0.4), 3%	N/A	N/A	N/A
Iterated Stiffness, (0.4), 7%	N/A	N/A	N/A
Doepker Iterated Stiffness, (0.8), 3%	-92.5%	-48.6%	164.3%
Doepker Iterated Stiffness, (0.8), 7%	-76.7%	-58.8%	-23.3%
Uniform Best Fit	-27.8%	-78.4%	68.9%
Uniform Best Fit, 3%	N/A	N/A	N/A
Uniform Best Fit, 7%	N/A	N/A	N/A
Uniform Best Fit, 3% FEMA	N/A	N/A	N/A
Uniform Best Fit, 7% FEMA	N/A	N/A	N/A
Variable Best Fit	-22.1%	-83.4%	72.3%

Table A- 28: Error in Roof Acceleration Prediction (Evaluation Method 5) for CAMUS C-3 Test Specimen

Specimen	CAMUS C - 3			
Test	Stage 1	Stage 2	Stage 3	Stage 4
Period (s)	0.30	0.40	0.57	0.74
Drifts	0.117%	0.347%	1.318%	2.274%
FIB 27 (0.3), 3%	-28.2%	37.5%	16.6%	184.6%
FIB 27 (0.3), 7%	-54.5%	-32.4%	-58.2%	100.6%
Adebar Upper, 3%	-31.1%	-23.4%	-8.0%	330.6%
Adebar Upper, 7%	-64.5%	-59.9%	-48.8%	249.6%
Adebar Lower, 3%	-52.4%	-100.6%	71.7%	58.5%
Adebar Lower, 7%	-61.5%	-12.2%	-4.8%	18.6%
FEMA Cracked, 3%	-84.4%	24.3%	39.0%	283.7%
FEMA Cracked, 7%	-79.7%	-25.5%	-7.4%	177.1%
FEMA Uncracked, 3%	-87.3%	-35.8%	-11.1%	396.8%
FEMA Uncracked, 7%	-86.6%	-63.7%	-46.1%	243.5%
Brown Iterated Stiffness, 3%	-28.2%	37.5%	-49.1%	125.2%
Brown Iterated Stiffness, 7%	-54.5%	-32.4%	75.2%	152.9%
Iterated Stiffness, (0.4), 3%	N/A	N/A	N/A	N/A
Iterated Stiffness, (0.4), 7%	N/A	N/A	N/A	N/A
Doepker Iterated Stiffness, (0.8), 3%	-21.5%	69.1%	-57.1%	150.6%
Doepker Iterated Stiffness, (0.8), 7%	-64.6%	-30.6%	61.6%	219.8%
Uniform Best Fit	-35.6%	-3.2%	-46.1%	124.2%
Uniform Best Fit, 3%	N/A	N/A	N/A	N/A
Uniform Best Fit, 7%	N/A	N/A	N/A	N/A
Uniform Best Fit, 3% FEMA	N/A	N/A	N/A	N/A
Uniform Best Fit, 7% FEMA	N/A	N/A	N/A	N/A
Variable Best Fit	-28.8%	5.2%	-41.9%	138.6%

Table A- 29: Error in Roof Acceleration Prediction (Evaluation Method 5) for CAMUS 2000 Test Specimen

Specimen	CAMUS 2000		
Test	Run 1	Run 2	Run 3
Period (s)	0.187	0.25	0.281
Drifts	0.088%	0.296%	0.384%
FIB 27 (0.3), 3%	69.5%	226.3%	-10.1%
FIB 27 (0.3), 7%	-13.6%	195.7%	18.8%
Adebar Upper, 3%	127.4%	293.0%	36.8%
Adebar Upper, 7%	26.1%	221.2%	26.5%
Adebar Lower, 3%	43.8%	347.5%	625.4%
Adebar Lower, 7%	16.5%	144.3%	276.5%
FEMA Cracked, 3%	62.3%	473.3%	507.2%
FEMA Cracked, 7%	-1.3%	229.0%	137.8%
FEMA Uncracked, 3%	64.1%	166.7%	378.7%
FEMA Uncracked, 7%	28.0%	116.6%	246.3%
Brown Iterated Stiffness, 3%	69.5%	203.1%	140.8%
Brown Iterated Stiffness, 7%	-13.6%	183.2%	62.6%
Iterated Stiffness, (0.4), 3%	138.0%	198.8%	159.3%
Iterated Stiffness, (0.4), 7%	-52.0%	195.7%	59.0%
Doepker Iterated Stiffness, (0.8), 3%	-2.5%	299.5%	138.1%
Doepker Iterated Stiffness, (0.8), 7%	-23.8%	178.9%	89.3%
Uniform Best Fit	10.2%	144.3%	88.4%
Uniform Best Fit, 3%	76.6%	194.4%	163.5%
Uniform Best Fit, 7%	10.4%	237.2%	137.5%
Uniform Best Fit, 3% FEMA	N/A	N/A	N/A
Uniform Best Fit, 7% FEMA	N/A	N/A	N/A
Variable Best Fit	-32.7%	159.6%	82.3%

Table A- 30: Error in Roof Acceleration Prediction (Evaluation Method 5) for Ecoleader Test Specimen

Specimen	CAMUS Ecoleader					
Test	**Run 1**	**Run 3**	**Run 4**	**Run 5**	**Run 6**	**Run 7**
Period (s)	0.22	0.25	0.37	0.40	0.46	0.56
Drifts	0.159%	0.195%	0.623%	0.872%	1.187%	1.303%
FIB 27 (0.3), 3%	-4.5%	-31.5%	-2.1%	-35.9%	45.0%	8.0%
FIB 27 (0.3), 7%	-18.1%	-58.0%	35.5%	-54.9%	-19.2%	7.2%
Adebar Upper, 3%	-22.1%	-69.1%	15.0%	140.3%	31.6%	181.0%
Adebar Upper, 7%	-36.4%	-63.7%	-37.8%	-48.0%	-8.9%	11.5%
Adebar Lower, 3%	18.6%	-75.1%	144.8%	127.7%	47.8%	93.7%
Adebar Lower, 7%	1.0%	-62.8%	87.1%	90.9%	-8.9%	56.7%
FEMA Cracked, 3%	18.7%	-89.0%	146.7%	202.9%	148.1%	180.5%
FEMA Cracked, 7%	2.4%	-92.9%	65.0%	73.0%	132.4%	114.0%
FEMA Uncracked, 3%	23.4%	-37.4%	102.2%	190.6%	179.8%	-80.7%
FEMA Uncracked, 7%	-1.4%	-45.8%	-35.9%	77.4%	59.0%	57.7%
Brown Iterated Stiffness, 3%	-4.5%	-31.5%	40.5%	117.7%	46.6%	517.0%
Brown Iterated Stiffness, 7%	-18.1%	-58.0%	35.5%	-54.9%	-13.2%	-32.4%
Iterated Stiffness, (0.4), 3%	N/A	N/A	N/A	N/A	N/A	N/A
Iterated Stiffness, (0.4), 7%	N/A	N/A	N/A	N/A	N/A	N/A
Doepker Iterated Stiffness, (0.8), 3%	-0.6%	-88.1%	-2.1%	46.3%	124.9%	270.0%
Doepker Iterated Stiffness, (0.8), 7%	-0.7%	-81.8%	-3.2%	-54.9%	-15.3%	29.3%
Uniform Best Fit	-19.7%	-64.5%	-11.4%	64.2%	108.2%	99.9%
Uniform Best Fit, 3%	N/A	N/A	N/A	N/A	N/A	N/A
Uniform Best Fit, 7%	N/A	N/A	N/A	N/A	N/A	N/A
Uniform Best Fit, 3% FEMA	N/A	N/A	N/A	N/A	N/A	N/A
Uniform Best Fit, 7% FEMA	N/A	N/A	N/A	N/A	N/A	N/A
Variable Best Fit	N/A	N/A	N/A	N/A	N/A	N/A

Table A- 31: Total Acceleration Error Normalized with Respect to Max Roof Acceleration (Evaluation Method 6) for UCSD Test Specimen

Specimen	UCSD		
Test	EQ1	EQ2	EQ3
Period (s)	0.65	0.84	0.96
Drifts	0.271%	0.761%	0.832%
Adebar Lower, 3%	20.1%	19.6%	25.4%
Adebar Lower, 7%	5.0%	13.1%	23.0%
FEMA Cracked, 3%	12.6%	11.7%	6.4%
FEMA Cracked, 7%	14.2%	16.5%	16.4%
FEMA Uncracked, 3%	12.2%	12.0%	23.7%
FEMA Uncracked, 7%	16.6%	16.7%	22.2%
Brown Iterated Stiffness, 3%	20.8%	20.8%	13.9%
Brown Iterated Stiffness, 7%	10.8%	6.4%	24.4%
Iterated Stiffness, (0.4), 3%	N/A	N/A	N/A
Iterated Stiffness, (0.4), 7%	N/A	N/A	N/A
Doepker Iterated Stiffness, (0.8), 3%	17.9%	20.8%	13.9%
Doepker Iterated Stiffness, (0.8), 7%	6.7%	5.8%	23.2%
Uniform Best Fit	8.5%	8.1%	17.6%
Uniform Best Fit, 3%	16.6%	20.8%	2.3%
Uniform Best Fit, 7%	5.2%	9.7%	10.0%
Uniform Best Fit, 3% FEMA	16.6%	N/A	N/A
Uniform Best Fit, 7% FEMA	16.6%	N/A	N/A
Variable Best Fit	9.4%	10.7%	17.1%

Table A- 32: Total Acceleration Error Normalized with Respect to Max Roof Acceleration (Evaluation Method 6) for CAMUS C-1 Test Specimen

Specimen	CAMUS C - 1			
Test	Stage 1	Stage 2	Stage 3	Stage 4
Period (s)	0.43	0.47	0.61	0.70
Drifts	0.352%	0.522%	1.313%	1.849%
Adebar Lower, 3%	N/A	N/A	N/A	N/A
Adebar Lower, 7%	N/A	N/A	N/A	N/A
FEMA Cracked, 3%	N/A	N/A	N/A	N/A
FEMA Cracked, 7%	N/A	N/A	N/A	N/A
FEMA Uncracked, 3%	N/A	N/A	N/A	N/A
FEMA Uncracked, 7%	N/A	N/A	N/A	N/A
Brown Iterated Stiffness, 3%	N/A	N/A	N/A	N/A
Brown Iterated Stiffness, 7%	N/A	N/A	N/A	N/A
Iterated Stiffness, (0.4), 3%	N/A	N/A	N/A	N/A
Iterated Stiffness, (0.4), 7%	N/A	N/A	N/A	N/A
Doepker Iterated Stiffness, (0.8), 3%	N/A	N/A	N/A	N/A
Doepker Iterated Stiffness, (0.8), 7%	N/A	N/A	N/A	N/A
Uniform Best Fit	N/A	N/A	N/A	N/A
Uniform Best Fit, 3%	N/A	N/A	N/A	N/A
Uniform Best Fit, 7%	N/A	N/A	N/A	N/A
Uniform Best Fit, 3% FEMA	N/A	N/A	N/A	N/A
Uniform Best Fit, 7% FEMA	N/A	N/A	N/A	N/A
Variable Best Fit	N/A	N/A	N/A	N/A

Table A- 33: Total Acceleration Error Normalized with Respect to Max Roof Acceleration (Evaluation Method 6) for CAMUS C-2 Test Specimen

Specimen	CAMUS C - 2		
Test	Stage 2	Stage 3	Stage 4
Period (s)	0.33	0.42	0.61
Drifts	0.082%	0.540%	1.912%
Adebar Lower, 3%	N/A	N/A	N/A
Adebar Lower, 7%	N/A	N/A	N/A
FEMA Cracked, 3%	N/A	N/A	N/A
FEMA Cracked, 7%	N/A	N/A	N/A
FEMA Uncracked, 3%	N/A	N/A	N/A
FEMA Uncracked, 7%	N/A	N/A	N/A
Brown Iterated Stiffness, 3%	N/A	N/A	N/A
Brown Iterated Stiffness, 7%	N/A	N/A	N/A
Iterated Stiffness, (0.4), 3%	N/A	N/A	N/A
Iterated Stiffness, (0.4), 7%	N/A	N/A	N/A
Doepker Iterated Stiffness, (0.8), 3%	N/A	N/A	N/A
Doepker Iterated Stiffness, (0.8), 7%	N/A	N/A	N/A
Uniform Best Fit	N/A	N/A	N/A
Uniform Best Fit, 3%	N/A	N/A	N/A
Uniform Best Fit, 7%	N/A	N/A	N/A
Uniform Best Fit, 3% FEMA	N/A	N/A	N/A
Uniform Best Fit, 7% FEMA	N/A	N/A	N/A
Variable Best Fit	N/A	N/A	N/A

Table A- 34: Total Acceleration Error Normalized with Respect to Max Roof Acceleration (Evaluation Method 6) for CAMUS C-3 Test Specimen

Specimen	CAMUS C - 3			
Test	Stage 1	Stage 2	Stage 3	Stage 4
Period (s)	0.30	0.40	0.57	0.74
Drifts	0.117%	0.347%	1.318%	2.274%
Adebar Lower, 3%	N/A	N/A	N/A	N/A
Adebar Lower, 7%	N/A	N/A	N/A	N/A
FEMA Cracked, 3%	N/A	N/A	N/A	N/A
FEMA Cracked, 7%	N/A	N/A	N/A	N/A
FEMA Uncracked, 3%	N/A	N/A	N/A	N/A
FEMA Uncracked, 7%	N/A	N/A	N/A	N/A
Brown Iterated Stiffness, 3%	N/A	N/A	N/A	N/A
Brown Iterated Stiffness, 7%	N/A	N/A	N/A	N/A
Iterated Stiffness, (0.4), 3%	N/A	N/A	N/A	N/A
Iterated Stiffness, (0.4), 7%	N/A	N/A	N/A	N/A
Doepker Iterated Stiffness, (0.8), 3%	N/A	N/A	N/A	N/A
Doepker Iterated Stiffness, (0.8), 7%	N/A	N/A	N/A	N/A
Uniform Best Fit	N/A	N/A	N/A	N/A
Uniform Best Fit, 3%	N/A	N/A	N/A	N/A
Uniform Best Fit, 7%	N/A	N/A	N/A	N/A
Uniform Best Fit, 3% FEMA	N/A	N/A	N/A	N/A
Uniform Best Fit, 7% FEMA	N/A	N/A	N/A	N/A
Variable Best Fit	N/A	N/A	N/A	N/A

Table A- 35: Total Acceleration Error Normalized with Respect to Max Roof Acceleration (Evaluation Method 6) for CAMUS 2000 Test Specimen

Specimen	CAMUS 2000		
Test	Run 1	Run 2	Run 3
Period (s)	0.187	0.25	0.281
Drifts	0.088%	0.296%	0.384%
Adebar Lower, 3%	56.6%	No Data	207.4%
Adebar Lower, 7%	18.7%	No Data	102.8%
FEMA Cracked, 3%	114.7%	No Data	177.7%
FEMA Cracked, 7%	38.2%	No Data	29.2%
FEMA Uncracked, 3%	72.6%	No Data	122.5%
FEMA Uncracked, 7%	18.6%	No Data	94.2%
Brown Iterated Stiffness, 3%	38.0%	No Data	44.6%
Brown Iterated Stiffness, 7%	17.6%	No Data	16.5%
Iterated Stiffness, (0.4), 3%	70.4%	No Data	50.2%
Iterated Stiffness, (0.4), 7%	44.7%	No Data	16.1%
Doepker Iterated Stiffness, (0.8), 3%	54.0%	No Data	47.0%
Doepker Iterated Stiffness, (0.8), 7%	53.3%	No Data	23.5%
Uniform Best Fit	17.5%	No Data	20.0%
Uniform Best Fit, 3%	75.3%	No Data	48.8%
Uniform Best Fit, 7%	17.6%	No Data	32.3%
Uniform Best Fit, 3% FEMA	N/A	No Data	N/A
Uniform Best Fit, 7% FEMA	N/A	No Data	N/A
Variable Best Fit	29.7%	No Data	24.2%

Table A- 36: Total Acceleration Error Normalized with Respect to Max Roof Acceleration (Evaluation Method 6) for Ecoleader Test Specimen

Specimen	CAMUS Ecoleader					
Test	Run 1	Run 3	Run 4	Run 5	Run 6	Run 7
Period (s)	0.22	0.25	0.37	0.40	0.46	0.56
Drifts	0.159%	0.195%	0.623%	0.872%	1.187%	1.303%
Adebar Lower, 3%	No Data	No Data	No Data	No Data	No Data	No Data
Adebar Lower, 7%	No Data	No Data	No Data	No Data	No Data	No Data
FEMA Cracked, 3%	No Data	No Data	No Data	No Data	No Data	No Data
FEMA Cracked, 7%	No Data	No Data	No Data	No Data	No Data	No Data
FEMA Uncracked, 3%	No Data	No Data	No Data	No Data	No Data	No Data
FEMA Uncracked, 7%	No Data	No Data	No Data	No Data	No Data	No Data
Brown Iterated Stiffness, 3%	No Data	No Data	No Data	No Data	No Data	No Data
Brown Iterated Stiffness, 7%	No Data	No Data	No Data	No Data	No Data	No Data
Iterated Stiffness, (0.4), 3%	No Data	No Data	No Data	No Data	No Data	No Data
Iterated Stiffness, (0.4), 7%	No Data	No Data	No Data	No Data	No Data	No Data
Doepker Iterated Stiffness, (0.8), 3%	No Data	No Data	No Data	No Data	No Data	No Data
Doepker Iterated Stiffness, (0.8), 7%	No Data	No Data	No Data	No Data	No Data	No Data
Uniform Best Fit	No Data	No Data	No Data	No Data	No Data	No Data
Uniform Best Fit, 3%	No Data	No Data	No Data	No Data	No Data	No Data
Uniform Best Fit, 7%	No Data	No Data	No Data	No Data	No Data	No Data
Uniform Best Fit, 3% FEMA	No Data	No Data	No Data	No Data	No Data	No Data
Uniform Best Fit, 7% FEMA	No Data	No Data	No Data	No Data	No Data	No Data
Variable Best Fit	No Data	No Data	No Data	No Data	No Data	No Data

Table A- 37: Maximum Story Acceleration Error (Evaluation Method 7) for UCSD Test Specimen

Specimen	UCSD		
Test	EQ1	EQ2	EQ3
Period (s)	0.65	0.84	0.96
Drifts	0.271%	0.761%	0.832%
Adebar Lower, 3%	43.9%	45.1%	34.9%
Adebar Lower, 7%	10.5%	20.6%	41.9%
FEMA Cracked, 3%	20.8%	23.3%	9.8%
FEMA Cracked, 7%	29.9%	35.2%	23.6%
FEMA Uncracked, 3%	23.0%	27.7%	44.6%
FEMA Uncracked, 7%	40.7%	25.5%	31.8%
Brown Iterated Stiffness, 3%	42.8%	33.2%	38.0%
Brown Iterated Stiffness, 7%	18.2%	14.3%	45.5%
Iterated Stiffness, (0.4), 3%	N/A	N/A	N/A
Iterated Stiffness, (0.4), 7%	N/A	N/A	N/A
Doepker Iterated Stiffness, (0.8), 3%	46.7%	33.2%	38.0%
Doepker Iterated Stiffness, (0.8), 7%	14.3%	18.8%	46.4%
Uniform Best Fit	24.8%	12.7%	31.0%
Uniform Best Fit, 3%	46.3%	33.2%	11.3%
Uniform Best Fit, 7%	11.4%	20.3%	16.8%
Uniform Best Fit, 3% FEMA	46.3%	N/A	N/A
Uniform Best Fit, 7% FEMA	46.3%	N/A	N/A
Variable Best Fit	28.6%	18.6%	32.1%

Table A- 38: Maximum Story Acceleration Error (Evaluation Method 7) for CAMUS C-1 Test Specimen

Specimen	CAMUS C - 1			
Test	Stage 1	Stage 2	Stage 3	Stage 4
Period (s)	0.43	0.47	0.61	0.70
Drifts	0.352%	0.522%	1.313%	1.849%
Adebar Lower, 3%	N/A	N/A	N/A	N/A
Adebar Lower, 7%	N/A	N/A	N/A	N/A
FEMA Cracked, 3%	N/A	N/A	N/A	N/A
FEMA Cracked, 7%	N/A	N/A	N/A	N/A
FEMA Uncracked, 3%	N/A	N/A	N/A	N/A
FEMA Uncracked, 7%	N/A	N/A	N/A	N/A
Brown Iterated Stiffness, 3%	N/A	N/A	N/A	N/A
Brown Iterated Stiffness, 7%	N/A	N/A	N/A	N/A
Iterated Stiffness, (0.4), 3%	N/A	N/A	N/A	N/A
Iterated Stiffness, (0.4), 7%	N/A	N/A	N/A	N/A
Doepker Iterated Stiffness, (0.8), 3%	N/A	N/A	N/A	N/A
Doepker Iterated Stiffness, (0.8), 7%	N/A	N/A	N/A	N/A
Uniform Best Fit	N/A	N/A	N/A	N/A
Uniform Best Fit, 3%	N/A	N/A	N/A	N/A
Uniform Best Fit, 7%	N/A	N/A	N/A	N/A
Uniform Best Fit, 3% FEMA	N/A	N/A	N/A	N/A
Uniform Best Fit, 7% FEMA	N/A	N/A	N/A	N/A
Variable Best Fit	N/A	N/A	N/A	N/A

Table A- 39: Maximum Story Acceleration Error (Evaluation Method 7) for CAMUS C-2 Test Specimen

Specimen	CAMUS C - 2		
Test	Stage 2	Stage 3	Stage 4
Period (s)	0.33	0.42	0.61
Drifts	0.082%	0.540%	1.912%
Adebar Lower, 3%	N/A	N/A	N/A
Adebar Lower, 7%	N/A	N/A	N/A
FEMA Cracked, 3%	N/A	N/A	N/A
FEMA Cracked, 7%	N/A	N/A	N/A
FEMA Uncracked, 3%	N/A	N/A	N/A
FEMA Uncracked, 7%	N/A	N/A	N/A
Brown Iterated Stiffness, 3%	N/A	N/A	N/A
Brown Iterated Stiffness, 7%	N/A	N/A	N/A
Iterated Stiffness, (0.4), 3%	N/A	N/A	N/A
Iterated Stiffness, (0.4), 7%	N/A	N/A	N/A
Doepker Iterated Stiffness, (0.8), 3%	N/A	N/A	N/A
Doepker Iterated Stiffness, (0.8), 7%	N/A	N/A	N/A
Uniform Best Fit	N/A	N/A	N/A
Uniform Best Fit, 3%	N/A	N/A	N/A
Uniform Best Fit, 7%	N/A	N/A	N/A
Uniform Best Fit, 3% FEMA	N/A	N/A	N/A
Uniform Best Fit, 7% FEMA	N/A	N/A	N/A
Variable Best Fit	N/A	N/A	N/A

Table A- 40: Maximum Story Acceleration Error (Evaluation Method 7) for CAMUS C-3 Test Specimen

Specimen	CAMUS C - 3			
Test	Stage 1	Stage 2	Stage 3	Stage 4
Period (s)	0.30	0.40	0.57	0.74
Drifts	0.117%	0.347%	1.318%	2.274%
Adebar Lower, 3%	N/A	N/A	N/A	N/A
Adebar Lower, 7%	N/A	N/A	N/A	N/A
FEMA Cracked, 3%	N/A	N/A	N/A	N/A
FEMA Cracked, 7%	N/A	N/A	N/A	N/A
FEMA Uncracked, 3%	N/A	N/A	N/A	N/A
FEMA Uncracked, 7%	N/A	N/A	N/A	N/A
Brown Iterated Stiffness, 3%	N/A	N/A	N/A	N/A
Brown Iterated Stiffness, 7%	N/A	N/A	N/A	N/A
Iterated Stiffness, (0.4), 3%	N/A	N/A	N/A	N/A
Iterated Stiffness, (0.4), 7%	N/A	N/A	N/A	N/A
Doepker Iterated Stiffness, (0.8), 3%	N/A	N/A	N/A	N/A
Doepker Iterated Stiffness, (0.8), 7%	N/A	N/A	N/A	N/A
Uniform Best Fit	N/A	N/A	N/A	N/A
Uniform Best Fit, 3%	N/A	N/A	N/A	N/A
Uniform Best Fit, 7%	N/A	N/A	N/A	N/A
Uniform Best Fit, 3% FEMA	N/A	N/A	N/A	N/A
Uniform Best Fit, 7% FEMA	N/A	N/A	N/A	N/A
Variable Best Fit	N/A	N/A	N/A	N/A

Table A- 41: Maximum Story Acceleration Error (Evaluation Method 7) for CAMUS 2000 Test Specimen

Specimen	CAMUS 2000		
Test	Run 1	Run 2	Run 3
Period (s)	0.187	0.25	0.281
Drifts	0.088%	0.296%	0.384%
Adebar Lower, 3%	114.1%	No Data	355.3%
Adebar Lower, 7%	47.5%	No Data	180.0%
FEMA Cracked, 3%	200.3%	No Data	306.8%
FEMA Cracked, 7%	65.7%	No Data	57.6%
FEMA Uncracked, 3%	127.2%	No Data	209.1%
FEMA Uncracked, 7%	43.7%	No Data	166.4%
Brown Iterated Stiffness, 3%	67.2%	No Data	79.1%
Brown Iterated Stiffness, 7%	45.6%	No Data	26.9%
Iterated Stiffness, (0.4), 3%	112.8%	No Data	75.4%
Iterated Stiffness, (0.4), 7%	82.5%	No Data	26.1%
Doepker Iterated Stiffness, (0.8), 3%	103.5%	No Data	83.9%
Doepker Iterated Stiffness, (0.8), 7%	98.5%	No Data	41.4%
Uniform Best Fit	47.0%	No Data	37.0%
Uniform Best Fit, 3%	137.8%	No Data	75.8%
Uniform Best Fit, 7%	47.0%	No Data	57.5%
Uniform Best Fit, 3% FEMA	N/A	No Data	N/A
Uniform Best Fit, 7% FEMA	N/A	No Data	N/A
Variable Best Fit	52.2%	No Data	34.4%

Table A- 42: Maximum Story Acceleration Error (Evaluation Method 7) for Ecoleader Test Specimen

Specimen	CAMUS Ecoleader					
Test	Run 1	Run 3	Run 4	Run 5	Run 6	Run 7
Period (s)	0.22	0.25	0.37	0.40	0.46	0.56
Drifts	0.159%	0.195%	0.623%	0.872%	1.187%	1.303%
Adebar Lower, 3%	No Data	No Data	No Data	No Data	No Data	No Data
Adebar Lower, 7%	No Data	No Data	No Data	No Data	No Data	No Data
FEMA Cracked, 3%	No Data	No Data	No Data	No Data	No Data	No Data
FEMA Cracked, 7%	No Data	No Data	No Data	No Data	No Data	No Data
FEMA Uncracked, 3%	No Data	No Data	No Data	No Data	No Data	No Data
FEMA Uncracked, 7%	No Data	No Data	No Data	No Data	No Data	No Data
Brown Iterated Stiffness, 3%	No Data	No Data	No Data	No Data	No Data	No Data
Brown Iterated Stiffness, 7%	No Data	No Data	No Data	No Data	No Data	No Data
Iterated Stiffness, (0.4), 3%	No Data	No Data	No Data	No Data	No Data	No Data
Iterated Stiffness, (0.4), 7%	No Data	No Data	No Data	No Data	No Data	No Data
Doepker Iterated Stiffness, (0.8), 3%	No Data	No Data	No Data	No Data	No Data	No Data
Doepker Iterated Stiffness, (0.8), 7%	No Data	No Data	No Data	No Data	No Data	No Data
Uniform Best Fit	No Data	No Data	No Data	No Data	No Data	No Data
Uniform Best Fit, 3%	No Data	No Data	No Data	No Data	No Data	No Data
Uniform Best Fit, 7%	No Data	No Data	No Data	No Data	No Data	No Data
Uniform Best Fit, 3% FEMA	No Data	No Data	No Data	No Data	No Data	No Data
Uniform Best Fit, 7% FEMA	No Data	No Data	No Data	No Data	No Data	No Data
Variable Best Fit	No Data	No Data	No Data	No Data	No Data	No Data

Table A- 43: Error in Base Shear Prediction (Evaluation Method 8) for UCSD Test Specimen

Specimen	**UCSD**		
Test	**EQ1**	**EQ2**	**EQ3**
Period (s)	0.65	0.84	0.96
Drifts	0.271%	0.761%	0.832%
FIB 27 (0.3), 3%	-23.7%	3.6%	8.8%
FIB 27 (0.3), 7%	-28.5%	-3.3%	52.5%
Adebar Upper, 3%	-143.1%	43.2%	68.9%
Adebar Upper, 7%	-107.1%	-5.0%	57.5%
Adebar Lower, 3%	27.1%	16.0%	66.6%
Adebar Lower, 7%	-10.6%	-20.1%	60.6%
FEMA Cracked, 3%	-35.4%	-17.4%	-3.5%
FEMA Cracked, 7%	-11.6%	-26.9%	47.0%
FEMA Uncracked, 3%	-15.0%	0.8%	61.5%
FEMA Uncracked, 7%	-33.6%	-32.8%	59.0%
Brown Iterated Stiffness, 3%	-23.7%	-2.1%	32.4%
Brown Iterated Stiffness, 7%	-28.5%	0.5%	63.1%
Iterated Stiffness, (0.4), 3%	N/A	N/A	N/A
Iterated Stiffness, (0.4), 7%	N/A	N/A	N/A
Doepker Iterated Stiffness, (0.8), 3%	-13.4%	-2.1%	32.4%
Doepker Iterated Stiffness, (0.8), 7%	-18.2%	-1.5%	59.7%
Uniform Best Fit	0.8%	-21.5%	48.5%
Uniform Best Fit, 3%	18.2%	-2.1%	4.0%
Uniform Best Fit, 7%	-10.5%	-21.4%	31.6%
Uniform Best Fit, 3% FEMA	18.2%	-28.9%	44.3%
Uniform Best Fit, 7% FEMA	18.2%	-17.3%	37.8%
Variable Best Fit	-0.8%	-33.5%	47.5%

Table A- 44: Error in Base Shear Prediction (Evaluation Method 8) for CAMUS C-1 Test Specimen

Specimen	**CAMUS C - 1**			
Test	**Stage 1**	**Stage 2**	**Stage 3**	**Stage 4**
Period (s)	0.43	0.47	0.61	0.70
Drifts	0.352%	0.522%	1.313%	1.849%
FIB 27 (0.3), 3%	19.6%	16.8%	-60.9%	-49.1%
FIB 27 (0.3), 7%	-23.6%	-38.8%	-29.7%	-28.0%
Adebar Upper, 3%	-16.8%	-32.2%	79.0%	53.1%
Adebar Upper, 7%	-54.5%	-62.9%	42.7%	48.3%
Adebar Lower, 3%	3.7%	-35.3%	-34.6%	-39.9%
Adebar Lower, 7%	-18.2%	-60.8%	-44.2%	-42.2%
FEMA Cracked, 3%	-2.2%	-9.0%	137.4%	143.1%
FEMA Cracked, 7%	-66.8%	-59.2%	95.0%	99.7%
FEMA Uncracked, 3%	-72.9%	-62.3%	178.2%	216.1%
FEMA Uncracked, 7%	-64.1%	-61.2%	115.7%	112.0%
Brown Iterated Stiffness, 3%	19.6%	-47.7%	-5.6%	-57.9%
Brown Iterated Stiffness, 7%	-23.6%	-38.8%	52.6%	-13.8%
Iterated Stiffness, (0.4), 3%	N/A	N/A	N/A	N/A
Iterated Stiffness, (0.4), 7%	N/A	N/A	N/A	N/A
Doepker Iterated Stiffness, (0.8), 3%	14.2%	-30.8%	-0.8%	-4.2%
Doepker Iterated Stiffness, (0.8), 7%	-48.2%	-50.0%	-11.3%	18.2%
Uniform Best Fit	-21.2%	-26.0%	7.9%	-11.9%
Uniform Best Fit, 3%	32.5%	5.1%	24.7%	-2.1%
Uniform Best Fit, 7%	-11.2%	-39.8%	6.7%	-4.8%
Uniform Best Fit, 3% FEMA	32.5%	5.1%	-2.3%	-12.3%
Uniform Best Fit, 7% FEMA	32.5%	5.1%	10.2%	-8.3%
Variable Best Fit	-20.3%	-28.5%	11.0%	-10.9%

Table A- 45: Error in Base Shear Prediction (Evaluation Method 8) for CAMUS C-2 Test Specimen

Specimen	CAMUS C - 2		
Test	Stage 2	Stage 3	Stage 4
Period (s)	0.33	0.42	0.61
Drifts	0.082%	0.540%	1.912%
FIB 27 (0.3), 3%	-62.4%	27.8%	46.3%
FIB 27 (0.3), 7%	-66.6%	-26.9%	57.5%
Adebar Upper, 3%	-31.3%	-53.9%	157.3%
Adebar Upper, 7%	-64.2%	-56.9%	179.2%
Adebar Lower, 3%	-84.7%	-8.9%	-22.5%
Adebar Lower, 7%	-72.0%	-42.5%	21.0%
FEMA Cracked, 3%	-7.8%	-10.8%	322.5%
FEMA Cracked, 7%	-44.1%	-47.8%	253.5%
FEMA Uncracked, 3%	-57.9%	-50.3%	363.3%
FEMA Uncracked, 7%	-71.5%	-55.0%	278.2%
Brown Iterated Stiffness, 3%	-3.4%	50.3%	74.6%
Brown Iterated Stiffness, 7%	-58.7%	-71.7%	136.8%
Iterated Stiffness, (0.4), 3%	N/A	N/A	N/A
Iterated Stiffness, (0.4), 7%	N/A	N/A	N/A
Doepker Iterated Stiffness, (0.8), 3%	-86.4%	-22.8%	161.4%
Doepker Iterated Stiffness, (0.8), 7%	-61.9%	-50.7%	110.6%
Uniform Best Fit	-0.5%	-62.4%	86.2%
Uniform Best Fit, 3%	N/A	N/A	N/A
Uniform Best Fit, 7%	N/A	N/A	N/A
Uniform Best Fit, 3% FEMA	N/A	N/A	N/A
Uniform Best Fit, 7% FEMA	N/A	N/A	N/A
Variable Best Fit	0.5%	-59.7%	86.6%

Table A- 46: Error in Base Shear Prediction (Evaluation Method 8) for CAMUS C-3 Test Specimen

Specimen	**CAMUS C - 3**			
Test	**Stage 1**	**Stage 2**	**Stage 3**	**Stage 4**
Period (s)	0.30	0.40	0.57	0.74
Drifts	0.117%	0.347%	1.318%	2.274%
FIB 27 (0.3), 3%	-30.0%	6.2%	0.3%	114.3%
FIB 27 (0.3), 7%	-51.4%	-36.4%	-66.5%	72.9%
Adebar Upper, 3%	-11.3%	-36.2%	-10.2%	195.2%
Adebar Upper, 7%	-52.5%	-58.5%	-37.2%	142.3%
Adebar Lower, 3%	-61.5%	33.5%	-105.9%	-14.1%
Adebar Lower, 7%	-108.6%	-15.0%	-74.4%	8.2%
FEMA Cracked, 3%	-76.8%	-18.4%	19.1%	151.7%
FEMA Cracked, 7%	-54.5%	-46.5%	-23.4%	229.4%
FEMA Uncracked, 3%	-80.1%	-38.9%	-4.8%	368.6%
FEMA Uncracked, 7%	-78.6%	-58.5%	-37.2%	255.3%
Brown Iterated Stiffness, 3%	-30.0%	6.2%	-62.7%	-1.5%
Brown Iterated Stiffness, 7%	-51.4%	-36.4%	51.9%	100.9%
Iterated Stiffness, (0.4), 3%	N/A	N/A	N/A	N/A
Iterated Stiffness, (0.4), 7%	N/A	N/A	N/A	N/A
Doepker Iterated Stiffness, (0.8), 3%	-6.3%	32.8%	-37.9%	-79.5%
Doepker Iterated Stiffness, (0.8), 7%	-31.1%	-43.5%	57.3%	93.9%
Uniform Best Fit	3.0%	-21.7%	-40.4%	-2.5%
Uniform Best Fit, 3%	N/A	N/A	N/A	N/A
Uniform Best Fit, 7%	N/A	N/A	N/A	N/A
Uniform Best Fit, 3% FEMA	N/A	N/A	N/A	N/A
Uniform Best Fit, 7% FEMA	N/A	N/A	N/A	N/A
Variable Best Fit	-2.0%	-20.3%	-39.6%	-0.2%

Table A- 47: Error in Base Shear Prediction (Evaluation Method 8) for CAMUS 2000 Test Specimen

Specimen	CAMUS 2000		
Test	Run 1	Run 2	Run 3
Period (s)	0.187	0.25	0.281
Drifts	0.088%	0.296%	0.384%
FIB 27 (0.3), 3%	10.7%	-24.0%	105.9%
FIB 27 (0.3), 7%	-51.2%	-5.6%	83.6%
Adebar Upper, 3%	-65.9%	-29.1%	12.7%
Adebar Upper, 7%	-110.7%	-12.7%	73.2%
Adebar Lower, 3%	-38.3%	-23.9%	-55.3%
Adebar Lower, 7%	-36.3%	-4.6%	6.7%
FEMA Cracked, 3%	-83.1%	3.1%	21.4%
FEMA Cracked, 7%	-51.9%	-7.3%	86.4%
FEMA Uncracked, 3%	2.4%	-17.6%	-71.0%
FEMA Uncracked, 7%	-20.0%	-3.4%	18.5%
Brown Iterated Stiffness, 3%	10.7%	78.0%	291.0%
Brown Iterated Stiffness, 7%	-51.2%	2.2%	144.3%
Iterated Stiffness, (0.4), 3%	-29.7%	47.0%	305.2%
Iterated Stiffness, (0.4), 7%	-26.6%	-5.6%	140.5%
Doepker Iterated Stiffness, (0.8), 3%	39.5%	44.7%	306.2%
Doepker Iterated Stiffness, (0.8), 7%	-31.9%	6.3%	163.0%
Uniform Best Fit	-41.4%	-19.2%	57.9%
Uniform Best Fit, 3%	-42.2%	33.9%	297.1%
Uniform Best Fit, 7%	-41.4%	-3.4%	165.5%
Uniform Best Fit, 3% FEMA	N/A	N/A	N/A
Uniform Best Fit, 7% FEMA	N/A	N/A	N/A
Variable Best Fit	-41.3%	-12.6%	86.1%

Table A- 48: Error in Base Shear Prediction (Evaluation Method 8) for Ecoleader Test Specimen

Specimen	CAMUS Ecoleader					
Test	Run 1	Run 3	Run 4	Run 5	Run 6	Run 7
Period (s)	0.22	0.25	0.37	0.40	0.46	0.56
Drifts	0.159%	0.195%	0.623%	0.872%	1.187%	1.303%
FIB 27 (0.3), 3%	-17.5%	-0.7%	77.7%	-39.2%	-28.3%	-58.5%
FIB 27 (0.3), 7%	-24.5%	-65.5%	-4.8%	-75.8%	-62.8%	-112.5%
Adebar Upper, 3%	-9.3%	-46.7%	131.0%	45.8%	23.1%	110.6%
Adebar Upper, 7%	-19.3%	-60.6%	54.2%	51.6%	-34.2%	63.7%
Adebar Lower, 3%	-5.2%	-70.7%	68.5%	93.5%	142.4%	34.3%
Adebar Lower, 7%	-10.3%	-70.0%	-10.3%	89.8%	53.4%	-112.4%
FEMA Cracked, 3%	-21.8%	-41.4%	241.0%	-34.1%	77.3%	31.0%
FEMA Cracked, 7%	-27.5%	-51.3%	93.6%	-38.0%	8.6%	-34.8%
FEMA Uncracked, 3%	8.6%	-61.1%	83.8%	49.0%	16.9%	237.1%
FEMA Uncracked, 7%	-8.5%	-61.3%	6.0%	-12.2%	27.1%	22.7%
Brown Iterated Stiffness, 3%	-17.5%	-0.7%	84.8%	81.4%	21.7%	166.6%
Brown Iterated Stiffness, 7%	-24.5%	-65.5%	-4.8%	-75.8%	-62.1%	-72.3%
Iterated Stiffness, (0.4), 3%	N/A	N/A	N/A	N/A	N/A	N/A
Iterated Stiffness, (0.4), 7%	N/A	N/A	N/A	N/A	N/A	N/A
Doepker Iterated Stiffness, (0.8), 3%	-22.9%	-60.5%	77.7%	-56.5%	148.7%	221.8%
Doepker Iterated Stiffness, (0.8), 7%	-30.8%	-62.2%	-29.2%	-75.8%	-45.2%	-6.3%
Uniform Best Fit	-2.1%	-78.4%	-10.6%	-30.3%	-11.9%	-2.9%
Uniform Best Fit, 3%	N/A	N/A	N/A	N/A	N/A	N/A
Uniform Best Fit, 7%	N/A	N/A	N/A	N/A	N/A	N/A
Uniform Best Fit, 3% FEMA	N/A	N/A	N/A	N/A	N/A	N/A
Uniform Best Fit, 7% FEMA	N/A	N/A	N/A	N/A	N/A	N/A
Variable Best Fit	N/A	N/A	N/A	N/A	N/A	N/A

Table A- 49: Average Error in Imposed Inertial Loads (Evaluation Method 9) for UCSD Test Specimen

Specimen	**UCSD**		
Test	**EQ1**	**EQ2**	**EQ3**
Period (s)	0.65	0.84	0.96
Drifts	0.271%	0.761%	0.832%
FIB 27 (0.3), 3%	12.6%	9.1%	0.7%
FIB 27 (0.3), 7%	10.9%	9.0%	3.6%
Adebar Upper, 3%	53.4%	2.7%	4.4%
Adebar Upper, 7%	40.0%	0.9%	3.7%
Adebar Lower, 3%	10.1%	1.3%	4.3%
Adebar Lower, 7%	5.6%	1.4%	3.9%
FEMA Cracked, 3%	14.1%	12.5%	7.2%
FEMA Cracked, 7%	15.7%	17.4%	21.1%
FEMA Uncracked, 3%	13.3%	13.7%	27.7%
FEMA Uncracked, 7%	17.8%	16.7%	26.5%
Brown Iterated Stiffness, 3%	12.6%	11.6%	19.2%
Brown Iterated Stiffness, 7%	10.9%	6.1%	28.4%
Iterated Stiffness, (0.4), 3%	N/A	N/A	N/A
Iterated Stiffness, (0.4), 7%	N/A	N/A	N/A
Doepker Iterated Stiffness, (0.8), 3%	10.1%	11.6%	19.2%
Doepker Iterated Stiffness, (0.8), 7%	7.2%	19.9%	26.9%
Uniform Best Fit	8.6%	10.3%	22.8%
Uniform Best Fit, 3%	8.1%	11.6%	4.3%
Uniform Best Fit, 7%	9.1%	9.4%	14.8%
Uniform Best Fit, 3% FEMA	8.1%	N/A	N/A
Uniform Best Fit, 7% FEMA	8.1%	N/A	N/A
Variable Best Fit	4.1%	11.8%	22.9%

Table A- 50: Average Error in Imposed Inertial Loads (Evaluation Method 9) for CAMUS C-1 Test Specimen

Specimen	CAMUS C - 1			
Test	Stage 1	Stage 2	Stage 3	Stage 4
Period (s)	0.43	0.47	0.61	0.70
Drifts	0.352%	0.522%	1.313%	1.849%
FIB 27 (0.3), 3%	N/A	N/A	N/A	N/A
FIB 27 (0.3), 7%	N/A	N/A	N/A	N/A
Adebar Upper, 3%	N/A	N/A	N/A	N/A
Adebar Upper, 7%	N/A	N/A	N/A	N/A
Adebar Lower, 3%	N/A	N/A	N/A	N/A
Adebar Lower, 7%	N/A	N/A	N/A	N/A
FEMA Cracked, 3%	N/A	N/A	N/A	N/A
FEMA Cracked, 7%	N/A	N/A	N/A	N/A
FEMA Uncracked, 3%	N/A	N/A	N/A	N/A
FEMA Uncracked, 7%	N/A	N/A	N/A	N/A
Brown Iterated Stiffness, 3%	N/A	N/A	N/A	N/A
Brown Iterated Stiffness, 7%	N/A	N/A	N/A	N/A
Iterated Stiffness, (0.4), 3%	N/A	N/A	N/A	N/A
Iterated Stiffness, (0.4), 7%	N/A	N/A	N/A	N/A
Doepker Iterated Stiffness, (0.8), 3%	N/A	N/A	N/A	N/A
Doepker Iterated Stiffness, (0.8), 7%	N/A	N/A	N/A	N/A
Uniform Best Fit	N/A	N/A	N/A	N/A
Uniform Best Fit, 3%	N/A	N/A	N/A	N/A
Uniform Best Fit, 7%	N/A	N/A	N/A	N/A
Uniform Best Fit, 3% FEMA	N/A	N/A	N/A	N/A
Uniform Best Fit, 7% FEMA	N/A	N/A	N/A	N/A
Variable Best Fit	N/A	N/A	N/A	N/A

Table A- 51: Average Error in Imposed Inertial Loads (Evaluation Method 9) for CAMUS C-2 Test Specimen

Specimen	CAMUS C - 2		
Test	Stage 2	Stage 3	Stage 4
Period (s)	0.33	0.42	0.61
Drifts	0.082%	0.540%	1.912%
FIB 27 (0.3), 3%	N/A	N/A	N/A
FIB 27 (0.3), 7%	N/A	N/A	N/A
Adebar Upper, 3%	N/A	N/A	N/A
Adebar Upper, 7%	N/A	N/A	N/A
Adebar Lower, 3%	N/A	N/A	N/A
Adebar Lower, 7%	N/A	N/A	N/A
FEMA Cracked, 3%	N/A	N/A	N/A
FEMA Cracked, 7%	N/A	N/A	N/A
FEMA Uncracked, 3%	N/A	N/A	N/A
FEMA Uncracked, 7%	N/A	N/A	N/A
Brown Iterated Stiffness, 3%	N/A	N/A	N/A
Brown Iterated Stiffness, 7%	N/A	N/A	N/A
Iterated Stiffness, (0.4), 3%	N/A	N/A	N/A
Iterated Stiffness, (0.4), 7%	N/A	N/A	N/A
Doepker Iterated Stiffness, (0.8), 3%	N/A	N/A	N/A
Doepker Iterated Stiffness, (0.8), 7%	N/A	N/A	N/A
Uniform Best Fit	N/A	N/A	N/A
Uniform Best Fit, 3%	N/A	N/A	N/A
Uniform Best Fit, 7%	N/A	N/A	N/A
Uniform Best Fit, 3% FEMA	N/A	N/A	N/A
Uniform Best Fit, 7% FEMA	N/A	N/A	N/A
Variable Best Fit	N/A	N/A	N/A

Table A- 52: Average Error in Imposed Inertial Loads (Evaluation Method 9) for CAMUS C-3 Test Specimen

Specimen	**CAMUS C - 3**			
Test	**Stage 1**	**Stage 2**	**Stage 3**	**Stage 4**
Period (s)	0.30	0.40	0.57	0.74
Drifts	0.117%	0.347%	1.318%	2.274%
FIB 27 (0.3), 3%	N/A	N/A	N/A	N/A
FIB 27 (0.3), 7%	N/A	N/A	N/A	N/A
Adebar Upper, 3%	N/A	N/A	N/A	N/A
Adebar Upper, 7%	N/A	N/A	N/A	N/A
Adebar Lower, 3%	N/A	N/A	N/A	N/A
Adebar Lower, 7%	N/A	N/A	N/A	N/A
FEMA Cracked, 3%	N/A	N/A	N/A	N/A
FEMA Cracked, 7%	N/A	N/A	N/A	N/A
FEMA Uncracked, 3%	N/A	N/A	N/A	N/A
FEMA Uncracked, 7%	N/A	N/A	N/A	N/A
Brown Iterated Stiffness, 3%	N/A	N/A	N/A	N/A
Brown Iterated Stiffness, 7%	N/A	N/A	N/A	N/A
Iterated Stiffness, (0.4), 3%	N/A	N/A	N/A	N/A
Iterated Stiffness, (0.4), 7%	N/A	N/A	N/A	N/A
Doepker Iterated Stiffness, (0.8), 3%	N/A	N/A	N/A	N/A
Doepker Iterated Stiffness, (0.8), 7%	N/A	N/A	N/A	N/A
Uniform Best Fit	N/A	N/A	N/A	N/A
Uniform Best Fit, 3%	N/A	N/A	N/A	N/A
Uniform Best Fit, 7%	N/A	N/A	N/A	N/A
Uniform Best Fit, 3% FEMA	N/A	N/A	N/A	N/A
Uniform Best Fit, 7% FEMA	N/A	N/A	N/A	N/A
Variable Best Fit	N/A	N/A	N/A	N/A

Table A- 53: Average Error in Imposed Inertial Loads (Evaluation Method 9) for CAMUS 2000 Test Specimen

Specimen	CAMUS 2000		
Test	Run 1	Run 2	Run 3
Period (s)	0.187	0.25	0.281
Drifts	0.088%	0.296%	0.384%
FIB 27 (0.3), 3%	38.4%	78.7%	42.5%
FIB 27 (0.3), 7%	30.5%	62.7%	25.8%
Adebar Upper, 3%	58.7%	98.4%	19.9%
Adebar Upper, 7%	65.8%	71.7%	22.6%
Adebar Lower, 3%	22.8%	84.7%	96.3%
Adebar Lower, 7%	25.8%	61.5%	25.5%
FEMA Cracked, 3%	49.4%	159.6%	77.0%
FEMA Cracked, 7%	30.8%	91.8%	26.6%
FEMA Uncracked, 3%	15.6%	55.4%	93.4%
FEMA Uncracked, 7%	21.2%	53.7%	18.4%
Brown Iterated Stiffness, 3%	38.4%	61.9%	89.8%
Brown Iterated Stiffness, 7%	30.5%	56.8%	44.5%
Iterated Stiffness, (0.4), 3%	53.3%	57.2%	94.1%
Iterated Stiffness, (0.4), 7%	27.5%	62.7%	43.3%
Doepker Iterated Stiffness, (0.8), 3%	23.5%	88.1%	94.4%
Doepker Iterated Stiffness, (0.8), 7%	21.5%	54.3%	50.3%
Uniform Best Fit	27.2%	51.7%	17.8%
Uniform Best Fit, 3%	28.1%	55.6%	91.6%
Uniform Best Fit, 7%	27.1%	77.3%	51.0%
Uniform Best Fit, 3% FEMA	N/A	N/A	N/A
Uniform Best Fit, 7% FEMA	N/A	N/A	N/A
Variable Best Fit	26.5%	49.9%	26.6%

Table A- 54: Average Error in Imposed Inertial Loads (Evaluation Method 9) for Ecoleader Test Specimen

Specimen	**CAMUS Ecoleader**					
Test	**Run 1**	**Run 3**	**Run 4**	**Run 5**	**Run 6**	**Run 7**
Period (s)	0.22	0.25	0.37	0.40	0.46	0.56
Drifts	0.159%	0.195%	0.623%	0.872%	1.187%	1.303%
FIB 27 (0.3), 3%	No Data	No Data	No Data	No Data	No Data	No Data
FIB 27 (0.3), 7%	No Data	No Data	No Data	No Data	No Data	No Data
Adebar Upper, 3%	No Data	No Data	No Data	No Data	No Data	No Data
Adebar Upper, 7%	No Data	No Data	No Data	No Data	No Data	No Data
Adebar Lower, 3%	No Data	No Data	No Data	No Data	No Data	No Data
Adebar Lower, 7%	No Data	No Data	No Data	No Data	No Data	No Data
FEMA Cracked, 3%	No Data	No Data	No Data	No Data	No Data	No Data
FEMA Cracked, 7%	No Data	No Data	No Data	No Data	No Data	No Data
FEMA Uncracked, 3%	No Data	No Data	No Data	No Data	No Data	No Data
FEMA Uncracked, 7%	No Data	No Data	No Data	No Data	No Data	No Data
Brown Iterated Stiffness, 3%	No Data	No Data	No Data	No Data	No Data	No Data
Brown Iterated Stiffness, 7%	No Data	No Data	No Data	No Data	No Data	No Data
Iterated Stiffness, (0.4), 3%	No Data	No Data	No Data	No Data	No Data	No Data
Iterated Stiffness, (0.4), 7%	No Data	No Data	No Data	No Data	No Data	No Data
Doepker Iterated Stiffness, (0.8), 3%	No Data	No Data	No Data	No Data	No Data	No Data
Doepker Iterated Stiffness, (0.8), 7%	No Data	No Data	No Data	No Data	No Data	No Data
Uniform Best Fit	No Data	No Data	No Data	No Data	No Data	No Data
Uniform Best Fit, 3%	No Data	No Data	No Data	No Data	No Data	No Data
Uniform Best Fit, 7%	No Data	No Data	No Data	No Data	No Data	No Data
Uniform Best Fit, 3% FEMA	No Data	No Data	No Data	No Data	No Data	No Data
Uniform Best Fit, 7% FEMA	No Data	No Data	No Data	No Data	No Data	No Data
Variable Best Fit	No Data	No Data	No Data	No Data	No Data	No Data

Table A- 55: Maximum Story Error in Imposed Inertial Loads (Evaluation Method 10) for UCSD Test Specimen

Specimen	UCSD		
Test	EQ1	EQ2	EQ3
Period (s)	0.65	0.84	0.96
Drifts	0.271%	0.761%	0.832%
FIB 27 (0.3), 3%	26.7%	23.3%	24.7%
FIB 27 (0.3), 7%	22.6%	25.8%	68.4%
Adebar Upper, 3%	143.1%	39.6%	66.3%
Adebar Upper, 7%	110.6%	18.1%	64.9%
Adebar Lower, 3%	22.9%	24.9%	66.3%
Adebar Lower, 7%	22.2%	19.6%	71.6%
FEMA Cracked, 3%	45.9%	35.0%	19.6%
FEMA Cracked, 7%	52.9%	56.1%	53.1%
FEMA Uncracked, 3%	45.9%	34.8%	75.1%
FEMA Uncracked, 7%	62.0%	48.4%	61.0%
Brown Iterated Stiffness, 3%	26.7%	19.4%	67.4%
Brown Iterated Stiffness, 7%	22.6%	20.0%	76.5%
Iterated Stiffness, (0.4), 3%	N/A	N/A	N/A
Iterated Stiffness, (0.4), 7%	N/A	N/A	N/A
Doepker Iterated Stiffness, (0.8), 3%	19.5%	19.4%	67.4%
Doepker Iterated Stiffness, (0.8), 7%	19.8%	57.3%	76.3%
Uniform Best Fit	21.0%	27.7%	61.2%
Uniform Best Fit, 3%	17.4%	19.4%	19.9%
Uniform Best Fit, 7%	32.6%	25.4%	47.3%
Uniform Best Fit, 3% FEMA	17.4%	N/A	N/A
Uniform Best Fit, 7% FEMA	17.4%	N/A	N/A
Variable Best Fit	8.7%	33.5%	62.3%

Table A- 56: Maximum Story Error in Imposed Inertial Loads (Evaluation Method 10) for CAMUS C-1 Test Specimen

Specimen	CAMUS C - 1			
Test	Stage 1	Stage 2	Stage 3	Stage 4
Period (s)	0.43	0.47	0.61	0.70
Drifts	0.352%	0.522%	1.313%	1.849%
FIB 27 (0.3), 3%	N/A	N/A	N/A	N/A
FIB 27 (0.3), 7%	N/A	N/A	N/A	N/A
Adebar Upper, 3%	N/A	N/A	N/A	N/A
Adebar Upper, 7%	N/A	N/A	N/A	N/A
Adebar Lower, 3%	N/A	N/A	N/A	N/A
Adebar Lower, 7%	N/A	N/A	N/A	N/A
FEMA Cracked, 3%	N/A	N/A	N/A	N/A
FEMA Cracked, 7%	N/A	N/A	N/A	N/A
FEMA Uncracked, 3%	N/A	N/A	N/A	N/A
FEMA Uncracked, 7%	N/A	N/A	N/A	N/A
Brown Iterated Stiffness, 3%	N/A	N/A	N/A	N/A
Brown Iterated Stiffness, 7%	N/A	N/A	N/A	N/A
Iterated Stiffness, (0.4), 3%	N/A	N/A	N/A	N/A
Iterated Stiffness, (0.4), 7%	N/A	N/A	N/A	N/A
Doepker Iterated Stiffness, (0.8), 3%	N/A	N/A	N/A	N/A
Doepker Iterated Stiffness, (0.8), 7%	N/A	N/A	N/A	N/A
Uniform Best Fit	N/A	N/A	N/A	N/A
Uniform Best Fit, 3%	N/A	N/A	N/A	N/A
Uniform Best Fit, 7%	N/A	N/A	N/A	N/A
Uniform Best Fit, 3% FEMA	N/A	N/A	N/A	N/A
Uniform Best Fit, 7% FEMA	N/A	N/A	N/A	N/A
Variable Best Fit	N/A	N/A	N/A	N/A

Table A- 57: Maximum Story Error in Imposed Inertial Loads (Evaluation Method 10) for CAMUS C-2 Test Specimen

Specimen	CAMUS C - 2		
Test	Stage 2	Stage 3	Stage 4
Period (s)	0.33	0.42	0.61
Drifts	0.082%	0.540%	1.912%
FIB 27 (0.3), 3%	N/A	N/A	N/A
FIB 27 (0.3), 7%	N/A	N/A	N/A
Adebar Upper, 3%	N/A	N/A	N/A
Adebar Upper, 7%	N/A	N/A	N/A
Adebar Lower, 3%	N/A	N/A	N/A
Adebar Lower, 7%	N/A	N/A	N/A
FEMA Cracked, 3%	N/A	N/A	N/A
FEMA Cracked, 7%	N/A	N/A	N/A
FEMA Uncracked, 3%	N/A	N/A	N/A
FEMA Uncracked, 7%	N/A	N/A	N/A
Brown Iterated Stiffness, 3%	N/A	N/A	N/A
Brown Iterated Stiffness, 7%	N/A	N/A	N/A
Iterated Stiffness, (0.4), 3%	N/A	N/A	N/A
Iterated Stiffness, (0.4), 7%	N/A	N/A	N/A
Doepker Iterated Stiffness, (0.8), 3%	N/A	N/A	N/A
Doepker Iterated Stiffness, (0.8), 7%	N/A	N/A	N/A
Uniform Best Fit	N/A	N/A	N/A
Uniform Best Fit, 3%	N/A	N/A	N/A
Uniform Best Fit, 7%	N/A	N/A	N/A
Uniform Best Fit, 3% FEMA	N/A	N/A	N/A
Uniform Best Fit, 7% FEMA	N/A	N/A	N/A
Variable Best Fit	N/A	N/A	N/A

Table A- 58: Maximum Story Error in Imposed Inertial Loads (Evaluation Method 10) for CAMUS C-3 Test Specimen

Specimen	CAMUS C - 3			
Test	Stage 1	Stage 2	Stage 3	Stage 4
Period (s)	0.30	0.40	0.57	0.74
Drifts	0.117%	0.347%	1.318%	2.274%
FIB 27 (0.3), 3%	N/A	N/A	N/A	N/A
FIB 27 (0.3), 7%	N/A	N/A	N/A	N/A
Adebar Upper, 3%	N/A	N/A	N/A	N/A
Adebar Upper, 7%	N/A	N/A	N/A	N/A
Adebar Lower, 3%	N/A	N/A	N/A	N/A
Adebar Lower, 7%	N/A	N/A	N/A	N/A
FEMA Cracked, 3%	N/A	N/A	N/A	N/A
FEMA Cracked, 7%	N/A	N/A	N/A	N/A
FEMA Uncracked, 3%	N/A	N/A	N/A	N/A
FEMA Uncracked, 7%	N/A	N/A	N/A	N/A
Brown Iterated Stiffness, 3%	N/A	N/A	N/A	N/A
Brown Iterated Stiffness, 7%	N/A	N/A	N/A	N/A
Iterated Stiffness, (0.4), 3%	N/A	N/A	N/A	N/A
Iterated Stiffness, (0.4), 7%	N/A	N/A	N/A	N/A
Doepker Iterated Stiffness, (0.8), 3%	N/A	N/A	N/A	N/A
Doepker Iterated Stiffness, (0.8), 7%	N/A	N/A	N/A	N/A
Uniform Best Fit	N/A	N/A	N/A	N/A
Uniform Best Fit, 3%	N/A	N/A	N/A	N/A
Uniform Best Fit, 7%	N/A	N/A	N/A	N/A
Uniform Best Fit, 3% FEMA	N/A	N/A	N/A	N/A
Uniform Best Fit, 7% FEMA	N/A	N/A	N/A	N/A
Variable Best Fit	N/A	N/A	N/A	N/A

Table A- 59: Maximum Story Error in Imposed Inertial Loads (Evaluation Method 10) for CAMUS 2000 Test Specimen

Specimen	CAMUS 2000		
Test	Run 1	Run 2	Run 3
Period (s)	0.187	0.25	0.281
Drifts	0.088%	0.296%	0.384%
FIB 27 (0.3), 3%	77.6%	114.1%	61.5%
FIB 27 (0.3), 7%	38.6%	106.1%	36.2%
Adebar Upper, 3%	89.0%	146.6%	49.2%
Adebar Upper, 7%	91.9%	115.0%	36.4%
Adebar Lower, 3%	31.4%	127.4%	153.3%
Adebar Lower, 7%	38.8%	104.9%	52.9%
FEMA Cracked, 3%	66.0%	296.9%	154.9%
FEMA Cracked, 7%	40.3%	163.2%	31.8%
FEMA Uncracked, 3%	27.8%	82.5%	142.8%
FEMA Uncracked, 7%	32.1%	92.2%	39.2%
Brown Iterated Stiffness, 3%	77.6%	152.0%	145.2%
Brown Iterated Stiffness, 7%	38.6%	103.3%	72.5%
Iterated Stiffness, (0.4), 3%	72.2%	136.4%	130.4%
Iterated Stiffness, (0.4), 7%	53.4%	106.1%	69.5%
Doepker Iterated Stiffness, (0.8), 3%	30.6%	182.8%	144.5%
Doepker Iterated Stiffness, (0.8), 7%	37.1%	103.0%	96.7%
Uniform Best Fit	41.4%	70.0%	36.5%
Uniform Best Fit, 3%	42.4%	127.3%	133.8%
Uniform Best Fit, 7%	41.2%	128.4%	94.0%
Uniform Best Fit, 3% FEMA	N/A	N/A	N/A
Uniform Best Fit, 7% FEMA	N/A	N/A	N/A
Variable Best Fit	43.9%	73.9%	30.4%

Table A- 60: Maximum Story Error in Imposed Inertial Loads (Evaluation Method 10) for Ecoleader Test Specimen

Specimen	CAMUS Ecoleader					
Test	**Run 1**	**Run 3**	**Run 4**	**Run 5**	**Run 6**	**Run 7**
Period (s)	0.22	0.25	0.37	0.40	0.46	0.56
Drifts	0.159%	0.195%	0.623%	0.872%	1.187%	1.303%
FIB 27 (0.3), 3%	No Data	No Data	No Data	No Data	No Data	No Data
FIB 27 (0.3), 7%	No Data	No Data	No Data	No Data	No Data	No Data
Adebar Upper, 3%	No Data	No Data	No Data	No Data	No Data	No Data
Adebar Upper, 7%	No Data	No Data	No Data	No Data	No Data	No Data
Adebar Lower, 3%	No Data	No Data	No Data	No Data	No Data	No Data
Adebar Lower, 7%	No Data	No Data	No Data	No Data	No Data	No Data
FEMA Cracked, 3%	No Data	No Data	No Data	No Data	No Data	No Data
FEMA Cracked, 7%	No Data	No Data	No Data	No Data	No Data	No Data
FEMA Uncracked, 3%	No Data	No Data	No Data	No Data	No Data	No Data
FEMA Uncracked, 7%	No Data	No Data	No Data	No Data	No Data	No Data
Brown Iterated Stiffness, 3%	No Data	No Data	No Data	No Data	No Data	No Data
Brown Iterated Stiffness, 7%	No Data	No Data	No Data	No Data	No Data	No Data
Iterated Stiffness, (0.4), 3%	No Data	No Data	No Data	No Data	No Data	No Data
Iterated Stiffness, (0.4), 7%	No Data	No Data	No Data	No Data	No Data	No Data
Doepker Iterated Stiffness, (0.8), 3%	No Data	No Data	No Data	No Data	No Data	No Data
Doepker Iterated Stiffness, (0.8), 7%	No Data	No Data	No Data	No Data	No Data	No Data
Uniform Best Fit	No Data	No Data	No Data	No Data	No Data	No Data
Uniform Best Fit, 3%	No Data	No Data	No Data	No Data	No Data	No Data
Uniform Best Fit, 7%	No Data	No Data	No Data	No Data	No Data	No Data
Uniform Best Fit, 3% FEMA	No Data	No Data	No Data	No Data	No Data	No Data
Uniform Best Fit, 7% FEMA	No Data	No Data	No Data	No Data	No Data	No Data
Variable Best Fit	No Data	No Data	No Data	No Data	No Data	No Data

Table A- 61: Error in Base Moment Prediction (Evaluation Method 11) for UCSD Test Specimen

Specimen	UCSD		
Test	EQ1	EQ2	EQ3
Period (s)	0.65	0.84	0.96
Drifts	0.271%	0.761%	0.832%
FIB 27 (0.3), 3%	-9.3%	-8.4%	-14.2%
FIB 27 (0.3), 7%	-21.3%	-14.0%	-62.3%
Adebar Upper, 3%	-142.5%	37.9%	-67.0%
Adebar Upper, 7%	-105.9%	-6.6%	-60.8%
Adebar Lower, 3%	20.0%	15.4%	-65.6%
Adebar Lower, 7%	-14.8%	-15.9%	-65.2%
FEMA Cracked, 3%	-39.0%	-27.2%	-6.3%
FEMA Cracked, 7%	-27.2%	-39.4%	-49.3%
FEMA Uncracked, 3%	-27.7%	-15.2%	-64.8%
FEMA Uncracked, 7%	-45.1%	-40.4%	-60.4%
Brown Iterated Stiffness, 3%	-9.3%	3.9%	-45.9%
Brown Iterated Stiffness, 7%	-21.3%	-5.7%	-67.0%
Iterated Stiffness, (0.4), 3%	N/A	N/A	N/A
Iterated Stiffness, (0.4), 7%	N/A	N/A	N/A
Doepker Iterated Stiffness, (0.8), 3%	-3.9%	3.9%	-45.9%
Doepker Iterated Stiffness, (0.8), 7%	-16.7%	-7.0%	-64.5%
Uniform Best Fit	-3.0%	-23.4%	-54.4%
Uniform Best Fit, 3%	14.8%	3.9%	-9.7%
Uniform Best Fit, 7%	-14.5%	-18.3%	-36.2%
Uniform Best Fit, 3% FEMA	14.8%	-31.1%	-48.7%
Uniform Best Fit, 7% FEMA	14.8%	-19.0%	-41.6%
Variable Best Fit	-2.9%	-25.4%	-53.7%

Table A- 62: Error in Base Moment Prediction (Evaluation Method 11) for CAMUS C-1 Test Specimen

Specimen	CAMUS C - 1			
Test	Stage 1	Stage 2	Stage 3	Stage 4
Period (s)	0.43	0.47	0.61	0.70
Drifts	0.352%	0.522%	1.313%	1.849%
FIB 27 (0.3), 3%	7.0%	3.5%	-62.2%	-53.0%
FIB 27 (0.3), 7%	-32.2%	-45.5%	-36.3%	-38.4%
Adebar Upper, 3%	-25.4%	-40.1%	59.1%	34.7%
Adebar Upper, 7%	-59.6%	-67.4%	25.8%	30.6%
Adebar Lower, 3%	-6.2%	-42.5%	-41.2%	-52.3%
Adebar Lower, 7%	-26.1%	-65.3%	-45.2%	-49.5%
FEMA Cracked, 3%	-11.1%	-20.1%	115.1%	107.8%
FEMA Cracked, 7%	-69.7%	-64.4%	79.5%	73.4%
FEMA Uncracked, 3%	-76.0%	-66.9%	156.4%	176.2%
FEMA Uncracked, 7%	-68.4%	-66.0%	98.1%	86.3%
Brown Iterated Stiffness, 3%	7.0%	-86.5%	-10.1%	-58.8%
Brown Iterated Stiffness, 7%	-32.2%	-45.5%	41.5%	-23.3%
Iterated Stiffness, (0.4), 3%	N/A	N/A	N/A	N/A
Iterated Stiffness, (0.4), 7%	N/A	N/A	N/A	N/A
Doepker Iterated Stiffness, (0.8), 3%	1.8%	-37.6%	-6.0%	-15.2%
Doepker Iterated Stiffness, (0.8), 7%	-53.5%	-56.0%	-23.3%	5.3%
Uniform Best Fit	-28.5%	-34.8%	-1.3%	-58.3%
Uniform Best Fit, 3%	20.3%	-6.8%	16.0%	-11.6%
Uniform Best Fit, 7%	-19.5%	-47.1%	-2.4%	-13.9%
Uniform Best Fit, 3% FEMA	20.3%	-6.8%	-10.5%	-22.1%
Uniform Best Fit, 7% FEMA	20.3%	-6.8%	2.6%	-18.4%
Variable Best Fit	-28.2%	-36.9%	11.0%	-59.0%

Table A- 63: Error in Base Moment Prediction (Evaluation Method 11) for CAMUS C-2 Test Specimen

Specimen	**CAMUS C - 2**		
Test	**Stage 2**	**Stage 3**	**Stage 4**
Period (s)	0.33	0.42	0.61
Drifts	0.082%	0.540%	1.912%
FIB 27 (0.3), 3%	-65.3%	13.4%	39.0%
FIB 27 (0.3), 7%	-67.9%	-35.6%	44.9%
Adebar Upper, 3%	-32.8%	-60.2%	135.7%
Adebar Upper, 7%	-64.6%	-62.4%	153.8%
Adebar Lower, 3%	-85.3%	-18.7%	-32.0%
Adebar Lower, 7%	-73.4%	-48.9%	6.4%
FEMA Cracked, 3%	-12.2%	-21.8%	284.4%
FEMA Cracked, 7%	-46.0%	-54.5%	223.1%
FEMA Uncracked, 3%	-59.6%	-56.6%	325.4%
FEMA Uncracked, 7%	-71.7%	-100.0%	-99.7%
Brown Iterated Stiffness, 3%	-65.7%	33.2%	58.0%
Brown Iterated Stiffness, 7%	-119.3%	-74.4%	118.3%
Iterated Stiffness, (0.4), 3%	N/A	N/A	N/A
Iterated Stiffness, (0.4), 7%	N/A	N/A	N/A
Doepker Iterated Stiffness, (0.8), 3%	-87.6%	-31.9%	145.2%
Doepker Iterated Stiffness, (0.8), 7%	-63.3%	-55.6%	84.9%
Uniform Best Fit	-3.8%	-67.4%	21.5%
Uniform Best Fit, 3%	N/A	N/A	N/A
Uniform Best Fit, 7%	N/A	N/A	N/A
Uniform Best Fit, 3% FEMA	N/A	N/A	N/A
Uniform Best Fit, 7% FEMA	N/A	N/A	N/A
Variable Best Fit	-3.3%	-65.1%	17.2%

Table A- 64: Error in Base Moment Prediction (Evaluation Method 11) for CAMUS C-3 Test Specimen

Specimen	CAMUS C - 3			
Test	Stage 1	Stage 2	Stage 3	Stage 4
Period (s)	0.30	0.40	0.57	0.74
Drifts	0.117%	0.347%	1.318%	2.274%
FIB 27 (0.3), 3%	-35.3%	-8.5%	-11.0%	86.5%
FIB 27 (0.3), 7%	-55.4%	-45.6%	-70.6%	48.1%
Adebar Upper, 3%	-20.1%	-45.3%	-20.6%	158.0%
Adebar Upper, 7%	-57.4%	-64.9%	-48.7%	111.3%
Adebar Lower, 3%	-70.3%	13.7%	88.5%	-22.9%
Adebar Lower, 7%	-73.2%	-27.9%	19.7%	-7.8%
FEMA Cracked, 3%	-79.3%	-28.9%	5.3%	120.1%
FEMA Cracked, 7%	-60.2%	-53.7%	-32.0%	183.9%
FEMA Uncracked, 3%	-82.3%	-48.0%	-17.2%	299.6%
FEMA Uncracked, 7%	-80.9%	-64.9%	-45.7%	201.7%
Brown Iterated Stiffness, 3%	-35.3%	-8.5%	-66.1%	-15.4%
Brown Iterated Stiffness, 7%	-55.4%	-45.6%	36.8%	72.9%
Iterated Stiffness, (0.4), 3%	N/A	N/A	N/A	N/A
Iterated Stiffness, (0.4), 7%	N/A	N/A	N/A	N/A
Doepker Iterated Stiffness, (0.8), 3%	-15.3%	14.1%	-47.4%	-78.7%
Doepker Iterated Stiffness, (0.8), 7%	-39.5%	-51.6%	37.8%	66.3%
Uniform Best Fit	-8.6%	-32.6%	-47.7%	-12.0%
Uniform Best Fit, 3%	N/A	N/A	N/A	N/A
Uniform Best Fit, 7%	N/A	N/A	N/A	N/A
Uniform Best Fit, 3% FEMA	N/A	N/A	N/A	N/A
Uniform Best Fit, 7% FEMA	N/A	N/A	N/A	N/A
Variable Best Fit	-12.4%	-31.7%	-47.2%	-10.2%

Table A- 65: Error in Base Moment Prediction (Evaluation Method 11) for CAMUS 2000 Test Specimen

Specimen	**CAMUS 2000**		
Test	**Run 1**	**Run 2**	**Run 3**
Period (s)	0.187	0.25	0.281
Drifts	0.088%	0.296%	0.384%
FIB 27 (0.3), 3%	195.3%	4.2%	-8.2%
FIB 27 (0.3), 7%	38.1%	11.2%	4.3%
Adebar Upper, 3%	74.7%	10.9%	-11.0%
Adebar Upper, 7%	-35.8%	10.1%	2.7%
Adebar Lower, 3%	59.3%	7.7%	17.2%
Adebar Lower, 7%	78.9%	11.4%	-8.4%
FEMA Cracked, 3%	-16.3%	72.5%	34.1%
FEMA Cracked, 7%	33.2%	25.0%	6.4%
FEMA Uncracked, 3%	86.7%	-3.7%	7.7%
FEMA Uncracked, 7%	108.3%	7.8%	-10.4%
Brown Iterated Stiffness, 3%	195.3%	71.8%	107.6%
Brown Iterated Stiffness, 7%	38.1%	14.7%	36.9%
Iterated Stiffness, (0.4), 3%	143.2%	50.0%	112.8%
Iterated Stiffness, (0.4), 7%	23.8%	11.2%	34.7%
Doepker Iterated Stiffness, (0.8), 3%	186.3%	66.6%	110.9%
Doepker Iterated Stiffness, (0.8), 7%	33.1%	16.8%	49.9%
Uniform Best Fit	69.2%	-5.9%	0.4%
Uniform Best Fit, 3%	67.2%	40.3%	111.0%
Uniform Best Fit, 7%	69.0%	22.3%	54.8%
Uniform Best Fit, 3% FEMA	N/A	N/A	N/A
Uniform Best Fit, 7% FEMA	N/A	N/A	N/A
Variable Best Fit	69.9%	-1.6%	5.9%

Table A- 66: Error in Base Moment Prediction (Evaluation Method 11) for Ecoleader Test Specimen

Specimen	**CAMUS Ecoleader**					
Test	**Run 1**	**Run 3**	**Run 4**	**Run 5**	**Run 6**	**Run 7**
Period (s)	0.22	0.25	0.37	0.40	0.46	0.56
Drifts	0.159%	0.195%	0.623%	0.872%	1.187%	1.303%
FIB 27 (0.3), 3%	-6.0%	-62.0%	68.4%	-41.4%	-16.4%	-44.4%
FIB 27 (0.3), 7%	-15.0%	-63.2%	13.4%	-71.8%	-56.3%	-94.2%
Adebar Upper, 3%	6.2%	-67.2%	116.2%	67.7%	32.7%	165.1%
Adebar Upper, 7%	-6.4%	-66.6%	43.2%	25.8%	-24.9%	68.8%
Adebar Lower, 3%	4.8%	-49.0%	105.5%	100.5%	109.8%	73.9%
Adebar Lower, 7%	-6.4%	-57.3%	16.1%	85.6%	46.2%	-1.1%
FEMA Cracked, 3%	-4.0%	-49.0%	235.8%	12.9%	72.8%	83.8%
FEMA Cracked, 7%	-13.2%	-57.5%	99.8%	-15.1%	22.9%	17.6%
FEMA Uncracked, 3%	22.9%	-52.7%	104.0%	79.6%	67.9%	164.2%
FEMA Uncracked, 7%	2.4%	-55.4%	13.7%	17.2%	32.9%	50.7%
Brown Iterated Stiffness, 3%	-6.0%	-62.0%	85.6%	86.7%	31.5%	302.6%
Brown Iterated Stiffness, 7%	-15.0%	-63.2%	13.4%	-71.8%	-54.9%	-57.9%
Iterated Stiffness, (0.4), 3%	N/A	N/A	N/A	N/A	N/A	N/A
Iterated Stiffness, (0.4), 7%	N/A	N/A	N/A	N/A	N/A	N/A
Doepker Iterated Stiffness, (0.8), 3%	-8.2%	-65.1%	68.4%	-30.8%	118.5%	275.0%
Doepker Iterated Stiffness, (0.8), 7%	-16.0%	-64.7%	-16.9%	-71.8%	-36.4%	41.3%
Uniform Best Fit	1.3%	-71.6%	-3.0%	-21.5%	24.7%	32.5%
Uniform Best Fit, 3%	N/A	N/A	N/A	N/A	N/A	N/A
Uniform Best Fit, 7%	N/A	N/A	N/A	N/A	N/A	N/A
Uniform Best Fit, 3% FEMA	N/A	N/A	N/A	N/A	N/A	N/A
Uniform Best Fit, 7% FEMA	N/A	N/A	N/A	N/A	N/A	N/A
Variable Best Fit	N/A	N/A	N/A	N/A	N/A	N/A

Appendix B: Zero Error Damping Results

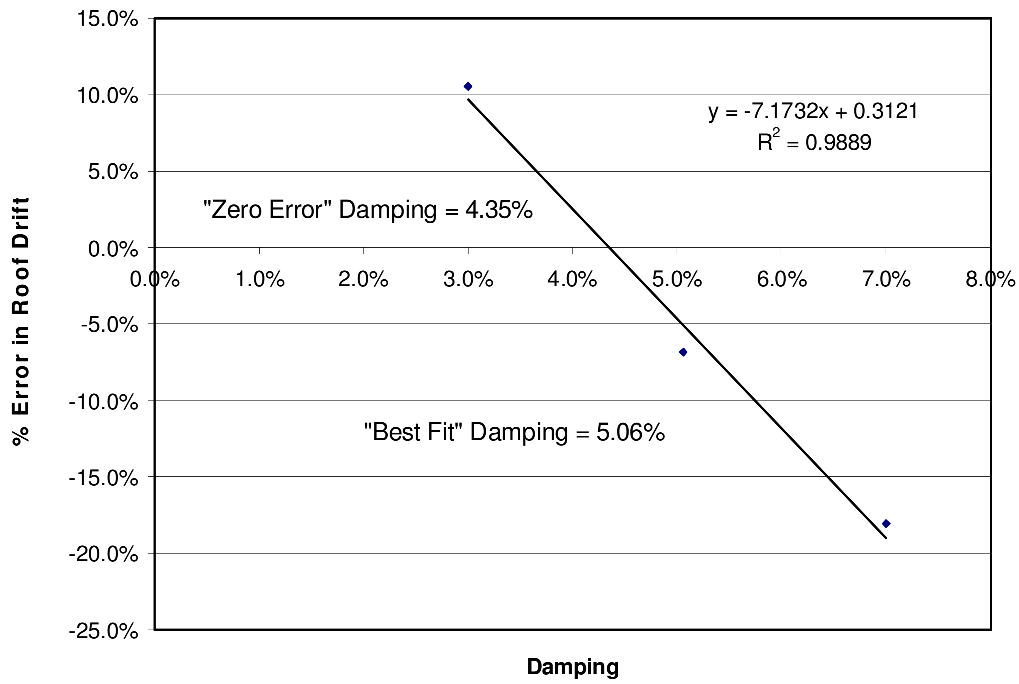

Figure B- 1: UCSD EQ 1 – Error in Roof Drift with Respect to Damping

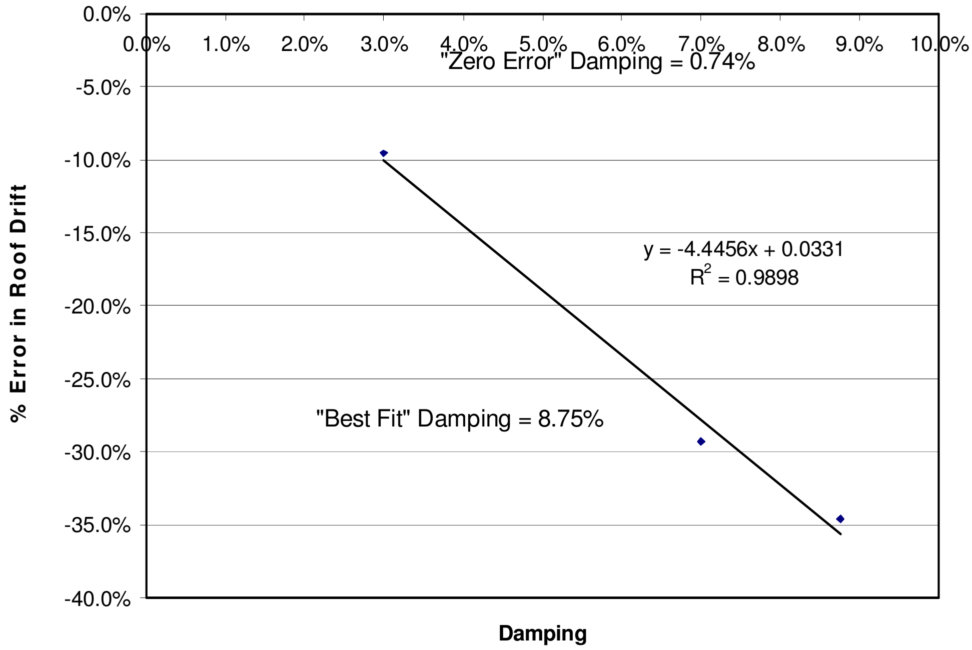

Figure B- 2: UCSD EQ 2 – Error in Roof Drift with Respect to Damping

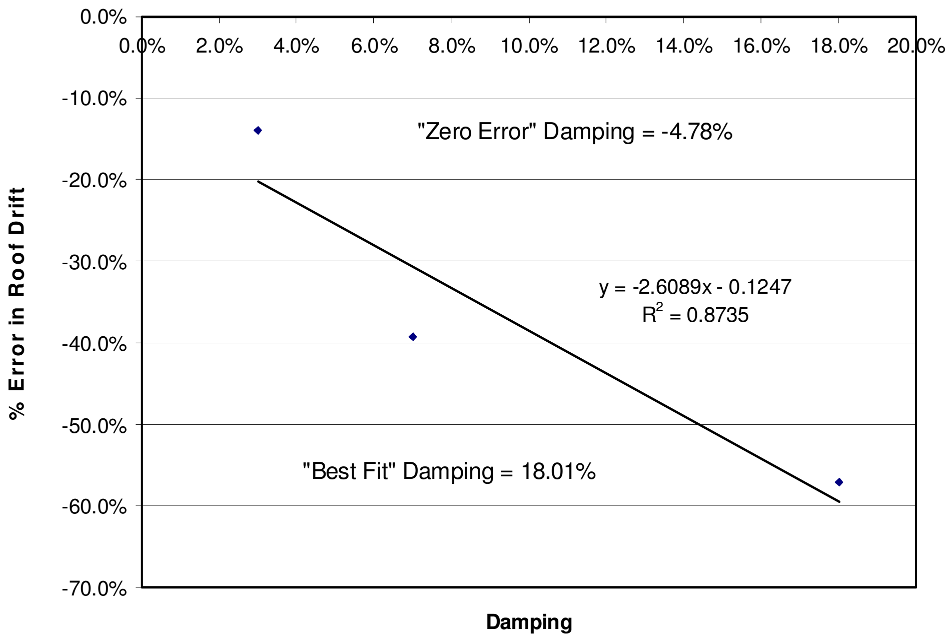

Figure B- 3: UCSD EQ 3 – Error with Respect to Damping

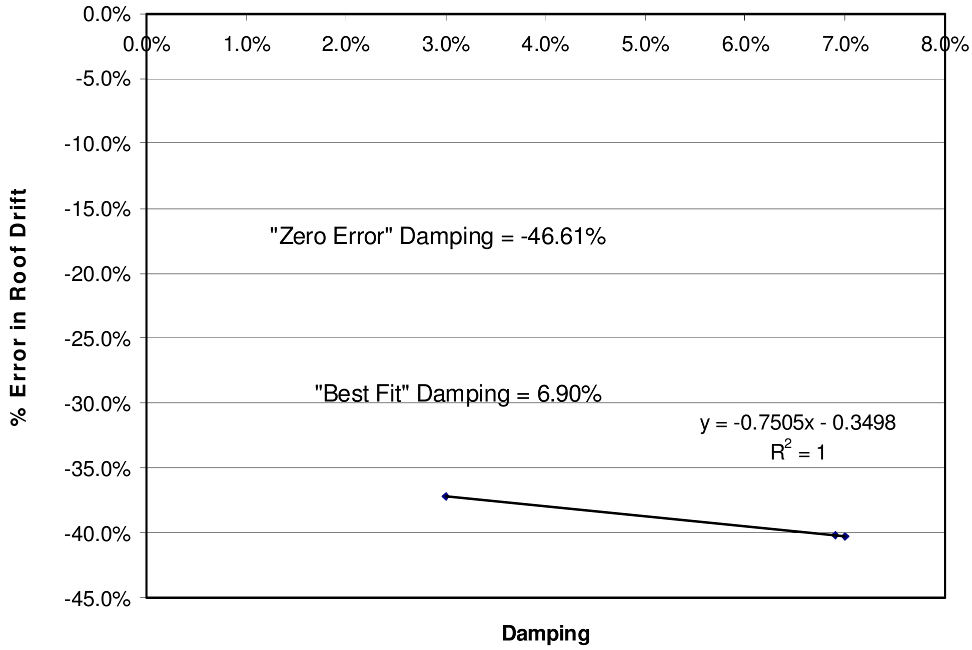

Figure B- 4: CAMUS 2000 Test 1 – Error in Roof Drift with Respect to Damping

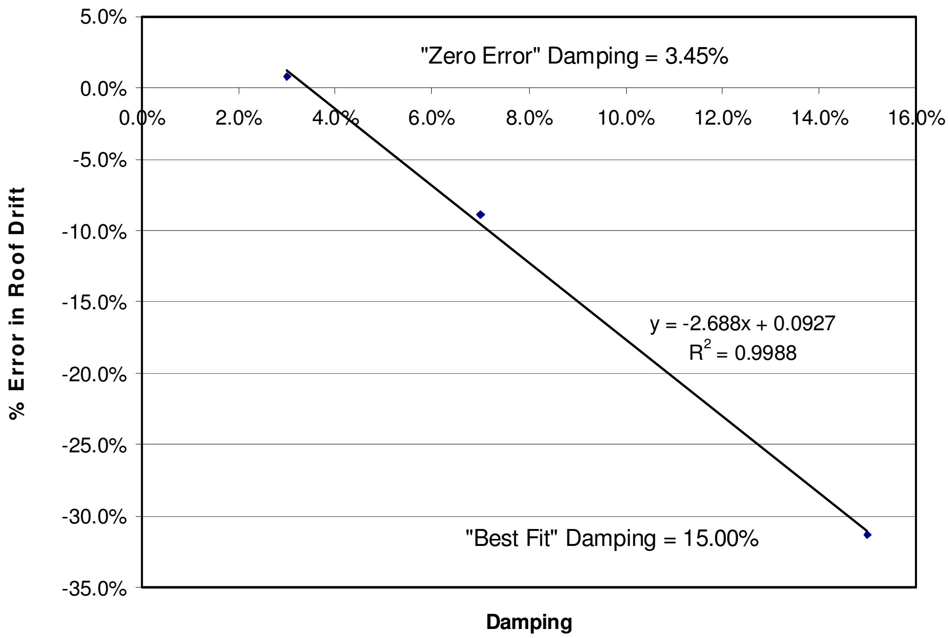

Figure B- 5: CAMUS 2000 Test 2 – Error in Roof Drift with Respect to Damping

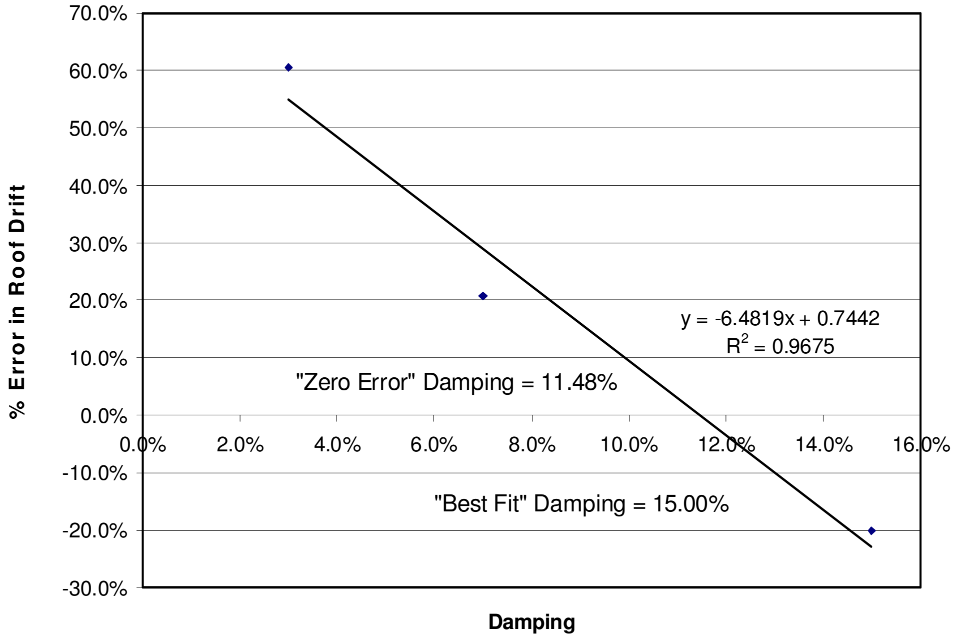

Figure B- 6: CAMUS 2000 Test 3 – Error in Roof Drift with Respect to Damping

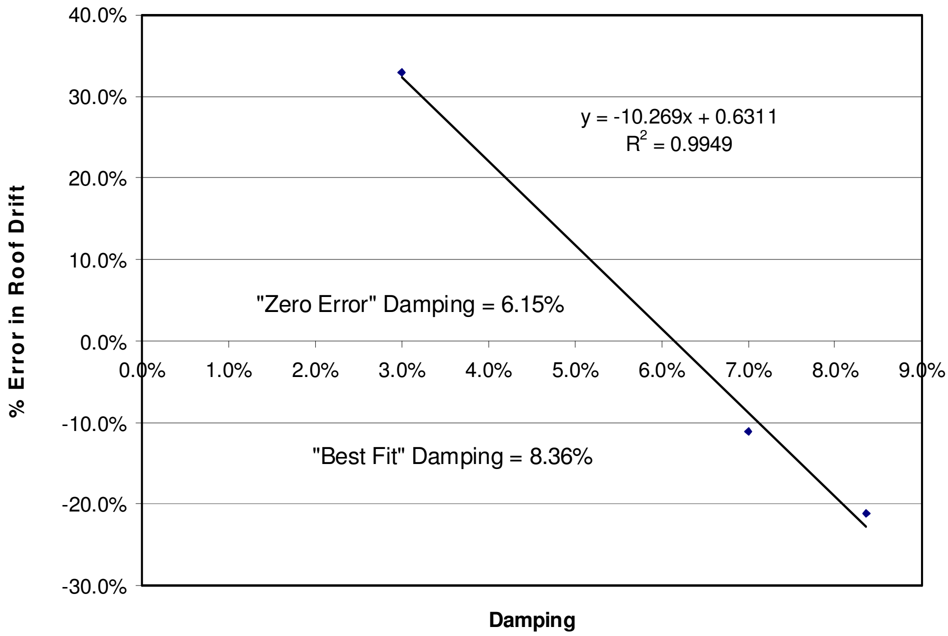

Figure B- 7: CAMUS C-1 Stage 1 – Error in Roof Drift with Respect to Damping

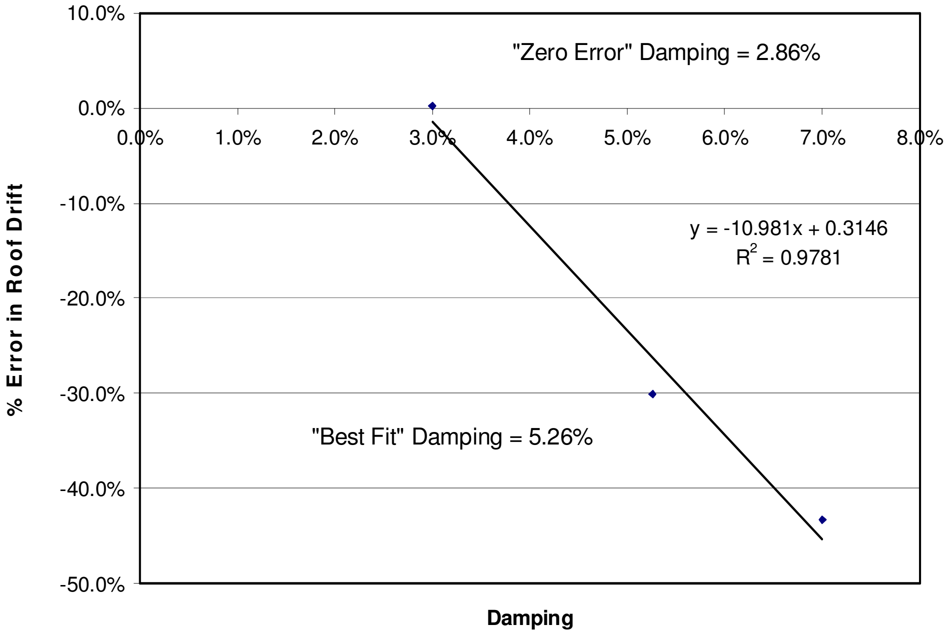

Figure B- 8: CAMUS C-1 Stage 2 – Error in Roof Drift with Respect to Damping

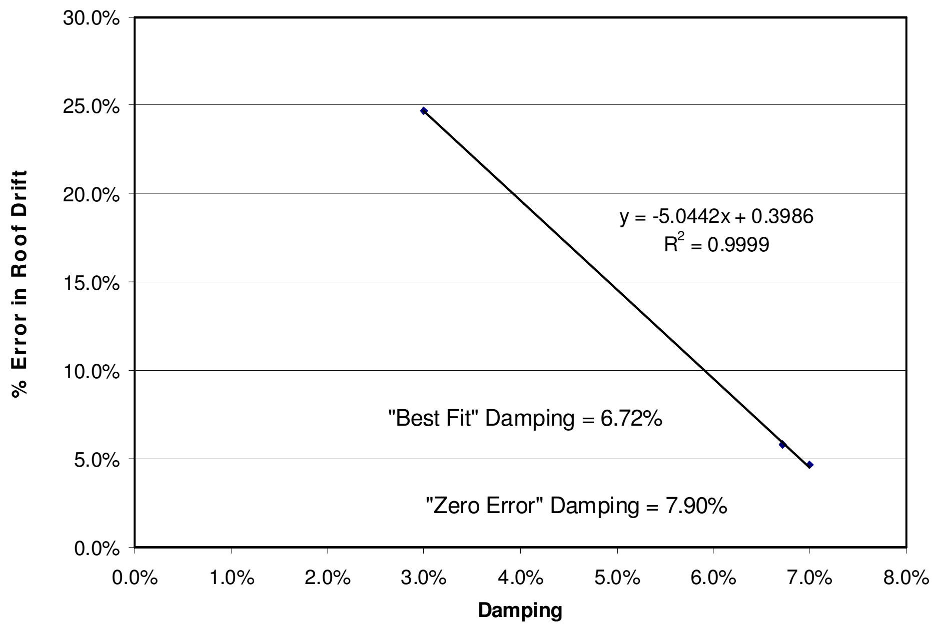

Figure B- 9: CAMUS C-1 Stage 3 – Error in Roof Drift with Respect to Damping

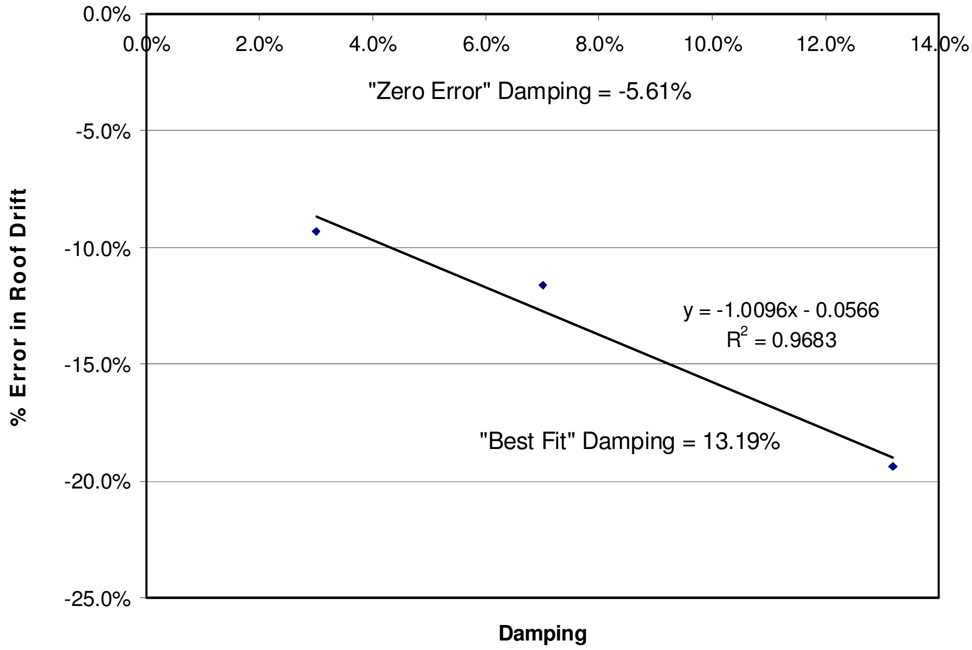

Figure B- 10: CAMUS C-1 Stage 4 – Error in Roof Drift with Respect to Damping

Appendix C: Determining Flexural Deformation by Subtracting Rigid Body Rotation

In order to accurately assess the damage state of a reinforced concrete wall subjected to lateral loading, a method was derived to exclude rigid body rotation so as to get a clear indication of the amount of flexural deformation occurring. This derivation can be seen below:

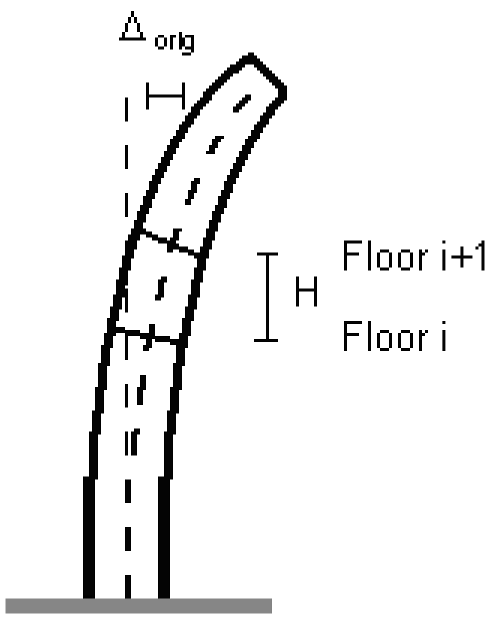

Figure C- 1: Example of Wall under Imposed Drift

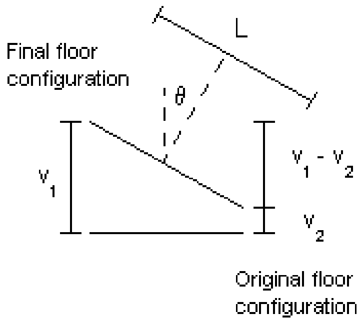

Figure C- 2: Floor Configuration During Deformation

$$\sin\theta = \frac{|v_1 - v_2|}{L}$$

$$\theta = \left|\arcsin\left(\frac{v_1 - v_2}{L}\right)\right|$$

where L = width of wall

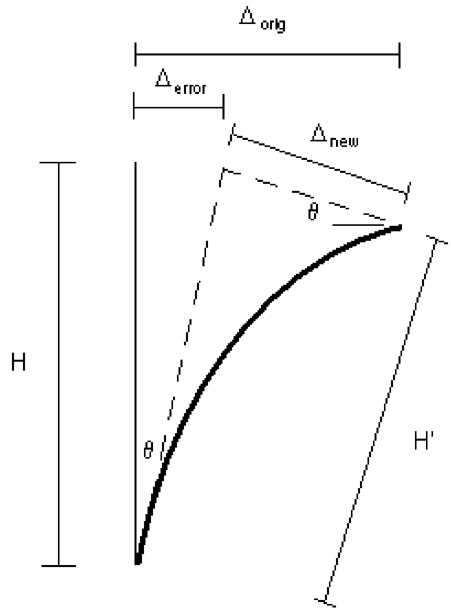

Figure C- 3: Wall Deformation between Two Stories

$$H' = \frac{H}{\cos\theta} \approx H$$

$$\tan\theta = \frac{\Delta_{error}}{H}$$

$$\Delta_{error} = H \times \tan\theta$$

$$\cos\theta = \frac{\Delta_{orig} - \Delta_{error}}{\Delta_{new}}$$

$$\Delta_{new} = \frac{\Delta_{orig} - \Delta_{error}}{\cos\theta}$$

$$drift_{old} = \frac{\Delta_{orig}}{H}$$

$$drift_{NRB} = \frac{\Delta_{orig} - \Delta_{error}}{H}$$

where NRB = no rigid body rotation

Appendix D: Results of Attempts to Apply Brown Regression for a Variable Stiffness.

The method for subtracting out rigid body rotation from Appendix C was applied with the Brown Regression to establish a variable stiffness. The following summarizes the method and explains the results.

1. Run an analysis with 0.3, as was done in the updated uniform stiffness.
2. Extract floor displacements, determine story drifts subtracting out rigid body rotation.
3. Using Brown's equation, determine new stiffness for each story.
4. Rerun the model, extract the data.

However, upon attempting to do this for the UCSD test, no story saw sufficient drift to warrant further reduction in stiffness. This ultimately led to a stiffer system than was observed in the updated uniform stiffness. The following table shows the results of displacement profile, and the corresponding drifts and stiffness values.

Table D- 1: **Results of Brown's Recommended Stiffness Values for Measured and 0.3 Model**

	Displacement Profile					
	Measured			0.3 Models		
Height Above Base	**EQ1**	**EQ2**	**EQ3**	**EQ1**	**EQ2**	**EQ3**
0	0.00	0.00	0.00	0.00	0.00	0.00
108	0.12	0.43	0.48	0.08	0.26	0.30
216	0.32	1.09	1.17	0.27	0.88	1.02
324	0.67	2.01	2.19	0.54	1.77	2.06
432	0.99	2.86	3.08	0.89	2.82	3.30
540	1.32	3.81	4.14	1.26	3.93	4.62
648	1.71	4.81	5.26	1.65	5.05	5.95
756	1.94	5.50	5.94	2.02	6.12	7.22
1st Story Drift (%)	0.11	0.40	0.45	0.07	0.24	0.28
Brown Stiffness (story 1)	**0.38**	**0.27**	**0.25**	**0.39**	**0.32**	**0.31**
Bottom 2 Story Drift (%)	0.15	0.50	0.54	0.12	0.41	0.47
Brown Stiffness (story 1&2)	**0.36**	**0.23**	**0.23**	**0.37**	**0.26**	**0.24**
Bottom 3 Story Drift (%)	0.21	0.62	0.68	0.17	0.55	0.64
Brown Stiffness (story 1-3)	**0.33**	**0.20**	**0.19**	**0.35**	**0.22**	**0.20**
Roof Drift (%)	0.26	0.73	0.79	0.27	0.81	0.95
Brown Stiffness (uniform)	**0.32**	**0.18**	**0.17**	**0.31**	**0.16**	**0.14**

To clarify, the stiffness values highlighted are:

- Brown stiffness story 1 – This is the drift between the base and the first floor. This drift was then used to compute a stiffness value. Note, any values over 0.3 would be capped to 0.3, I just left those values in to show how close we are to a stiffness reduction.
- Story 1&2 – The drift in this case is between the 2nd floor and the base.
- Story 1&3 – The drift in this case is between the 3rd floor and the base
- Roof – This is the value if we wanted to provide a uniform stiffness.

In every case the stiffness of the uniform model will be more flexible (in many cases quite substantially) than for any variable stiffness model.

Appendix E: Additional Information for Shake Table Tests

E.1: UCSD

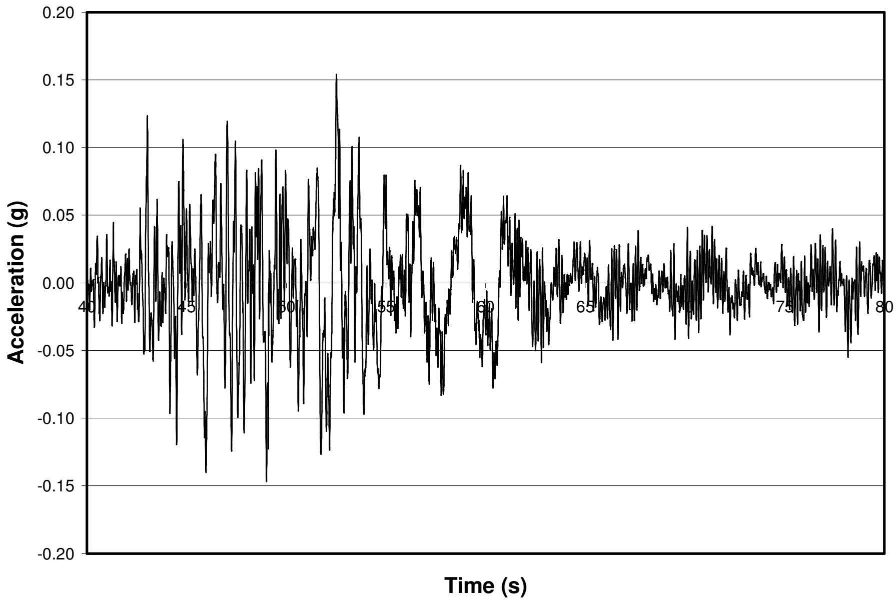

Figure E- 1: Recorded Strong Motion Portion of Ground Motion EQ 1 at Table Surface

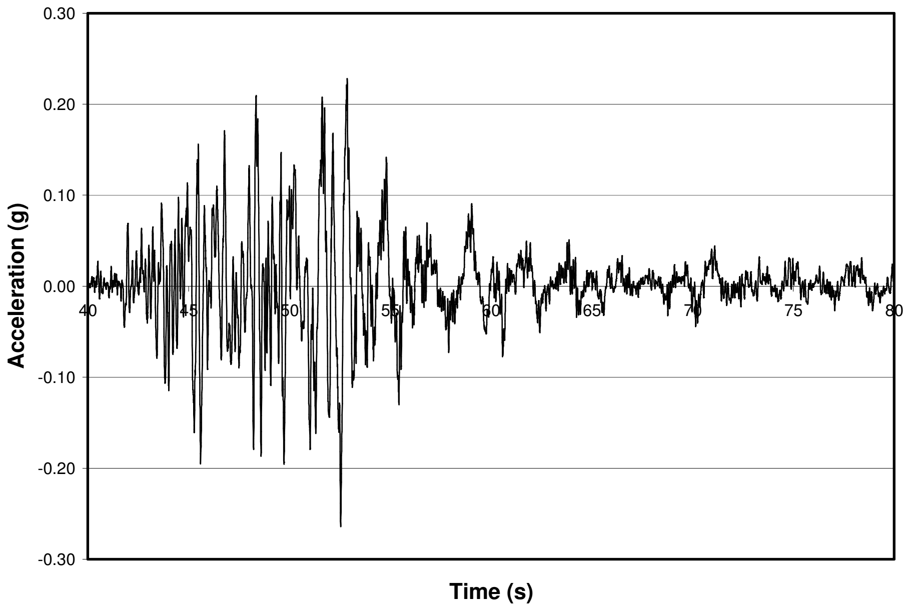

Figure E- 2: Recorded Strong Motion Portion of Ground Motion EQ 2 at Table Surface

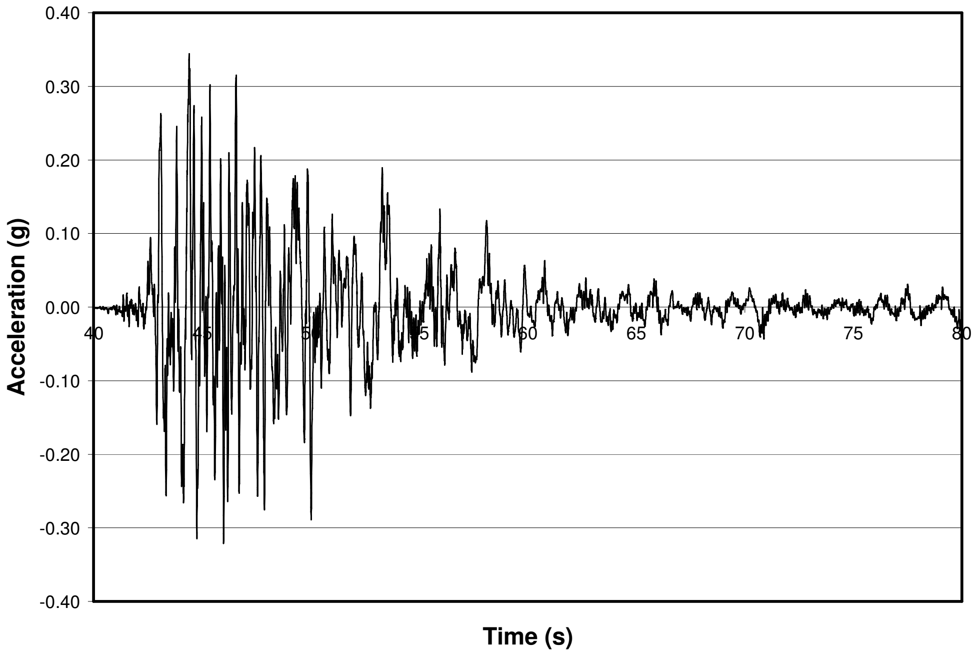

Figure E- 3: Recorded Strong Motion Portion of Ground Motion EQ 3 at Table Surface

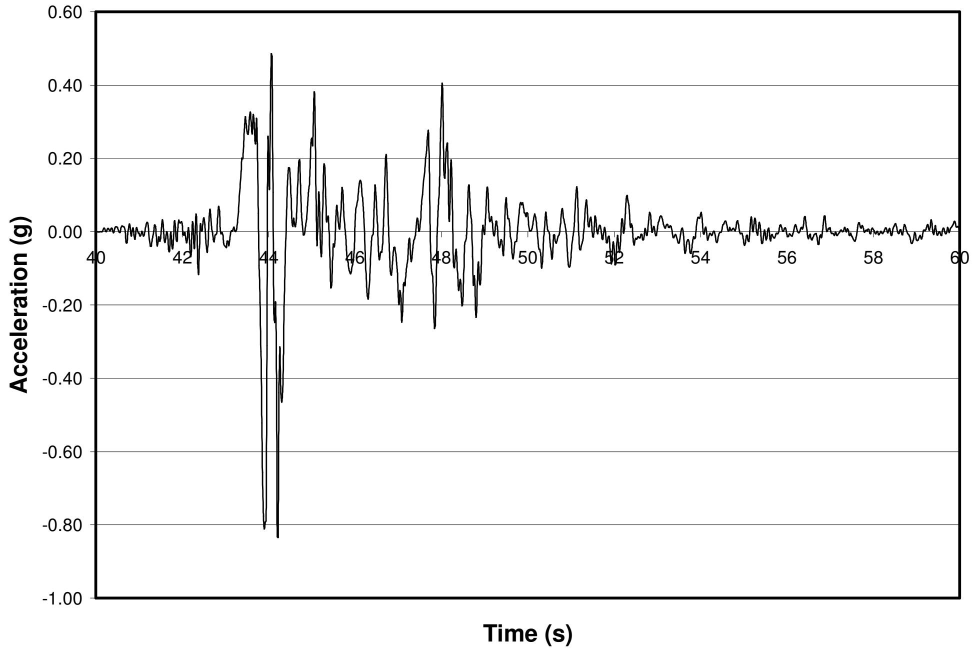

Figure E- 4: Recorded Strong Motion Portion of Ground Motion EQ 4 at Table Surface

E.2: CAMUS 2000

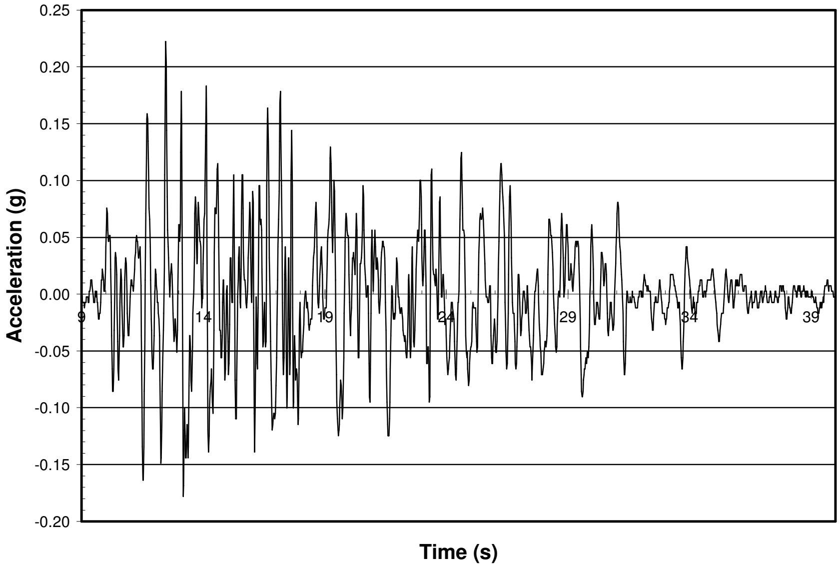

Figure E- 5: Recorded Strong Motion Portion of Run 1 in the Wall (X) Direction at Table Surface

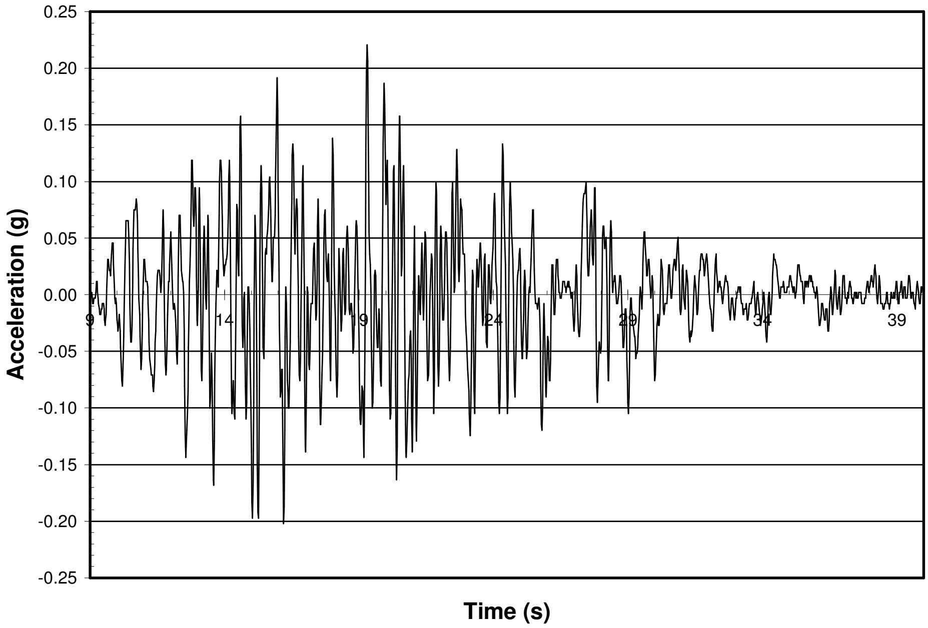

Figure E- 6: Recorded Strong Motion Portion of Run 1 in the Brace (Y) Direction at Table Surface

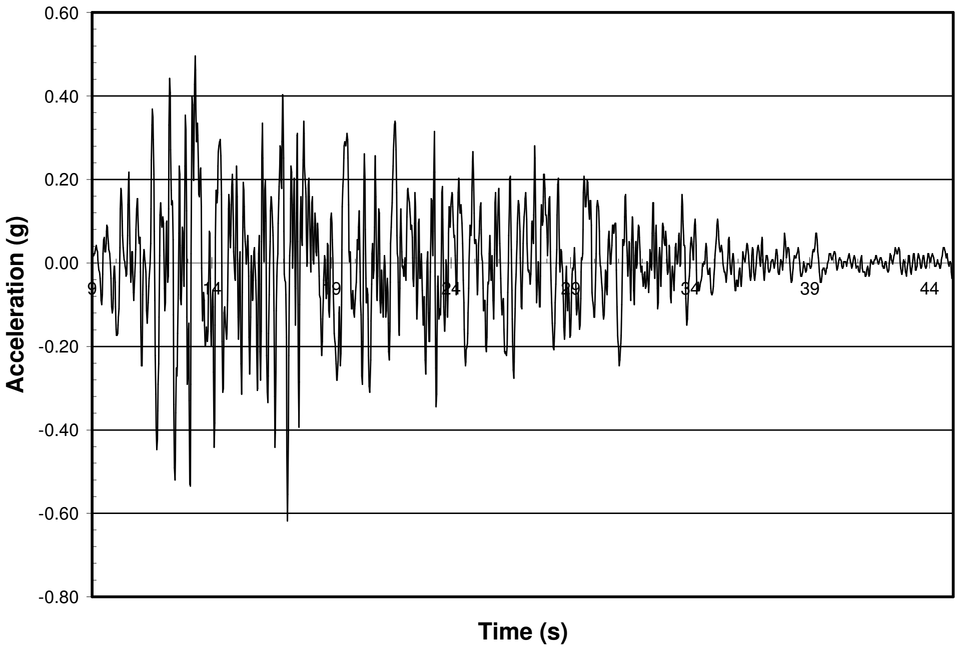

Figure E- 7: Recorded Strong Motion Portion of Run 2 in the Wall (X) Direction at Table Surface

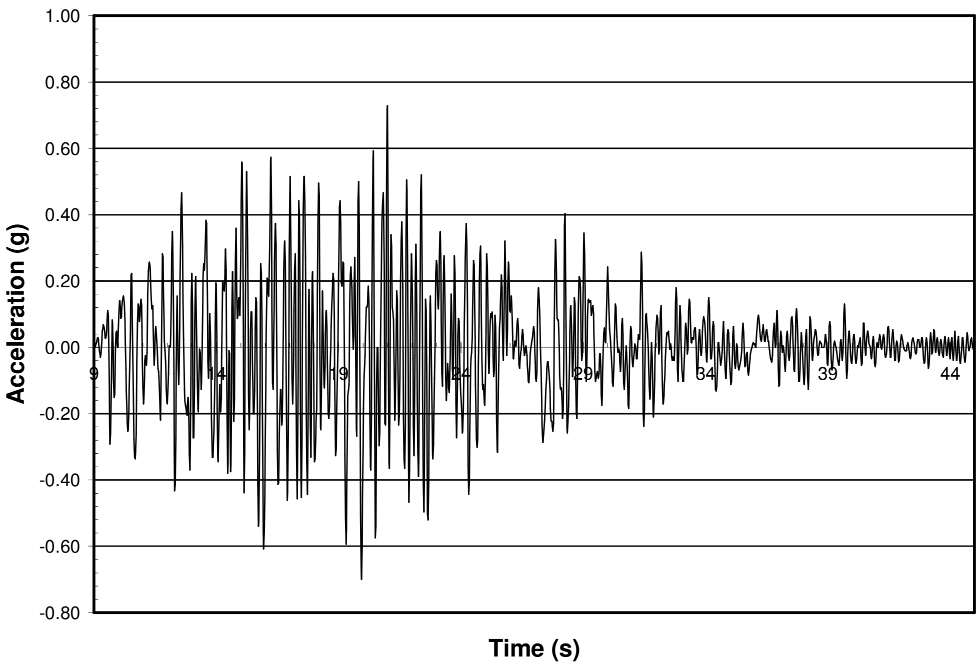

Figure E- 8: Recorded Strong Motion Portion of Run 2 in the Brace (Y) Direction at Table Surface

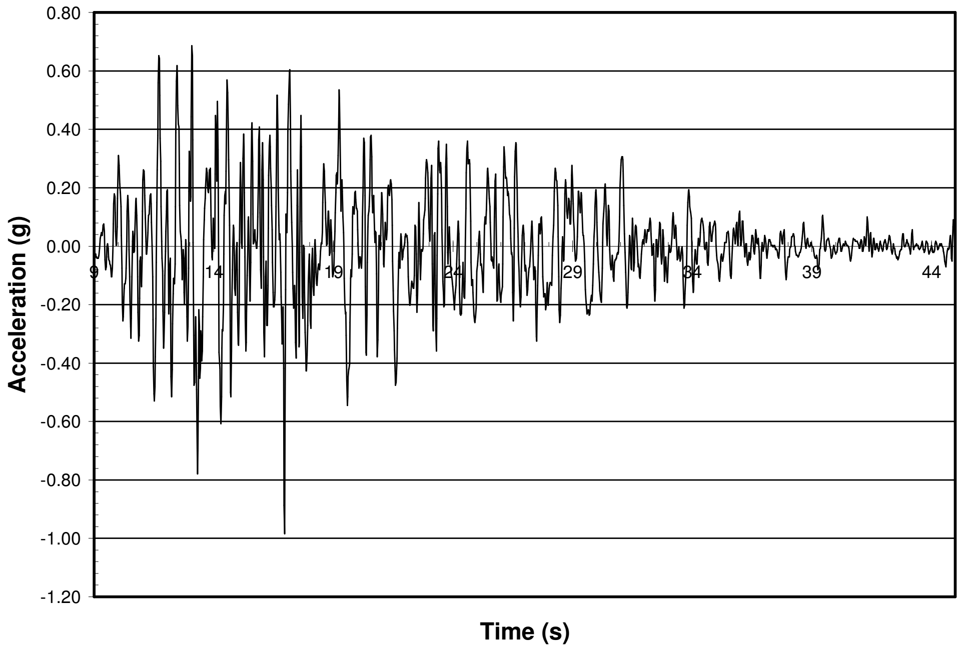

Figure E- 9: Recorded Strong Motion Portion of Run 3 in the Wall (X) Direction at Table Surface

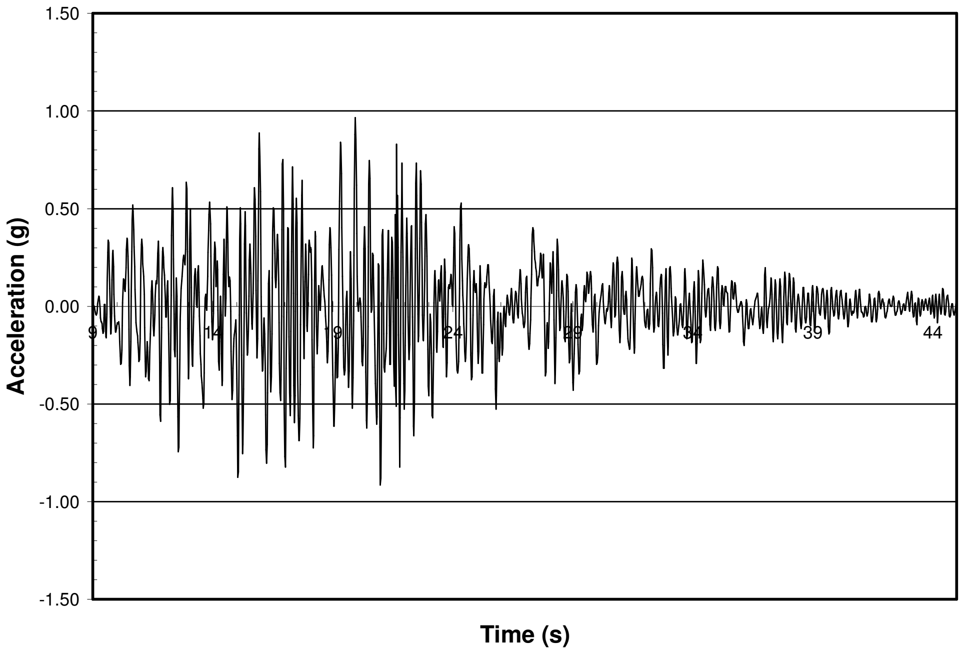

Figure E- 10: Recorded Strong Motion Portion of Run 3 in the Brace (Y) Direction at Table Surface

E.3: CAMUS Ecoleader

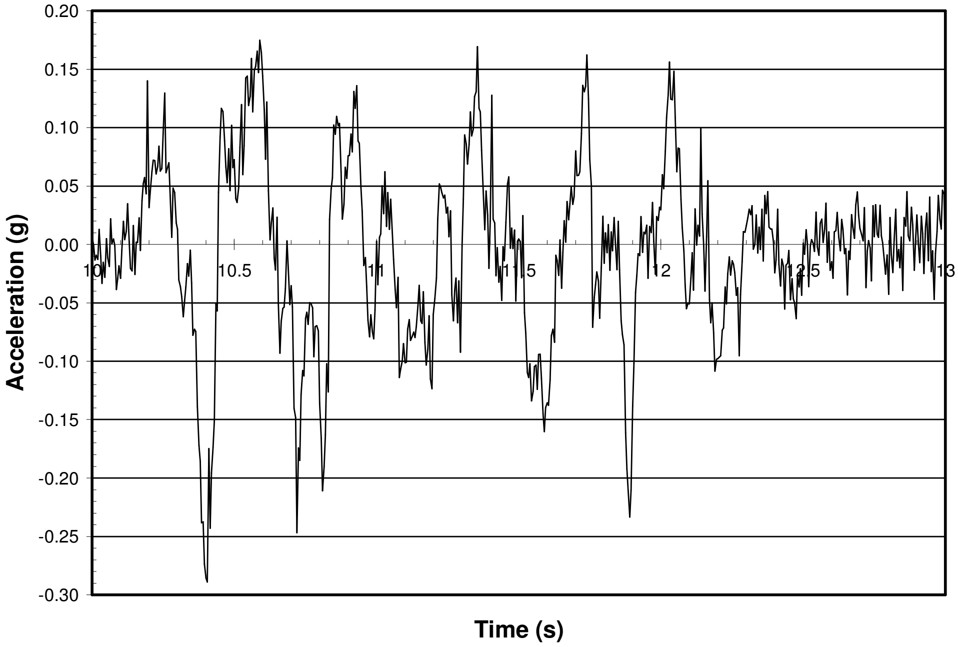

Figure E- 11: Recorded Strong Motion Portion of Run T0-X at Table Surface

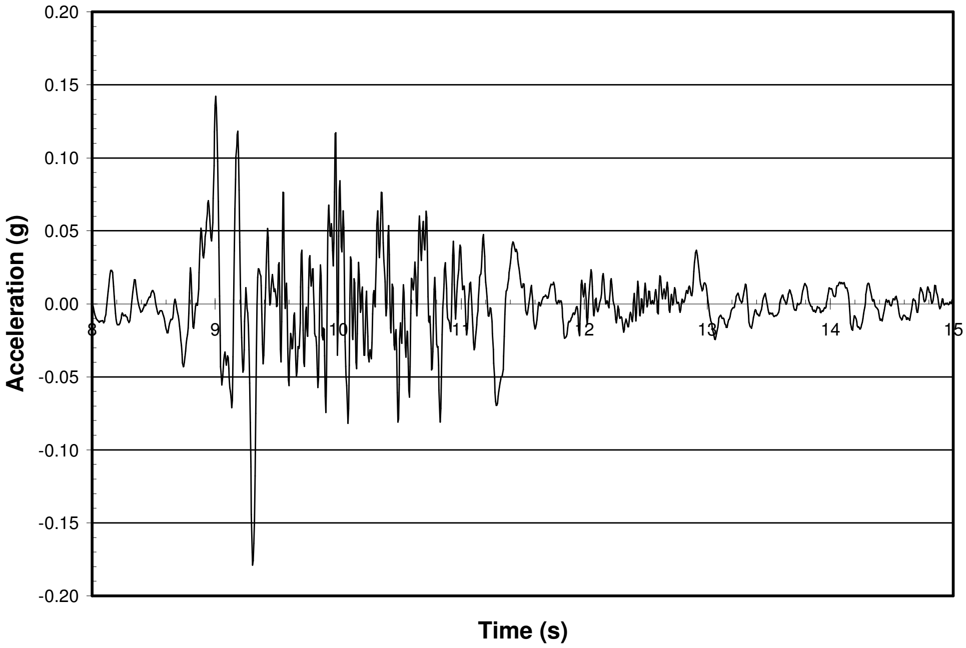

Figure E- 12: Recorded Strong Motion Portion of Run T1-Y at Table Surface

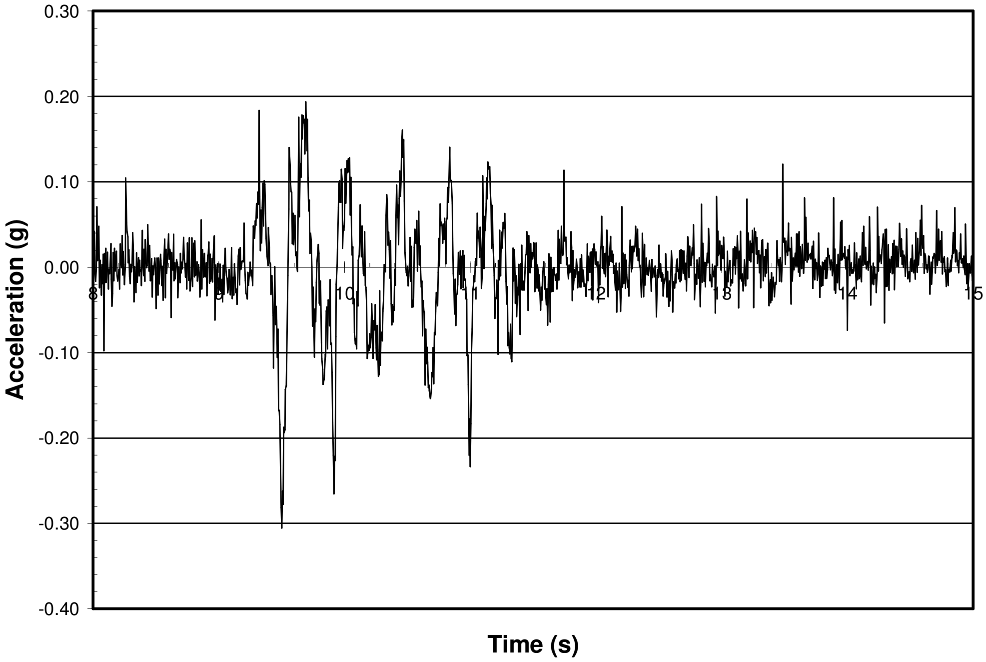

Figure E- 13: Recorded Strong Motion Portion of Run T2-X at Table Surface

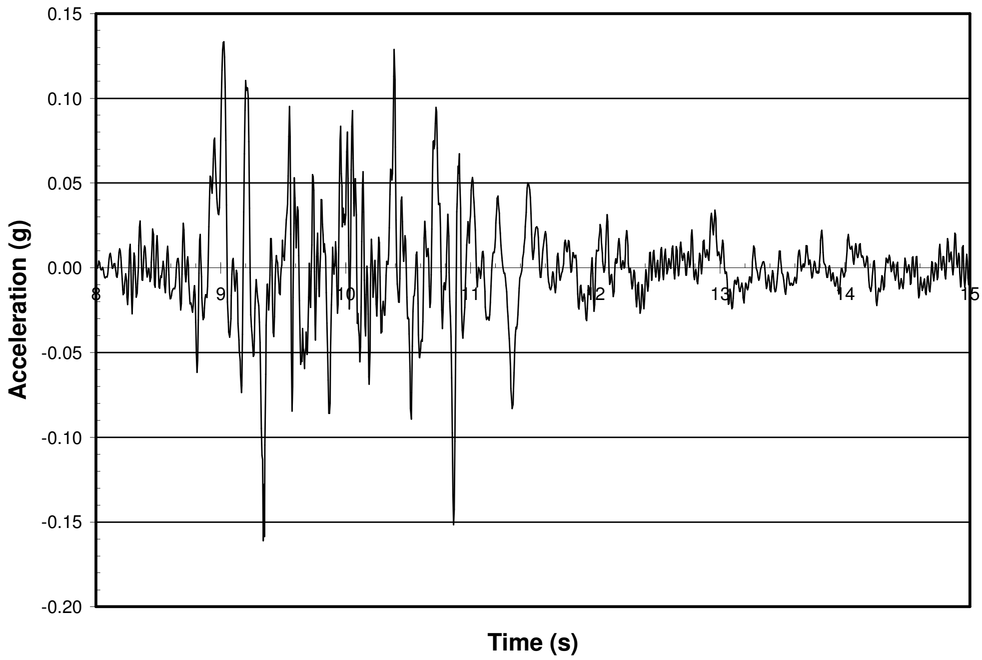

Figure E- 14: Recorded Strong Motion Portion of Run T2-Y at Table Surface

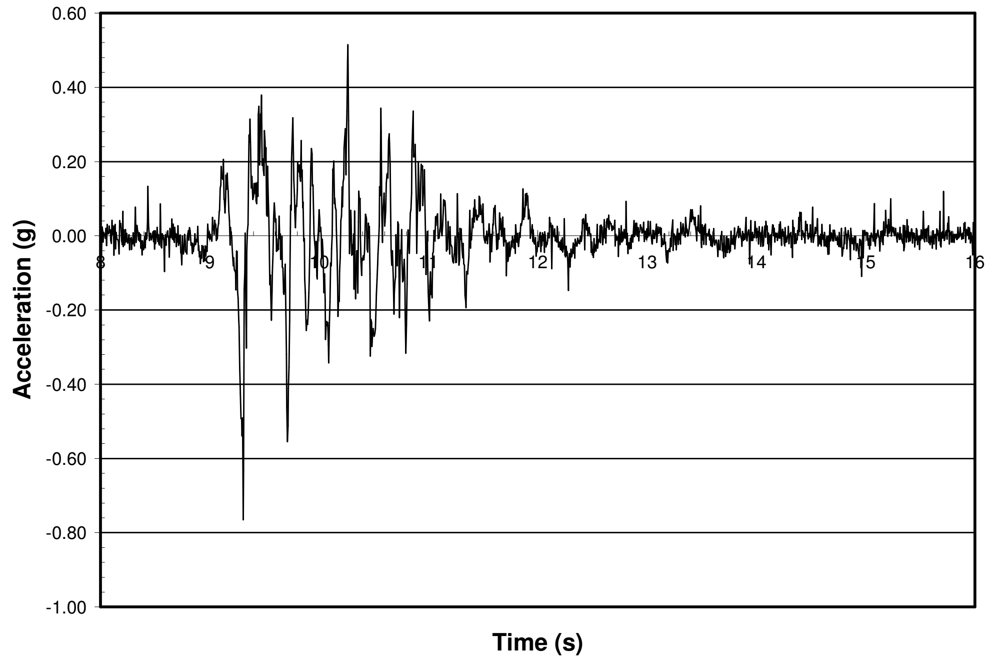

Figure E- 15: Recorded Strong Motion Portion of Run T3-X at Table Surface

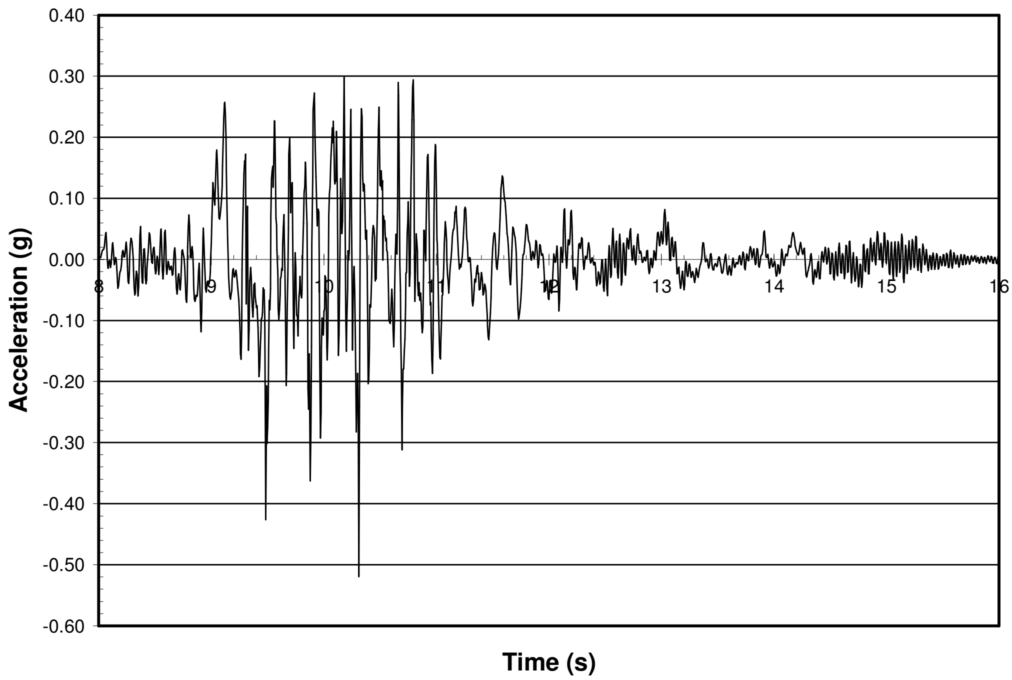

Figure E- 16: Recorded Strong Motion Portion of Run T3-Y at Table Surface

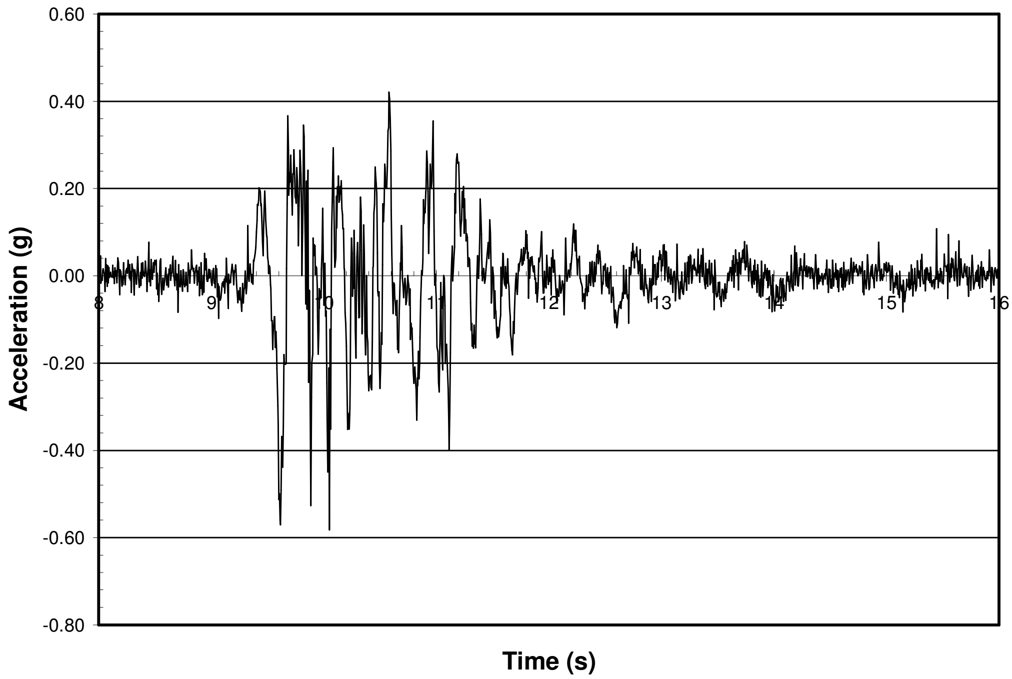

Figure E- 17: Recorded Strong Motion Portion of Run T4-X at Table Surface

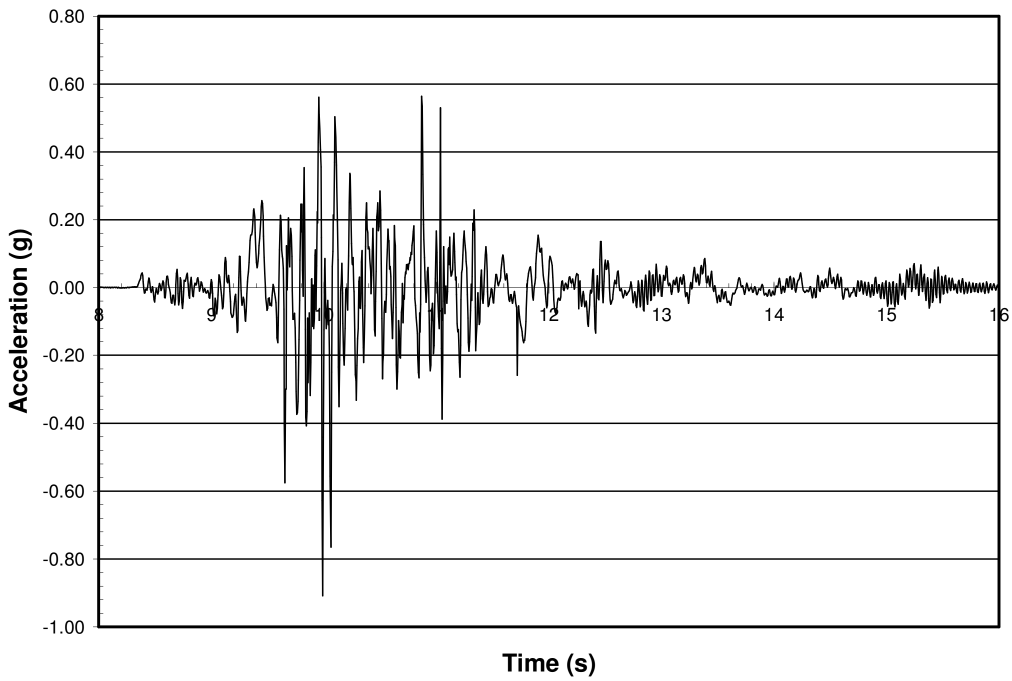

Figure E- 18: Recorded Strong Motion Portion of Run T4-Y at Table Surface

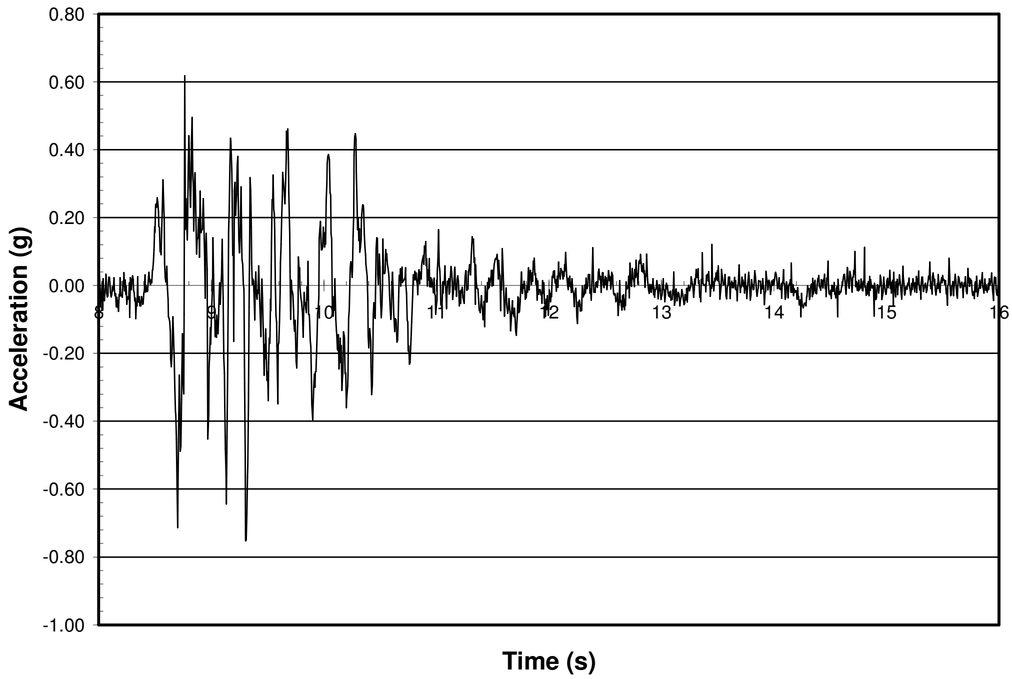

Figure E- 19: Recorded Strong Motion Portion of Run T5-X at Table Surface

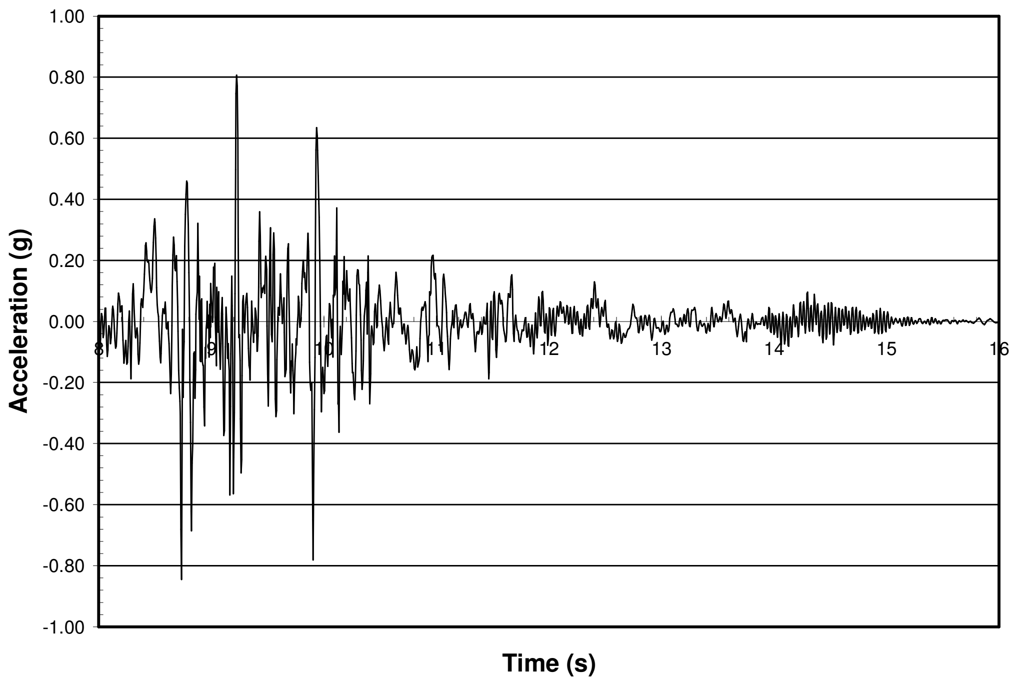

Figure E- 20: Recorded Strong Motion Portion of Run T5-Y at Table Surface

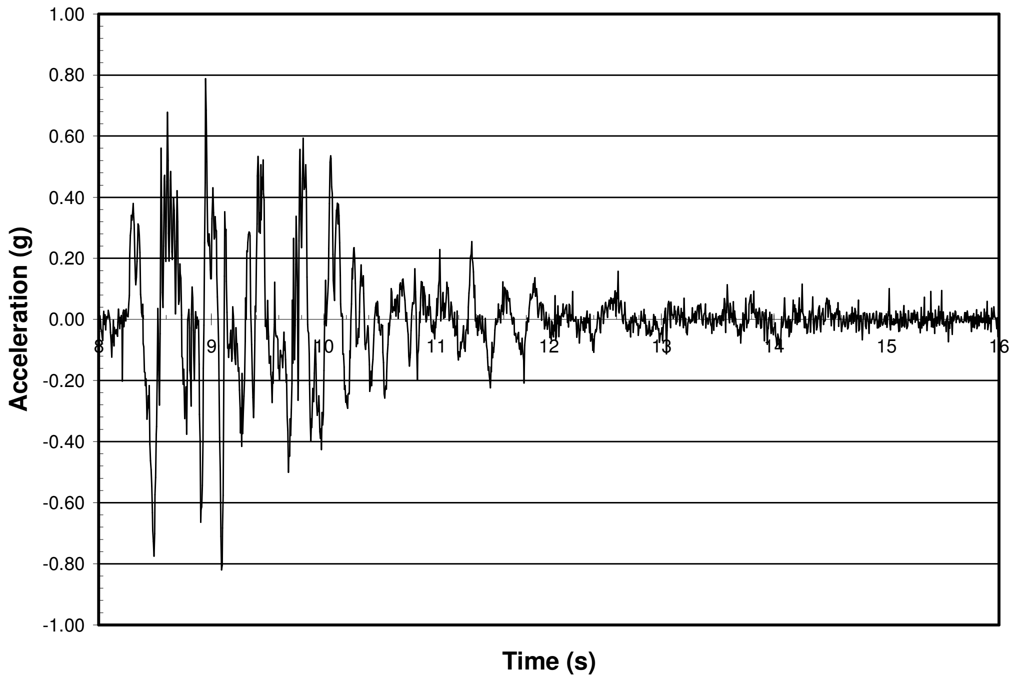

Figure E- 21: Recorded Strong Motion Portion of Run T6-X at Table Surface

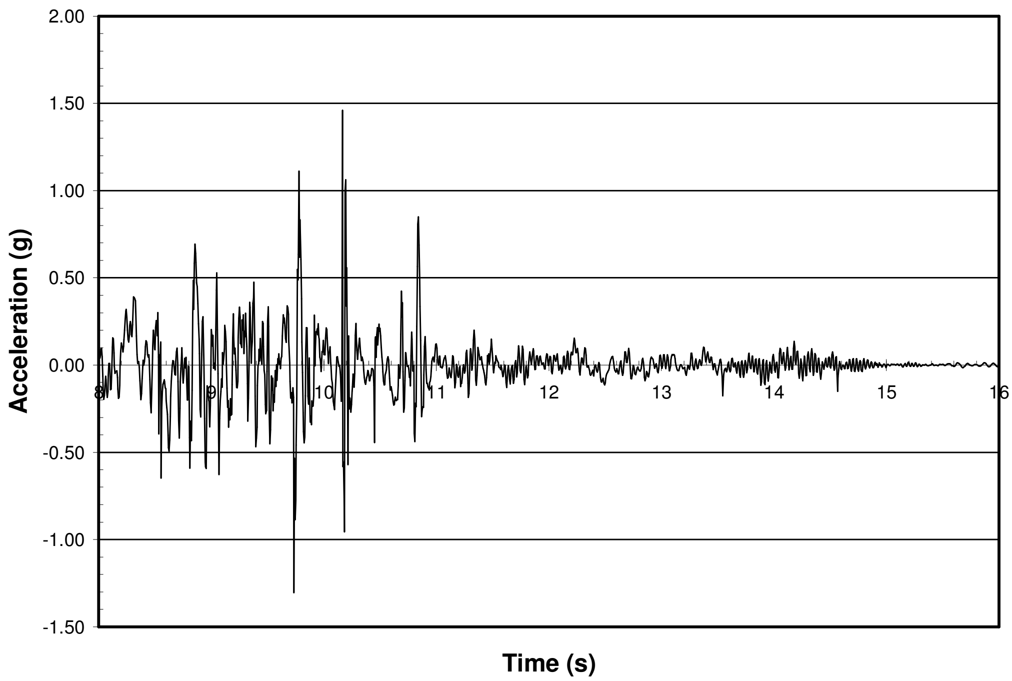

Figure E- 22: Recorded Strong Motion Portion of Run T6-Y at Table Surface

E.4: CAMUS C-Shaped Wall

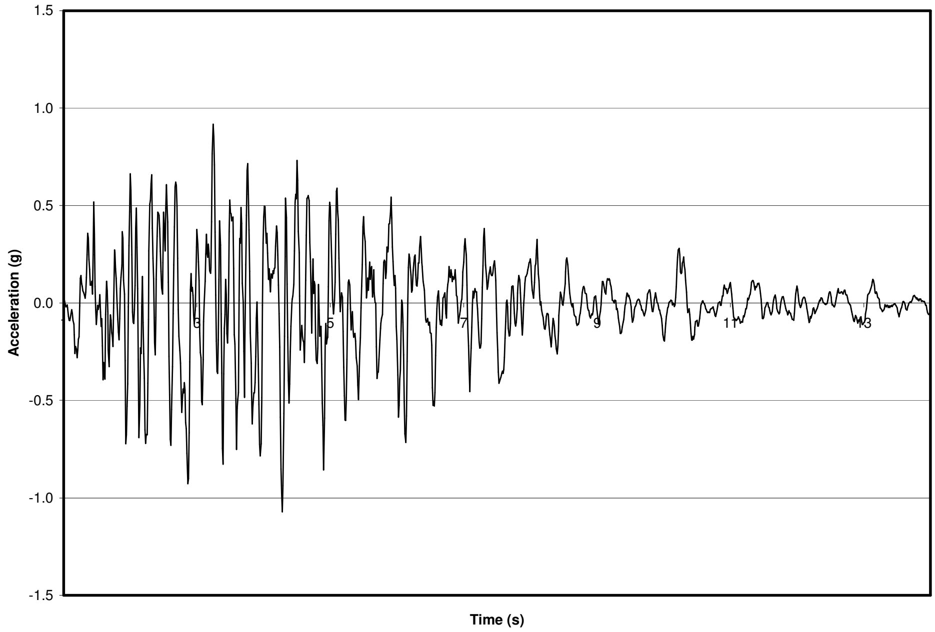

Figure E- 23: Motion 1 – Recorded Strong Motion Time History Acceleration at the Table Surface for Specimen 3, stage 5.

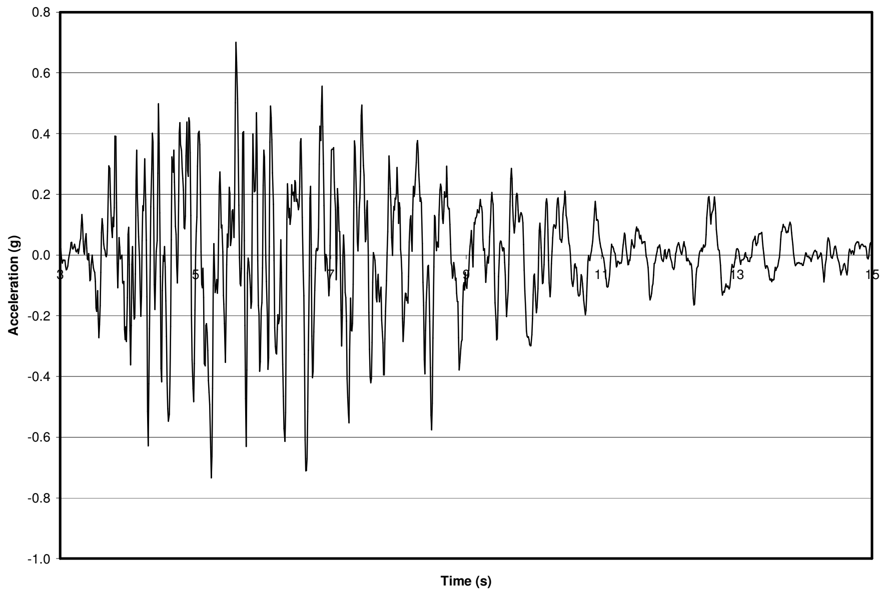

Figure E- 24: Motion 2 - Recorded Strong Motion Time History Acceleration at the Table Surface for Specimen 0, stage 5.

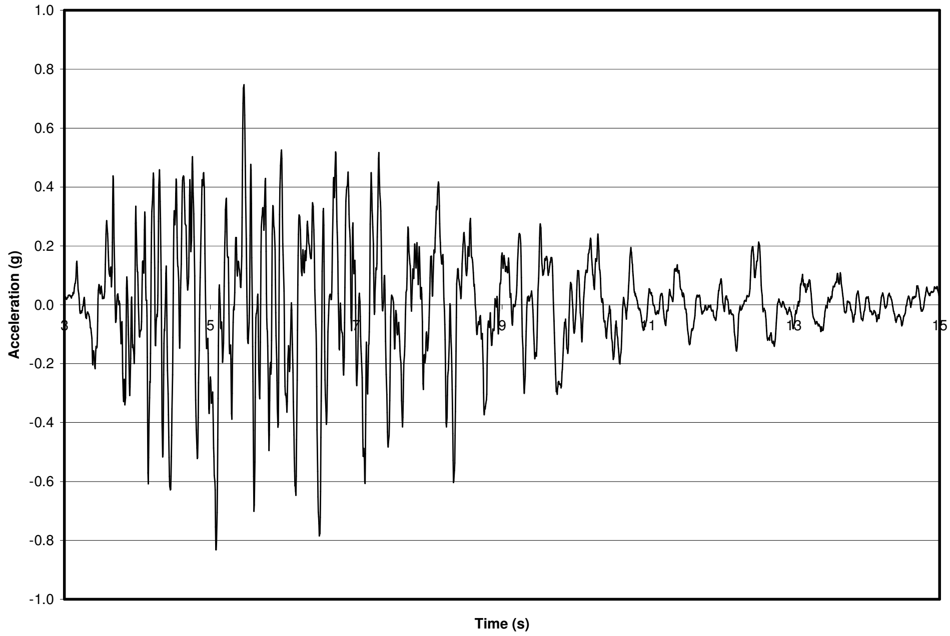

Figure E- 25: Motion 3 - Recorded Strong Motion Time History Acceleration at the Table Surface for Specimen 2, stage 5.

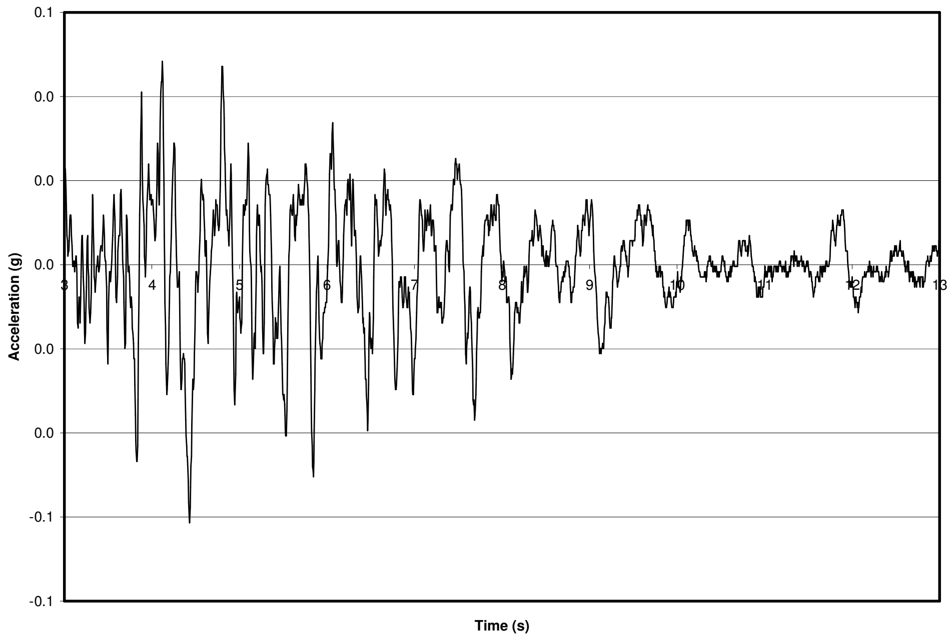

Figure E- 26: Motion 4 - Recorded Strong Motion Time History Acceleration at the Table Surface for Specimen 2, stage 2.

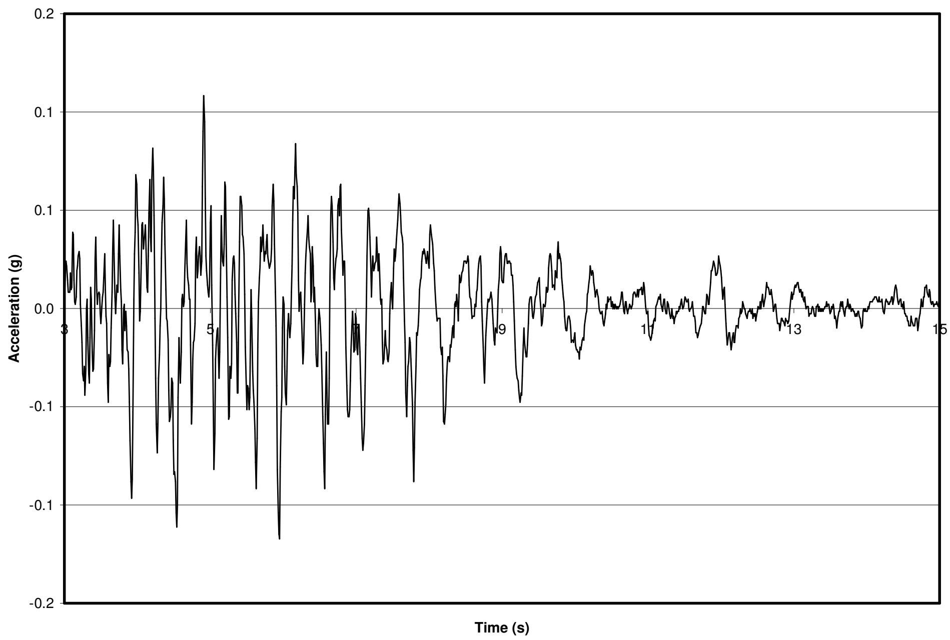

Figure E- 27: Motion 5 - Recorded Strong Motion Time History Acceleration at the Table Surface for Specimen 0, stage 2.